The expression patterns of non-classical and classical forms of HLA-B27 in spondyloarthritis

Thesis submitted for the degree of D.Phil

University of Oxford

Hilary Term 2015

Oliwia Rysnik

Green Templeton College

Botnar Research Centre
Institute of Musculoskeletal Sciences
Nuffield Department of Orthopaedics, Rheumatology and Musculoskeletal Sciences (NDORMS)
Oxford

Supervisors: Professor Paul Bowness
and Dr Simon Kollnberger

Oliwia Rysnik
Green Templeton College, University of Oxford
Thesis submitted for the degree of Doctor of Philosophy (D.Phil) in Musculoskeletal Sciences, Hilary Term 2015

The expression patterns of non-classical and classical forms of HLA-B27 in spondyloarthritis

Abstract

The strong association of the human leukocyte antigen HLA-B27 (B27), with spondyloarthropathies (SpA), was discovered more than four decades ago, yet the role B27 plays in disease pathogenesis remains unclear. It has been demonstrated that HLA-B27 can form non-classical FHC forms, including B27 FHC homodimers ($B27_2$) and misfolded FHCs. Two leading theories of SpA pathogenesis proposed that both cell surface NC-B27 (the B27 homodimer theory) and intracellular (the B27 misfolding and UPR theory) can drive immune responses in SpA. Several studies demonstrated that cell surface NC-B27 binds to immune receptors and suggested that these interactions can activate Th17 immunity. My DPhil project focuses on the investigation of the cell surface expression of NC-B27 molecules in cells and tissues obtained from AS patients and B27 TG^2 rats. I used both existing reagents and a novel HD6 antibody, generated against $B27_2$, to examine the expression of HLA-B27 by flow cytometry, confocal microscopy and immunoprecipitation. This thesis provides evidence that the expression of HD6- and HC10-reactive molecules in AS patients is rather restricted to specific cell types (e.g. osteoclasts) and possibly particular environmental factors and tissue types (e.g. synovial fluid and joint tissue). My data using B27 TG^2 rats demonstrated that resident joint cells express HD6- and HC10-reactive molecules before the onset of clinical manifestations. Furthermore, I showed increased expression of NC-B27 on antigen presenting cells (APCs), and $CD161^+$ and $CD8^+$ cell populations in blood and secondary lymphoid organs. Based on these findings I hypothesized that cell surface expression of NC-B27 may not only be crucial for activation of Th17-driven immune responses, but may also shift the balance between immune tolerance and activation. Importantly, the expression of potentially pathogenic HD6-reactive molecules is restricted to specific cell and tissue types hence HD6 antibody may be a potential future therapeutic agent in SpA.

Declaration:

I declare that the work presented in this D.Phil thesis entitled: "The expression patterns of non-classical and classical forms of HLA-B27 in spondyloarthritis" is entirely my own work. No part of my thesis has been submitted for any degree or other qualification in the University of Oxford or elsewhere.

Oliwia Rysnik

Hilary Term 2015
Green Templeton College, University of Oxford

Acknowledgements:

I would like to thank my supervisors Paul Bowness and Simon Kollnberger and all the Bowness' lab members, especially Kirsty McHugh, for their help, guidance, support and encouragement over the course of my D.Phil ☺

I wish to thank Prof. Beaten, Leonie van Duivenvoorde and Melissa van Tok for the great collaboration and all their help ☺

My greatest gratitude goes to my family and friends, especially Billy Bob, Mitchy, V. Fiona, MC Phil, Momo, Jaco and Adam who have GREATLY supported me over the course of this long D.Phil journey ☺

I wish to express my sincere thanks to Arthritis Research UK, Green Templeton College and NDORMS for their financial support ☺

Thank you ALL!

Your sincerely,

Oliwia Rysnik

Table of contents

List of Abbreviations

AA - amino acid
AAU - acute anterior uveitis
AIDS - acquired immunodeficiency syndrome
ANKENT – murine ANKylosing ENThesopathy model
ANTXR2 - anthrax toxin receptor 2
APCs - antigen presenting cells
AREs - AU-rich elements
AS - Ankylosing spondylitis
ASAS - Assessment of SpondyloArthritis international Society
ASDAS - Ankylosing Spondylitis Disease Activity Score
ATF4 - transcription factor 4
ATF6 - transcription factor 6
axSpA - axial SpA
B27 TG – HLA-B27 transgenic rats
B27 TG^1 – 33-3 HLA-B27 transgenic rat model
B27 TG^2 – (21-3 x 283-2)F_1 HLA-B27 transgenic rat model
B27+ve - HLA-B27-positive
B27$_2$ - B27 homodimers
B7 TG - HLA-B7 transgenic rats
BAS-G - Bath Ankylosing Spondylitis Global Score
BASDAI - Bath Ankylosing Spondylitis Disease Activity Index
BASFI - Bath Ankylosing Spondylitis Funcional Index
BASMI - Bath Ankylosing Spondylitis Metrology Index
BCL - Epstein-Barr Virus (EBV)-transformed B cell line
BiP - immunoglobulin binding protein
BM – bone marrow
BMP - bone morphogenic protein
cAMP - cyclic adenosine monophosphate
CHOP - CCAAT/enhancer-binding protein homologous protein
CIA - collagen induced arthritis
CNX - calnexin
COPI - coat protein complex I
COPII - coat protein complex II
COX-2 -cyclooxygenase-2
Coxibs - COX-2 inhibitors
CRP - C-reactive protein
CRT - calreticulin
CTLs - cytotoxic $CD8^+$ T cells
Cys67 - cysteine at position 67
DCs - dendritic cells
DCs - dendritic cells
DKK-1 - Dickkopf-1
DMARDs - disease-modifying antirheumatic drugs
E.coli - *Esherichia coli*
EBV - Epstein-Barr Virus
EESG - European Spondyloarthropathy Study Group
EMA - European Medicines Agency
ER - endoplasmic reticulum
ERAD - ER-associated degradation
ERAP-1 - Endoplasmic reticulum aminopeptidase-1
ERGIC - ER-Golgi intermediate compartment

ESR - erythrocyte sedimentation rate
EULAR - European League Against Rheumatism
FasL - Fas ligand
FcγR - Fc receptor gamma chain
FHC - free heavy chain
FHC - free heavy chains
FSC or FS - forward scatter
GeoMean - geometric mean
GF - germ-free
GM-CSF - granulocyte macrophage colony stimulating factor
GRAPPA - Group for Research and Assessment of Psoriasis and Psoriatic Arthritis
GWAS - Genome Wide Association Studies
HC – heavy chain
HCV - hepatitis C virus
HIV - human immunodeficiency virus
HLA-B27 - human leukocyte antigen B27
HMW - high molecular weight
IBD - inflammatory bowel disease
IBP - inflammatory back pain
IFNα - interferon alpha
IFNβ – interferon beta
IFNγ – interferon gamma
Ig-like - immunoglobulin-like
IHC - immunohistochemistry
IL-1 - Interleukin-1
IL-12 - interleukin-12
IL-17 - interleukin-17
IL-23 - interleukin-23
IL-23R - Interleukin-23 receptor
IL-6 - interleukin 6
IL-8 - interleukin 8
IP - immunoprecipitation
IRE1 - Inositol-requiring kinase 1
ITAMs - immunoreceptor tyrosine-based activation motifs
ITIMs - immunoreceptor tyrosine-based inhibitory motifs
JAK - Janus kinase
JSpA Juvenile SpA
KIR3DL2 - killer cell immunoglobulin-like receptor 3DL2
KIRs - killer Ig-like receptors
LCL - lymphoblastoid B cell line
LILRs - leukocyte Ig-like receptors
LNs - lymph nodes
LPS - lipopolysaccharide
M-CSF - macrophage colony-stimulating factor
M.tb. - *Mycobacterium tuberculosis*
mAb - monoclonal antibody
MFI - mean fluorescence intensity
MHCI - Major Histocompatibility Complex class I
MHCII - Major Histocompatibility Complex class II
mNY - modified New York
moDCs - monocyte-derived dendritic cells
MPA - Murine progressive ankylosis
MRI - magnetic resonance imaging
MTX - methotrexate
Mφ - macrophages

NC-B27 - non-classical forms of HLA-B27
NF-κB - nuclear factor kappa B
NK - natural killer cells
NKT - natural killer T cells
NOG - noggin
nr-axSpA - non-radiographic axial SpA
NSAIDs - nonsteroidal anti-inflammatory drugs
OA - osteoarthritis
OCs - osteoclasts
PBMC - peripheral blood mononuclear cell
pDCs - plasmacytoid DCs
PDE4 - Phosphodiesterase 4
PERK - pancreatic ER eIF2a kinase
PGE_2 - prostaglandin E_2
PGIA - proteoglycan/aggrecan (PG)-induced arthritis
PGISp - PG-induced spondylitis
PGs - prostaglandins
PLC - peptide loading complex
poly I:C - polyinosinic:polycytidylic acid
PsA - psoriatic arthritis
pSpA - peripheral SpA
PTGER4 - prostaglandin E receptor 4
RA - rheumatoid arthritis
RANKL - receptor activator of nuclear factor kappa-B ligand
ReA - reactive arthritis
S.typhimurium - *Salmonella typhimurium*
SDS - sodium dodecyl sulfate
SEM - standard error of the mean
SF - synovial fluid
SFMC - synovial fluid mononuclear cells
SI – sacroiliac
SLZ – sulfasalazine
SOST - sclerostin
SpAs - Spondyloarthropathies
SPLC - splenocytes
SSC or SS - side-scatter
STAT - Signal Transducer and Activator of Transcription
TAP - transporter associated with antigen processing
TG - transgenic
TLR3 - Toll-like receptor 3
TLR4 - Toll-like receptor 4
TLR9 - Toll-like receptor 9
TNFRI - TNFα receptor I
TNFα - tumour necrosis factor α
TPN - tapasin
UPR - unfolded protein response
Wnt - Wingless-type like
WT - wild type
XBP1 - X-box binding protein 1
β2-m - β2-microglobulin

List of Tables

Chapter One:

Chapter Two:

Chapter Four:

Chapter Five:

List of Figures

Chapter One:

Chapter Three:

Chapter Four:

Chapter Five:

Chapter Six:

Chapter One: Introduction

1.1 The concept of spondyloarthropathies

Spondyloarthropathies (SpAs) are a group of heterogeneous chronic inflammatory diseases with common clinical and genetic features. SpAs are divided into two main subgroups based on clinical manifestation. The first of these groups is axial SpA (axSpA), which includes Ankylosing spondylitis (AS) and non-radiographic axial SpA (nr-axSpA). The second subgroup is a peripheral SpA (pSpA), with psoriatic arthritis (PsA), reactive arthritis (ReA) and arthritis associated with inflammatory bowel disease (IBD). Inflammatory back pain (IBP) caused by axial skeleton inflammation, including sacroiliitis and spondylitis, is one of the main characteristic clinical manifestations in axSpA and nr-axSpA. Peripheral joint arthritis is commonly found in the second group of SpA. Other clinical manifestations frequently observed in SpA patients consist of: enthesitis, acute anterior uveitis (AAU), dactylitis, psoriasis and Crohn's disease. Juvenile SpA (JSpA) is an early onset (>6 year of age) form of SpA that occurs predominantly in males. Sacroiliac joint inflammation (visible on magnetic resonance imaging (MRI)), peripheral arthritis and/or enthesitis are the main characteristic features of JSpA.

One of the common features of SpAs is their strong association with the human leukocyte antigen B27 (HLA-B27). In the European Caucasian population more than 90% of AS patient, depending on the geographical origin, carry the HLA-B27 gene. In other forms of SpA the prevalence of HLA-B27 gene varies from 70% in white ReA patients, 60-70% in psoriatic spondyloarthritis, 50-60% in spondyloarthritis associated with IBD, 50% in uveitis and about 25% in peripheral psoriatic arthritis (Garg, Bosch, and Deodhar 2014). The prevalence of HLA-B27 can reach 76% in JSpA (Sonkar, Usha, and Singh 2008). However, globally only ~2% of the HLA-B27-positive (B27+ve) individuals develop SpA (Braun et al. 1998). Therefore it has been suggested that other genetic and environmental factors contribute to disease susceptibility. Remarkable progress in the Genome Wide Association Studies (GWAS) in the past few years has led to the discovery of a significant number of novel genes strongly associated with SpA. Genetic associations with AS, as a prototype of SpA, are so far the best-studied. However, the number of studies investigating genetic associations with non-AS SpA, especially PsA, is growing. Interleukin-23 receptor (IL-23R) is according to GWAS the second most prominent gene associated with SpA. To date, the strong association of IL-23R gene has been identified in AS (Davidson et al. 2013; Dennis et al. 2012; Dong et al. 2013; Karaderi et al. 2009; Pimentel-Santos et al. 2009), PsA (Eirís et al. 2014; Jadon et al. 2013), AAU (Robinson et al. 2015) and in arthritis associated with IBD (Duerr et al. 2006; Reveille 2011). Endoplasmic reticulum aminopeptidase-1 (ERAP-1) is another gene candidate strongly associated with SpA (Agrawal and Brown 2014; Davidson et al. 2009; Jadon et al. 2013; Pimentel-Santos et al. 2009; Tsui et al. 2010). Furthermore, a number of genes located in the interleukin-1 (IL-1) family cluster have also been associated with AS and some other forms of SpA (Guo et al. 2010; Kim et al. 2008; Monnet et al. 2012; Sims et al. 2008).

Importantly, carrying specific variants of the disease-associated genes predispose individuals to SpA. However environmental factors also play a substantial role in disease development. Since subclinical gut inflammation is found in up to 60% of SpA patients (Mielants et al. 1985, 1988, 1996) and about 6% of B27+ve AS patients develop IBD (Mielants et al. 1995; De Vos et al. 1996) gut microbiota dysbiosis was suggested as a key environmental factor in SpA pathogenesis.

1.2 SpA classification criteria

Recognition of AS as a separate disease, proposed for the first time in 1961 at the European Congress of Rheumatology in Rome, gave rise to the concept of SpA (Kellgren, J.H., Jeffrey, M. R., and Ball, J., The Epidemiology of Chronic Rheumatism, vol.1, page 326, Blackwell, Oxford, 1963). The first AS classification criteria consisted of: lower back pain and stiffness for ≥3 months, that is not relieved by rest; limited motion of the lumbar spine; pain and stiffness in the thoracic region; X-ray showing bilateral sacroiliiac (SI) joint changes typical for AS (which exclude osteoarthritis (OA)). Five years later a grading of sacroiliitis and more specific definitions of AS was published in the New York criteria. In 1974 Moll and Wright introduced a new concept of seronegative polyarthritis, different from rheumatoid arthritis (RA) and with a similarity to AS. Ten years later the modified New York (mNY) criteria included a definition of inflammatory back pain (IBP) distinct from mechanical lower back pain. According to the mNY criteria, IBP has an insidious origin, is persistent at night and improves with exercise.

Although the strong association of HLA-B27 with AS and other forms of seronegative arthritis was discovered in the 70's (Cheatum 1975; R. I. Morris et al. 1974; R. Morris et al. 1974; Schlosstein et al. 1973), HLA typing was only introduced in SpA diagnosis 16 years later by the Amor criteria (Amor, Dougados, and Mijiyawa 1990). The Amor and European Spondyloarthropathy Study Group (EESG) (Dougados et al. 1991) criteria developed in the 90s were based on the overlap between the clinical features of axSpA and pSpA. Hence, an improved earlier diagnosis was possible in patients with predominantly peripheral clinical features, such as enthesitis, psoriasis, uveitis or gut manifestations, and with less significant spinal manifestations at the time of diagnosis.

Further need to diagnose SpA at its early stages, along with the advance in the use of magnetic resonance imaging (MRI) as a diagnostic tool, led to the development of the Assessment of SpondyloArthritis international Society (ASAS) classification criteria in 2009 (M Rudwaleit et al. 2009). Notably, over the past five years ASAS developed a new definition of IBP and an active SI joint inflammation on MRI. Moreover, the new classification criteria for axial SpA covered patients with both radiographic and nr-axSpA. The most up-to-date ASAS classification criteria are presented in Table 1.1 (Rudwaleit et al. 2011). Importantly, the new ASAS classification criteria included peripheral SpA. In patients with peripheral symptoms only, SpA classification is based on arthritis, enthesitis or dactylitis in peripheral joints (Table 1.1). The final set of ASAS classification criteria demonstrated the best combination of sensitivity (~78%) and specificity (~83%) compared with EESG and the Amor criteria (Rudwaleit et al. 2011).

The SpAs are an extremely challenging group of diseases when it comes to an early diagnosis. However, ongoing discussion on the SpA classification criteria, increasing number of post-diagnosis reports and the development of novel diagnostic techniques and tools will likely improve the efficacy of early axSpA and pSpA diagnosis.

Table 1.1 Current Assessment of SpondyloArthritis international Society (ASAS) classification criteria for axSpA and pSpa

ASAS Classification Criteria of Axial and Peripheral SpA	
ASAS Classification Criteria for axial Spondyloarthritis:	**ASAS Classification Criteria for Peripheral Spondyloarthritis:**
In patients with ≥ 3 months of back pain and age of onset <45 years **Sacroiliitis on imaging* plus ≥1 SpA features**** **OR** **HLA B27 plus ≥2 SpA features**:** *** Sacroiliitis on imaging:** • Active (acute) inflammation on MRI highly suggestive of sacroiliitis associated with SpA • Definite radiographic sacroiliitis according to modified NY criteria **** SpA Features:** • Inflammatory back pain • Arthritis • Enthesitis (heel) • Uveitis • Dactylitis • Psoriasis • Chron's colitis • Good response to NSAIDs • Family history of SpA • HLA B27 • Elevated CRP	**Arthritis or Enthesitis or Dactylitis** **Plus ≥1 of:** • Psoriasis • Inflammatory bowel disease • Previous infection • HLA B27 • Uveitis • Sacroiliitis on imaging (radiographs or MRI) **OR** **Plus ≥2 of the remaining:** • Arthritis • Dactylitis • Enthesitis • IBP in the past • Positive family history of SpA

Adapted from the http://www.asas-group.org and (Rudwaleit et al., 2009)

1.3 Assessment of the disease activity and treatment outcome in AS

Due to the heterogeneity of clinical manifestations and the lack of reliable markers of disease progression there is no gold standard for measuring AS activity. The Bath Ankylosing Spondylitis Disease Activity Index (BASDAI) was developed in 1994 to meet the needs of clinicians for a sensitive to change, reliable and a comprehensive form of AS activity measure (Calin et al. 1994). BASDAI consists of six questions (of a 1-10 scale) assessing pain and discomfort in the spine and peripheral joints, patient tiredness/fatigue and morning stiffness (Table 1.2). The formula calculating the final BASDAI score (in 0-10 scale) gives each symptom equal weighting. BASDAI score ≥ 4 indicate a high activity of the disease. The Bath Ankylosing Spondylitis Funcional Index (BASFI) (Calin et al. 1994) and the Bath Ankylosing Spondylitis Metrology Index (BASMI) (Jenkinson et al. 1994) were developed at the same time in order to assess the degree of funcional limitation in patients and accurately measure changes in spinal movement. Additionally, in 1996 Jones *et al.* introduced The Bath Ankylosing Spondylitis Global Score (BAS-G) to provide a global assessment of patient well-being over a given period of time (Jones et al. 1996).

However, in Bath indices clinical symptoms are not distinguished according to their importance. Furthermore, some questions asked in the same questionnaire cover similar symptoms. Hence, to encounter the unmet needs for the more accurate SpA diagnosis ASAS suggested in 2009 an improved disease activity index (Lukas et al. 2009). The Ankylosing Spondylitis Disease Activity Score (ASDAS) formula for the first time took into consideration statistical relevance of diffirent factors involved in the assessment of disease (Table 1.3) (D van der Heijde et al. 2009; Lukas et al. 2009).

Table 1.2 The Bath Ankylosing Spondylitis Disease Activity Index (BASDAI)

BASDAI

Please place a mark on each line below to indicate your answer to each question relating to the past week

1. How would you describe the overall level of fatigue/tiredness you have experienced?

NONE ____ VERY SEVERE

2. How would you describe the overall level of AS neck, back or hip pain you have had?

NONE ____ VERY SEVERE

3. How would you describe the overall level of pain/swelling in joints other than neck, back, hips you have had?

NONE ____ VERY SEVERE

4. How would you describe the overall level of discomfort you have had from any areas tender to touch or pressure?

NONE ____ VERY SEVERE

5. How would you describe the overall level of morning stiffness you have had from the time you wake up?

NONE ____ VERY SEVERE

6. How long does your morning stiffness last from the time you wake up?

____

0 hrs $^{1}/_{2}$ 1 1 $^{1}/_{2}$ 2 or more hrs

Calculation of BASDAI:

- **Compute the mean of questions 5 and 6**
- **Calculate the sum of questions 1-4 and add the result to the mean of questions 5 and 6**
- **Divide the result by 5**

Adapted from http://basdai.com and (Garrett et al., 1994)

The ASDAS score calculation formula includes five disease activity variables with only partial overlap and measurement of acute phase reactant, preferentially C-reactive protein (CRP) measurement ($ASDAS_{CRP}$) or the alternative version with erythrocyte sedimentation rate (ESR) measurement ($ASDAS_{ESR}$). Additionally, ASAS developed ASDAS cut-offs for the disease status scores: < 1.3 for incactive disease; 1.3 < > 2.1 for moderate disease activity; 2.1 < > 3.5 for high disease activity and < 3.5 for very high disease activity (Machado et al. 2011). Furthermore, the cut-offs for improvement scores were developed in order to measure AS improvement: a change ≥ 1.1 for clinically important improvement and ≥ 2.0 for major improvement (Machado et al. 2011).

The need for a novel criteria to measure the improvement of AS in the placebo-controlled nonsteroidal anti-inflammatory drugs (NSAIDs) clinical trials led to the development of ASAS response criteria (ASAS 20, ASAS 5/6 and ASAS 40) (Table 1.4) and BASDAI 50. Regarding the BASDAI 50, a major clinical response is defined as a 50% improvement of the initial BASDAI score after 12 weeks of treatment with an active drug (Rudwaleit et al. 2004b).

Taken together, both Bath and ASAS disease assessment criteria are currently gold standards in the measurment of AS progression, while ASAS 20, ASAS 40 and ASAS 5/6 and BASDAI 50 response criteria are the most commonly used in AS clinical trials and recommended by the European Medicines Agency (EMA) and the European League Against Rheumatism (EULAR) (Braun, Van Den Berg, et al. 2012).

Table 1.3 Ankylosing Spondylitis Disease Activity Score (ASDAS)

Calculation of the ASDAS

ASDAS $_{CRP}$

0.12 x Total Back Pain + 0.06 x Duration of Morning Stiffness + 0.11 x Patient Global + 0.07 x Peripheral pain/ Swelling + 0.58xLn (CRP+1)

ASDAS $_{ESR}$

0.08 x Total Back Pain + 0.07 x Duration of Morning Stiffness + 0.11 x Patient Global + 0.09 x Peripheral pain/ Swelling + 0.29x√ESR

* CRP in mg/l and ESR in mm/h
** All patient assessment scores in a 10cm scale

Adapted from the http://www.asas-group.org and (Lukas et al., 2009)

Table 1.4 ASAS 20, ASAS 5/6 and ASAS 40 improvement criteria

ASAS 20

Improvement of ≥ 20% and ≥ 1 unit* in at least 3 out of 4 domains

Patient Global
Pain
Function
Inflammation**

No worsening of ≥ 20% and ≥ 1 unit in the remaining domain

ASAS 5/6

Improvement of ≥ 20% in at least 5 out of 6 domains

Patient Global
Pain
Function
Inflammation**
CRP
Spinal mobility

ASAS 40

Improvement of ≥ 40% and ≥ 2 units* in at least 3 out of 4 domains

Patient Global
Pain
Function
Inflammation**

No worsening in the remaining domain

* on a 0-10 scale
** mean of BASDAI questions 5 and 6

Adapted from the http://www.asas-group.org and (Anderson, Baron, Van Der Heijde, Felson, & Dougados, 2001; Brandt et al., 2004)

1.4 Treatment recommendations in the management of SpA

The correct and early diagnosis of SpA is necessary for the best possible choice of treatment. Importantly, based on our current knowledge about the pathophysiology of joint inflammation and efficacy of treatment in axSpA vs pSpA, it has been suggested that axial and peripheral joint inflammation may be driven by different mechanisms. Hence, the use of ASAS diagnosis criteria and distinguishing axSpA from pSpA can lead to more targeted and efficient treatment.

According to the current ASAS recommendations, NSAIDs are suggested as the first line drugs in axSpA, pSpA and ReA (Braun, Van Den Berg, et al. 2012). Additionally the use of single local injection of corticosteroids is recommended in pSpA and ReA with peripheral joint inflammation. In axSpA a four week trial treatment with two different types of NSAIDs (in total) are recommended before switching to second line treatment (Table 1.5). In axSpA patients with peripheral symptoms one local steroid injection or a short-term course of disease-modifying antirheumatic drugs (DMARDs), preferably sulfasalazine (SLZ), is recommended. Furthermore, NSAIDs, preferably selective COX-2 inhibitors (Coxibs), are proved as safe drugs for short-term therapy in patients with arthritis related with IBD. In PsA the Group for Research and Assessment of Psoriasis and Psoriatic Arthritis (GRAPPA), suggests using the best treatment strategy based on clinical features, which in case of peripheral and axial musculoskeletal manifestations are similar to recommendations for AS (Table 1.6).

Table 1.5 Management of Ankylosing spondylitis - ASAS recommendations

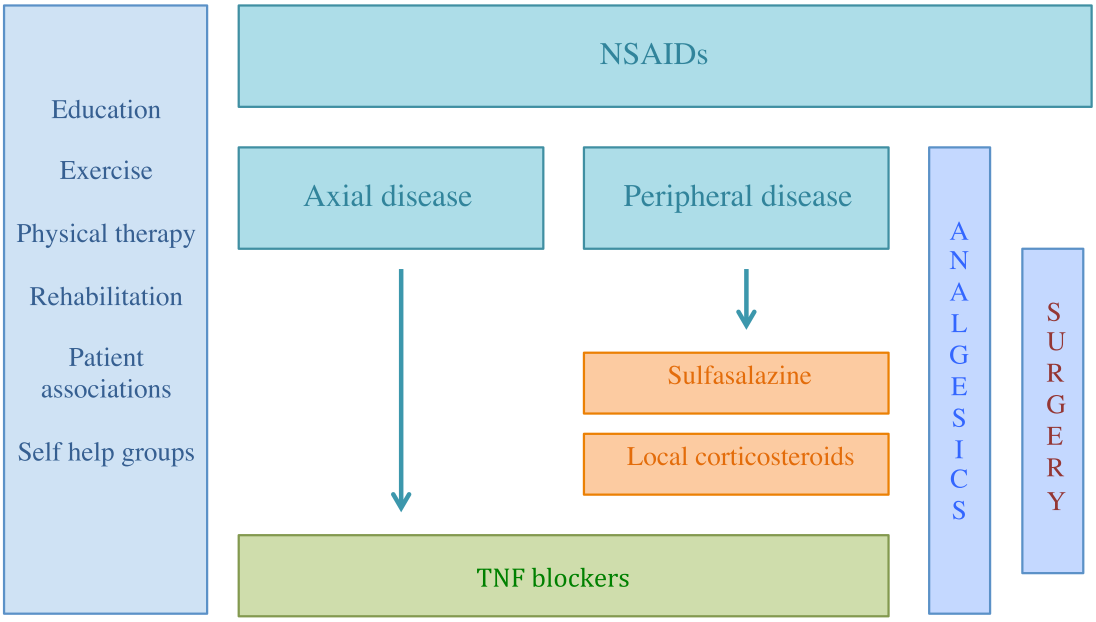

Adapted from http://www.asas-group.org and (Braun et al., 2012)

Table 1.6 Management of PsA - GRAPPA recommendations

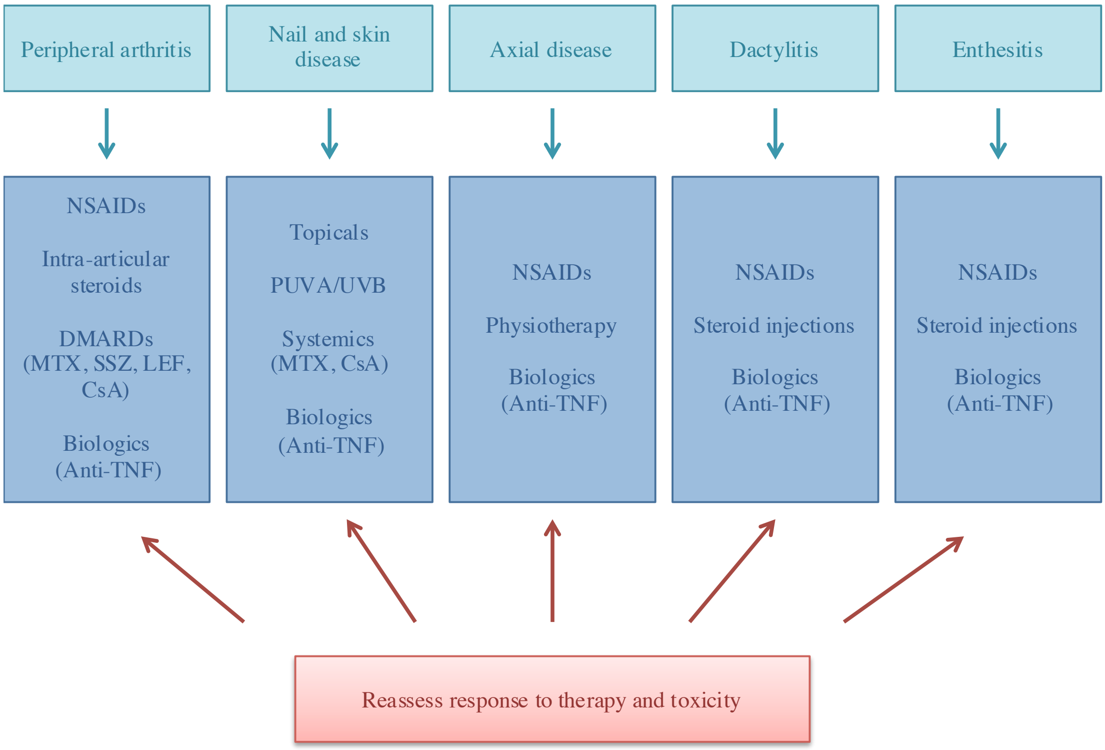

Adapted from http://www.asas-group.org and (Kavanaugh et al., 2006)

1.4.1 DMARDs

The most recent ASAS recommendations for the management of SpA (Braun, Van Den Berg, et al. 2012) suggested that DMARDs, despite a proven high efficacy in the treatment of rheumatoid arthritis (RA), are questionable in the management of axSpA and pSpA. Methotrexate (MTX) and sulfasalazine (SLZ) are amongst the most commonly used DMARDs in SpA treatment.

MTX can inhibit pro-inflammatory cytokine production by activated T cells, indirectly inhibit osteoclast formation and may indirectly contribute to the anti-angiogenesis effects (Wessels, Huizinga, and Guchelaar 2008). However, the recent Cochrane review concluded that the evidence of benefit from treatment is insufficient to support the use of MTX in SpA patients (Chen, Liu, and Lin 2006).

The potential mechanism of action of SLZ is an inhibition of nuclear factor kappa B (NF-κB) (Wahl et al. 1998). SLZ was shown to inhibit the synthesis of prostaglandins (PGs) and leukotrienes, modulate leukocyte function and proliferation, as well as colonic microbiome (Dahan and Amidon 2009; Desreumaux and Ghosh 2006; Hawkey, Boughton-Smith, and Whittle 1985; Liptay et al. 2002). Notably, two major active metabolites of SLZ, 5-aminosalicylic acid and sulfapyridine, are chemically attracted to collagen rich tissues, such as synovial and joint tissues (Gowdie 2011; Pfizer 2013). Hence, SLZ may act as an anti-inflammatory agent directly in inflamed joints. Results obtained from 11 independent clinical trials demonstrated reduced morning stiffness and ESR in AS patients treated with SLZ (Chen and Liu 2005). However there was no significant improvement in IBP, spinal mobility, physical function, enthesitis and global assessment, by both patient and doctor.

Thus, ASAS do not recommend DMARDs as a first line therapy for axSpA, yet SLZ can be considered as a second line drug for peripheral disease.

1.4.2 NSAIDs – a golden standard in the first line SpA treatment

ASAS recommends the use of NSAIDs as a first line treatment in axSpA (both advanced, radiographic axial inflammation and nr-axSpA) and pSpA. NSAIDs were shown to inhibit cyclooxygenases, the enzymes responsible for the synthesis of prostaglandins and leukotriens.

PGs can bind to nociceptors and consequently increase the perception of pain. Hence, blocking PG synthesis leads to the decrease in pain sensation. Furthermore, PGs play an important role in the bone and cartilage homeostasis (Brochhausen et al. 2006) and were shown to modulate both bone resorption (Dietrich, Goodson, and Raisz 1975) and new bone formation (Flanagan and Chambers 1992). Recent studies demonstrated that they can activate osteoblast formation in a concentration dependent manner (Blackwell, Raisz, and Pilbeam 2010). Moreover, the binding of prostaglandin E_2 (PGE_2) to its receptor mediates new bone formation and the generation of syndesmophytes (Aguirre et al. 2007). Thus, different PGs present locally at distinct sites of axial or peripheral joint may drive in parallel bone resorption and new bone formation. Interestingly, recent GWAS studies discovered the association between prostaglandin E receptor 4

(PTGER4) and AS. Taken together, these findings suggest the importance of PGs in joint pathology and may explain the efficacy of NSAIDs at certain stages of the disease. Selective cyclooxygenase-2 (COX-2) inhibitors (coxibs), such as celecoxib, are commonly used in SpA treatment. Yet, both selective and non-selective coxibs were shown to have similar efficiency in SpA treatment (Barkhuizen et al. 2006; Dougados et al. 1999; Sieper et al. 2008; van der Heijde et al. 2005a). Treatment with NSAIDs can significantly improve lower back pain in 60% of AS patients (Amor et al. 1995; Van Der Heijde et al. 2005; Sieper et al. 2008) compared to 15% in patients with mechanical back pain (Amor et al. 1995). Importantly, several studies demonstrated inhibition of radiographic progression in axSpA patients post NSAID treatment and showed positive outcome in patients with nr-axSpA in a course of two years (Poddubnyy and Sieper 2012; Poddubnyy et al. 2011; Wanders et al. 2005). Thus, SpA patients with axial skeleton manifestations can benefit from fast symptomatic effectiveness of NSAIDs and their disease-modifying abilities.

However, high gastrointestinal toxicity of coxibs and their capacity to increase cardiovascular diseases are two major limiting factors. Therefore, ASAS recommends detailed assessment of gastrointestinal and cardiovascular factors before choosing the treatment regimen with NSAIDs. Furthermore, the use of gastroprotective agents is recommended in combination with non-selective COX inhibitors in order to increase the safety of treatment. Less toxic, selective COX-2 inhibitors can be used alone in patients with moderate gastrointestinal risk. However, in patients with a high cardiovascular and/or gastrointestinal risk alternative therapies are recommended.

1.4.3 Non-pharmacological intervention in SpA treatment

Regarding the most recent ASAS/EULAR update on the management of SpA, non-pharmacological treatment is as important as NSAIDs in first line treatment (Braun, Van Den Berg, et al. 2012; Dagfinrud and Hagen 2001; Passalent 2011). It has been demonstrated that exercise, particularly group physiotherapy, correlated with an improvement in spinal mobility, function, respiratory symptoms and decreased back pain and disease activity. Moreover, patients suffered from less fatigue, less depression and a general quality of life was improved with exercise (Passalent 2011).

1.4.4 Tumour Necrosis Factor α (TNFα) inhibitors – a second line treatment

SpA patients who failed a first line treatment with NSAIDs are classified for a second line treatment. The ASAS recommendations for the use of TNFα antagonists are summarized in Table 1.7.

TNFα along with interleukin 6 (IL-6), interleukin 1 (IL-1), interleukin 8 (IL-8) and granulocyte macrophage colony stimulating factor (GM-CSF) were the first pro-inflammatory cytokines identified in RA synovial fluids and tissues (Feldmann, Brennan, and Maini 1996). Feldmann *et al*. hypothesized that TNFα, as one of the fast-release cytokines, may be a key upstream regulator of the other pro-inflammatory cytokines found in the synovial fluid and tissue from RA patients (Brennan et al. 1989). Notably, results from their study demonstrated that the addition of a neutralizing, monoclonal anti-TNFα antibody to a synovial cell culture significantly decreased IL-1 levels. Later studies confirmed an inhibitory effect of anti-TNFα treatment on the production of GM-CSF (Haworth et al. 1991) and IL-6 (Feldmann et al. 1996). Subsequently, TNFα antagonists were introduced to clinical trials for RA treatment in the early 90s.

Despite the proven high effectiveness of TNFα inhibitors in RA treatment, the first two clinical trials using Infliximab, a monoclonal anti-TNFα antibody, in AS patients were performed ten years later (Van den Bosch et al. 2000; Brandt et al. 2000). To date four TNFα inhibitors (Infliximab, Etanerecept, Adalimumab and Golimumab) are approved for SpA treatment, all of which demonstrated high efficacy in axSpA patients who did not respond to a first line treatment with NSAIDs (Davis et al., 2005; Inman et al., 2008; Lambert et al., 2007; Désirée Van Der Heijde et al., 2006; Désirée Van Der Heijde, Dijkmans, et al., 2005). Yet, several two-year follow up post-treatment reports suggested no substantial inhibition of radiographic progression in patients treated with anti-TNFα compared with non-treated patients (Braun et al. 2013; Braun, Baraliakos, et al. 2012; Désirée van der Heijde et al. 2009; Van Der Heijde et al. 2008; Heijde et al. 2008). A recent study demonstrated that combination therapy with anti-TNFα and NSAIDs is more successful in both clinical and radiographic post treatment outcomes (Sieper et al. 2014). Yet, up to date ASAS recommendations suggest using combined treatment only in patients with high risk factors for developing radiographic progression and with clinical indications for NSAIDs treatment (Braun, Van Den Berg, et al. 2012).

Notably, a high efficacy of anti-TNFα inhibitors observed in nr-axSpA patients with active disease (high CRP levels and/or inflammation visible on MRI) and the ones who failed first line treatment (Barkham et al. 2009; Burness and Deeks 2012; Sieper et al. 2012; Song et al. 2013) led to the further extension of official labels for the use of

Adalimumab (a monoclonal anti-TNFα antibody, know as Humira). However, as yet its use is limited to nr-axSpA patients under the given circumstances (Committee for Medicinal Products for Human Use 2012).

Importantly, about 40% of SpA patients do not respond to the anti-TNFα treatment due to drug inefficacy and/or intolerance (Paramarta and Baeten 2013). Young age, signs of active inflammation on the MRI, elevated CRP/ESR levels, short disease duration, HLA-B27 status and a low level of functional disability are amongst positive prediction factors of the anti-TNFα therapy in axSpA patients (Martin Rudwaleit et al. 2009; Rudwaleit et al. 2004a; Vastesaeger et al. 2011). It has been demonstrated that RA (Bartelds et al. 2010; van der Laken et al. 2007, 2008) and AS (de Vries et al. 2007) non-responders, and patients who lost their response to TNFα inhibitors after long periods of treatment, can produce elevated levels of anti-Adalimumab or anti-Infliximab antibodies and antibody complexes (van Schouwenburg et al. 2012). Hence, it has been proposed that TNFα inhibitors may be blocked by these antibodies and/or eliminated from circulation and tissues in non-responders.

Another important disadvantage of TNFα inhibitors is the lack of long-lasting remission after the interruption of treatment. In consequence nearly 100% of axSpA patients relapse after a couple of months from the discontinuation of the drug (Baraliakos et al. 2005; Brandt et al. 2003, 2005; Breban et al. 2002; Heldmann et al. 2011; Paramarta, Heijda, and Baeten 2013; Song et al. 2012). Thus, due to the necessity for a lifelong treatment in SpA patients further adjustments in the frequency and doses of administrated drugs could be beneficial.

Table 1.7 Anti-TNFα treatment - ASAS recommendations

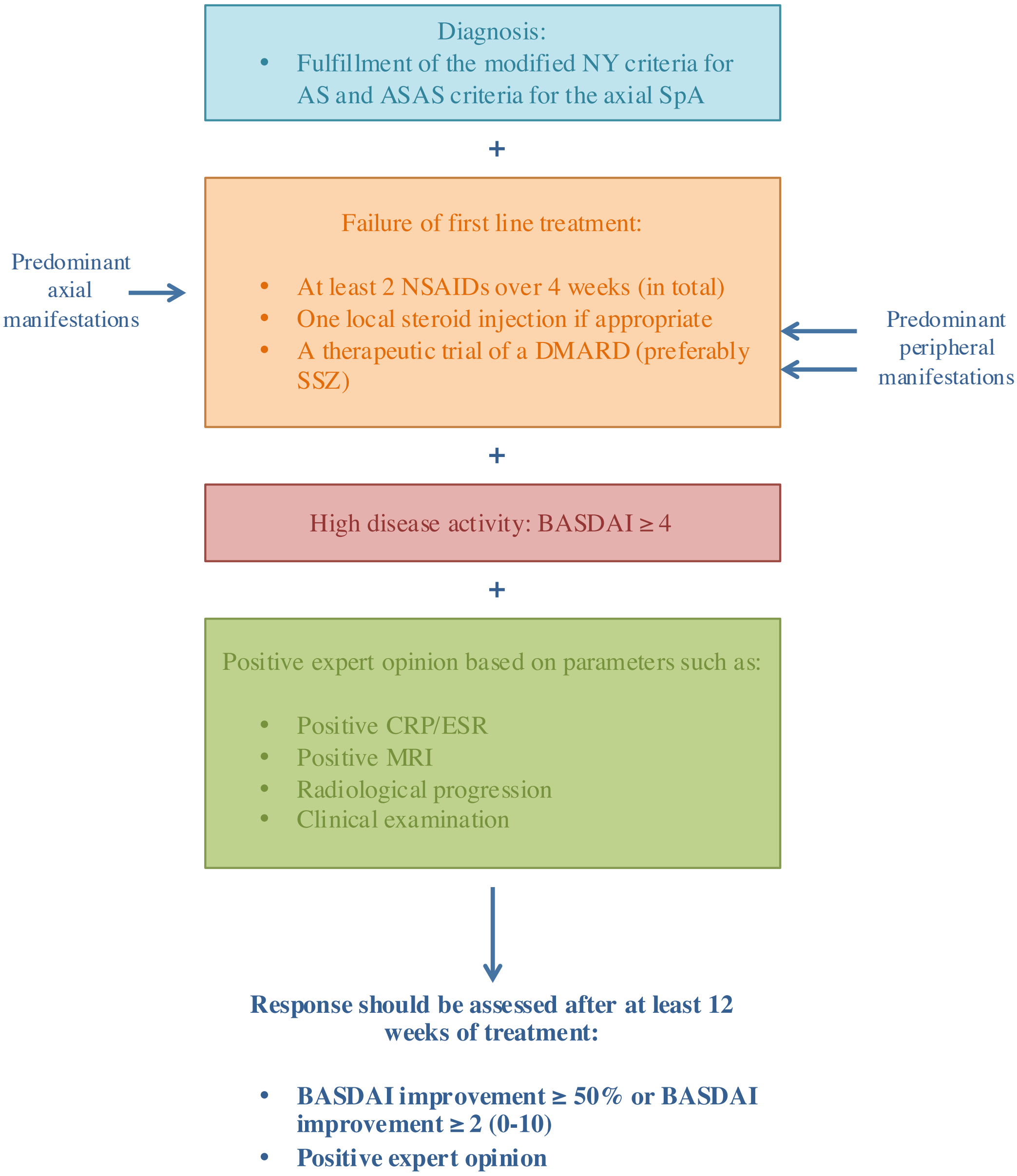

Adapted from http://www.asas-group.org and (van der Heijde et al., 2011)

Finally, although TNFα antagonists were shown to improve bone destruction within one year after treatment in PsA (D. Van Der Heijde et al., 2007) and AS patients (Gengenbacher, Sebald, Villiger, Hofstetter, & Seitz, 2008), their effectiveness in the treatment of new bone formation is questionable (Braun et al. 2013; Heijde et al. 2008; Poddubnyy and Sieper 2012). Thus, it has been hypothesized that new bone formation may not be dependent on TNFα and could be driven by molecular mechanisms different from osteoproliferation.

1.4.5 Development of novel treatments for SpA

The emerging knowledge about genetic factors and molecular mechanisms involved in SpA pathogenesis has pushed forward the development of potential novel treatments.

B cell-targeted therapies with Rituximab (anti-CD20 antibody) (Nocturne et al. 2009; Wendling et al. 2012) and T cell synapse-targeted therapies with Abatacept (antibody blocking CD80/86:CD28 interactions) (Song et al. 2011) failed to bring positive outcomes in SpA patients (Braun et al. 2015; Song and Poddubnyy 2011). Furthermore, inhibition of TNFα 'downstream' cytokines (IL-1 and IL-6) showed low or no efficacy, with a small difference between AS and PsA patients (Braun et al. 2015; Song and Poddubnyy 2011).

However, targeting the interleukin-23/interleukin-17 (IL-23/IL-17) pathway in SpA patients gave promising results. Ustekinumab is a human monoclonal antibody against a subunit shared between IL-23 and interleukin-12 (IL-12) (p40). Ustekinumab showed efficacy in clinical trials and was recently approved for treatment in PsA (McInnes et al.

2013; Toussirot et al. 2013) and Crohn's disease (Sandborn et al. 2008, 2012). However, only 65% of AS patients with active disease responded to Ustekinumab in the first proof-of-concept clinical trial (Poddubnyy et al. 2014). Three other drugs targeting IL-23 are in ongoing clinical trials in SpA patients, yet no data is available from these studies.

To date none of the anti-IL-17 biologics have been approved for treatment. However, Secukinumab, a fully human anti-IL-17A antibody, is currently in several ongoing clinical trials in psoriasis, PsA, Crohn's disease, Behçet's disease and AS. Recent reports have suggested high efficiency of Secukinumab in psoriasis, but lower effectiveness in PsA (Langley et al. 2014; McInnes et al. 2014; Rich et al. 2012). Furthermore, significant clinical and biological efficacy was observed in 60% of AS patients after two infusions of Secukinumab in a recent small cohort study (Baeten et al. 2013). Notably, the treatment outcome was measured only 6 weeks from the first injection of the drug. Yet, in the latter clinical trial the higher susceptibility of bacterial infections post-treatment raised questions about the safety of Secukinumab. Additionally, two other agents, Brodalumab (anti-IL-17 receptor antibody) and Ixekizumab (a fully human anti-IL-17A antibody), are currently in the phase II clinical trials for psoriasis and PsA. Both Brodalumab and Ixekizumab significantly improved skin plague treatment in psoriatic patients (K. A. Papp et al. 2012; Spuls and Hooft 2012). Furthermore, a recent report from a clinical trial with Brodalumab has demonstrated a significant increase in the response rate in PsA patients (Mease et al. 2014). These findings are promising, although more clinical trials with a larger number of participants need to be performed to enable the approval of anti-IL-17 therapeutics as a safe and effective drugs for psoriasis, PsA and AS treatment.

Another potential alternative to anti-TNFα agents are small molecule inhibitors targeting proteins involved in signaling pathways implicated in activation of pro-inflammatory responses. Phosphodiesterase 4 (PDE4) inhibitors, lead to the increase in intracellular cyclic adenosine monophosphate (cAMP) and consequently have an antagonistic effect on the production of pro-inflammatory factors. Apremilast, a specific (PDE4) inhibitor, have been effective in the treatment of PsA (Schett et al. 2012; Strand et al. 2013) and psoriasis (Gottlieb et al. 2008; K. Papp et al. 2012; Papp et al. 2013). However, in the small pilot study in AS only 35% of patients achieved ASAS20 responses (Pathan et al. 2012). Additionally, two novel inhibitors of Janus kinase (JAK)/Signal Transducer and Activator of Transcription (STAT) signaling pathway have been recently used in clinical trials for the treatment of RA, PsA, psoriasis and IBD. High efficacy of Tofacitinib (TOF), a selective JAK1 and JAK3 inhibitor, has been demonstrated in several clinical trials in RA (Fleischmann et al. 2012; Van Der Heijde et al. 2013; Lee et al. 2014; Tanaka et al. 2011; van Vollenhoven et al. 2012) and psoriasis (Hsu and Armstrong 2014; Mamolo et al. 2014; Ports et al. 2013; Tan et al. 2013). Yet, no data is available for PsA and AS. Moreover, Baricitinib and Ruoxinimab, a specific JAK1 and JAK2 and other small JAK/STAT inhibitors are currently in development.

In summary, increasing the number of head to head trials with traditionally used drugs, the advances in novel treatment development, and our knowledge about the disease pathology bring a promising future for a novel, more targeted and efficient therapy for SpA.

1.5 Immunopathogenesis of SpA and AS

SpA is a highly heterogeneous group of chronic inflammatory diseases. Although it has been demonstrated that the IL-23/IL-17 axis play a key role in the pathogenesis of SpA, there is increasing evidence that the different clinical manifestations occurring in each of the SpA subgroups can be driven by distinct molecular mechanisms. To date studies demonstrate that the complex combination of genetic and environmental factors can predispose to the development of a particular form of SpA.

1.5.1 HLA-B27

The association of HLA-B27 with AS was discovered over four decades ago. Although there is still debate in how HLA-B27 can contribute to disease pathogenesis, HLA-B27 is confirmed by a number of studies as one of the strongest genetic factors associated with SpA. Importantly, HLA-B27 is present in ~90% of AS patients and in 76%-25% of patients with other forms of SpA. Our current knowledge suggests that HLA-B27 could be a key player in both the activation of pro-inflammatory IL-23/IL-17 pathway and the induction of bone pathogenesis in the IL-23/IL-17-independent manner. The role of HLA-B27 in health and disease and potential pathogenic mechanisms by which B27 molecules may drive SpA pathogenesis are discussed in the next chapter (see Chapter 1.6).

1.5.2 IL-23/IL-17 pathway

Based on genetic and clinical studies it has been suggested that the IL-23/IL-17 pathway is a key player in SpA pathogenesis. IL-23 drives the differentiation and proliferation of pathologic T-helper 17 (Th17) cells that produce pro-inflammatory cytokines (IL-17, TNFα, IL-6 and IL-8) (Iwakura and Ishigame 2006; McKenzie, Kastelein, and Cua 2006). Importantly, GWAS studies have identified IL-23R as one of the strongest genetic associations with SpA and IBD, after HLA-B27 (Chen et al. 2012; Dong et al. 2013; Duerr et al. 2006; Eirís et al. 2014; Jadon et al. 2013; Pimentel-Santos et al. 2009). Moreover, macrophages (Mφ) and monocyte-derived dendritic cells (moDCs) obtained from AS patient blood produced higher amounts of IL-23 upon stimulation compared with similar cells from RA patients (Prevosto, Goodall, & Gaston, 2012; Zeng, Lindstrom, & Smith, 2011). Additionally, elevated levels of both IL-23 and IL-17 have been observed in sera from AS patients (Mei et al. 2011) and in supernatants from *in vitro* cultured peripheral blood mononuclear cell (PBMC) (Wang et al. 2009). Furthermore, elevated numbers of circulating Th17 cells have been found in blood isolated from AS patients (Shen, Goodall, and Hill Gaston 2009). Notably, Bowness group have previously demonstrated increased number of Th17 cells expressing the killer cell immunoglobulin-like receptor 3DL2 (KIR3DL2) in the blood of AS patients. These $CD4^+$ T cells with KIR3DL2 produce more IL-17 in response to stimulation with B27-expressing cell lines (Bowness and Ridley et al. 2011). Interestingly, Bautista *et al*. identified decreased numbers of circulating Th17 and Th1 cells in B27+ve patients with early nr-axSpA compared with B27-ve nr-axSpA controls (Bautista-caro et al. 2013). Moreover, there is increasing evidence that joint inflammation in SpA is dependent on the IL-23/IL-17 axis. However, it has been hypothesized that axial and peripheral joint manifestations may be driven by different molecular mechanisms (Paramarta and Baeten 2013). Importantly, restricted availability of axial and peripheral joint tissue samples is a major obstacle to study this hypothesis. As yet, only a single study has investigated pathogenic changes in facet joints obtained from AS patients with severe ankylosis (Appel et al. 2011). Appel *et al.* demonstrated increased numbers of infiltrating IL-17^{+}/CD15^{+} neutrophils in AS patient facet joints compared with control OA samples (Appel et al. 2011). On the other hand, Noordenbos *et al.* have recently suggested that mast cells are the main source of IL-17 in inflamed synovial tissue from the peripheral joints of SpA patients (Noordenbos et al. 2012). Notably, these findings indicate that the source of IL-17 may be different in axial and peripheral joints. Hence distinct molecular mechanisms may be responsible for driving the immune responses at distinct sites. Furthermore, recent data from an animal model (Sherlock et al. 2012) further supported the importance of IL-23/IL-17 pathway and showed the presence of a novel IL-23R^{+} entheseal resident T cell population, which can drive enthesitis in response to local production of IL-23.

Taken together, these findings suggest that the IL-23/IL-17 pro-inflammatory pathway plays a key role in SpA pathogenesis.

1.5.3 Wnt and BMP signaling pathways and joint pathology

There is increasing evidence that bone destruction and new bone formation processes are heterogeneous. Findings from animal models implicate genes involved in the Wingless-type like (Wnt) and the bone morphogenic protein (BMP) signaling pathways with TNFα-independent new bone and cartilage formation (Braem and Lories 2012;

Lories, Derese, and Luyten 2008; Lories, Luyten, and de Vlam 2009; Lories and Schett 2012). Moreover, GWAS studies have recently implicated two risk loci in Han Chinese AS patients in the *HAPLNI-EDIL3* and *ANO6* genes, which are also thought to be involved in new bone formation (Lin et al. 2012). Furthermore, several genetic studies have reported association of the anthrax toxin receptor 2 (*ANTXR2)* gene with AS (Bang et al. 2011; Guo et al. 2012). Notably, ANTXR2 can bind to a low-density lipoprotein receptor-related protein 6 (LRP6), which is an important component of the Wnt signaling pathway (Cryan and Rogers 2011; Deuquet et al. 2011).

In the limited number of clinical studies investigating the molecular mechanisms of pathogenic new bone formation in SpA patients, it has been demonstrated that sclerostin (SOST), a Wnt/β-catenin pathway antagonist, is absent in tissues from AS patient joints compared with RA and OA patients (Appel et al. 2009). Furthermore, continuous inflammation in AS patients receiving anti-TNFα treatment is correlated with low SOST serum levels (Saad et al., 2012). Additionally, it has been recently demonstrated that sera from AS and AS IBD patients have elevated levels of novel antibodies against SOST and noggin protein (NOG) (Tsui et al. 2013). NOG binds to the bone morphogenic proteins (BMP) and can negatively control the formation of new bone controlled via BMP pathway (Devlin et al. 2003; Lories et al. 2006; Wan et al. 2007; Wu et al. 2003). Hence, the presence of autoantibodies against SOST and NOG may explain the low detection levels of these molecules in patient sera. Moreover the binding of these antibodies may affect the function of SOST and NOG. Thus, these findings suggest that decreased levels of SOST and NOG could lead to the induction of Wnt/β-catenin and BMP pathways and drive uncontrolled osteoproliferation.

In conclusion, more studies need to be performed in order to support these novel findings and provide a better understanding of the immunology and pathology of axial and peripheral joint inflammation in SpA.

1.6 HLA-B27 as a MHC class I molecule

1.6.1 Structure of MHC class I and HLA-B27

The Human Leukocyte Antigen (HLA) B27 belongs to the highly polymorphic Major Histocompatibility Complex (MHC) class I family of proteins. The majority of nucleated cell types express cell surface MHCI. There are six isotypes of MHCI: highly polymorphic HLA-A, -B and -C; oligomorphic HLA-E and HLA-G; and monomorphic HLA-F isotype (Khan 2013). Furthermore, HLA class I isotypes have various number of subtypes called allotypes. Each different HLA allotype confers the ability to bind different peptides. HLA-B is known for the highest number of different allotypes. So far 105 subtypes of HLA-B27 have been identified, starting from HLA-B*27:01 to HLA-B*27:106. Additionally each subtype is associated with different genetic variability. For instance HLA-B*27:02 and HLA-B*27:90 have 2 alleles, HLA-B*27:04 and HLA-B*27:07 4 alleles, while there are 21 different alleles of HLA-B*27:05 (Khan 2013). Canonical MHCI forms a complex of heavy chain (HC) non-covalently associated with β2-microglobulin (β2-m) and peptide (usually 8-11 amino acids). The α1 and α2 domains of FHC form the peptide binding groove, while the α3 domain docks FHC in the cell membrane. The peptide binding groove consists of 8 antiparallel beta-strands surrounded by alpha-helices (Madden 1995). The B pocket in the HLA-B27 peptide binding groove interacts with an amino acid (AA) at position 2 (P2) of the bound peptide. A unique combination of AA residues (His9, Thr24, Glu45 and Cys67) and adjacent residues (Ala69, Lys70 and Ala71) forms a deep negatively charged binding pocket of HLA-B27. As suggested by predictions based on the HLA-B27 crystal structure and further confirmed by sequencing of eluted peptides, the HLA-B27 B pocket preferentially binds peptides with Arg at P2 (Feltkamp, Khan, and Lopez de Castro 1996; Madden 1995).

1.6.2 Function of MHC class I molecules in health and disease

MHCI antigen presentation

The main characterized role of MHCI is to present cellular peptides to cytotoxic $CD8^+$ T cells (CTLs) via the endogenous presentation pathway. Thus, MHCI molecules are key players in immune defence against intracellular pathogens and tumour cells, as well as in the induction of self-tolerance. $CD8^+$ T cells develop tolerance to self-peptides derived from proteins produced by healthy cells. On the other hand, peptides derived from tumorogenic cells, viruses and other intracellular pathogens, so called "danger peptides", can activate CTLs and induce adaptive immune responses. Notably, the interaction between CTLs, primed by "danger peptides" presented in the MHCI context, and specialized antigen presenting cells (APCs), such as DCs, is crucial for the activation of the CTL effector function. Activated effector CTLs can directly kill infected or tumour cells by release of cytotoxic granules, with perforins and granzymes, or alternatively by activation of the Fas-Fas ligand (FasL) cell death cytolytic pathway. Furthermore, effector CTLs can indirectly eliminate dangerous cells by the production of pro-inflammatory cytokines and factors (Andersen et al. 2006). In addition to the conventional MHCI presentation pathway, cross presentation of extracellularly derived self and foreign peptides by MHCI plays an important role in the induction of allogeneic responses and immune tolerance (Duan and Srivastava 2012; Joffre et al. 2012; Merzougui et al. 2011; Spel et al. 2013). Originally MHCI cross presentation was considered as a characteristic feature of DCs, however several studies have reported cross presentation by other APCs, such as macrophages, B cells and osteoclasts (Brode and MacAry 2004; Heit et al. 2004; Kiesel, Buchwald, and Aurora 2009; Mariño et al. 2012). Hence, APCs presenting self and foreign peptides in both a MHCI and MHCII-dependent manner can communicate with diverse immune cells, such as $CD8^{+}$ T cells, natural killer cells (NK), natural killer T cells (NKT) and $CD4^{+}$ T cells. This specific feature of APCs allows them to bridge adaptive and innate immune responses and consequently eliminate dangerous cells and pathogens more efficiently. Furthermore, MHCI cross-presentation of self-derived peptides plays a key role in the induction of cross-tolerance by promoting the deletion of autoreactive CTLs (Dresch et al. 2012; Heath and Carbone 2001; Joffre et al. 2012). Recent studies demonstrated that plasmacytoid DCs (pDCs) cross-presenting self-DNA peptide complexes released by neutrophils, are involved in the pathogenesis of systemic lupus erythematosus (SLE) (Lande et al. 2011) and diabetes (Diana et al. 2013). On the other hand, selective depletion of pDCs in the collagen induced arthritis (CIA) animal model of RA resulted in increased T and B cell autoimmune responses (Jongbloed et al. 2009). Thus, abnormalities in the endogenous and cross-presentation MHCI pathways can lead to the induction of both autoimmune and autoinflammatory responses. Hence, HLA-B27 presentation of self and/or foreign peptides may play a role in the SpA pathogenesis.

MHCI binding to Immunoglobulin (Ig)-like receptors

Another role of MHCI is binding to immunoglobulin-like (Ig-like) receptor family, consisting of killer Ig-like receptors (KIRs) and leukocyte Ig-like receptors (LILRs). The highly polymorphic KIRs are mainly expressed on NK cells, although they are also found on subsets of effector αβ $CD4^+$ and $CD8^+$ and γδ T cells (Parham 2005). On the other hand, LILRs are more commonly distributed and can be expressed on NK cells, T and B cells, myeloid cells and mast cells (Martin et al. 2002). Notably, KIRs bind to specific HLA class I alleles (Table 1.8), while LILRs can associate with a wider variety of different HLA class I molecules (Campbell and Purdy 2011; Held and Mariuzza 2008).

KIRs are formed from 2 or 3 extracellular Ig-like domains (2D or 3D) and 1-5 long (L) or short (S) cytoplasmic domain(s), hence the nomenclature e.g. KIR2DS1, KIR3DL2. "Inhibitory" KIRs, with a long cytoplasmic tail (DL), incorporate 1 or 2 immunoreceptor tyrosine-based inhibitory motifs (ITIMs) (Figure 1.1) (McVicar & Burshtyn, 2001). Upon binding to KIR ligand phosphorylated ITIMs recruit tyrosine phosphatases and modulate immune function (Ravetch & Lanier, 2000). "Stimulatory" KIRs, with a short cytoplasmic tail (DS), incorporate charged amino acids which interact with a transmembrane signaling adaptor protein (DAP12) fitted with immunoreceptor tyrosine-based activation motifs (ITAM) activated upon phosphorylation by Syk/ZAP-7 (Figure 1.1) (Humphrey, Lanier, and Nakamura 2005). However, there is increasing evidence for activating functions of ITIMs, as well as inhibitory role of ITAMs (Barrow and Trowsdale 2006).

Table 1.8 Specificity of inhibitory and activating KIRs

Receptor	Ligand
KIR2DL1	HLA-C, Group 2: C*02, C*04, C*05, C*06
KIR2DL2	HLA-C Group1: C*01, C*03, C*07, C*08; Group 2: C*0202, C*0501; HLA-B: B*4601, B*7301
KIR2DL3	HLA-C Group1: C*01, C*03, C*07, C*08; Group 2: C*0202, C*0501; HLA-B: B*4601, B*7301 (weaker affinity than KIRDL2)
KIR3DL1	Bw4 epitopes among HLA-B alleles: B*08, B*27, B*57; some HLA-A: A*24
KIR3DL2	Certain HLA-A alleles: A*03, A*11
KIR2DL4	HLA-G
KIRDS1	HLA-C Group 2: C*02, C*04, C*05, C*06
KIR2DS2	HLA-C Group 1: C*01, C*03, C*07, C*08
KIR2DS3	HLA-C Group 1: C*01, C*03, C*07, C*08
KIR2DS4	HLA-C some of both Group 1 and 2: C*0501, C*1601, C*0202; HLA-A: A*1102
KIR3DS1	Possibly HLA-Bw4

Red – inhibitory receptors
Green – activating receptors

Adapted from (Campbell & Purdy, 2011)

Similar to KIRs, LILRs can mediate inhibitory and activating signals (Colonna et al. 1999). The "inhibitory" LILRs contain 2 or 4 homologous extracellular C-2 type Ig-superfamily (SF) domains and a long cytoplasmic tail containing ITIMs. The "activating" LILRs consist of 4 extracellular domains, but lack the cytoplasmic tail. Cell activation and signal transduction via the activating receptors is mediated by association with the Fc receptor gamma chain (FcγR)(Colonna et al. 1999).

Interestingly, LILRs can interact with MHCI molecules in both a classical (*trans*) conformation or *cis* conformation (Held and Mariuzza 2008). *Trans* interactions occur when Ig-like receptor and MHCI molecule are present at the surface of different cells. Whereas, *cis* conformation occurs when receptor and MHCI are interacting at the surface of the same cell. Although, it has been suggested that *cis* and *trans* interactions between MHCI and Ig-like receptors may be important in the control of immunity, as yet the role and function of these interactions remain poorly understood (Held and Mariuzza 2008; Li et al. 2013).

Unusual interactions between HLA-B27 and KIRs and/or LILRs could play a role in driving immune responses in SpA.

Figure 1.1 The structure of inhibitory and activating KIRs

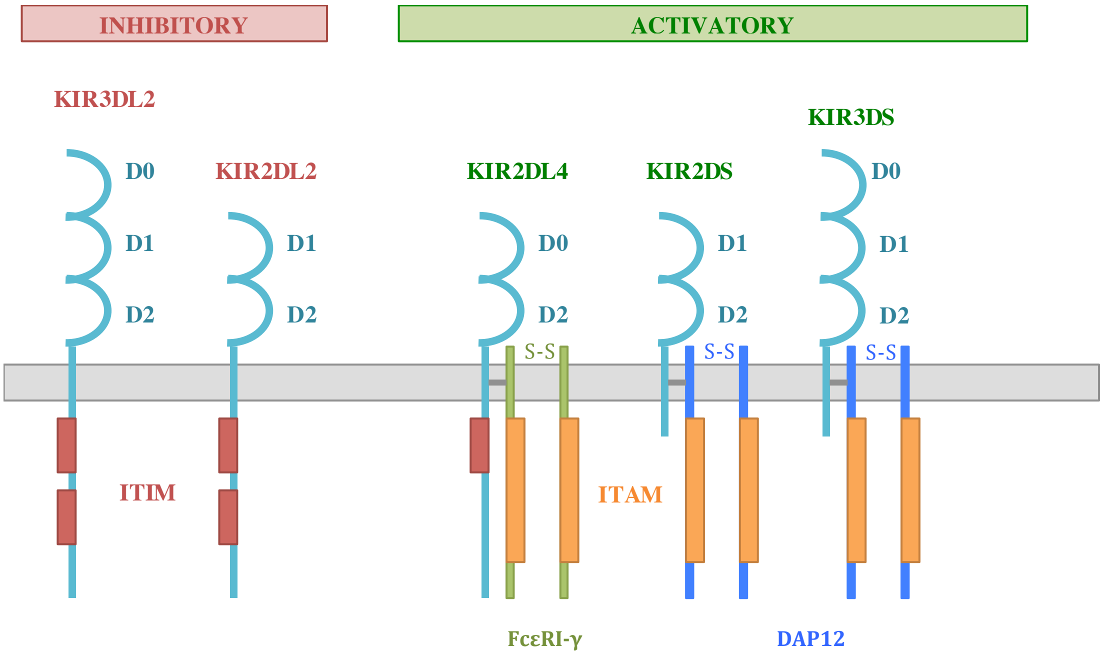

Adapted from (Campbell & Purdy, 2011)

MHCI antigen processing, loading and presentation

In the conventional MHCI presentation pathway endogenous peptides are loaded onto MHCI molecules in the endoplasmic reticulum (ER) using a specialized peptide loading complex (PLC) machinery (Dong et al. 2009; Hulpke and Tampé 2013; Parcej and Tampé 2010). Newly synthesized MHCI free heavy chains (FHCs) in the ER first associate with the ER chaperone immunoglobulin binding protein (BiP). BiP binding facilitates the proper folding and post-translational modifications of FHCs. A properly folded FHC associates with calnexin (CNX), a chaperone located in the ER membrane, and subsequently assembles with β2 microglobulin (β2m). Upon binding to β2m CNX is replaced by the ER-soluble, lectin-like chaperone, calreticulin (CRT). Next, FHC/β2m/CRT complex is joined by the thiol-disulfide oxidoreductase (ERp57) and tapasin (TPN). The peptide loading complex is completed once this newly formed pentameric complex binds to the transporter associated with antigen processing (TAP). TAP consists of two transmembrane ER proteins, TAP1 and TAP2. In the final step, cellular peptides derived from the proteasome are transported via TAP into the ER lumen where they are loaded onto MHCI/β2m heterodimers (Hulpke and Tampé 2013).

The proteasome is a multi-subunit enzyme complex involved in cellular protein degradation in the cytosol. The length of peptides generated by the proteasome for transport into the ER lumen via TAP is between 3 and 33 AAs (Hulpke, Baldauf, and Tampe 2012). Some peptides entering the ER are ready to be loaded onto the MHCI molecules directly. However, the majority of peptides is too long and has to be processed by endoplasmic reticulum aminopeptidases (ERAPs) before association with MHCI. Humans express ERAP1 and ERAP2, whereas rodents lack the ERAP2 ortholog (Evnouchidou et al. 2014).

A diverse array of ER chaperones and proteins ensure the high quality of MHCI/β2m/peptide complexes reaching the cell surface. MHCI complexes are translocated from the ER to the ER-Golgi intermediate compartment (ERGIC) via the coat protein complex II (COPII), ER membrane vesicles. Subsequently, ERGIC vesicles fuse with the *cis*-Golgi membrane (Appenzeller-Herzog and Hauri 2006). Notably, both properly loaded and peptide-receptive forms of MHCI have been found in the ERGIC and *cis*-Golgi. Hence, the multistep trafficking system associated with the quality control of protein export (e.g. Rab, TPN and CRT) plays an important role in the prevention of presentation of low quality MHCI/peptide complexes at the cell surface. Several studies have suggested that peptide-receptive forms of class I can be recycled to the ER via coat protein complex I (COPI) vesicles (Appenzeller-Herzog and Hauri 2006; Garstka et al. 2007a; Wang et al. 2010). Rab proteins have been shown to play a key role in the retrograde transport from the ERGIC and *cis*-Golgi (Appenzeller-Herzog and Hauri 2006). Furthermore, it has been suggested that TPN and CRT can chaperone MHCI complexes in the ERGIC and *cis*-Golgi compartments and may thus play a role in the elimination of peptide-receptive MHCI complexes (Garstka et al. 2007b; Howe et al. 2009).

ER-associated degradation (ERAD) pathways are responsible for the elimination of the misfolded or defective (e.g. with site mutations) proteins (Bernasconi and Molinari 2011). These potentially dangerous and/or dysfunctional proteins are recognized by chaperones (e.g. CNX and CRT) and are targeted, ubiquitinated and translocated to the proteasome for degradation. Proteins that fail to be degraded accumulate in the ER and cytosol leading to the activation of ER stress and an unfolded protein response (UPR). Inositol-requiring kinase 1 (IRE1), pancreatic ER eIF2a kinase (PERK) and activating transcription factor 6 (ATF6) are the main sensors in the ER membrane for detecting misfolded protein (Cao and Kaufman 2012). High levels of unfolded and/or misfolded proteins accumulating in the ER luminal space activate these sensors and subsequently induce transcription factors: ATF6, activating transcription factor 4 (ATF4) and X-box binding protein 1 (XBP1). ATF6 can enhance the transcription of ER chaperones or proteins involved in ER biogenesis and inflammatory responses. XBP1 can additionally activate transcription of ERAD components. ATF4 besides induction of ER chaperone transcription can also drive amino acid synthesis, antioxidant responses, ER-Golgi trafficking and transcription of the CCAAT/enhancer-binding protein homologous protein (CHOP) (Cao and Kaufman 2012). However, if the induction of UPR and ER stress fails to resolve the accumulation of misfolded proteins, defective cells are eliminated via apoptosis. Notably, UPR and ER stress responses have been associated with number of neurodegenerative, neoplastic, metabolic and autoimmune responses, and have also been suggested to play a role in the HLA-B27-driven SpA pathogenesis.

1.7 The unusual nature of HLA-B27

HLA-B27 due to its well known strong association with SpA is one of the best-studied MHCI molecules. Early studies investigating the nature of HLA-B27 molecules demonstrated the presence of a characteristic unpaired cysteine at position 67 (Cys 67), located in the $\alpha 2$ domain above peptide binding groove (MacLean et al. 1992). Yet, Cys67 is also found in several other HLA-B alleles (B14, B15, B38, B39, B73) three of which B14, B38 and B39 have been associated with the AS independently (Díaz-Peña, López-Vázquez, and López-Larrea 2012). Although, Cys67 does not significantly influence the structure of B27 FHC it has been suggested to play an important role in FHC dimerization (Allen et al. 1999).

Slow folding kinetics and the predisposition to misfold are another unusual feature of HLA-B27 (Colbert et al. 2009; Mear et al. 1999; Santos, Powis, and Arosa 2004). Excessive accumulation of misfolded forms of HLA-B27 can lead to the activation of ER stress and UPR (Smith et al. 2008; Turner et al. 2005; Turner, Delay, Bai, Klenk, and R. A. Colbert 2007). Notably, Mear *et al.* demonstrated that replacement of the crucial AAs characteristic for the HLA-B27 B pocket in the peptide binding groove with motifs specific for the HLA-A2 (HLA-B27. A2B), resulted in more efficient folding and transport of HLA-B27 to the cell surface (Mear et al. 1999). Furthermore, Colbert *et al.* have shown that newly synthesized HLA-B27 FHCs can bind to BiP for a prolonged time compared with other MHCI, suggesting that B27 misfolding in the ER occurs prior to association with β2m (Colbert et al. 2009).

Importantly, Allen *et al.* first demonstrated the presence of HLA-B27 FHC homodimers, both intracellularly and at the cell surface, and proposed that formation and accumulation of these misfolded, non-classical forms of HLA-B27 (NC-B27) results from slow folding kinetics (Allen et al. 1999). Further studies, suggested that cell surface B27 homodimers ($B27_2$) originated from the properly folded cell surface MHCI molecules, rather than NC-B27 accumulating in the intracellular compartments (Bird et al. 2003). Notably, cell surface NC-B27 molecules bind strongly to KIR3DL2 and LILRB2 (Cauli et al. 2013; Kollnberger et al. 2002, 2007; Wong-Baeza et al. 2013). Subsequent investigations demonstrated the importance of conserved Cys101 and Cys164 for formation of FHC homodimers (Lenart et al. 2012).

Efficient peptide loading and trafficking of properly folded MHCI molecules to the cell surface is controlled by TPN and TAP. The degree of dependency on these two proteins varies amongst different HLA class I alleles. For instance HLA-B*4402 and HLA-B8 are strongly dependent on TPN for efficient peptide loading in the ER (Hermann et al. 2013; Peh et al. 1998; Rizvi et al. 2014; Zernich et al. 2004). Therefore, deletion of functional TPN in cell lines expressing HLA-B44.02 or B8 leads to very low expression or complete absence of these molecules at the cell surface. On the other hand, a number of HLA class I alleles, such as HLA-B*2705 and HLA-B*4405, are less dependent on TPN and TAP (Zernich et al. 2004). Notably, cell lines carrying these alleles preserve normal expression of cell surface MHCI molecules even in the absence of functional TPN or TAP. Hence, TPN independence could promote the binding of lower affinity peptides and contribute to HLA-B27 misfolding, both intracellularly and at the cell surface.

HLA-B27 molecules were shown to bind to a wider repertoire of peptides, including longer and lower affinity peptides compared with other MHCI alleles (Peh et al., 1998; Urban et al., 1994). This characteristic feature of B27 can be directly related with its unusual associations with the PLC chaperones, enzymes (such as ERAP 1) and slow folding kinetics. Notably, according to GWAS, ERAP1 is, after HLA-B27, the second strongest genetic association with AS (Bang et al. 2011; Davidson et al. 2009; Pimentel-Santos et al. 2009; Tsui et al. 2010). ERAP1 polymorphisms are also associated with JIA (Hinks et al. 2011) and Behçet's disease (Kirino et al. 2013). Chen *et al.* recently demonstrated that ERAP1 silencing in cell lines expressing HLA-B27 results in the presentation of longer peptides (11-13-mers) compared with ERAP1 expressing B27+ve cell and cells expressing other HLA class I (which typically present 9-10-mers) (Chen et al. 2014).

However, the unusual nature of HLA-B27 is a double-edged sword, as this allele also has a protective effect in certain viral infections. Importantly, viral load in human immunodeficiency virus (HIV) infected B27+ve individuals is significantly decreased compared with individuals carrying other MHCI alleles (Altfeld et al. 2006; Carrington and O'Brien 2003; Hendel et al. 1999; Kaur and Mehra 2009; Neumann-Haefelin 2011). Furthermore, HLA-B27 was associated with the delayed progression to acquired immunodeficiency syndrome (AIDS). Additionally, HLA-B27 is correlated with the spontaneous clearance of hepatitis C virus (HCV) (Neumann-Haefelin et al. 2006). It has been suggested that the protective ability of HLA-B27 in these infections is linked with its unusual capacity to bind and present immunodominant $CD8^+$ specific viral epitopes (Altfeld et al. 2006; Neumann-Haefelin et al. 2006). Yet, there are several other HLA class I alleles which present with a similar protective capacity in HIV (HLA-B51, HLA-B57, HLA-B58 and HLA-A25) and HCV (HLA-B57 and HLA-A3) infections (Hendel et al. 1999). Importantly, it has been demonstrated that viral immune escape is significantly more challenging in B27+ve individuals, as it requires multiple mutations in the HIV and HCV specific epitopes (Ammaranond et al. 2011; Kelleher et al. 2001; Neumann-Haefelin et al. 2011; Schneidewind et al. 2008).

Taken together, to date a great number of studies have demonstrated that HLA-B27 can behave in many unusual ways. However, as yet we do not fully understand the molecular mechanisms behind its predisposition to misfold and accumulate, HLA-B27 interactions with chaperones and enzymes involved in the PLC, ERAD, ER stress and UPR, and the role of this molecule in the immune system in health and disease.

1.8 What have we learnt about disease pathogenesis from animal models?

Notably, studying the molecular mechanisms of SpA pathogenesis in patients is extremely challenging. Firstly, SpA diagnosis is often delayed due to the insidious nature of symptoms and the average time between the disease onset and diagnosis is 5-10 years (Feldtkeller and Erlendsson 2008). Secondly, as mentioned previously SpA is a very heterogenous group of diseases with a broad variety of axial, peripheral, gut and skin clinical manifestations. Finally, investigation of the inflammatory processes *in situ* in SpA patient axial and peripheral joints is extremely limited due to low availability of tissue samples. Hence, development of animal models of SpA is particularly beneficial and can bring us better insight into the disease pathogenesis and future treatment targets.

1.8.1 Mouse models of SpA

HLA-B27

The first animal model developed for investigating the role of HLA-B27 molecule in disease pathogenesis was developed 15 years after the discovery of it's strong genetic association with AS (Nickerson, Hanson, and David 1990; Taurog et al. 1988). However, the expression of human HLA-B27 (B27) gene in mice failed to induce SpA-like symptoms. Further investigation suggested that intracellular expression of B27 molecules was relatively high, but they were absent at the cell surface. Hence, it was hypothesized that the presence of murine MHC class I alleles and/or β2 microglobulin (β2m) could influence trafficking of B27 to the cell surface. Consequently, in the next approach the B27 gene was introduced into mice lacking murine β2m expression (HLA-B27/$\beta2^{-/-}$). HLA-B27/$\beta2^{-/-}$ transgenic (TG) animals (mainly males) developed spontaneous arthritis in hind paws, nail changes and hair loss was observed (Khare, Luthra, and David 1995). Furthermore, animals living in germ-free conditions remained healthy, suggesting the importance of pathogens for disease development. Nevertheless, the HLA-B27/$\beta2^{-/-}$ TG mouse model was not extensively used in further studies.

In addition, several models investigating the role of key inflammatory cytokines (TNFα and IL-6) and proteins involved in bone remodeling, as well as spontaneous models of SpA have been generated over the past four decades.

TNFα

Transgenic mouse lines carrying 3'-modified human TNFα gene construct (hTNF TG) develop chronic inflammatory polyarthritis with bilateral erosive sacroiliitis and elevated levels of IL-6 in joints (Keffer et al. 1991). In hTNF TG animals, arthritis is characterized by synovial inflammation, driven by osteoclast-mediated bone destruction and the lack of the new bone formation. Notably, in hTNF TG mice treated with Dickkopf-1 (DKK-1), a Wnt signaling pathway antagonist, osteoclastogenesis and joint destruction were significantly inhibited. However, at the same time new bone formation was induced both in peripheral and axial skeletal joints (Uderhardt et al. 2010). Furthermore, studies using IL-6-deficient hTNF TG (hTNF TG/$IL6^{-/-}$) mice demonstrated that joint inflammation in this animal model is independent of IL-6 production, as sacroiliitis was similar in both IL-6-deficient and proficient animals.

In the $TNF^{\Delta ARE}$ mouse model, deletion of AU-rich elements (AREs) at the 3'end of the TNFα gene, leads to overexpression of TNFα. As a consequence $TNF^{\Delta ARE}$ mice develop peripheral arthritis, enthesitis and sacroiliitis without visible ankylosis, as well as additional gastrointestinal inflammation (Kontoyiannis et al. 1999). Bone marrow engraftment experiments using this mouse model suggested that expression of TNFα receptor I (TNFRI) on stromal cells (such as mesenchymal stromal cells, fibroblasts and endothelial cells) is sufficient to induce RA- and IBD-like symptoms in these mice (Armaka et al. 2008).

Taken together, these findings suggest that osteoclast-driven bone erosion, but not new bone formation, is dependent on TNFα and further support findings from clinical studies in human SpA. At the same time, these findings raise the question whether axSpA patients without peripheral joint manifestations can benefit from treatment with anti-TNFα.

PGISp

The proteoglycan/aggrecan (PG)-induced arthritis (PGIA) or PG-induced spondylitis (PGISp) model, was the first animal model to develop disease resembling axial skeletal inflammation observed in human AS (Mikecz, Glant, and Poole 1987). In the PGISp model, immunization of susceptible murine strains (BALBc and C3H) with PG derived from human cartilage induced inflammation in the sacroiliac joint and entheseal tissue, followed by manifestations in vertebral discs (Bárdos et al. 2005; Glant et al. 2001;

Mikecz et al. 1987). Interestingly, findings from these studies suggest that arthritis in peripheral joints and inflammatory responses in axial skeleton occur independently and can be driven by different mechanisms. Furthermore, Haynes *et al*. have recently shown that excessive bone formation in the PGISp mouse model is correlated with decreased levels of DKK-1 and SOST in inflamed joints (Haynes et al. 2012). These findings suggest that abnormalities in the Wnt signaling pathway could lead to new bone formation and axial joint ankylosis in SpA.

Together with the induced arthritis mouse models, several spontaneous models of SpA have been developed over the past four decades.

ank/ank

Murine progressive ankylosis (MPA) is caused by a spontaneous mutation of the gene located on chromosome 15 (named *ank*) and described for the first time by Sweet and Green (1981). This model was the prototype of the spontaneous mouse model of human AS (*ank/ank)* (Krug, Mahowald, and Clark 1989). In *ank/ank* animals a homozygous recessive genetic defect causes inflammatory responses in the peripheral and axial skeleton leading to complete joint ankylosis (Krug et al. 1989). Despite, these promising findings, recent data from GWAS studies in AS patients have failed to confirm a genetic link between the human homolog of *ank* (*ANKH)* and susceptibility to AS.

ANKENT

In the murine ankylosing enthesopathy (ANKENT) model, male C57B1/10 mice spontaneously develop ankylosis and enthesitis in ankle and tarsal joints. Disease progresses with age, but only when male mice are caged in groups with other males. Males caged alone and in groups with females remain healthy (Weinreich et al. 1996). Moreover, C57B1/10 males caged together are more susceptible to ANKENT due to bite-related bacterial infections. Hence, these findings identified the importance of endocrine pathways and bacterial infection in the ankylosis and joint inflammation. Furthermore C57Bl/10 male mice caged in groups in germ-free (GF) conditions spontaneously developed ANKENT upon colonization with a mixture of bacteria species containing *Bacteroides* spp. and *Enterococcus* sp., but remained healthy when colonized with *Lactobacillus* spp. (Šinkorová et al. 2008). Thus, these results demonstrated the importance of microbes in ANKENT development and the protective effect of GF conditions.

Aging DBA/1

Aging DBA/1 mice spontaneously develop arthritis characterized by clinical features similar to human PsA, with ankylosing enthesitis in the peripheral joints and dactylitis (Nordling et al. 1992). Investigation of BMP signaling pathway in DBA/1 animals demonstrated overexpression of BMP2 in early and proliferating chondrogenic cells. On the other hand, BMP7 was up-regulated in pre-hypertrophic chondrocytes and BMP6 was present in hypertrophic chondrocytes (R. J. Lories, Derese, and Luyten 2005). Subsequently, Lories *at al*. have demonstrated that overexpression of NOG, a BMP antagonist, inhibits the onset and progression of arthritis in DBA/1 animals (R. J. U. Lories, Derese, and Luyten 2005). These findings suggest that overexpression of BMPs on the proliferating progenitor cells in the entheseal cartilage is sufficient to induce pathological changes and may drive the inflammation.

1.8.2 HLA-B27 transgenic rats

Since, B27 TG mice failed to develop SpA-like manifestations spontaneously there was an unmet need for an animal model investigating the role of HLA-B27 in the disease pathogenesis. Subsequently, several B27 TG rat lines were generated based on the previous observations that rats were more susceptible to arthritis compared with mice. Moreover, some of the existing arthritis models were specific to rats. The B27 TG rat line expressing human β2m was first described in 1990 (Hammer et al. 1990). Subsequently, three B27 TG rat lines were selected for further studies based on the development of SpA-like features: two on the Lewis background (Lewis) and one on the Fisher inbred background (F344) (Table 1.9). The 21-4H Lewis rat line was characterized by the highest gene copy number of both human B27 (hB27) (150 copies) and hβ2m (90 copies), while the other 21-3 Lewis rats expressed only 20 copies of hB27 and 15 of hβ2m. The 33-3 (F344) rats carried 55 copies of hB27 gene and 60 copies of hβ2m. Notably, both 21-4H and 33-3 heterozygous animals developed diarrhea spontaneously within 10 and 8 weeks of age, respectively (Hammer et al. 1990). Interestingly, these results demonstrated that the earlier disease onset in the 33-3 (55 hB27; 66 hβ2m) rats compared with age-matched 21-4H (150 hB27; 90 hβ2m) animals, could be due to higher expression levels of cell surface HLA-B27 molecules in young 33-3 rats. Importantly, the presence of clinical manifestations was dependent on the hB27 and hβ2m gene copy number, as 21-4L (6 hB27; 6 hβ2m) rats and heterozygous 21-3 (20 hB27; 15 hβ2m) rats remained healthy. Furthermore, clinical features were exacerbated with animal age and the consequent increase in the HLA-B27 expression both intracellularly and at the cell surface (Hammer et al. 1990; Taurog et al. 1993).

Both female and male rats from disease prone lines presented gastrointestinal inflammation similar to human IBD, whereas peripheral arthritis was initially observed specifically in males (Hammer et al. 1990). Further studies in the 21-4H and 33-3 rats revealed a similar prevalence of arthritis, but with a slower onset, in female animals (Taurog et al. 1993). Approximately 50% of 21-4H and 33-3 rats developed peripheral arthritis in both hind limbs, characterized by swelling, tarsal joint tenderness and erythema. Histological analysis of affected joints demonstrated the presence of hyperplastic synovium and significant number of neutrophil and plasma cell infiltrates in the inflamed joints. Moreover, destruction of articular cartilage and pannus formation, leading to fibrous ankylosis and osteophyte formation were observed upon inflammation. Notably, the 21-4H and 33-3 male rats developed axial skeleton manifestations, however with a lower prevalence compared with arthritis in peripheral joints. Affected vertebral discs presented inflammatory changes in the outer annulus fibrosus, accompanied by lymphocyte, neutrophil and plasma cell infiltrates. Additionally, active bone resorption at the insertion of the annulus fibrosus and the activation of adjacent periosteum were observed in axial joints from 21-3H male rats. However, as yet the full analysis of pathological changes in axial joints at different stages of the disease has not been described for the 21-4H and 33-3 rat lines. Furthermore, the majority of diseased male rats developed genital tract inflammation with lymphocyte infiltrates, epididymitis and orchitis. Several animals developed psoriasiform hyperplasia and nail dystrophy, resembling human psoriasis, and active inflammatory lesions in heart tissue with associated cellular infiltrates.

In order to exclude the possibility that clinical manifestations observed in the 21-3H and 33-3 rats were simply a consequence of the high copy number of human MHCI and/or hβ2m, subsequent control rat lines were produced (Taugor et al. 1999).

The 120-4 HLA-B7 (B7) (26 hB7 and 5 hβ2m) rat line was generated as a line expressing a control HLA-B allele. Notably, B7 TG rats remained healthy, even when homozygous and after 1 year of life. Importantly, despite low copy number of hβ2m (5 gene copies in heterozygous rats) cell surface levels of HLA-B7 molecules in the 120-4 rats were similar or even higher compared with B27 TG animals (21-4H and 33-3). Thus, these findings suggest that the disease phenotype is not an artifact of the HLA-B allele and is specific for HLA-B27 TG animals. Disease could possibly result from the unusual nature of HLA-B27 molecule.

Given that HLA-Cw6 is known for its association with psoriasis vulgaris, the 201-3 HLA-Cw6 (Cw6) rat line (55 hCw6 and 21 hβ2m) was produced as a control for another auto-inflammatory disease in human. The majority of the 201-3 Cw6 TG animals remained healthy, while a minority of homozygous rats exhibited temporary mild diarrhea and swelling and/or erythema in one or more digits of the front paws. Notably, arthritis and dactylitis in the hands and fingers is a characteristic feature of human PsA. Nevertheless, none of these clinical manifestations were persistent in the 201-3 Cw TG rats and the majority of animals remained healthy.

Table 1.9 HLA-B27 and control transgenic rat lines

LINE	HLA-B chain transgene	HLA heavy chain transgene copy number **	Huβ2m transgene copy number **	Occurrence of disease	
				Hemizygotes	Homozygotes
21-4H	B*2705	150	90	Yes	ND
21-4L	B*2705	6	6	No	No
21-3	B*2705	20	50	No	Yes
33-3	B*2705	55	66	Yes	ND
(21-3 × 283-2) F_1	B*2705	20	50	Yes	ND
120-4	B*0702	26	5	No	No
201-3	Cw*0601	53	21	No	Yes
283-2	None	---	35	No	No

* Gene copy number in the hemizygous transgene locus

Adapted from (Hammer, Maika, Richardson, Tang, & Taurog, 1990; Taugor et al., 1999; Tran et al., 2006)

Because of the associated disease symptoms, the B27 TG 21-3H and 33-3 rat lines were developed as models of human SpA. Subsequent studies demonstrated that gastrointestinal inflammation and peripheral arthritis, but not skin and genital lesions, are strictly dependent on the bacterial environment (Taurog et al. 1994). B27 TG rats raised in GF conditions remained healthy, whereas transfer to the conventional caging environment induced colitis and joint inflammation. Rath *et al.* showed that *Bacteroides spp.* were important for induction of pro-inflammatory responses in the 33-3 rats (Rath et al. 1996). Further investigation on the specificity of pro-pathogenic bacteria revealed that GF rats reconstituted with a *Bacteroides spp.* monoculture, but not *Escherichia coli*, developed colitis and gastritis comparable to that observed after administration of a mixed bacterial cocktail (Rath, Wilson, and Sartor 1999). However Rath *et al.* did not assess inflammation in axial and peripheral joints, so it is unclear from these studies whether joint inflammation is also dependent on the specificity of gastrointestinal commensal bacteria.

Notably, bone marrow (BM) transfer from diseased B27 TG rats was sufficient to induce multisystem inflammatory responses in healthy TG rats and wild type (WT) animals (Breban, M., Hammer, R. E., Richardson, J. A. & Taurog 1993). The induction of disease upon bone marrow engraftment suggested that resident BM cells in 21-4H and 33-3 rats could be the main effector cell population driving SpA-like inflammation. To further support this hypothesis, histological analysis of inflamed rat joints demonstrated extensive BM inflammation adjacent to the enthesis with little or no inflammation at the enthesis itself. Similarly, engraftment of fetal liver cells from 21-4H or 33-3 rats to the low copy number 21-4L or non-transgenic control Lewis rats induced inflammatory responses (Breban et al. 1996). Interestingly, arthritis was present less frequently in graft recipient animals compared with 21-4H and 33-3 rats. Furthermore, the severity of joint manifestations developed in graft recipients was significantly higher when 21-4H donor cells with the highest human gene copy number were used.

In order to investigate the role of T cells and the thymus in the disease pathogenesis Breban *et al*. generated the athymic *rnu/rnu* F344 rat line, carrying the disease-prone HLA-B27 gene locus from 33-3 (F344) rats (Breban et al. 1996). Notably, disease was completely abrogated in athymic rats and transfer of $CD4^+$ T cells, and to a less extent $CD8^+$ T cells, from 33-3 TG rats with established disease was sufficient to induce gastrointestinal and genital tract inflammation in male *rnu/rnu* recipients. Interestingly, very low or no arthritis was observed in *rnu/rnu* recipient rats. These findings suggested that thymic exposure to HLA-B27 and possibly negative selection of auto-reactive $CD8^+$ T cells, are not required for the induction of inflammatory manifestations in the gastrointestinal and genital tract. However, due to the low purity of donor $CD8^+$ T cells and possible contamination with $CD4^+$ T cells, it was not possible to draw final conclusions about the role of these two T cell populations in the disease pathogenesis. Hence, May *et al*. consequently developed a model investigating the role of $CD8^+$ T cells (May et al. 2003). In this model depletion of $CD8^+$ T cells with anti-CD8α monoclonal antibody (mAb) in thymectomized B27 TG rats (21-4H and 33-3) failed to prevent gut and joint manifestation. Furthermore, their results suggested that other cell populations expressing CD8α chain, such as NK cells and the $CD4^+/CD8^+/CD11bc^+/CD161a^+/CD172a^+$ monocyte population were still detected after depletion and may play a role in disease pathogenesis. Notably, the severity of arthritis, but not gastrointestinal inflammation, was reduced upon persistent treatment with anti-

CD8α mAb and elimination of NK cells and the monocytic cell population expressing CD8α.

Subsequently, Taurog *et al*. generated the 21-3H and 33-3 rats with a heritable CD8α-null mutation. The lack of functional CD8α resulted in almost complete abrogation of allogeneic CTL responses (Taurog et al. 2009). Their results further confirmed that $CD8^+$ T cell-dependent interaction with HLA-B27 is not necessary for the initiation of the clinical manifestations in B27 TG rat model. However, due to the low number of animals per study group and relatively low incidence of arthritis combined with the lack of axial manifestations in CD8α-null B27 TG rats, it remains unclear whether joint manifestations are fully independent on $CD8\alpha^+$ cell populations.

In summary, these findings suggested that thymic exposure to HLA-B27 and possibly negative selection of auto-reactive $CD8^+$ T cells, as well as the presence of conventional CD8α T cells, are not required for the induction of IBD-like clinical manifestation in B27 TG rats. However, the role of other cell types expressing CD8α and conventional $CD8^+$ T cells in joint inflammation remains unclear.

Given that the transfer of $CD4^+$ T cells from diseased B27 TG rats was sufficient for the induction of gut inflammation, and to some extent joint manifestations, several studies further investigated the role of $CD4^+$ T cells in disease pathogenesis. Qian *et al.* demonstrated that $CD4^+$ T mesenteric lymph node (MLN) cells isolated from diseased B27 TG (33-3) rats expressed decreased levels of cell surface MHCI and elevated levels of MHC class II (MHCII) compared with healthy GF 33-3 rats (Qian, Tonkonogy, and Balfour Sartor 2006). Furthermore, B27+ve $CD4^+$ T cells from diseased rats produced interferon γ (IFNγ) when co-cultured with both B27 TG or WT antigen presenting cells (APCs) pulsed with commensal caecal bacterial antigens. Notably, blocking HLA-B27 or MHCII molecules on APCs with specific mAbs completely abrogated IFNγ production by B27+ve $CD4^+$ T cells (Qian et al. 2006). Hence, these findings highlight the key role of $CD4^+$ T cells in the induction of IFNγ-driven pro-inflammatory responses in the 33-3 TG rats. Moreover they also suggest that HLA-B27 and MHCII molecules expressed at the surface of APCs, as well as the exposure to commensal gut microbiota are necessary for activation of IFNγ production by B27+ve $CD4^+$ T cells.

Notably, Breban *et al.* have recently demonstrated increased number of IL-17, TNFα and IFNγ producing $CD4^+$ T cells in mesenteric and popliteal LNs isolated from B27 TG rats compared with non-TG and B7 TG rats. Notably, Th17 cells were present in the affected peripheral joints in B27 TG animals and increased expansion of Th17 cells, but not Th1 and T_{reg} cells, correlated with the severity of clinical manifestations. Furthermore, B27+ve dendritic cells (DCs) favored the differentiation and expansion of pro-inflammatory Th17 cell in a contact dependent manner.

The role of APCs in the disease pathogenesis was properly investigated for the first time fourteen years after the generation of B27 TG rat model (Hacquard-Bouder et al. 2004). Firstly, Hacquard-Bouder *et al* demonstrated striking defective stimulation of allogeneic and syngeneic T lymphocytes by DCs isolated from B27 TG rats, but not control B7 TG and WT animals. Despite similar expression levels of co-stimulatory molecules and maturation markers (CD80, CD86, CD40, MHC class II, ICAM-1) B27 TG DCs formed fewer conjugates with T cells. Further analysis demonstrated that CD86 molecules were less used in the synapse formation in 33-3 rats. Hence, it has been suggested that the impaired ability of B27 TG DCs to form immunologic synapses may lead to the loss of HLA-B27 tolerance. Additionally, subsequent studies have demonstrated altered cytoskeletal dynamics in B27 TG DCs, and further confirmed the impaired capacity of B27-expressing DCs to stimulate T cells (Hacquard-Bouder et al. 2007). Later studies revealed up-regulated expression of proteins involved in the MHCI loading complex and UPR, and simultaneous decreased expression of MHCII molecules in B27 TG DCs compared with B7 TG rats (Dhaenens et al. 2009). Additionally, B27 TG DCs were characterized by decreased motility and altered morphology compared with control DCs. Interestingly, Dhaenens *et al*. have observed reduced viability of a potentially tolerogenic $CD103^{+}CD4^{-}$ DC population in B27 TG rats. On the other hand, Utriainen *et al*. have recently shown that expression of HLA-B27 in 33-3 rats can lead to enhanced DC apoptosis, the loss of a migratory DC population and increased production of IL-17 by $CD4^{+}$ T cells upon stimulation with surviving DCs (Utriainen et al. 2012). Notably, several genes induced by IFNγ were down-regulated in purified splenic $CD103^{+}/CD4^{+}$ DCs from B27 TG rats compared with control B7 TG and non-TG rats (Fert et al. 2014). In conclusion, these findings suggest the importance of B27-expressing DCs in SpA pathogenesis.

To date, several studies have investigated the role of UPR in B27 TG rats. Firstly, Colbert *et al*. showed increased UPR upon TNFα and IFNγ stimulation in cells derived from B27 TG animals compared with B7 TG controls (Turner et al. 2005). The presence of UPR was correlated with elevated expression levels of HLA-B27 and was characterized by intracellular accumulation of B27 oligomers and B27 free heavy chains (FHCs) which bound BiP (Turner, Delay, Bai, Klenk, and R. a Colbert 2007). Notably, the ratio of misfolded to folded B27 FHCs at steady state was consistently higher in

B27-expressing cells compared with B7 controls. Smith *et al*. showed that the induction of a UPR in B27 TG rat macrophages lead to enhanced responses to Toll-like receptor 3 (TLR3) (polyinosinic:polycytidylic acid (poly I:C)) and Toll-like receptor 4 (TLR4) (LPS) stimulation, with increased IFNβ production (Smith et al. 2008). Furthermore, recent studies showed increased ER stress and production of IL-1α and IL-1β in BM monocytes derived from B27 TG rats upon TNFα stimulation (Layh-Schmitt et al. 2013). Notably, their results suggested that HLA-B27 expression in monocytes promoted TNFα-driven and IL-1α and IL-1β-dependent osteoclastogenesis. Thus, UPR and HLA-B27 misfolding seem to play a role in the activation of pro-inflammatory immune responses in B27 TG rats.

In order to investigate whether stabilization of HLA-B27 molecules could decrease misfolding and UPR, Tran *et al*. created a rat line with high copy number of hβ_2m by crossing 33-3 (55 hB27; 66 hβ_2m) rats with disease-free 283-2 (35 hβ_2m) rats (Tran, Dorris, Satumtira, J. A. Richardson, et al. 2006). Surprisingly, although additional hβ_2m decreased HLA-B27 misfolding and UPR exacerbated arthritis and spondylitis were observed in the presence of gastrointestinal manifestations. Next, to investigate whether increased expression of hβ_2m can trigger disease independently on the high HLA-B27 gene copy number, female 21-3 rats (20 hB27; 15 hβ_2m) were crossed with male 283-2 rats (B27 TG^2) (Tran, Dorris, Satumtira, J. a Richardson, et al. 2006). Interestingly, male offspring showed extremely high, 70% prevalence of arthritis. Notably, arthritis was more severe and persistent and affected more limbs compared with arthritis in other B27 TG rat models. Importantly, for the first time axial skeleton manifestations were detected in the majority of male rats and animals presented with histological features characteristic of human SpA. These features included osteoproliferation in the vertebral discs and persistent inflammation with fibrosis and enthesitis. Furthermore, none of the B27 TG^2 rats developed histological gut inflammation. Histological analysis of axial joints from B27 TG^2 rats revealed the presence of inflammatory cell infiltrates in the mildly inflamed connective tissue adjacent to the junction between the annulus fibrosus and vertebrae (van Duivenvoorde et al. 2012). No infiltrates were detected in the enthesis. Furthermore, increased numbers of activated osteoclasts were initially found in the cartilage outside the vertebral end plate and subsequently spread to vertebrae and the adjacent bone marrow. Notably, osteoproliferation was slightly delayed compared with bone destruction and was situated at distinct location, in the periosteum surrounding the vertebral joint. Similarly to bone destruction, osteoproliferation progressed with inflammation.

Thus, the B27 TG^2 rat model seems to resemble human SpA to a greater degree compared with previously studied animal models and could thus provide better insights into the mechanisms leading to axial and peripheral joint pathology.

1.9 HLA-B27 and SpA - three leading theories

Three leading theories, discussed in the following, try to explain the possible role of HLA-B27 in disease pathogenesis. The findings from studies in human and B27 TG rodents gave some evidence to support or argue against these theories, however as yet there is no definitive answer to how HLA-B27 can be involved in SpA pathogenesis.

1.9.1 Arthritogenic peptide theory

The 'arthritogenic' peptide theory, was developed in 1990 and speculated about the role of HLA-B27 in disease pathogenesis (Benjamin and Parham 1990). It originated from an understanding of the conventional role of MHCI molecules in immune responses to present self and foreign cellular peptides to cytotoxic CD8$^+$ T cells. The theory postulates that disease associated HLA-B27 molecules can present 'arthritogenic' peptide(s) derived from intracellular pathogens that mimic self-derived peptides (Benjamin and Parham 1990). Consequently, CTLs activated against these mimetic, bacterial peptides can cross-react with self-peptides presented in the HLA-B27 context in the joint tissue and drive pro-inflammatory responses. ReA, a form of SpA associated with HLA-B27, is triggered by intracellular Gram-negative bacteria, such as *Chlamydia*, *Salmonella*, *Yersinia*, *Campylobacter* and *Shigella* (Sieper 2007; Sieper et al. 2002). Notably, several peptides derived from *Chlamydia* and *Yersinia* are homologous to human peptides and have a high affinity for the HLA-B27 binding pocket (Alvarez-Navarro et al. 2013; Cragnolini and de Castro 2008; Ramos et al. 2002; Ugrinovic et al. 1997). Furthermore, Hermann *et al*. have found CTL clones with specific cytotoxicity against B27-expressing cell lines in the synovial fluids (SFs) from 4 ReA patients and 1 AS patient (Hermann et al. 1993). Interestingly, cytotoxic CD8$^+$ T cells with specificity for a nonapeptide (LRRYLENGK) presented by HLA-B27, derived from B27 heavy chain itself, were found in B27+ve AS patient PBMCs, and were absent in B27+ve healthy controls (Frauendorf et al., 2003). However the LRRYLENGK peptide is commonly found in other HLA-A and -B alleles, which are not associated with SpA. Interestingly, *E.coli, Bacillus megaterium, P. aeruginosa* were demonstrated to produce peptides homologous to LRRYLENGK. Hence, these findings suggest that presence of this nonapeptide itself is not sufficient to activate cross-reactive CD8$^+$ T cells and additional factors, such as specific bacteria or unusual properties of HLA-B27 molecules may induce the loss of self-tolerance.

Subsequently, Atagunduz *et al*. proposed that peptides derived from proteins found in cartilage, but not mimetic bacterial peptides, could activate specific auto-reactive CTLs (Atagunduz et al. 2005). Based on the computer analysis 121 cartilage-derived peptides were predicted to have a binding motif to HLA-B*27:05 allele. Notably, only one peptide induced auto-reactive cytotoxic CD8$^+$ T cells from B27+ve AS patient synovial fluid. Interestingly this nonameric peptide originated from type VI collagen, a protein found in the cartilage and extracellular matrix of the human joint and intervertebral disc. Importantly, CTL responses against this nonameric peptide were less significant in PBMCs, and were absent in both PBMCs and synovial fluid mononuclear cells (SFMCs) derived from RA patients and healthy controls. Thus, these studies suggest that B27+ve AS patients may be predisposed to induce auto-reactive CD8$^+$ T cells against proteins present in the joint. However, as yet it is not clear if the presence of these CTLs is the cause of immune responses in joints or rather the result of cartilage destruction initiated by other pro-inflammatory events.

Notably, it has been shown that HLA-B27 can bind longer peptides compared with other HLA class I alles (Peh et al., 1998; Urban et al., 1994). Furthermore, peptides eluted from B27+ve cell lines after ERAP1 silencing were longer (11-13-mers) compared with controls (9-10-mers) (Chen et al. 2014). Importantly, this study showed that other genetic factors (e.g. ERAP1) can influence the length of peptides presented by B27 and might contribute to disease pathogenesis. Thus, these findings suggest that the escape from immune tolerance and activation of auto-reactive CTLs may result from the ability of B27 to bind longer peptides, rather than the specificity of peptides presented by B27.

1.9.2 The HLA-B27 misfolding, UPR and ER stress theory

The unfolded protein response (UPR) hypothesis proposes that misfolding and consequent accumulation of HLA-B27 molecules in the ER and intracellular compartments lead to the activation of pro-inflammatory cytokine production, such as IL-23, IL-6, IFNβ, TNFα, which drives SpA pathogenesis. As mentioned previously, studies using B27 TG rats have demonstrated that UPR can occur upon upregulation of HLA-B27 and increases with animal age (Turner et al. 2005; Turner, Delay, Bai, Klenk, and R. a Colbert 2007). Moreover, the induction of HLA-B27 resulted in FHC misfolding, oligomerization and binding to ER chaperone, BiP, in the ER. These observations were specific for B27 TG animals and were absent in B7 TG rats. Notably, BiP levels were increased upon stimulation with interferons and TNFα (Turner, Delay, Bai, Klenk, and R. a Colbert 2007). However, stabilization of B27 molecules, by additional copies of β2m led to the reduction of BiP levels, but failed to prevent arthritis in B27 TG^2 rats. These findings suggest that UPR activation and the resulting induction of pro-inflammatory cytokines is not sufficient to induce SpA-like disease in B27 TG^1 rats (Tran, Dorris, Satumtira, J. a Richardson, et al. 2006). On the other hand, the induction of UPR, either by the chemical agent or HLA-B27 misfolding, in lipopolysaccharide (LPS) stimulated macrophages from B27 TG^1 rats induced production of IL-23 (DeLay et al. 2009). Furthermore, increased levels of IL-23 were observed in the colon tissues from B27 TG^1 rats and colitis was associated with enhanced expansion of Th17 cells (DeLay et al. 2009). Layh-Schmitt *et al.*, recently demonstrated up-regulation of HLA-B27 expression and ER stress responses, upon TNFα stimulation in BM monocytes isolated from B27 TG[1] rats (Layh-Schmitt et al. 2013). Furthermore, BM-derived monocytes treated with TNFα produced elevated levels of IL-1α and IFNβ and formed more osteoclasts compared with control B7 monocytes. In conclusion, it is not clear whether activation of UPR and ER stress responses in B27 TG rats is a cause or rather an effect of on going inflammation. Furthermore, it could simply be a result of the overexpression of human HLA-B27 and β2m in rats.

Nevertheless, as yet there is no strong evidence on the importance of UPR and ER stress responses in SpA pathogenesis from human studies. Notably, no activation of UPR and ER stress responses was observed in AS patient-derived macrophages upon cytokine stimulation (Smith et al. 2008; Zeng et al. 2011). Importantly in this study AS patient macrophages produced increased amounts of IL-23 in response to LPS and IFNγ stimulation. Similar observations were reported using LPS-treated AS patient monocyte-derived DCs (Campbell et al. 2011). Despite up-regulation of FHC expression, BiP and XBP1 splicing were unaffected in these moDCs. However, the expression of BiP was increased in macrophages isolated from the peripheral joints of AS patients, compared with OA patients (Dong et al. 2008). In this study, BiP levels positively correlated with IL-6 and TNFα levels in the synovial fluid and serum levels of IL-6. Furthermore, Feng *et al.* demonstrated higher expression of CHOP, XBP1 and BiP in monocytes and macrophages from AS and ReA PBMCs, compared with OA patients and healthy controls (Feng et al. 2012).

Taken together, although, there is a strong evidence from the B27 TG animal model supporting the critical role of UPR and ER stress responses in colitis, the role of these responses in arthritis is less clear. On the other hand, data from human studies have shown increased UPR and ER stress responses only in peripheral and synovial fluid cells from AS patients with active disease. However, at the same time increased production of IL-23 by AS patient-derived cells was observed independently from UPR. Hence, it is still unclear whether inflammation occurs primarily as a result of the activation of the UPR and ER stress responses, or the UPR and ER occur as a result of active disease and ongoing pro-inflammatory responses.

1.9.3 The B27 homodimer theory

The third theory was proposed after the discovery that soluble, misfolded B27 FHCs can refold *in vitro* and form disulfide-bonded homodimers via an unpaired Cys67 (Allen et al. 1999). It has been proposed that these NC-B27 molecules are induced at the surface of cells in response to environmental factors (such as bacterial infection, local joint environment) or upon co-expression of other disease-predisposing genes. Subsequently NC-B27 binding to immune receptors could lead to development of pathogenic immune responses in SpA (Shaw, Hatano, and Kollnberger 2014).

The main obstacle to study the expression and role of these NC-B27 forms has been the lack of HLA-B27 and $B27_2$ specific antibodies. Although, the commonly used HC10 antibody recognizes both FHCs and FHC homodimers, it is not a HLA-B27 specific tool and also binds to other HLA-A, -B and -C alleles (Fleur Sernee, Ploegh, and Schust 1998; Perosa et al. 2003; Stam et al. 1990; Stam, Spits, and Ploegh 1986). On the other hand, the W6/32 antibody recognizes epitopes in both β2m and α2 FHC domain and has been demonstrated to bind to properly folded MHCI molecules of all alleles, as well as recognize a subset of B27 FHC homodimers (Stam et al. 1986). The third commonly used tool to study HLA-B27 molecules is the ME1 antibody which has high affinity for properly folded HLA-B27, -B7 and -Bw22 molecules (Ellis, Taylor, and McMichael 1982). Hence, studying the expression patterns of NC-B27 forms at the cell surface in SpA patient-derived cells and B27+ve cell lines, requires the use of a combination of techniques, such as flow cytometry, immunoprecipitation, standard and 2D isoelectric gel electrophoresis.

Kollnberger *et al*. demonstrated that HC10-reactive MHCI FHCs are abundantly expressed on B27+ve AS patient PBMCs and SFMCs, and subsequent 2D-gel electrophoresis confirmed the presence of cell surface B27 FHC homodimers (Kollnberger et al. 2002). Furthermore, they and other authors also showed that KIR3DL1, KIR3DL2 and LILRB2 can bind these NC-B27 molecules (Kollnberger et al. 2002, 2007). Subsequently, Bird *et al*. showed abundant expression of surface FHC homodimers in B27-expressing cell lines and demonstrated that these non-classical forms originate from properly folded cell surface MHCI molecules via endosomal recycling, rather than directly from the intracellular ER compartments (Bird et al. 2003). Therefore, this study suggests that cell surface B27 homodimers arise from a pool of HLA-B27 molecules trafficking to the cell surface distinct from the intracellular pool, which elicits UPR and ER stress responses. Moreover, studies using B27 TG rodent models showed the presence of both intracellular and cell surface HC10-reactive FHC homodimers and multimers in splenic cells (Kollnberger et al. 2004). This study also suggested that mouse paired Ig-like receptors (PIRs) bind NC-B27 forms. Notably, Chan *et al*. subsequently demonstrated increased expression of KIR3DL2 on NK and $CD4^+$ T cells in PBMCs and SFMCs obtained from SpA and juvenile enthesitis-related arthritis (ERA) patients compared with RA controls (Chan et al. 2005). Additionally, they showed an activated phenotype in disease, and increased viability of KIR3DL2+ve NK cells after co-culture with B27-expressing cell lines. Later studies have shown that FHC and B27 homodimers bind to the KIR3DL2 with a higher avidity compared with properly folded HLA-B27 and other MHC class I FHCs and heterotrimers (Wong-Baeza et al. 2013). Further investigation by Ridley *et al*. has demonstrated enhanced proliferation, survival and IL-17 production by superantigen-stimulated AS and SpA patient-derived $KIR3DL2^+$ $CD4^+$ T cells after co-culture with B27-expressing cell lines (Bowness and Ridley et al. 2011).

Importantly, Payeli *et al*. recently characterized a novel HD6 antibody generated by phage display library against $B27_2$ (Payeli et al. 2012). It has been shown previously by flow cytometry that the HD6 antibody binds specifically to B27+ve cell lines, B27 TG rat cells and to some extent to B27+ve AS patient monocytes (McHugh et al. 2014; Payeli et al. 2012). Notably, binding of HD6 to B27 TG rat splenic cells was shown to be dependent on the amount of cell surface HLA-B27 molecules, which increased with animal age (McHugh et al. 2014). Moreover increased levels of HD6-reactive molecules were detected by flow cytometry at the surface of B27+ve AS patient PBMCs following brief low pH treatment. Additionally, stabilization of properly folded cell surface HLA-B27 by addition of high affinity B27-binding peptides resulted in decreased amount of cell surface NC forms of B27. These findings suggest that HD6 staining is relatively high in B27+ve cell lines and B27 TG rat cells expressing high levels of surface HLA-B27 molecules. Yet they are detected only at low frequency on primary monocyte cells from B27+ve AS patient blood. These observations could result either from HD6 epitope masking at the cell surface of B27+ve patient-derived cells or very low expression of HD6-reactive, molecules on peripheral cells form patients.

Thus, based on our current knowledge the third theory proposes that NC-B27 molecules expressed at the surface of B27+ve AS patient cells in circulation or joint tissue under certain circumstances, can bind to KIR3DL2 receptors, and possibly some other Ig-like receptors, present at the surface of T or NK cells. These interactions are proposed to promote pro-inflammatory responses and cytokine production. Further functional studies of these interactions along with characterization of potential cell and tissue types expressing these NC-B27 molecules in AS patients will advance understanding of the role of HLA-B27 in SpA pathogenesis.

In conclusion, although HLA-B27 remains the strongest genetic factor associated with SpA, to date studies on these three theories do not yet fully explain the role of this molecule in disease pathogenesis. Our current knowledge suggests that there could be several different mechanisms by which HLA-B27 can activate immune responses in SpA patient joints and predispose to disease. Development of SpA seems to be rather a consequence of complex interplay of unique molecular features of B27 and genetic and environmental factors.

DPhil Project Objectives

To date, HLA-B27 is the strongest genetic factor predisposing to the development of SpA. However its role in disease pathogenesis remains unclear. Over the past four decades three main theories about mechanisms by which HLA-B27 could activate immune responses and joint inflammation in SpA have been extensively studied. Studies using B27 TG rats demonstrated that peripheral joint inflammation and gut manifestations occur in the absence of $CD8^+$ T cells and provided evidence against the arthritogenic peptide theory. Hence, both UPR/ER stress and B27 homodimer theory have been studied more extensively in past years. Nevertheless, the recent discovery of the ERAP1 association with SpA and subsequent studies gave a new perspective for the arthritogenic theory. It has been suggested that not specificity, but quality and length of peptides presented by B27-expressing cells in the presence or absence of ERAP1 may be a key factor contributing to the impaired $CD8^+$ T cell immune responses in SpA. On the other hand, unstable HLA-B27 complexes, loaded with low quality peptides could give rise to NC-B27 forms, which promote Th17 responses via KIR interactions. Thus, cell surface expression of HLA-B27 in combination with certain environmental and other genetic factors could be involved in both driving the IL-23/Th17 immune responses and impairing self-tolerance.

Importantly, our group has previously investigated the B27 homodimer theory and confirmed presence of cell surface HC10-reactive NC-B27 forms in cell lines, B27 TG rats and AS patient PBMCs. However, due to the broad specificity of HC10 antibody (FHC and FHC homodimers of HLA-A, -B and -C) investigation of the $B27_2$ expression in SpA patient cells and tissues by flow cytometry and confocal microscopy has been highly limited. Therefore, subsequently in order to meet experimental needs a specific B27 homodimer antibody was generated by screening a phage display library in collaboration with Renner group from Zurich. The novel HD6 antibody, which was identified from this screen, has been shown to bind to B27+ve cell lines and B27 TG[1] rat cells by flow cytometry. However, staining of AS patient-derived PBMCs has been more challenging as although one study suggested the presence of HD6+ve monocytes (Payeli et al. 2012), a number of subsequent experiments failed to confirm HD6 staining in PBMCs or SFMCs obtained from other AS patients (McHugh et al., 2014 and unpublished data). Nevertheless, cell surface HD6-reactive molecules could be induced specifically at the surface of B27+ve AS patient PBMCs following brief acid treatment (McHugh et al. 2014). These findings suggest that potentially pathogenic HD6-reactive molecules are not broadly expressed in the circulation and indicate the possibility of their expression only by specific cell and tissue types and under particular environmental conditions. Furthermore, as yet the expression and cell surface segregation patterns of these NC-B27 molecules have not been investigated. Studying the expression patterns of NC-B27 forms both *in vitro* and *in vivo* will give us a better understanding of the role of HLA-B27 in SpA pathogenesis.

Thus, the objectives of my DPhil project were focused on the investigation of the HD6-reactive molecule cell surface expression and segregation patterns in:

I. B27-transfected human cell lines and cell lines with the natural expression of HLA-B27 by immunoprecipitation and confocal microsopy.

II. AS patient blood-derived cells (DCs, Mφ and osteoclasts (OCs)) and SFMCs by flow cytometry and confocal microscopy, as well as tissue sections from SpA patients by immunohistochemistry.

III. Cells derived from the circulation, lymphoid tissue, ankle joints and axial skeleton of B27 TG[2] rats, using flow cytometry and immunohistochemistry.

Chapter Two: Materials and Methods

2.1 General cell culture

Suspension and adherent cells were cultured in various, sterile cell culture plastic ware (flasks or plates, BD Falcon™ , BD Biosciences, UK) at 37°C with 5% CO_2. For cell line details see Table 2.1. For cell culture media details see Table 2.2.

2.1.1 HeLa cells

Adherent HeLa cells were seeded in D10 media at density of $1x10^6$ cells/ml in $25cm^2$ or $75cm^2$ flasks (BD Bioscience, UK). Cells were split when fully-confluent. Media was aspirated and flask was washed with PBS to remove any traces of D10. Cells were detached with 3-5ml of warm trypsin-EDTA (CC-5012, Lonza, UK) for 5-10min at 37°C. For flow cytometry and confocal microscopy experiments HeLa cells were detached with lidocaine (4mg/ml) (Sigma-Aldrich, UK) / 10µM EDTA (Sigma-Aldrich, UK) in sterile ddH_2O in order to preserve untouched cell surface MHCI epitopes.

2.1.2 LBL.721.220 and LBL.721.221 cells

220 and 221 and transduced 220-B27, 221-B27, 220-B27 TPN, 220-B7, 221-B35 cell lines were seeded in R10 media at density of $1x10^6$ cells/ml, and cultured in a suspension in $25cm^2$ or $75cm^2$ flasks. Every 2-3 days cells were span down and resuspended in R10 media at density of $\sim 1x10^6$ cells/ml.

2.1.3 Monocyte-derived dendritic cells (moDCs)

Peripheral blood mononuclear cell (PBMC)-derived $CD14^+$ monocytes (described below) were seeded at $5x10^5$ cells/ml in R10 media supplemented with 1000U/ml recombinant human (rh) GM-CSF (Peprotech, UK) and 500U/ml rh IL-4 (Peprotech, UK). On day 3 of culture, 1/3 of the media volume was replaced with fresh R10 supplemented with 1000U/ml rh GM-CSF and 500U/ml rh IL-4.

On day 5 or 6 immature moDCs were stimulated with 100 ng/ml of lipopolysaccharide (LPS) *Escherichia coli* (*E.coli*, 0111:B4) or *Salmonella enterica*, serotype *thyphimurium* (*S.thyphimurium*) (both Sigma-Aldrich, UK) and/or TNFα and IFNα, IFNβ, IFNγ (20ng/ml, Peprotech, UK). In some experiments TLR9 stimuli 10μM CpG oligodeoxynucleotide (CpG ODN, Sigam-Aldrich, UK) and TLR3 stimuli 10μM polyinosinic:polycytidylic acid (Poly I:C, Sigma-Aldrich, UK) were used along LPS and cytokine stimulation to induce DC maturation and activation. On day 6 or 7 unstimulated and stimulated moDCs were stained with anti-MHCI (HD6, HC10, ME1, W6/32) antibodies and analyzed by flow cytometry or confocal microscopy.

2.1.4 Monocyte-derived macrophages

PBMC-derived $CD14^+$ monocytes were seeded at $5x10^5$ cells/ml in R10 media supplemented with 25ng/ml recombinant human Macrophage Colony-Stimulating Factor (rh M-CSF) (Peprotech, UK) on 24-well Imaging Plate FC, with Fluorocarbon Film Bottom (Cat.no. PAA21313231, PAA, UK). On day 3 of culture 1/3 of the media volume was replaced with fresh R10 suplemented with 25ng/ml rh M-CSF. On day 5 of culture cells were stimulated with 100ng/ml of LPS (Sigma-Aldrich, UK) and/or TNFα or IFNγ (20ng/ml) (Peprotech, UK). Following day unstimulated and stimulated cells were used in flow cytometry or confocal microsocpy experiments.

2.1.5 Monocyte-derived osteoclasts

PBMC-derived $CD14^+$ monocytes were cultured on 24-well Imaging Plate FC, with Fluorocarbon Film Bottom (Cat.no. PAA21313231, PAA, UK) at density of 0.3-0.4 $x10^6$ cells/500ml of MEM10 suplemented with recombinant human soluble Receptor Activator of NFϰB Ligand (rh sRANKL) (100ng/ml) and rh M-CSF (25ng/ml) (both from Peprotech, UK). Every 2-3 days 50% of the culture media volume was replaced with fresh MEM10 supplemented with 100ng/ml rh sRANKL and 25ng/ml rh M-CSF. On day 10-12, when mature osteoclasts were formed, cells were stained on plates and analyzed by confocal microscopy.

2.1.6 PBMC-derived osteoclasts

PBMCs were cultured at density of $1x10^6$ cells/ml on 24-well Imaging Plate FC, with Fluorocarbon Film Bottom (Cat.no. PAA21313231, PAA, UK) in MEM10 suplemented with 100ng/ml rh RANKL and 25ng/ml rh M-CSF (both from Peprotech, UK) (OC MEM10). On second/third day of culture, when adherent cells reached the confluency of 60-80%, suspension cells were gently removed from wells and adherent cells were resuspended in 500μl/well of fresh MEM10 supplemented with 100ng/ml rh RANKL and 25ng/ml rh M-CSF. Every 2-3 days OC culture media was replaced with fresh OC MEM10. On day 10-12, when mature osteoclasts were formed, cells were stained on plates and analyzed by confocal microscopy.

2.2 Lentiviral transfection of HeLa cells

HeLa-B27 cell line was generated using the supernatant from cultured HEK 293T cells that had been transiently transfected to produce lentiviral particles. 293T cells cultured in D10 media were co-transfected at with 3 different plasmids: the HLA-B*27:05 lentiviral plasmid pHR-SIN-BX- IRES-Em, an HIV-based packaging plasmid (pCMVR8.91) and an HIV-based envelope plasmid (pMD-G). 0.7μg of each vector was added in a 1.5ml sterile screw-cap tube to 150μl of transfection mix, GeneJuice® transfection reagent (Cat.no. 70967, Novagen, Merck Millipore, UK) and R0, prepared as per manufacturer's instructions. Transfection mix with plasmid vectors was incubated for 20min at RT and subsequently 100μl was added to 293T cells (~60% confluent) in 6 well plates with 1ml of D10 media and cells were incubated at 37°C for 4 days. Supernatant was aspirated and centrifuged (3000rpm, 15min). 100μl of SN was used to infect $2x10^5$ HeLa cells in 24-well plates. After 5 days, the expression of HLA-B27 in transfected cells was evaluated by flow cytometry using ME1 antibody.

2.3 Isolation of human PBMCs and CD14$^+$ monocytes

All blood samples were obtained with informed consent from all donors and with appropriate ethical permission (COREC06/Q1606/139). AS patient (20-30ml) and healthy control (50ml) venous blood were collected in a heparin coated (100μl/tube) 50ml Falcon™ tube (BD Biosciences, UK) or 10ml glass, heparin coated BD Vacutainer® Blood Collection Tube (Cat.no. 366480, BD Biosciences, UK). Blood was diluted with an equal volume of pre-warmed R0 media and layered onto 15ml of Histopaque® (Cat.no. 10771, Sigma-Aldrich, UK). PBMCs were isolated by the density gradient centrifugation (20min, 2000rpm, with a breaking rate 0). PBMCs were aspirated from the layer between the Histopaque® and the plasma. After isolation PBMCs were washed 2 times in R10 at 1800rpm, 10min, followed by 1 wash at 1500rpm, 10min. Cells were counted using the automated cell counter (AbX pentra 60, Horiba ABX Diagnostics) or resuspended in 0.4% trypan blue solution (T8154, Sigma-Aldrich, UK) and counted manually using a hemocytometer. Monocytes were isolated by positive selection using CD14 MicroBeads (Cat.no. 130-050-201, MACS® Cell Separation technology, Miltenyi Biotec, UK).

2.4 Cryopreservation of cells

Cells were centrifuged at 1500rpm, 5min. Supernatants were discarded and cell pellets were resuspended in 1ml per up to $10x10^6$ cells of filter-sterilized FBS supplemented with 10% dimethyl sulphoxide (DMSO) (D2650, Sigma-Aldrich, UK) (freezing media). Cells were transferred to 2.0ml cryovials (Nalgene, Sigma-Aldrich, UK) and stored at -80°C in Mr. Frosty™ freezing containers (Thermo Scientific, UK). For long-term storage cryovials with frozen cells were transferred to liquid nitrogen.

Frozen cells were thawed immidiately after beeing removed from -80°C or liquid nitrogen at 37°C in a water bath. Cell suspensions were gently transferred with a pippete (by dropping) into warm R10 and centrifuged at 1500rpm for 5min. Cells were washed 2 times with fresh R10 and counted manually in hemocytometer in a 0.4% trypan blue solution (T8154, Sigma-Aldrich, UK).

2.5 Low pH iso-osmotic treatment of cells

Cells were washed 3 times in R0 prior to the procedure. $0.5\text{-}5x10^6$ cells were gently resuspended in 0.3ml of filter-sterilized pH 2.4 PBS/1% bovine serum albumin

(BSA)(Cat.no. A9418, Sigma-Aldrich, UK)/300mM glycine (Cat.no. 410225, Sigma-Aldrich, UK) and incubated for 2min at RT. Acidic media was neutralized by adding 25ml of R0 to the cell pellet. Cells were washed 2 times with PBS/1%FBS and directly used in flow cytometry, confocal microscopy or IP experiments.

2.6 Flow cytometry

2.6.1 Flow cytometry of human cell lines and PBMC-derived cells

Suspension and adherent cells were transferred to 96-well, round bottom plates at 2-5x10^5 cells/well and washed 3 times with 200µl/well of PBS/1%FBS by centrifugation (1500rpm, 3min). In order to eliminate unspecific antibody binding, blood- and tissue-derived cells were incubated for 30min on ice in 30-50µl/well of blocking buffer (PBS/1%FBS/10% normal goat serum (NGS)/10% normal rabbit serum (NRS)/ 10%-50% heat inactivated (HI) human serum). Alternatively, human blood- and tissue-derived cells were blocked for 10min on ice using a commercial human FcR blocking reagent (1:10, Cat.no. 130-059-901, MACS Miltenyi Biotec, UK). Unconjugated, primary antibodies (HD6, HC10, ME1, W6/32, IgG2a, IgG1, see Table 2.3) at 1µg/well were added directly to the non-commercial blocking buffer and incubated for 45-60min on ice. Cells incubated with the human FcR blocking reagent were washed 3 times with PBS/1%FBS and subsequently incubated with primary antibodies at 1µg/well. After incubation with primary antibodies, cells were washed 3 times with PBS/1%FBS and incubated for 30-45min on ice, in the dark with a mixture of secondary antibody (0.25-0.5µg/well, see Table 2.3) and a 1:100 diluted LIVE/DEAD® violet stain (4µl/well, Cat.no. L34955, Invitrogen, UK). Cells were washed 3 times with PBS/1%FBS and fixed in 200µl/well of PBS/1.5% formaldehyde (fix buffer) (Cat.no. F1635, Sigma-

Aldrich, UK). Fixed cells were transferred to 5ml BD Falcon™ FACS tubes (BD Biosciences, UK) and acquired with the 9-colour CyAnADP flow cytometer (Dako, Denmark) or BD LSRFortessa™ cell analyzer (BD Biosciences, UK). Flow cytometry data were analyzed using FlowJo 8.7 software (Tree Star Inc.).

2.6.2 Flow cytometry of rat-derived cells

Spleens and lymph nodes (LNs) were gently mashed using 2ml syringe plunger on a 20µm cell strainer placed in a sterile Petri dish. Cell strainer was washed 3 times using 1ml of PBS/1%FBS. Cell suspension was aspirated from the Petri dish and placed in a BD Falcon™ 15ml tubes (BD Biosciences, UK). Cells were span down (1500rpm, 5min) at RT, followed by 3 washes with PBS/1%FBS. Subsequently splenocytes and LN cells were stained with anti-MHCI (see Table 2.3) or non-MHCI antibodies for phenotypic screening (see Table 2.5) using a standard flow cytometry protocol and acquired with BD LSRFortessa™ cell analyzer (BD Biosciences, UK). Flow cytometry data were analyzed using FlowJo 8.7 software (Tree Star Inc.).

2.7 Confocal microscopy

2.7.1 Confocal microscopy of suspension cells

Suspension cells were stained with anti-MHCI antibodies (HD6, HC10, ME1 and W6/32) using a standard flow cytometry staining protocol. Subsequently, in order to stain nuclei cells were incubated with 200µl/well of 2.5µM SYTO®Green Fluorescent Nucleic Acid Stain (Invitrogen, UK) for 1h at 4°C. Cells were washed 2 times with PBS/1%FBS, resuspended in 300µl/well of fix buffer and visualized on 24-well Imaging Plate FC, with Fluorocarbon Film Bottom (Cat.no. PAA21313231, PAA, UK) using Zeiss LSM510 confocal microscope or Zeiss LSM710 multiphoton confocal microscope (Zeiss, UK). Confocal microscopy images were analyzed using ZEN software (Zeiss, UK).

2.7.2 Confocal microscopy of adherent cells

HeLa cells

Adherent HeLa cells were cultured on 24-well Imaging Plate FC, with Fluorocarbon Film Bottom. Cells were washed on plates with 1ml of PBS/1%FBS for 5min and fixed with 4% methanol-free formaldehyde in PBS (Cat.no 28906, Pierce 16% Formaldehyde (w/v), Methanol-free, Thermo Scientific) for 15min at RT. Fixative was aspirated from wells and cells were washed 3 times/5min with 1ml of PBS/1%FBS. Cells were incubated with 150µl/well of blocking buffer (PBS/1%FBS/10%NGS/10%NRS) for 30min on ice and washed 3 times/5min. Subsequently cells were incubated with primary, anti-MHCI antibodies (HD6, HC10, ME1 and W6/32) at 1µg/well in blocking buffer, for 1h on ice. Cells were washed 3 times/5min in PBS/1%FBS and incubated with 150µl/well of secondary antibody (0.5µg/well) on ice, in the dark. In order to stain cell nuclei, cells were washed 3 times/5min in PBS/1%FBS and incubated with 200µl/well of 2.5µM SYTO®Green Fluorescent Nucleic Acid Stain (Invitrogen,UK) for 1h at 4°C. Cells were washed 3 times with PBS, resuspended in 300µl/well of fix buffer and visualized using Zeiss LSM710 multiphoton confocal microscope. Confocal microscopy images were analyzed using ZEN software (Zeiss, UK).

Human blood-derived cells

Monocyte-derived macrophages and monocyte- or PBMC-derived osteoclasts cultured on 24-well Imaging Plate FC, with Fluorocarbon Film Bottom, were gently washed 3 times on plates with 1ml of PBS/1%FBS. Unspecific antibody binding was blocked with non-commercial blocking buffer for 30min, on ice. Alternatively in some experiments OCs were blocked with commerical human FcR blocking reagent (MACS Miltenyi Biotec, UK) for 10min, on ice and washed 3 times/5min on plates with 1ml of PBS/1%FBS. Subsequently, cells were stained with anti-MHCI primary antibodies for 1h on ice. After 3 times/5min washes on plates with 1ml of PBS/1%FBS secondary antibody staining was performed. In order to stain nuclei cells were incubated with 200µl/well of 2.5µM SYTO®Green Fluorescent Nucleic Acid Stain (Invitrogen, UK). Cells were washed 3 times/5min in PBS/1%FBS, resuspended in 4% methanol-free formaldehyde in PBS (Cat.no 28906, Pierce 16% Formaldehyde (w/v), Methanol-free, Thermo Scientific, UK) and visualized on plates using Zeiss LSM710 multiphoton confocal microscope. Confocal microscopy images were analyzed using ZEN software (Zeiss, UK).

2.8 Immunoprecipitation (IP) of cell surface proteins

$10x10^6$ cells were washed with 25-40ml of PBS/1%FBS in a 50ml Falcon™ tube. Cell pellets were resuspended in 200µl/10µg/well of HD6 or HC10 antibody and incubated for 1h on ice. Cells were washed 5 times with 25-40ml of PBS. Subsequently cells were resuspended in 1ml of cell lysis buffer, PBS supplemented with: 20mM Tris, 150mM NaCl, 0.5% Nonidet P40 (NP40) (Cat.no. 56009 2L, BDH Laboratory Supplies, UK), 10mM iodoacetamide (IAA) (Cat.no. 1149, Sigma-Aldrich, UK), 1x diluted protease inhibitor (Cat.no. 05892791001, CompleteULTRA®Tablets, Mini, EDTA-free, Roche, UK) and transferred to eppendorfs. Cell were incubated in lysis buffer for 1h at 4°C, on the rotor. In order to pellet cell debris post lysis, eppendorfs were centrifuged (13000rpm, 15min, 4°C). Supernatants were transferred to new eppendorfs and incubated for 1h at 4°C, on the rotating mixer with 50µl/eppendorf of Dynabeads® Sheep anti-Mouse IgG (Cat.no. 112-01D, Novex®, Life Technologies, UK). Magnetic beads with bound proteins were washed 4 times with 1ml of lysis buffer on a magnet, followed by 2 washes with 1ml of lysis buffer base without NP40. In order to increase the efficiency of washing steps, the solution of proteins with bound Dynabeads® in lysis buffer were transferred to new eppendorfs. After last wash magnetic beads with bound proteins were resuspended in 50-60µl of 1x NuPAGE® lithium dodecyl sulfate (LDS) sample loading buffer (Cat.no. NP0007, Life Technologies, UK). In order to dissociate proteins from Dynabeads® LDS solutions were incubated for 5min in thermal block (90°C), cooled down to RT and briefly centrifugated. Eppendorfs with solutions containing immunoprecipitated HD6- or HC10-reactive molecules were placed on a magnet to separate proteins from magnetic beads. Immunoprecipitated proteins were analyzed by gel electophoresis followed by western blot with HC10-HRP conjugated antibody.

2.9 Gel electrophoresis and western blot

Samples were diluted in 1x LDS sample buffer, 10-20µl was loaded into well of NuPAGE® Novex® 4-12% Bis-Tris Gel (Cat.no. NP0322, Life Technologies, UK) and run a 1x solution of NuPAGE® MOPS SDS Running Buffer (Cat.no. NP0001, Life Technologies, UK). Proteins were transferred onto PVDF membrane using iBlot Transfer Stack and iBlot 7-minute Blotting System (Life Technologies, UK). Membranes were soaked in deionized (DI) water, followed by 30min incubation with blocking buffer: 5% Nonfat Dry Milk (Cat.no. 9999S, Cell Signaling TECHNOLOGY®, UK) in PBS/0.5% Tween®20 (Cat.no. P5927, Sigma-Aldrich, UK) at RT, on a shaker. Subsequently membranes were incubated overnight (O/N) with 1/1000 of HC10-HRP mAb in a blocking buffer, at 4°C, on a shaker. After O/N incubation with detection antibody membranes were washed 3 times/10min with PBS/0.5% Tween®20. Membranes were incubated for 1min with ECL™ Western Blotting Detection Reagent (Cat.no. RPN2209, Amersham™, GE Healthcare, UK). Detection reagent was removed, membranes were exposed to Hyperfilm™ ECL (Cat.no 28906837, Amersham™, GE Healthcare, UK) in the dark room and filmes were developed using CRUX60 Agfa film processor (Agfa, UK).

2.10 Exogenous peptide addition to cell culture

HLA-B27-binding peptide, SRYWAIRTR (influenza nucleoprotein (NP), residues 383-391) or control HLA-A2-binding peptide, GILGFVFTL (influenza matrix protein, residues 58-66) were resuspended in R0 solution at 1mg/ml and filter sterilized. Peptides were added at the final concentration of 100μM to 220-B27 TPN cells cultured at $1x10^6$ cells/ml. Peptide-pulsed cells were incubated for 20h prior immunoprecipitation. Peptides were synthesized and kindly provided by Dr Kati di Gleria and Zhanru Yu.

2.11 Preparation and immunohistochemistry (IHC) of paraffin-embedded tissue sections

2.11.1 IHC of patient-derived knee synovial tissue sections

Paraffin-embedded knee synovial tissue sections derived from inflamed joints of B27+ve or B27-ve SpA (including PsA) patients were kindly provided by Prof. Baeten's lab (Academic Medical Centre, University of Amsterdam). Tissue sections on slides were stored at 4°C. Slides were adjusted to RT before deparaffinization procedure. Tissue sections were stretched at 60°C for 15min and subsequently adjusted to RT. Next, tissue sections were deparaffinized by 2x4min incubation in a xylene (Sigma-Aldrich, UK) bath, followed by 2x4min incubation in 100% ethanol (VWR International Ltd., UK), 1x4min 96% ethanol and 1x4min 70% ethanol. Deparaffinized slides were washed 2x4min in tap water followed by 3x5min wash in PBS. Slides were briefly dried and tissues were marked with the ImmEdge™ Pen (Cat.no. H-4000, Vector Labs). Tissue sections were incubated with few drops of dual endogenous enzyme block for 10min at RT (Cat.no. S2003, DAKO, UK) and washed 3 times/5min in PBS. Unspecific FcR antibody binding was blocked by 15min incubation at RT with human FcR blocking reagent (MACS Miltenyi, UK) (1/10 in PBS/1%FBS). Tissue sections were washed 3 times/5min in PBS and incubated for 30min at RT in PBS/1%FBS/10%NGS blocking buffer, followed by 3 times, 5min washes in PBS. Next, tissue sections were incubated O/N with primary antibodies: 1μg/ml of HD6, 0.5μg/ml of HC10 or isotype controls: 1μg/ml IgG1 and 0.5μg/ml IgG2a in PBS/1%FBS in a humid box, at 4°C. After O/N incubation slides were washed 3-5 times/5-10min in PBS.

HD6 staining

Tissues stained with HD6 and IgG1 antibodies were incubated for 30min at RT with secondary Goat anti-Mouse IgG1-biotynylated antibody (Cat.no. 1070-08, Southern Biotech, UK) at 1/2500 dilution in PBS/1%FBS. HD6- and IgG1-stained tissue sections were washed 3 times/5min with PBS, followed by 30min incubation with streptavidin-HRP (Cat.no. P0397, DAKO, UK) (1/200) at RT. Slides were washed 3 times/5min with PBS.

HC10 staining

Slides stained with HC10 or IgG2a primary antibodies were washed 3-5 times/5-10min and incubated for 30min at RT with peroxidase labelled polymer conjugated to Goat anti-Mouse immunoglobins (IgGs) (Cat.no. K4001, DAKO, UK). Slides were washed 3 times/5min with PBS.

Subsequently both HD6- and HC10-stained tissue sections and isotype controls were washed 3 times/5min in PBS and incubated with Ready-to-Use AEC+High Sensitivity Substrate Chromogen (Cat.no. K3469, DAKO, UK) for 5-30min (until the desired change of red staining appeared) at RT. After rinsing with DI water, tissue sections were incubated for 5-10min with Mayer's Hematoxilin in order to stain cell nuclei. To increase the intensity of nucelar blue stain tissue sections were incubated for 10min in warm tap water. In a final step, slides were washed in a DI water and dried O/N by air. Dried tissue sections were mounted with Keiser's glycerol gelatine (Cat.no. 109242, Merck Milipore, UK) and covered with glass coverslips (VWR International Ltd., UK). Slides were scanned using Aperio CS2 Scanner (Leica Biosystems, UK) and analyzed using Aperio ImageScope software (Leica Biosystems, UK).

2.11.2 Preparation and IHC of rat-derived tissues

Tissue section preparation

Rat tail and ankle joint tissues were obtained from B27 TG, B7 TG and WT Lewis animals (Table 2.4). Skin and excessive muscle tissue were removed with scissors. Joints were fixed in PBS/4% formalin for 48h and decalcified for 3 months in Osteosoft® solution (Cat.no. 101728, Merck Milipore) by Baeten's lab (Academic Medical Centre, University of Amsterdam). Decalcified joint tissues were embedded in paraffin blocks (at the Academic Medical Centre, University of Amsterdam). Paraffin-embedded tissues were sectioned in 4μm slices using disposable microtome blades (Feather, N35, VWR International Ltd., UK) with Leica microtome. Tissue sections were gently floated at the surface DI water (in a 37°C water bath) and attached to Superfrost® adhesion glass slides (VWR International Ltd., UK). Tissue sections were stretched and fixed to the glass slides by O/N incubation at 56°C. After O/N incubation slides were adjusted to RT and stored at 4°C.

IHC staining of rat tissue sections

Rat tail and ankle joint tissue sections were deparaffinized and prepared for the IHC staining as described for human-derived tissue sections. Slides were washed 3 times/5min in PBS and incubated with blocking buffer (PBS/1%FBS/10%NGS/10% rat serum) for 1h at RT. Tissue sections were washed and stained with HD6, HC10 or isotype control antibodies according to the previously described for human tissue sections IHC protocol. Stained tissue sections were scanned using Aperio CS2 Scanner (Leica Biosystems, UK) and images were analyzed with Aperio ImageScope software (Leica Biosystems, UK).

Table 2.1 Cell lines and AS patient and healthy donor blood-derived cells

Cell type	Description	Source
HeLa	Human epithelial carcinoma cell line. Cultured in D10.	ATCC Number CCL-2
HeLa-B27	HeLa cell line lentivirally transduced with HLA-B27 plasmid. Cultured in D10.	Rysnik O.
LB 721.220 (220)	Human lymphoblastoid B cell line (LCL) 220 lacks the expression of HLA-A, HLA-B alleles and functional tapasin (Copeman, Bangia, Cross, & Cresswell, 1998). Cultured in R10.	Elliot T.
LB 721.220-B27 (220-B27)	220 cell line lentivirally transduced with HLA-B27 plasmid. Cultured in R10.	McHugh K.
LB 721.220-B27 TPN (220-B27 TPN)	220 cell line lentivirally transduced with TPN and HLA-B27 plasmids. Cultured in R10.	McHugh K.
LB 721.220-B7 (220-B7)	220 cell line lentivirally transduced with HLA-B7 plasmid. Cultured in R10.	McHugh K.
LB 721.221 (221)	Human lymphoblastoid cell line (LCL) 221 lacks expression of all HLA-A, -B and -C MHC class I alleles (Shimizu, Geraghty, Koller, Orr, & DeMars, 1988). Cultured in R10.	McHugh K.
LB 721.221-B27 (221-B27)	221 cell line lentivirally transduced with HLA-B27 plasmid. Cultured in R10.	McHugh K.
LB 721.221-B35 (221-B35)	221 cell line lentivirally transduced with HLA-B35 plasmid. Cultured in R10.	McHugh K.
Jesthom B27+ve BCL	Commercially available non-AS donor blood-derived B cell line with the natural MHCI expression homozygous: HLA-B*27:05, HLA-A*02:01 and HLA-Cw*01:02. Cultured in R10.	McHugh K.
B27+ve BCL	In house generated non-AS donor blood-derived B cell line with the original MHCI expression carrying HLA-B*27:05 allele. Other HLA class I alleles unknown. Cultured in R10.	McHugh K.
B27-ve BCL	In house generated healthy donor blood-derived B cell line with the original MHCI expression, HLA-B27-ve. Other HLA class I alleles unknown. Cultured in R10.	McHugh K.
Monocyte-derived dendritic cells, macrophages and osteoclasts	Cells cultured from monocytes isolated from AS patient- or healthy control-derived PBMCs. Cultured in R10 with cytokine supplements (see text).	Rysnik O.
Synovial tissue cells	AS patient-derived synovial tissue cells. Samples obtained from the hip replacement.	Ridley A.

Table 2.2 Cell culture media

Media	Descrition	Use
R0	Roswell Park Memorial Institute (RPMI)-1640 media (Cat.no. R8758, Sigma, UK).	Washing steps (PBMCs isolation, post acid treatment)
R10	R0 supplemented with 2mM L-glutamine (Cat.no. BE17-605E), 50U/ml penicillin/streptomycin (Cat.no. DE17-603E, Lonza Group Ltd, Switzerland) and 10% HI FBS (Cat.no. F9665, Sigma,UK).	Cell culture LCLs and BCLs
R10 + G418	R10 supplemented with selective antibiotic 0,5mg/ml Geneticin®, G418 sulphate (Cat.no. 11811, Gibco, UK).	Selection media, lentiviral-transduced cells
R10 + cytokines	R10 supplemented with 1000U/ml recombinant human GM-CSF (Cat.no. 300-03, Peprotech, UK) and 500U/ml recombinant human IL-4 (Cat.no. 200-04, Peprotech, UK) or recombinant human M-CSF 25ng/ml (Cat.no. 300-25, Peprotech, UK)	AS patient and healthy donor moDC or Mϕ culture
MEM10	Minium Essential Medium (MEM) Alpha Medium, (-) Ribonucleosides, (-) Deoxyribonucleosides (Cat.no. 22561, Gibco® by Life Technologies™) supplemented with 2mM L-glutamine (Cat.no.BE17-605E), 50U/ml penicilin /streptomycin (Cat.no.DE17-603E, Lonza Group Ltd, Switzerland) and 10% heat-inactivated (HI) fetal bovine serum (FBS) (Lonza. Cat.no AE-1480/FH).	AS patient and healthy donor monocyte- and PBMC-derived osteoclast culture
D10	Dulbecco's Modified Eagle Medium (DMEM) (Cat.no.D5786, Sigma, UK) 2mM L-glutamine, 50U/ml penicillin/streptomycin, 10% FBS.	HeLa and HeLa-B27 cell culture

Table 2.3 MHCI staining antibodies

Antibody	Description	Source/ used concentration
HC10 **(Mouse IgG2a)**	Recognises unfolded, FHCs, not associated with β2-microglobulin (β2m) HLA-B, -C, and some -A alleles (Stam, Spits, & Ploegh, 1986). Used in flow cytometry/confocal microsocpy/IP.	Made in house $1\mu g$ / $0.5\text{-}1.0\text{x}10^6$ cells
HC10-HRP	HC10 conjugated with HRP used in western blots.	Made in house 1/5000
ME1 **(Mouse IgG1)**	Was reported to recognise HLA-B27, -B7, B-14 alleles (Barnstable et al., 1978).	Made in house $1\mu g$ / $0.5\text{-}1.0\text{x}10^6$ cells
W6/32 **(Mouse IgG2a)**	Recognises folded MHCI molecules (Ellis, Taylor, & McMichael, 1982).	Made in house $1\mu g$ / $0.5\text{-}1.0\text{x}10^6$ cells
HD6 **(IgG1)**	Antibody generated in the phage display technology against $B27_2$ (Payeli et al., 2012). Chimeric antibody with human Fab and mouse Fc fragment.	Renner C. (University of Zurich), in house $1\mu g$ / $0.5\text{-}1.0\text{x}10^6$ cells
Alexa Fluor 633 or 647 **Goat Anti-Mouse IgG F(ab')$_2$**	Secondary antibody used in flow cytometry and confocal microscopy experiments.	Invitrogen $0.5\mu g$ / $1.0\text{x}10^6$ cells
Mouse IgG2a ϰ	Isotype control	BD Pharmingen™ $0.5\mu g$ / $1.0\text{x}10^6$ cells
Mouse IgG1 ϰ	Isotype control	BD Pharmingen™ $0.5\mu g$ / $1.0\text{x}10^6$ cells

Table 2.4 Rat lines used in flow cytometry and IHC experiments

Rat strain	Cell and tissue type	Source
(21-3x283-2)F1 HLA-B27 huβ2m transgenic rats (B27 TG[2])	Flow cytometry: PBMCs, SPLCs and LN cells; IHC: ankle and tail joints.	Prof. Baeten D. Academic Medical Centre, University of Amsterdam
(120-4x283-2)F1 HLA-B7 huβ2m transgenic rats (B7 TG)	Flow cytometry: SPLCs and LN cells; IHC: ankle and tail joints.	Prof. Baeten D. Academic Medical Centre, University of Amsterdam
Non-transgenic Lewis rats (WT)	Flow cytometry: SPLCs and LN cells; IHC: ankle and tail joints.	Prof. Baeten D. Academic Medical Centre, University of Amsterdam

Table 2.5 Non-MHCI antibodies used in flow cytometric analysis of rat cells

Antibody	Clone/Isotype/Cat.no.	Source
FITC **Mouse Anti-Rat CD4**	OX-38; IgG2a, ϰ Cat.no. 554843	BD Pharmingen
PerCP **Mouse Anti-Rat CD8α**	OX-8; IgG1, ϰ Cat.no. 558824	BD Pharmingen
PerCP **Mouse Anti-Rat RT1B (MHCII)**	OX-6; IgG1, ϰ Cat.no. 557016	BD Pharmingen
Alexa Fluor 488 **Mouse Anti-Rat CD11bc**	OX-42; IgG2a, ϰ Cat.no. 201812	BioLegend
Alexa Fluor 488 **Mouse Anti-Rat CD11b**	OX-42; IgG2a, ϰ Cat.no. MCA275A488	AbD Serotec
PE **Mouse Anti-Rat CD161**	3.2.3; IgG1, ϰ Cat.no. 205604	BioLegend
FITC **Mouse Anti-Rat CD45R**	HIS24; IgG2b, ϰ Cat.no. 554880	BD Pharmingen

Chapter Three: Expression of non-classical forms of HLA-B27 in human cell lines

3.1 Introduction

The lymphoblastoid B cell line (LCL) 721.220 (220) lacks the expression of HLA-A, HLA-B alleles and functional tapasin (TPN) (Copeman, Bangia, Cross, & Cresswell, 1998). Tapasin is one of the peptide loading complex (PLC) proteins. The PLC is crucial in MHCI processing and TPN catalyses peptide loading onto the MHCI molecules in endoplasmic reticulum (ER). There is a wide spectrum of TPN dependence between different HLA alleles and B27 is amongst the ones characterized by the low tapasin-dependency. Consequently, reduced quality control of peptides loaded onto B27 in the ER may promote binding of low-affinity peptides. These peptide-receptive MHCI complexes might escape the quality control in the ER and Golgi, reach cell surface and consequently form NC-B27 molecules.

LCL 721.221 (221) lacks expression of all HLA-A, -B and -C MHC class I alleles. This mutant cell line was derived from LCL 721 by immunoselection and subsequent gamma-ray mutagenesis that abolished expression of HLA-A, -B and -C alleles (Shimizu, Geraghty, Koller, Orr, & DeMars, 1988).

Hence, transfection of both 220 and 221 cell lines with a single HLA gene construct enables us to study the nature and behaviour of various MHCI molecules. Furthermore, 220 cell line is a great tool to study the dependence of different HLA class I alleles on TPN.

The Bowness group has previously proposed that non-classical forms of HLA-B27 (NC-B27), including free heavy chains (FHC) and FHC dimers ($B27_2$), may play a role in the pathogenesis of SpA (Bowness, Zaccai, Bird, & Jones, 1999; Cauli et al., 2013; Chen et al., 2014; Giles et al., 2012; Kollnberger et al., 2002; McHugh et al., 2014; Payeli et al., 2012; Wong-Baeza et al., 2013). It was postulated that these NC-B27 molecules can accumulate at the cell surface and bind to immune receptors such as KIRs and LILRs with a higher affinity than other MHCI molecules. Furthermore, although KIR3DL2 has been previously shown to bind HLA-A3 and -A11 in the peptide-dependent manner, its binding to NC-B27 molecules was a new concept. NC-B27:immune receptors interactions could lead to altered immune regulation and promote inflammation in AS. As mentioned in the introduction, the novel HD6 antibody has been shown to react specifically with recombinant $B27_2$ protein (Payeli et al., 2012). Therefore, studying the surface expression of HD6-reactive molecules in 220-B27 and 221-B27 cell lines by confocal microscopy and immunorecipitation could help understand the unusual nature of these NC-B27 molecules.

3.2 Investigation of cell surface expression of HLA-B27 by confocal microscopy

3.2.1 HD6-reactive molecules are detected in B27-expressing cell lines and form clusters at the cell surface

It has been demonstrated previously using flow cytometry that NC-B27 species detected with HD6 are present both intracellulary and at the cell surface of B27-transfected cells (including HeLa-B27, 220-B27 and 221-B27 cell lines) (McHugh et al., 2014). However, as yet no-one has investigated the cell surface expression of these NC-B27 molecules by confocal microscopy. Studying the expression patterns of NC-B27 in cell lines using the novel HD6 B27-reactive antibody by confocal microscopy could indicate the organization and behaviour of B27 at the cell surface, as well as enable to establish working protocols to investigate NC-B27 expression in AS patient-derived cells.

Importantly, surface-expressed MHCI molecules are sensitive to a variety of factors including cell fixatives, environmental factors, the composition of culture media and staining solutions, as well as to cell viability. For instance, cell fixatives (paraformaldehyde, methanol) and cell detachment methods (trypsinization), commonly used in staining protocols can affect the structure and antibody binding epitopes of properly folded and NC-B27 and their organization in a cell membrane. Therefore, my first aim was to optimise an immunofluorescence staining protocol for intact HLA proteins at the surface of live, adherent HeLa cells (see Materials and methods). Unconjugated primary antibodies (HD6, ME1, HC10 and W6/32) and fluorophore-conjugated secondary antibodies (see Material and methods for further antibody details) were used to characterise different forms of MHC class I molecules at the cell surface. Both HD6- and HC10-reactive molecules were observed as patches at the cell surface of B27-transfected HeLa cells (HeLa-B27) (Figure 3.1, A-C). Moreover, these forms of NC-B27 tended to accumulate above the perinuclear region, with HD6-reactive molecules almost exclusively confined to this region (Figure 3.1, A and B). Interestingly, this is in agreement with Matko *et al*. (Matko, Bushkin, Wei, & Edidinr, 1994) who also observed MHC class I free-heavy chains clustering at the cell surface. Importantly, properly folded B27 (ME1 staining) showed evenly distributed membrane staining (Figure 3.1, D).

To confirm the staining patterns observed by confocal microscopy, parallel flow cytometry analysis was carried out in B27-transfected and non-transfected HeLa cells with the same antibody set (Figure 3.2).

Figure 3.1 NC-B27 molecules form clusters at the surface of HeLa-B27 cells. Confocal microsocpy analysis of the MHCI expression patterns in HeLa-B27 cells. A) HD6; B) HD6, 63X objective; C) HC10; D) ME1 and E) IgG1 ; F) IgG2a isotype controls. Magenta (secondary antibody Alexa Fluor 633); Blue (nuclear stain DAPI). Pictures A, C, D, E and F were taken with a 40X objective using Zeiss LSM510 confocal microscope. Representative of n=3 experiments.

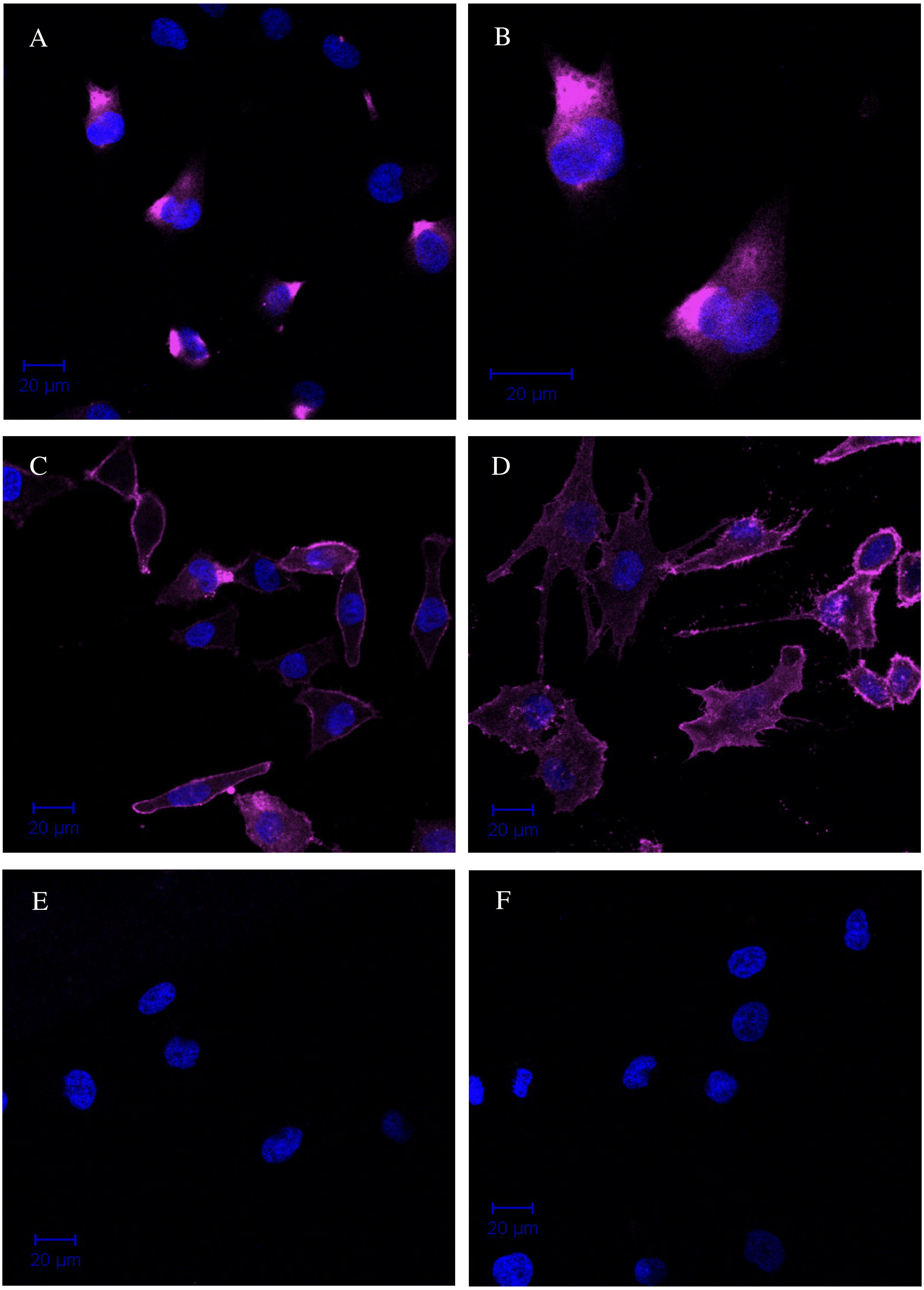

Figure 3.2 Flow cytometry analysis of MHCI expression in HeLa-B27 and non-transfected HeLa cells. A) HeLa-B27 and B) non-transfected HeLa cells. Green histograms - HD6; Orange histograms - HC10; Blue histograms - ME1; Gray histograms - IgG1 and IgG2a isotype controls. Numbers in the histogram legends - GeoMeanMFI. Representative of n=5 experiments.

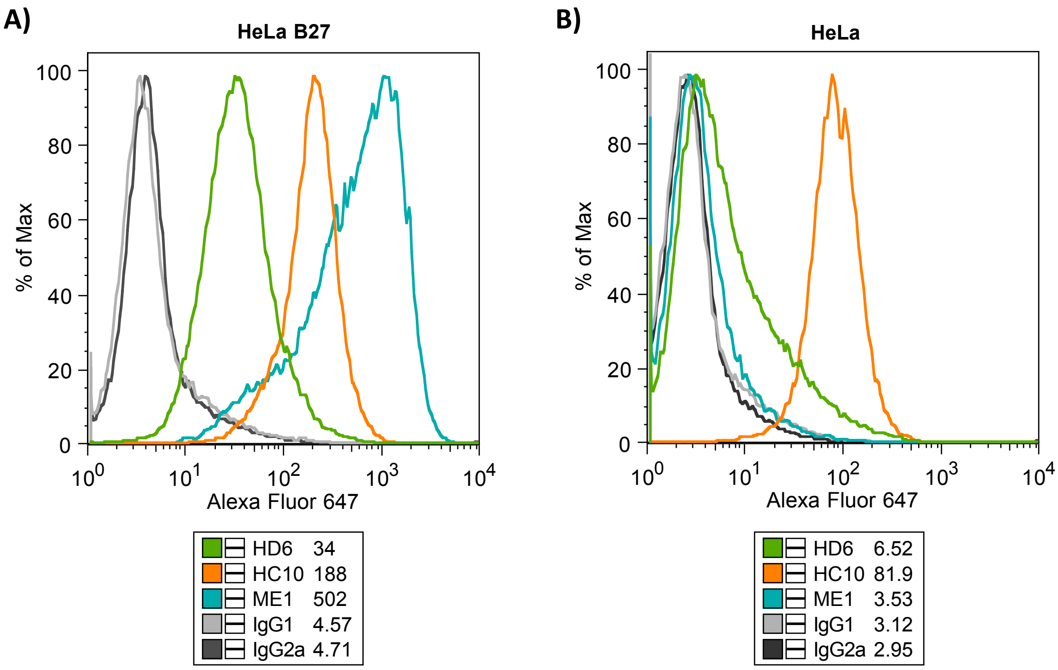

It has been previously demonstrated by flow cytometry that HD6-reactive molecules are expressed at relatively high levels at the surface of 220-B27 and 221-B27 cells (McHugh et al., 2014; Payeli et al., 2012), however their organization at the cell surface has not been investigated. Therefore, my next approach was to determine expression patterns of classical and NC-B27 molecules in 221-B27 and 220-B27, non-adherent cells using confocal microscopy. In contrast to HeLa cells, confocal microscopy of non-adherent cells was not as straightforward. One issue with imaging suspension cells is the need to attach them to coverslips, which may affect their phenotype and cell surface expression of MHC class I molecules. To address this I stained 221-B27 cells according to the standard flow cytometry protocol, then resuspended cells in a fixative on a fluorocarbon film bottomed 24-well plate and imaged with the confocal microscope. This enabled me to stain live cells and image them in a cell suspension without the need to attach them to the plate and risk modifying their cell surface molecules.

For the 221-B27 cells NC-B27, HD6 (Figure 3.3, A and B) and HC10 (Figure 3.3, C and D) were detected at the cell surface in clusters. Moreover, properly folded class I molecules (ME1) were evenly distributed at the cell surface and showed significantly distinct staining patterns compared with HD6 and HC10 (Figure 3.4, A and B). This is in agreement with the observed staining pattern of the B27-transduced HeLa cells. The different staining patterns observed with the ME1 compared with HD6 and HC10 antibodies could be due to different expression levels of classical and NC-B27 at the cell surface.

Fluorescence signals observed in staining using HC10 or HD6 antibodies are significantly lower in 221-B27 cells and B27-HeLa cells compared with signals detected using ME1. As before, parallel flow cytometry of 221-B27 cells and control cell lines (221 and 221-B35) was performed in order to confirm confocal microscopy results (Figure 3.5).

Figure 3.3 NC-B27 molecules form clusters at the surface of 221-B27 cells. Confocal microscopy of HD6 - A) and B), and HC10 staining - C) and D) in 221-B27 cells. Red (secondary antibody Alexa Fluor 647). Green (nuclear stain SytoGreen 21). Pictures A) and C) - 40X objective, B) and D) 2X magnification of pictures A) and C). Pictures taken with Zeiss LSM710 confocal microscope and analyzed using ZEN software. Representative of n=3 experiments.

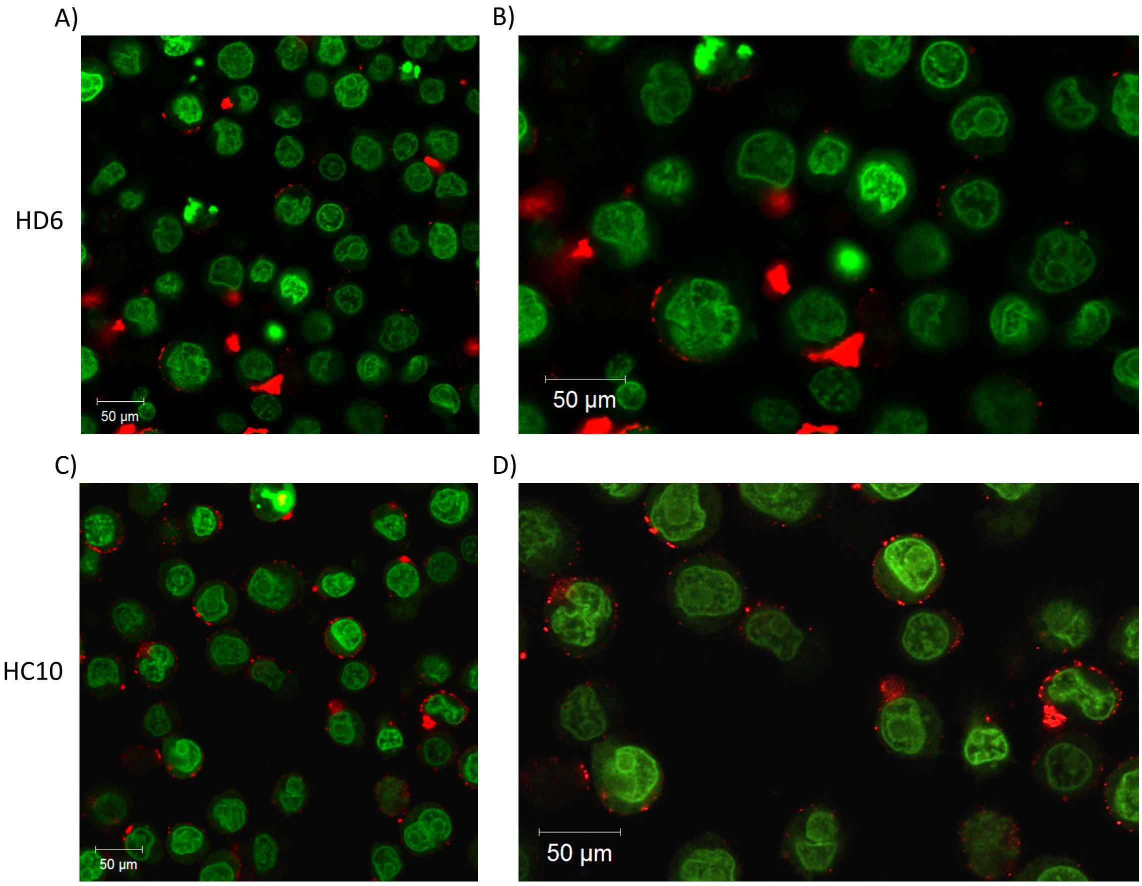

Figure 3.4 Cell surface ME1-reactive molecules are evenly distributed at the surface of 221-B27 cells. A) and B) ME1 staining in 221-B27 cells; C) ME1 staining in control 221 cells; D) IgG1 isotype control staining in 221-B27 cells. Red (secondary antibody Alexa Fluor 647). Green (nuclear stain SytoGreen 21). Pictures A, C, and D - 40X objective, B) 3X magnification of A). Pictures taken with Zeiss LSM710 confocal microscope and analyzed using ZEN software. Representative of n=3 experiments.

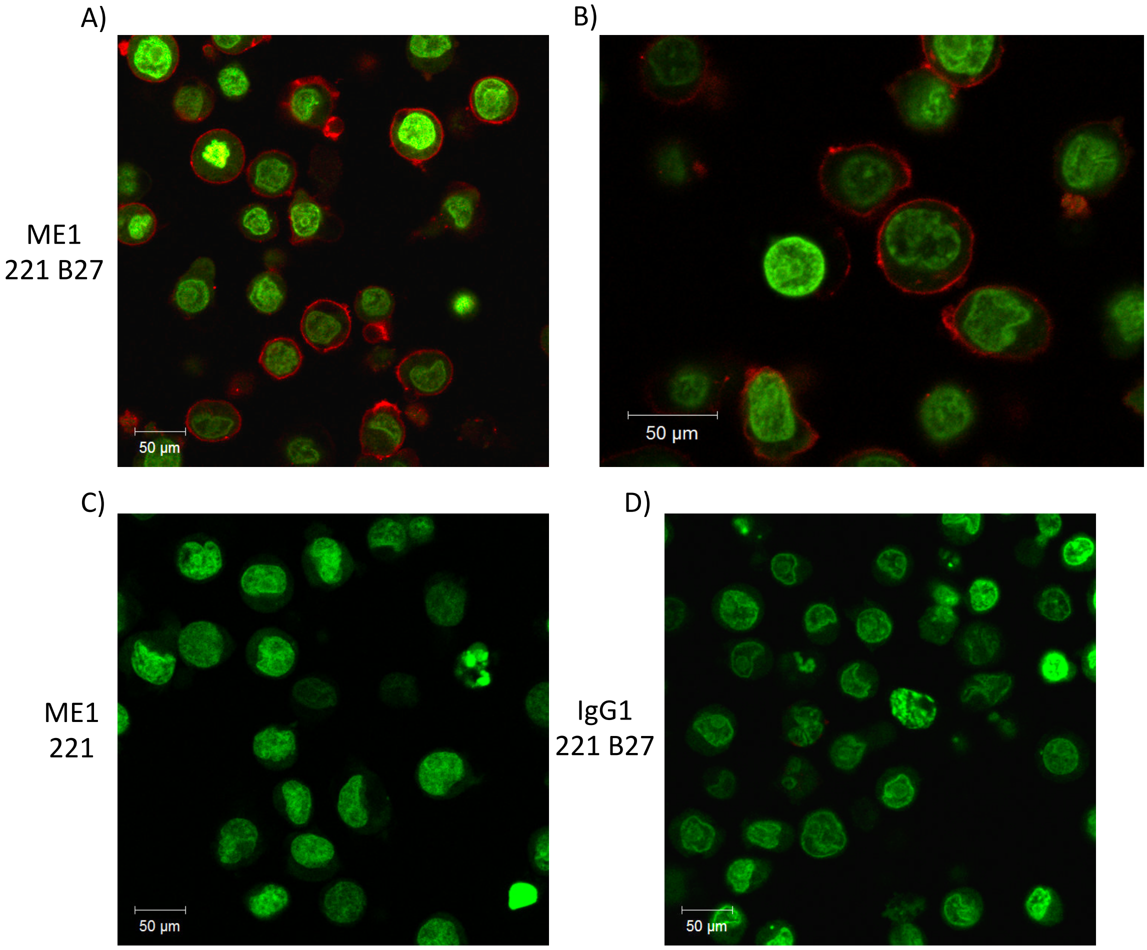

Figure 3.5 HD6-reactive molecules are expressed specifically in 220-B27 and 221-B27 cell lines. A) HD6 staining in 220-B27, 221-B27 (Green histograms) and control 220-B7 and 221-B35 (Blue histograms) cell lines. B) Expression of different forms of HLA-B27 molecules in 220-B27 cells. Representative flow cytometry histograms from n=5 experiments.

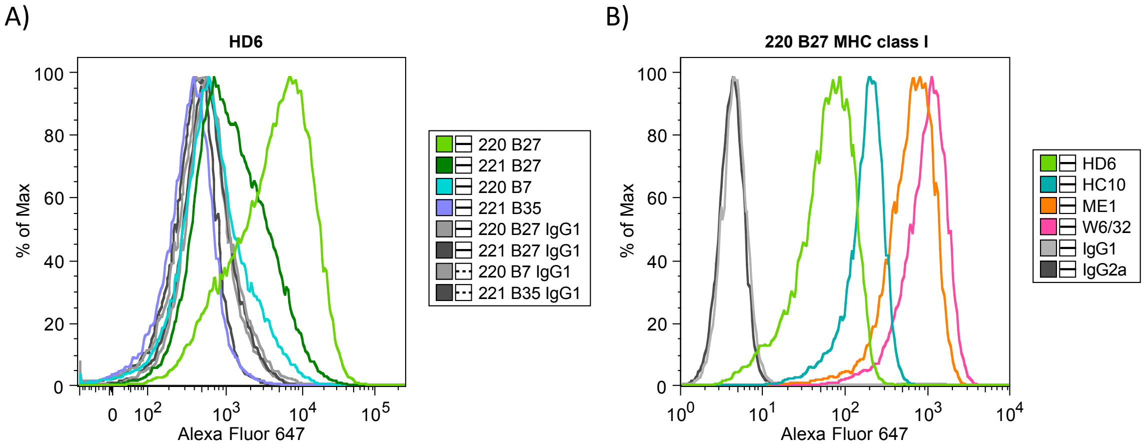

3.2.2 Low pH treatment of 221-B27 cells induces surface HD6- and HC10-reactive molecules detected by confocal microscopy

Brief low pH treatment (2 min, pH=2.4, 'acid treatment') of cells removes surface β2-microglobulin (β2m) and peptide from properly folded cell surface MHCI molecules, leaving heavy chains associated with the cell membrane (Malik, Klimovitsky, Deng, Boyson, & Strominger, 2002; Zeh et al., 1994). McHugh *et al*. previously showed by flow cytometry that acid treatment of B27-expressing cell lines can induce and/or increase surface staining of HD6 and HC10 (McHugh et al., 2014). However, how these 'induced NC-B27' molecules are organized at the cell surface was not investigated. Therefore I next sought to determine if acid treatment has an influence on NC-B27 organization in the cell membrane. This would enable us to investigate where these 'induced NC-B27' molecules originate from; they could be simply a consequence of stripping β2m and/or peptide from the folded cell surface B27 complexes, or alternatively the acid treatment may affect the transport of B27 molecules within the recycling compartments.

Suspension cells were subjected to a 2min acid treatment prior to antibody staining, and than analysed by confocal microscopy as before. For 221-B27 cells, acid treatment increased the levels of HD6 and HC10 staining detected at the cell surface compared with untreated cells (Figure 3.6, HD6 and HC10 - A vs B). In contrast, as expected, ME1 staining indicative of properly folded B27 molecules was almost completely removed from the surface by acid treatment (Figure 3.6, ME1 - A vs B). Notably, the distribution of NC-B27 molecules after acid treatment resembled the distribution of classical B27 molecules before acid treatment, with no obvious localization or clustering patterns at the cell surface.

Summary Chapter 3.2

Taken together, I have demonstarted by confocal microsocpy that in adherent HeLa cells NC-B27 forms (HD6 and HC10 staining) have a tendency to cluster at the cell surface. Moreover, similar clustering can be observed at the surface of non-adherent 221-B27 cells, however no accumulation of HD6 staining was detected in perinuclear region. Additionally, I have demonstrated that formation of cell surface clusters is undetectable, when HD6 and HC10 staining levels are increased upon acid treatment.

Figure 3.6 Cell surface HD6- and HC10-reactive molecules are induced in 221-B27 cells following acid treatment. HD6 staining A) before and B) after acid treatment; HC10 C) – ACID and D) + ACID; ME1 E) – ACID and F) + ACID in 221-B27 cells. Magenta (secondary antibody Alexa Fluor 633). Green (nuclear stain SytoGreen 21). Pictures taken with a 40X objcective using Zeiss LSM510 confocal microscope and analyzed using ZEN software. Representative of n=3 experiments.

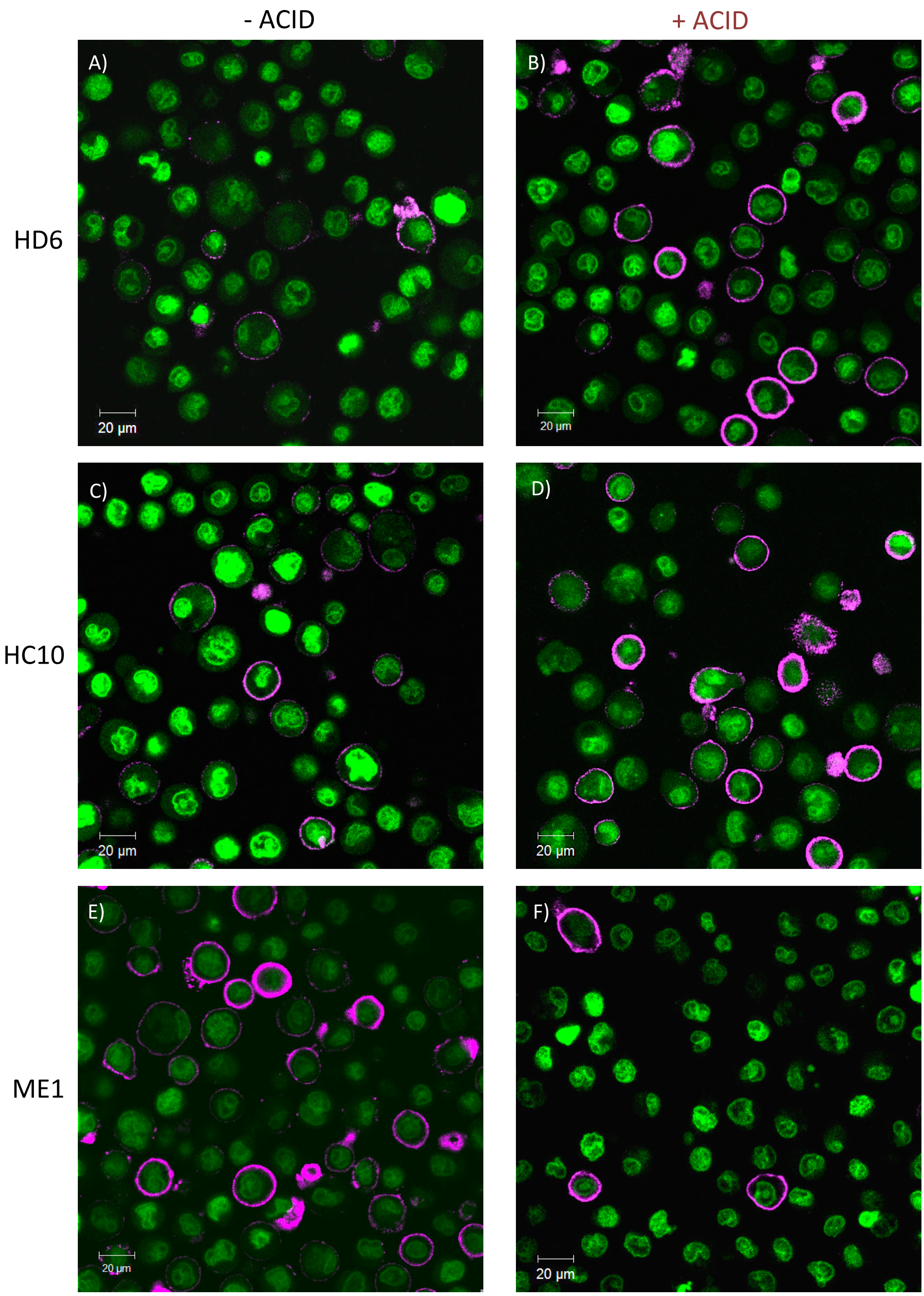

Figure 3.7 HD6- and HC10-reactive molecules are not detected in 221 control cell line before and after acid treatment. HD6 staining in control 221 cells A) before and B) after acid treatment. HC10 C) – ACID and D) + ACID. IgG1 isotype control staining in 221-B27 cells E) – ACID and F) + ACID. Magenta (secondary antibody, Alexa Fluor 633). Green (nuclear stain SytoGreen 21). Pictures taken with a 40X objective using Zeiss LSM510 confocal microscope and analyzed in ZEN software.

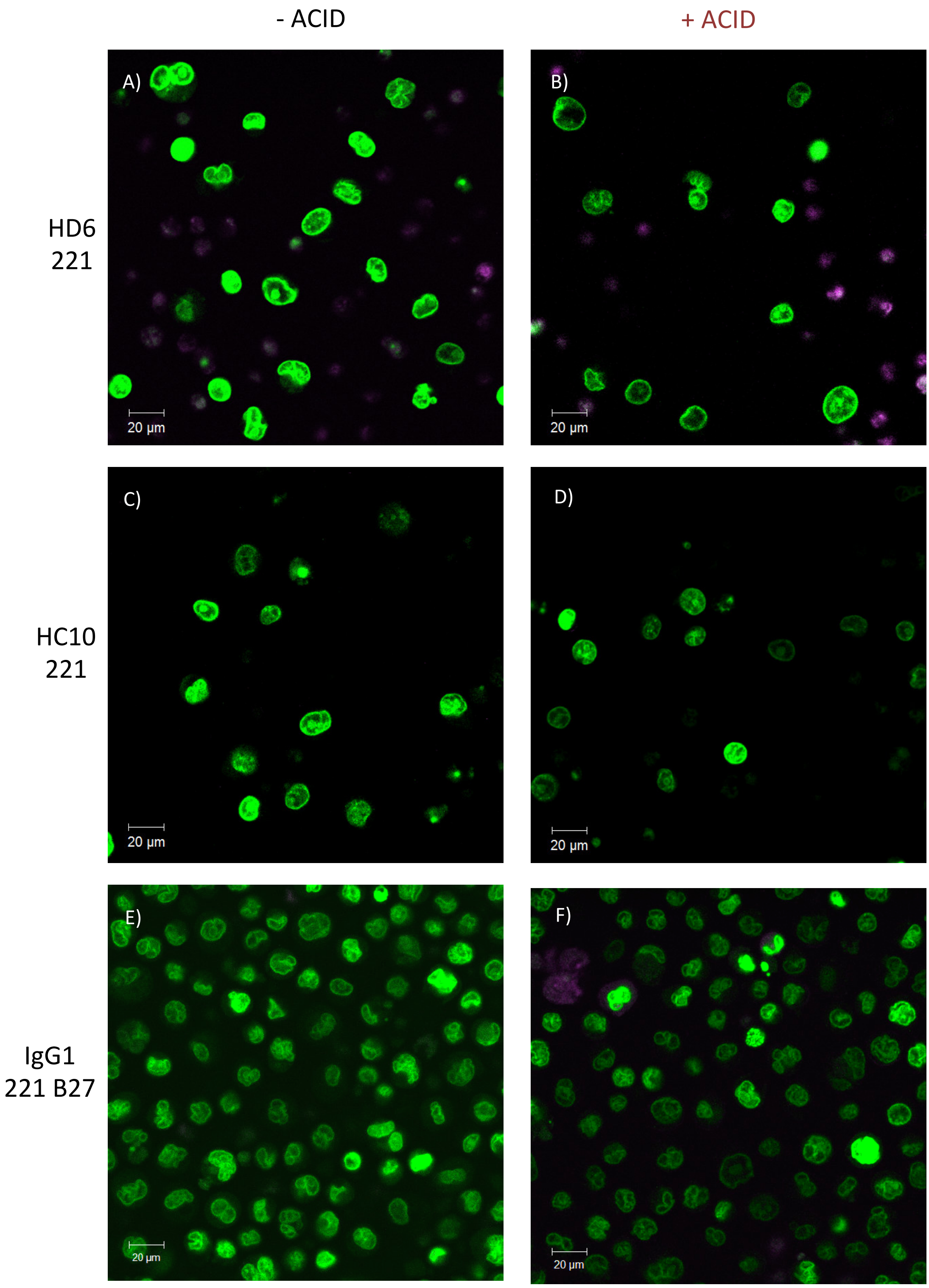

3.3 Immunoprecipitation of cell surface HD6-reactive molecules

3.3.1 HD6-reactive molecules can be immunoprecipitated from the surface of B27-expressing cell lines

Bird *et al*. have previously demonstrated that 220-B27 cells express HC10-reactive FHC homodimers both intracellulary and at the cell surface by immunoprecipitation (IP) (Bird et al., 2003). Two-dimensional gel electrophoresis confirmed that the high molecular weight (HMW) bands (>76kDa) observed in western blots consist of FHC. Further investigation of these NC-B27 molecules using the HD6 antibody also demonstrated the presence of NC-B27 at the surface of a number of B27-expressing cell lines, including 220-B27 and 221-B27 cells by flow cytometry (McHugh et al., 2014). In the previous section I have now also demonstrated that cell surface HD6-reactive molecules can be detected by confocal microscopy. However, nobody as yet has tested the HD6 antibody in cell surface IP experiments. Notably, cell surface IP experiments and subsequent western blot could give us a clue whether HD6-reactive molecules immunoprecipitated from the surface of B27+ve cell lines are represented by monomers (~45kDa) and/or HMW species (possibly FHC dimers and multimers).

Therefore, next 220-B27, 221-B27 and 221-B35 cell lines were stained on ice with the HD6 or HC10 antibody and subsequently lysed and immunoprecipitated with sheep anti-mouse IgG dynabeads. Iodoacetamide (IAA) was added to the lysis buffer to minimise post lysis dimer formation, as previously described (Bird et al., 2003). Non-reduced and reduced (+DTT) immunoprecipitated proteins were separated by gel electrophoresis and detected with HRP-conjugated HC10 antibody by western blot.

In the non-reduced samples, both monomeric FHC (~45kDa) and HMW species were immunoprecipitated from the surface of 220-B27 and 221-B27 cells with either HC10 or HD6 (Figure 3.8, A). Notably, there was a greater quantity of HMW species (>76kDa) compared with monomeric forms. Reducing conditions disrupt the disulphide bonds of proteins, including the predicted Cys67-Cys67 disulphide bond in B27 FHC homodimers, resulting in their reduction into monomers. As shown in Figure 3.8, B, under reducing conditions the majority of FHC dimers (HMW bands >76kDa) were reduced to monomers (~45kDa). These results suggest that HC10 and HD6 antibodies can immunoprecipitate FHC homodimers from the cell surface. Importantly, in both reduced and non-reduced IP samples, the HD6 antibody was specific to HLA-B27 molecules as no bands were seen in IP material from HLA-B35-expressing (221-B35) cells (Figure 3.8, Lane 6). Moreover, the HC10-reactive FHC and/or FHC homodimers were present in a greater quantity at the surface of B27-expressing cell lines compared with control 221-B35 cells (Figure 3.8, Lanes 1 and 3 vs Lane 5).

Figure 3.8 220-B27 and 221-B27 cell lines express relatively high levels of cell surface HD6- and HC10-reactive molecules in HMW form. Immunoprecipitation of cell surface HC10- and HD6-reactive molecules in 220-B27 (Lanes 1 and 2), 221-B27 (Lanes 3 and 4) and control 221-B35 (Lanes 5 and 6) cell lines. A) Non-reduced and B) reduced (+DTT) SDS-Page gel electrophoresis followed by western blot with HC10-HRP conjugated antibody.

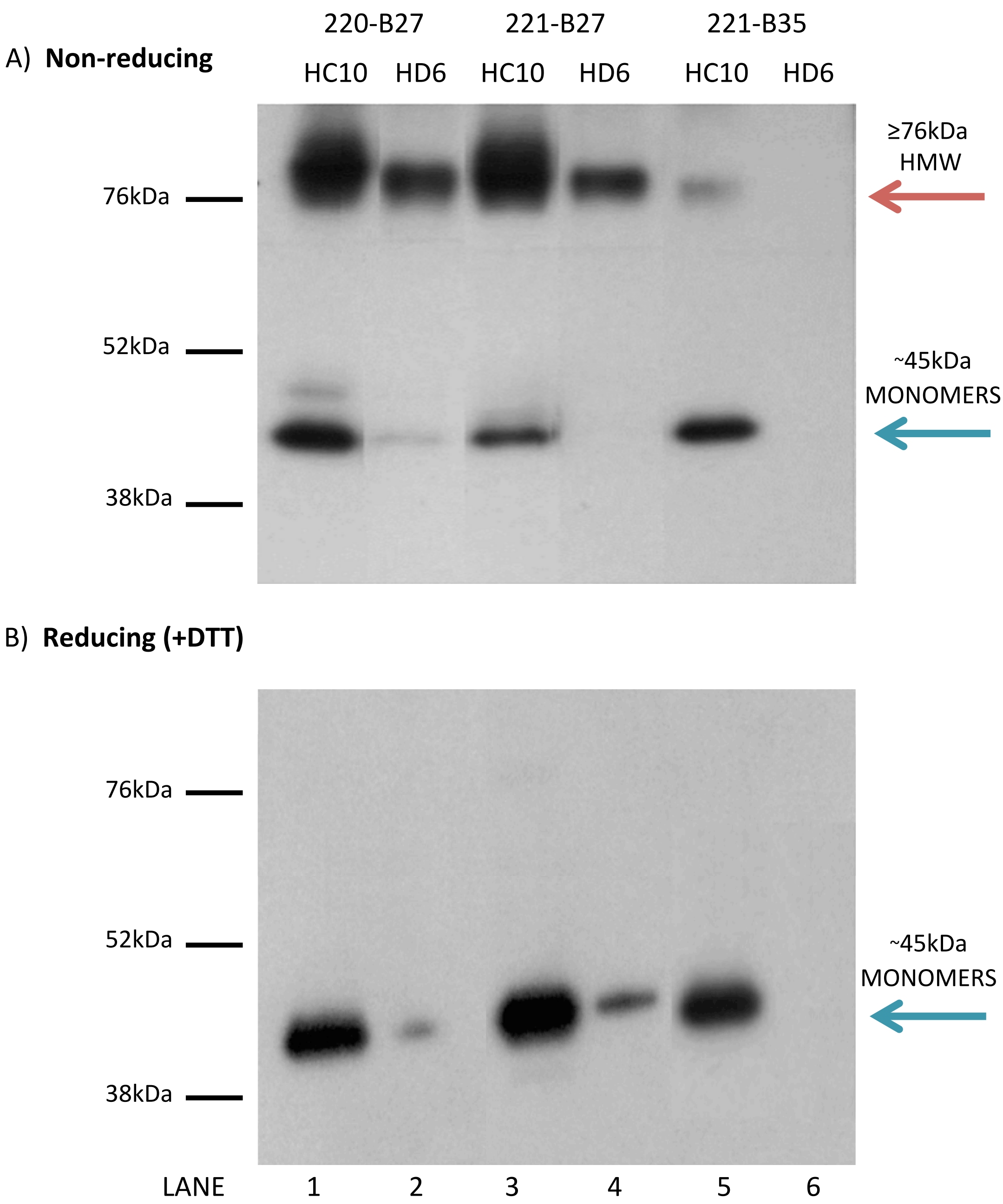

3.3.2 Acid-induced HD6-reactive molecules exist in a multimeric form at the cell surface in tapasin-proficient 221-B27 cells

As mentioned previously brief acid treatment removes β2 microglobulin and peptide from properly folded cell surface MHC class I molecules, leaving free heavy chains associated with cell membrane. It has been previously shown by flow cytometry that this acid treatment of B27-expressing cell lines increases and/or induces HC10 and HD6 staining (McHugh et al., 2014). Furthermore, these 'acid-induced'-NC-B27 species are functionally recognised by immune receptors, as detected in a KIR3DL2-CD3ε reporter cell assay (McHugh et al., 2014). Interestingly, acid treatment had no effect on levels of HD6-reactive molecules in the tapasin-defficient cell line 220-B27 (McHugh, unpublished data).

Therefore, I next sought to confirm these findings and investigate the nature of acid-induced HD6-reactive molecules in cell lines with and without functional tapasin.

Acid treatment of tapasin-expressing cell lines (220-B27 TPN and 221-B27) induced both HD6- and HC10-reactive molecules at the cell surface, in both monomeric and HMW forms, consistent with our previous findings by flow cytometry (Figure 3.9, 220-B27 TPN – A, Lanes 5-8 and 221-B27 – B, Lanes 3-6). As expected, no HD6-reactive molecules were observed both before and after acid treatment of the control 221-B35 (Figure 3.9, B, Lanes 9 and 10) and 221-B7 cell lines (Figure 3.9, B, Lanes 1 and 2). 221-B35 control cells however did express increased levels of HC-10-reactive molecules upon acid treatment, majority of which was in the monomeric form (Figure 3.9, B, Lanes 7 and 8). Acid treatment of 220-B27 cells (lacking functional tapasin), made little difference to the amount of HD6- and HC10-reactive molecules, again consistent with previous findings by flow cytometry (Figure 3.9, A, Lanes 1-4). Similarly, no significant differences in the amount of HC10-reactive FHC in 220-B7 cells after acid treatment (Figure 3.9, Lanes 9 and 10). Thus, in the presence of tapasin the acid-induced molecules in B27-expressing cells are mainly in the HMW form.

Notably, I observed an additional HMW band predominantly in B27-expressing cell lines (Figure 3.9, A and B bands >102kDa, labeled as MULTIMERS). This HMW species could represent multimeric forms of B27 FHC, $B27_2$ or complexes of FHCs associated with other molecules at the cell surface.

Importantly, after the addition of DTT only monomeric forms (45kDa) were detected in western blots (Figure 3.10, A and B).

Some of my data presented in this chapter were published in the paper: *Expression of aberrant HLA-B27 molecules is dependent on B27 dosage and peptide supply* (McHugh et al., 2014).

Figure 3.9 Acid treatment induces cell surface FHC and HMW FHC species. HD6 antibody recognises HMW forms only in B27-expressing cell lines. Immunoprecipitation of cell surface HC10- and HD6-reactive molecules, before and after acid treatment in 220-B27 (A, Lanes 1-4); 220-B27 TPN (A, Lanes 5-8); 221-B27 (B, Lanes 3-6) and control 220-B7 (A, Lanes 9,10 and B, Lanes 1,2); 220-B35 (B, Lanes 7-10) cell lines. Blue arrows – 45kDa FHC monomers; **Red arrows** – FHC dimers; Orange arrows – multimers. Non-reducing SDS-Page gel electrophoresis followed by western blot with HC10 HRP-conjugated antibody. A) and B) represent the same experiment, samples were run at the same time on two separate gels. Representative of n=5 independent experiments.

A) **NON-REDUCING SDS-PAGE**

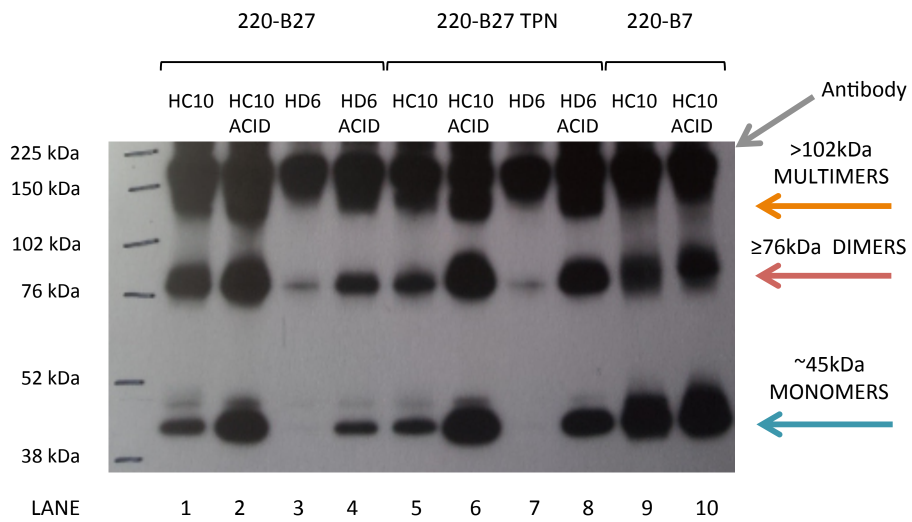

B) **NON-REDUCING SDS-PAGE**

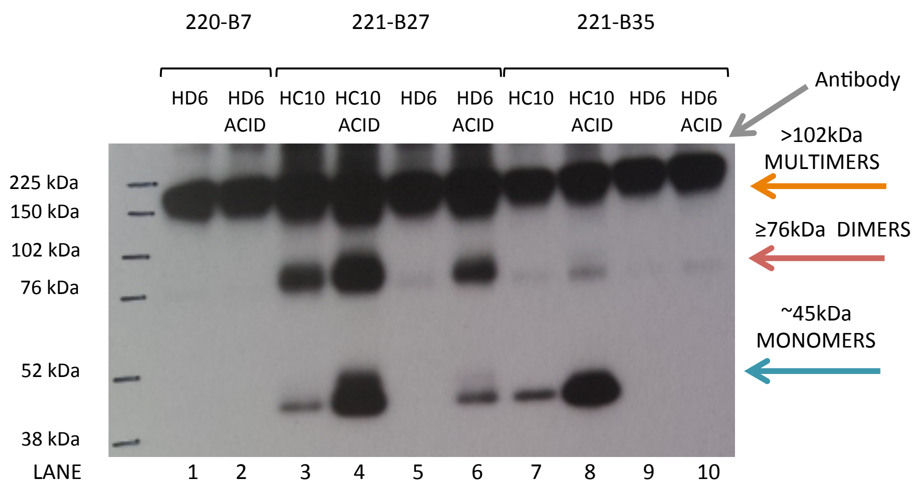

Figure 3.10 HMW forms immunoprecipitated with HD6 and HC10 antibodies are reduced to monomeric forms. Immunoprecipitation of cell surface FHC forms using HC10 and HD6 antibodies, before and after acid treatment in 220-B27 (A, Lanes 1-4); 220-B27 TPN (A, Lanes 5-8); 221-B27 (B, Lanes 3-6) and control 220-B7 (A, Lanes 9,10, B, Lanes 1,2); 220-B35 (B, Lanes 7-10) cell lines. Blue arrows – 45kDa FHC monomers; **Red arrows** – FHC dimers. Reducing (+DTT) SDS-Page gel electrophoresis followed by western blot with HC10 HRP-conjugated antibody. A) and B) represent the same experiment, samples were run at the same time on two separate gels. Representative of n=5 independent experiments.

A) **REDUCING SDS-PAGE (+DTT)**

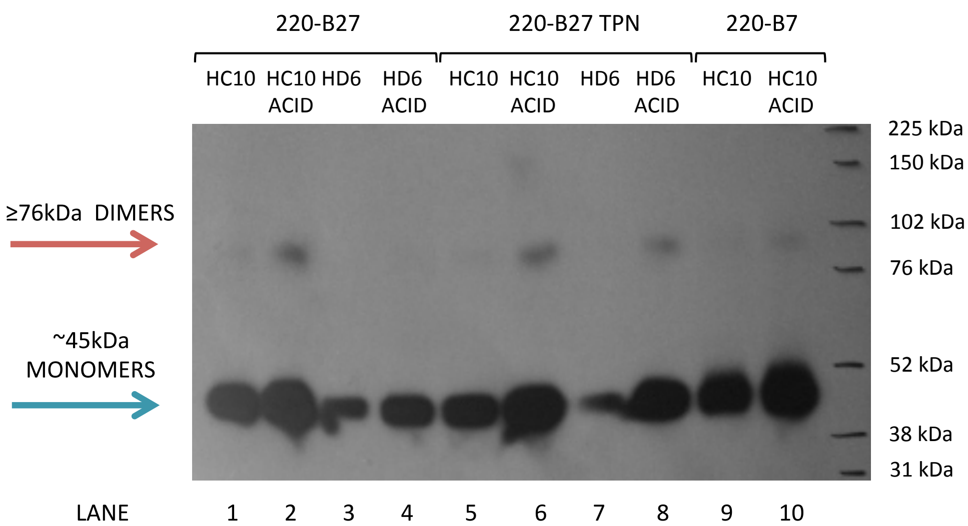

B) **REDUCING SDS-PAGE (+DTT)**

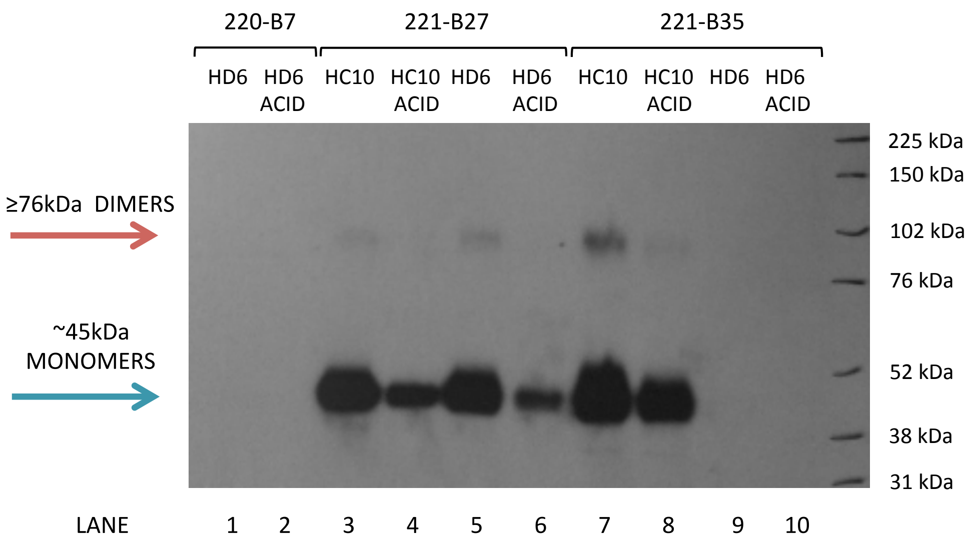

3.3.3 HD6-reactive molecules can be induced by acid treatment in EBV-trasformed B cell lines

220 and 221 B cell lines lack expression of their natural HLA-A and HLA-B alleles. Consequently, studying the behaviour of MHCI molecules in cell lines expressing a single HLA allele can be a great tool for investigation of that allele, but may not be a complete represantation of the *in vivo* behaviour. For example, co-expression of other MHCI alleles may influence the expression patterns of classical and non-classical forms of HLA-B27.

To address this problem, I next sought to determine whether HD6- and HC10-reactive forms of B27 can be immunoprecipitated from the surface of donor-derived Epstein-Barr Virus (EBV)-transformed B cell lines expressing the normal milieu of antigen presenting molecules. Cell surface protein immunoprecipitation with HD6 and HC10 antibodies was carried out as before, with 2 B27+ve BCLs from non-AS individuals: Jesthom (homozygous HLA-B*27:05) and BCL B27+ve (heterozygous HLA-B*27:05) along with control B27-ve cell lines (see Materials and methods). Importantly, no HD6 staining before acid treatment has been observed previously in these cell lines using flow cytometry, but significant HD6 staining can be induced upon acid treatment (McHugh, unpublished data).

Cell surface immunoprecipitation of the B27+ve BCLs yielded few if any HD6-reactive molecules prior to acid treatment, consistent with the previous flow cytometry findings (Figure 3.11, Lanes 3 and 8). Interestingly, upon acid treatment I detected more monomeric than dimeric forms of HD6-reactive molecules, a finding that is seemingly inconsistent with my data using 220-B27, 220-B27 TPN and 221-B27 cell lines (Figure

3.9, A, Lanes 3 vs 4 and 7 vs 8; and B, Lanes 5 vs 6). At the same time B27+ve BCLs abundantly expressed surface HC10-reactive molecules, of which a significant amount was detected as HMW bands (>76kDa), suggesting the presence of FHC homodimers (Figure 3.11, Lanes 1, 2, 5, 6). Importantly, in B27-ve BCLs the majority of immunoprecipitated HC10-reactive molecules were present in a monomeric form (~45kDa bands) (Figure 3.11, Lanes 9 and 10), while no HD6-reactive molecules could be detected.

Some of my data presented in this chapter were published in the paper: *Expression of aberrant HLA-B27 molecules is dependent on B27 dosage and peptide supply* (McHugh et al., 2014).

Figure 3.11 B27+ve BCLs express significantly higher levels of HC10-reactive HMW forms compared with control B27-ve cell lines. HD6-reactive species can be induced by low pH treatment specifically in B27+ve BCLs. Immunoprecipitation of cell surface free heavy chains using HC10 and HD6 antibodies, before and after acid treatment in B27+ve BCLs: B27$^{+/-}$BCL (Lanes 1-4) and Jesthom B27$^{+/+}$BCL (Lanes 5-8) and control BCL-ve (Lanes 9-12). Blue arrows – ~45kDa FHC monomers; Red arrows – ≥76 kDa, dimers. Non-reducing SDS-Page gel electrophoresis followed by western blot with HC10-HRP conjugated antibody. Representative of n=5 independent experiments.

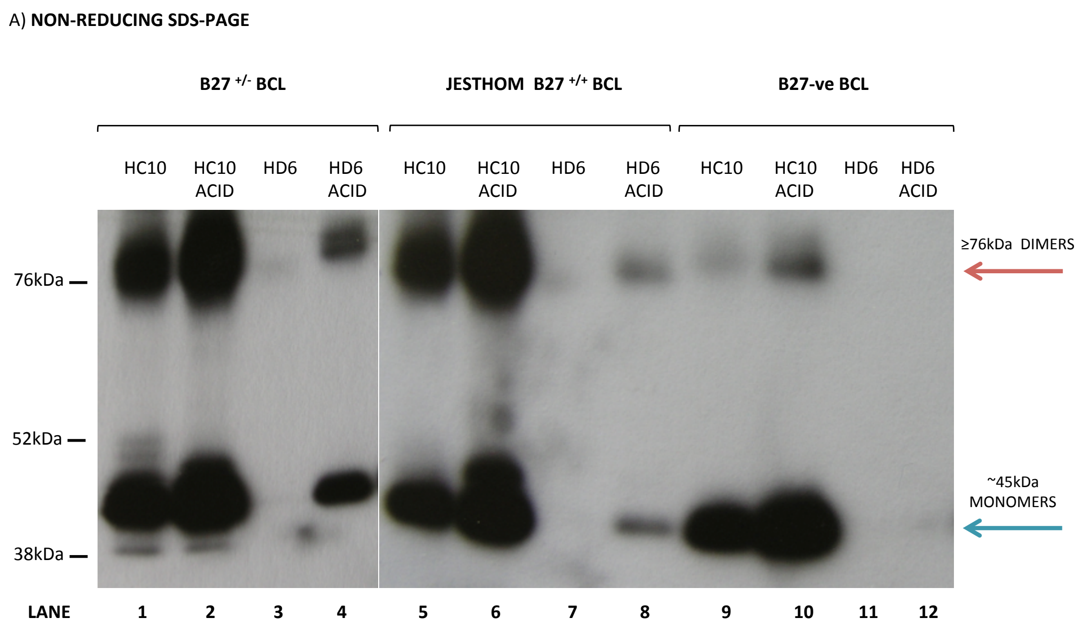

3.3.4 The amount of immunoprecipitated HD6-reactive molecules is decreased by addition of B27-binding peptides in tapasin-proficient cell lines

It has been previously demonstrated that addition of exogenous high affinity peptides can stabilize MHCI heterodimeric complexes both intracelullarly and at the cell surface (Baas et al., 1992; Townsend et al., 1989). Moreover, as shown by McHugh *et al.*, addition of HLA-B27-binding peptides to B27-expressing cells decreases the expression of HD6-reactive molecules. To support the flow cytometry data, I cultured 220 B27 TPN cells overnight with a B27-binding peptide (SRYWAIRTR, influenza nucleoprotein (NP), residues 383-391) or a control HLA-A2-binding peptide (GILGFVFTL, influenza matrix protein, residues 58-66) (see Materials and methods). Subsequently, I immunoprecipitated cell surface HC10- and HD6-reactive molecules using my standard IP protocol. The presence of the HLA-B27-binding peptide, but not the HLA-A2-binding peptide, reduced the amout of HD6-reactive molecules detected (Figure 3.12, Lanes 2 vs 4). Interestingly, I did not detect visible changes in the band intensities for the HC10-reactive molecules after addition of the HLA-B27-binding peptide (Figure 3.12, Lane 1 vs 3).

My data presented in this chapter were published in the paper: *Expression of aberrant HLA-B27 molecules is dependent on B27 dosage and peptide supply* (McHugh et al., 2014).

Figure 3.12 Addition of HLA-B27-binding peptide leads to the reduction of surface HD6-reactive molecules in 220-B27 TPN cells. Immunoprecipitation of surface HC10- and HD6-reactive molecules using 220-B27 TPN cells. 220-B27 TPN cells cutured without peptide addition (Lanes 1 and 2); with HLA-B27-binding peptide (Lanes 3 and 4) or HLA-A2-binding peptide (Lanes 5 and 6). Blue arrows – ~45kDa FHC monomers; Red arrows – ≥76 kDa dimers. Non-reducing SDS-Page gel electrophoresis followed by western blot with HC10-HRP conjugated antibody. Representative of n=2 independent IP experiments.

A) NON-REDUCING SDS-PAGE

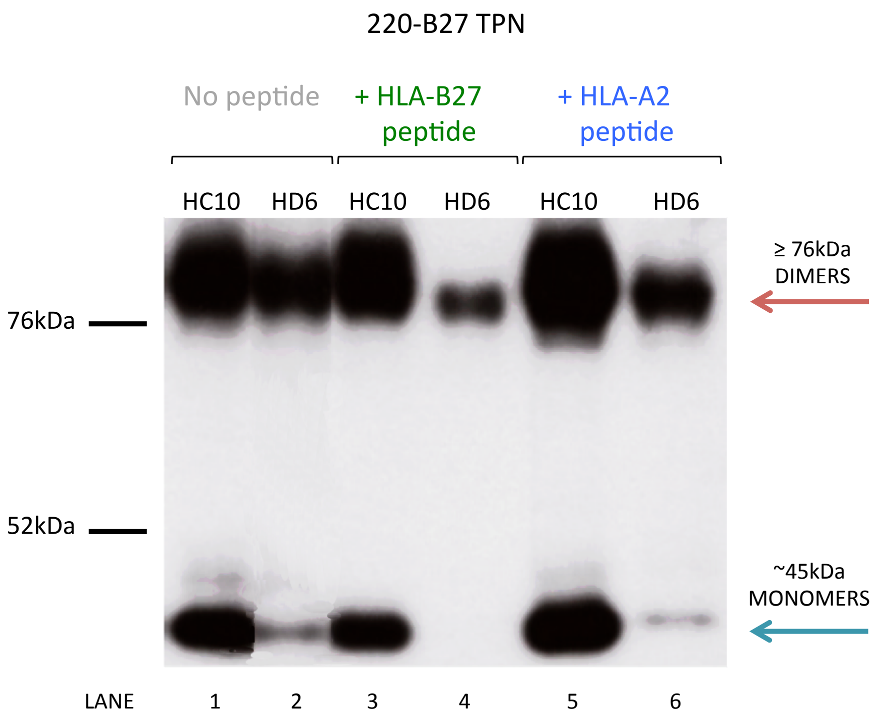

Summary Chapter 3.3

In summary, the majority of HD6-reactive molecules immunoprecipitated from the cell surface of LCLs expressing B27 molecules is represented by HMW forms. Acid treatment of tapasin proficent cell lines (220-B27 TPN and 221-B27) can further iduce HMW species of HD6- and HC10-reactive molecules.

Moreover, my findings suggest that HD6-reactive molecules can be found specifically at the cell surface of BCLs expressing HLA-B27, but only after acid treatment. In addition, these B27+ve cells expressed more HC10-reactive FHC in an HMW form compared with B27-ve cells, both before and after acid treatment.

Furthermore, addition of HLA-B27 specific peptide decreased the amount of cell surface HD6-reactive molecules, but had less influence on the HC10-reactive molecules.

3.4 Discussion Chapter Three

Importantly in this chapter I have investigated for the first time cell surface organization patterns of HD6- and HC10-reactive molecules in B27-expressing cell lines by confocal microscopy. In adherent HeLa cells, NC-B27 forms (both HD6 and HC10 staining) have a tendency to cluster at the cell surface. Notably, the majority of HD6 clusters was found exclusively in the perinuclear regions. Although, clustering of NC-B27 molecules was also detected at the surface of non-adherent 221-B27 cells, I did not observe the accumulation of HD6 staining in the perinuclear region. Accumulation of HD6 staining in the perinuclear regions in HeLa-B27, and not in 221-B27 cells, could be due to the differences in confocal microsocpy staining procedure of adherent and suspension cells. Notably, both protocols are optimized for the exclusive staining of the cell surface molecules. However, staining of adherent cells directly on microsocpy plates requires brief fixation with 4% methanol-free PFA prior to the staining procedure. Short incubation time (up to 15min) and the use of mild fixative (4% methanol-free PFA) should assure preservation of cell surface epitopes without permeabilization of the cell membrane. Yet, I can not exclude the possibility that observed staining was intracellular.

On the other hand, HD6 confocal microscopy staining patterns observed in HeLa-B27 vs 221-B27, could be different due to the morphological, functional and genetic characteristics, such as the expression of other HLA class I alleles. The HeLa cell line is a human epithelial-like carcinoma non-immune cell line, while the 221 cell line was derived from human B cells by the EBV-transformation (Shimizu et al., 1988). Notably, my flow cytometry data demonstrated relatively high levels of cell surface W6/32 and

HC10 staining, even in non-transfected HeLa cells, which confirms the expression of other MHCI molecules. Whereas, 221 cells have been shown to lack both intracellular and cell surface expression of HLA-A, -B and -C alleles (Shimizu et al., 1988), however were shown to express low levels of cell surface HLA-E molecules (Lo Monaco et al., 2008). Hence, trafficking of MHCI molecules, their association with peptides and stability at the cell surface are likely to be different in HeLa and 221 cells.

The observed clustering of cell surface NC-B27 molecules could be due to their association with the structured cell membrane domains known as lipid rafts. Lipid rafts are the glycolipoprotein domains of the cell membrane that act as organizing centres for signalling proteins, and can also facilitate endocytosis and internalization processes. Interestingly, although MHC class II molecules have been previously described to aggregate in lipid rafts (Goebel, Forrest, Flynn, Rao, & Roszman, 2002), as yet the association of MHCI with lipid rafts has not been reported. A number of studies showed evidence that viruses require lipid rafts in order to penetrate cell membrane and replicate (Campbell, Crowe, & Mak, 2001; Carter et al., 2009; Metzner, Salmons, Günzburg, & Dangerfield, 2008; Suzuki & Suzuki, 2006; Van Wilgenburg, Moore, James, & Cowley, 2014). Interestingly, HLA-B27 was shown to be protective in HIV and HCV infection (Goulder et al., 2001; Kelleher et al., 2001; López de Castro, 2005; Neumann-Haefelin, 2011; Schneidewind et al., 2008). Hence, there is a possibility that observed clustering of NC-B27 molecules at the cell surface could be co-localized with lipid rafts and may play a role in the viral resistance.

Since NC-B27 bind with the high affinity to immune receptors KIR3DL2 and LILRB2 (Bowness and Ridley et al., 2011; Chan, Kollnberger, Wedderburn, & Bowness, 2005;

Kollnberger et al., 2007; Wong-Baeza et al., 2013), this may cause their clustering at the cell surface and possible association with lipid rafts. Furthermore, it has been suggested that MHCI FHCs can bind to immune receptors (such as KIRs and LILRs) and other class I FHCs not only in a traditional, *trans* conformation, but also in the *cis* conformation (Held & Mariuzza, 2008; N. L. Li, Fu, Uchtenhagen, Achour, & Burshtyn, 2013; Masuda, Nakamura, Maeda, Sakamoto, & Takai, 2007). As mentioned previously 221 cells can express low levels of HLA-E and also were showed to express LILRs. Hence, the aggregation of surface NC-B27 observed in my microscopy experiments could be a consequence of their *cis* interactions with LILRs or other class I FHCs. Alternatively, clustering of NC-B27 at the cell surface could be related to MHCI recycling and endocytosis processes.

Since I did not observe cell surface clusters in 221-B27 cells stained with ME1 and W6/32 mAbs, this may be a characteristic feature of NC-B27 molecules. Yet, my data also suggest that high intensity staining may mask cell surface MHCI clusteres. Hence, the observed lack of ME1 and W6/32 aggregates at the cell surface could be related to the higher intensity of staining with these mAbs compared with HD6 and HC10.

Importantly, Bird *et al*. proposed that FHC homodimers present at the surface of 221-B27 cells originate from properly folded HLA-B27 molecules, rather than from NC-B27 accumulated in the ER compartments (Bird et al., 2003). Additionally, it has been suggested that the removal of β2m and peptide from the cell surface heterodimeric HLA-B27 complexes upon brief acid treatment can induce NC-B27 molecules (McHugh et al., 2014 and unpublished data). In agreement with our previous findings, my confocal microsopy data have demonstrated an increase in HD6 and HC10 staining, and simultaneous decrease in ME1 and W6/32 staining, post acid tretament. These findings further support the hypothesis that NC-B27 molecules can arise from the properly folded cell surface MHCI molecules.

Notably, although HD6 has been previously shown to bind to B27-expressing cells by flow cytometry, as yet nobody has investigated cell surface HD6-reactive molecules by immunoprecipitation. Here, I have demonstrated for the first time by IP the presence of cell surface HD6-reactive molecules in 220-B27, 220-B27TPN and 221-B27 cell lines. Notably, the majority of these MHCI heavy chains were immunoprecipitated in the HMW form (≥76kDa), suggesting the presence of $B27_2$. Additionally, I have demonstrated that cells lacking functional TPN (220-B27) express higher levels of cell surface HMW HD6- and HC10-reactive NC-B27 molecules compared with TPN-sufficient cell lines (220-B27 TPN and 221-B27). However, more NC-B27 molecules were immunoprecipitated from the surface of cells with functional TPN compared with 220-B27 following acid treatment. Hence, my results suggest that higher expression levels of properly folded cell surface MHCI in the presence of TPN, could give raise to the additional, newly formed HD6- and HC10-reactive NC-B27 molecules after acid treatment.

Importantly, cell surface HMW HD6-reactive molecules were specifically immunoprecipitated from the surface of B27-expressing cells and were absent in control cell lines. Furthermore, higher amounts of HMW HC10-reactive species were observed in IPs from B27-expressing cell lines compared with control cells expressing other HLA types. Thus, these findings suggest that HLA-B27 molecules are predisposed to misfold and possibly form FHC homodimers and other multimeric complexes at the cell surface.

Notably, my IP data demonstrated that cell surface HMW HC10-reactive molecules can be also detected in 220 cells expressing HLA-B7, while in 221-B35 cells the majority of FHCs is present in the monomeric form (~45kDa). However, whether this phenomenon is due to the lack of TPN in 220-B7 and the presence of TPN in 221-B35, or is simply a characteristic feature of these HLA types remains unclear.

In contrast to B27-expressing LCLs, I did not observe HD6-reactive molecules in surface IPs from the EBV-transformed BCLs carrying HLA-B27 genes. Importantly, B27+ve BCLs naturally express other HLA class I molecules. Hence, there is a possibility that in BCLs fewer unstable B27 and/or misfolded NC-B27 can reach cell surface due to the expression of other HLA class I molecules and consequent more rigorous control of MHCI processing. On the other hand, in 220-B27 and 221-B27 cell lines the overexpression of a single type of the MHCI molecule could result in the altered control of MHCI peptide loading and trafficking. As a consequence, higher number of low quality B27-complexes could reach cell surface, leading to increased MHCI misfolding and formation of NC-B27. Furthermore, the observed lower levels of cell surface HMW HD6- and HC10-reactive molecules in BCLs, could be a result of their faster MHCI recycling and endocytosis kinetics compared with LCLs.

Interestingly, the majority of HD6- and HC10-reactive molecules immunoprecipitated from B27+ve BCLs after acid treatment was represented by monomeric (~45kDa) species. These findings contradict my results from IP experiments using 220-B27 and 221-B27 cell lines, and suggest that properly folded HLA-B27 complexes reaching cell surface in B27+ve BCLs are more stable. Alternatively, faster kinetics of MHCI endocytosis and recycling in cells with the natural MHCI expression may prevent the abundant formation of HMW forms of FHC.

Notably, there is also a possibility that the lack of HD6-reactive species before acid treatment in immunoprecipitates from B27+ve BCLs could be due to the absence or masking of the antibody epitope. The HD6 antibody was generated using a phage display library screened against *in vitro* re-folded $B27_2$ derived from *E.coli* (Allen, O'Callaghan, McMichael, & Bowness, 1999; Payeli et al., 2012). Importantly, human and bacterial cells have different post-translational protein modification mechanisms (Cain, Solis, & Cordwell, 2014). Hence, human cell lines with the natural expression of MHCI molecules could lack the HD6 antibody epitope and/or the epitope could be masked by glycosylation sites. There is a possibility that acid treatment not only removes β2m and peptide from the cell surface heterotrimeric MHCI complexes, but could possibly also alter HLA-B27 conformation and open HD6 epitopes.

Furthermore, the HD6 epitope in surface NC-B27 forms present in B27+ve BCLs could be masked by binding of other proteins, such as chaperones, or KIRs, LILRs and other class I FHCs interacting in *cis*. Notably, to support this hypothesis a number of studies have demonstarted that MHCI molecules can bind to KIRs, LILRs and other MHCI FHCs in a *cis* conformation (Held & Mariuzza, 2008; Y. Li & Mariuzza, 2014; Masuda et al., 2007; Santos, Powis, & Arosa, 2004). These MHCI ligand interactions were suggested to be important in immune regulation and self-tolerance. Hence, they may occur specifically or more frequently in B27+ve BCLs compared with LCLs. In summary, the availability of HD6 antibody epitopes and possible interactions of NC-B27 with other proteins at the cell surface in BCLs and LCLs need further investigation.

Chapter Four: Investigation of the expression of HD6- and HC10-reactive molecules in AS patient blood-derived cells and SpA synovial tissue

4.1 Introduction

The FHC homodimer theory proposes that NC-B27 expressed at the cell surface of APCs can bind with a high affinity to immune receptors, such as KIR3DL2 and LILRB2, and activate Th17-driven immune responses. Hence, dendritic cells (DCs) and macrophages (Mφ), which are proffesional APCs could express potentially pathogenic NC-B27 molecules in AS patients.

DCs in B27 TG rats are characterized by impaired migration and synapse formation (Hacquard-Bouder et al., 2007; Utriainen et al., 2012). Although there is little known about the role of B27-expressing DCs in SpA, AS patient-derived moDCs have been demonstrated to express increased levels of *ERAP1* and decreased levels of BiP compared with control cells (Campbell, Fettke, Bhat, Morley, & Powis, 2011). Furthermore, AS patient-derived moDCs have been shown to produce higher levels of the Th17-associated cytokine IL-23 upon stimulation compared with RA moDCs (Prevosto, Goodall, & Gaston, 2012). Thus, DCs may play a role in driving immune responses in SpA.

Mφ have been found in tissues in early stages of inflammation and enthesitis (Baeten & Keyser, 2004), as well as in inflamed SpA synovial tissue isolated from peripheral joints (Ambarus, Noordenbos, de Hair, Tak, & Baeten, 2012). Moreover, it has been shown that AS patient monocyte-derived Mφ produce increased amounts of IL-23 upon LPS stimulation compared with healthy controls (Zeng et al., 2012). These findings implicate macrophages in SpA pathogenesis.

Another cell population that may be involved in the activation of Th17 responses in the joint are osteoclasts (OCs). Although there is still little known about their immune modulatory role, recent findings demonstrated that OCs can express MHCI and MHCII molecules and co-stimulatory molecules (CD80, CD86 and CD40), and can also take up antigens and present them to $CD4^+$ and $CD8^+$ T cells in a similar manner as APCs (Li et al., 2010). Moreover, OCs induce tolerance via the activation of FoxP3 expression on $CD8^+$ cells in a MHCI dependent manner (Kiesel, Buchwald, & Aurora, 2009). OCs are also well known for their role in bone remodeling processes. Higher number of OCs was observed in cartilage isolated from hip joints of AS patients with active disease compared with OA and RA patients (Appel et al., 2006; François, Neure, Sieper, & Braun, 2006). Moreover, increased osteoclastogenesis in response to RANKL was observed in monocyte-derived cells from AS patients compared with healthy controls (Im et al., 2009). Studies in B27 TG animal models of SpA have further reinforced the importance of bone erosion in the disease pathology (Layh-Schmitt, Yang, Kwon, & Colbert, 2013; van Duivenvoorde et al., 2012). Hence, high frequency of OCs expressing NC-B27 might impair the balance between immune tolerance and activation and/or may drive Th17 immune responses.

In the previous chapter I demonstrated by confocal microscopy and immunoprecipitation that surface HD6-reactive molecules are present in B27-expressing cell lines and/or their expression can be induced by acid treatment. Next I sought to determine whether these potentially pathogenic NC-B27 molecules are present in primary cells derived from AS patient blood. Payeli *et al.* observed HD6 staining on a $CD14^+$ population from AS patient PBMCs (Payeli et al., 2012), however, as yet, nobody has investigated the expression of HD6-reactive molecules on other monocytic cell types derived from AS patient PBMCs. Moreover, the expression patterns of NC-B27 forms in the inflamed joints of SpA patients has not been investigated. Therefore, I first sought to determine cell surface expression of HD6- and HC10-reactive molecules in AS patient monocyte-derived dendritic cells (moDCs), macrophages (Mφ) and monocyte- or PBMC-derived osteoclasts. Notably, potentially pathogenic NC-B27 molecules could be expressed more abundantly and/or specifically by either resident or infiltrating cells in joints, rather than in circulation. Hence, in this chapter I investigated additionally HD6 and HC10 epression by flow cytometry in cells isolated from synovial fluid and tissue, and by immunohistochemistry in synovial tissue samples isolated from SpA patients.

4.2 Expression of non-classical and classical forms of MHCI molecules in AS patient moDCs

4.2.1 LPS treatment of the AS patient derived moDCs induces high levels of cell surface HC10-reactive molecules without any detectable HD6 staining

It has been previously demonstrated that surface expression of HD6-reactive molecules appears to depend on the overall levels of B27, as high levels of HD6 staining were observed in cells overexpressing this HLA allele (McHugh et al., 2014). In contrast, EBV-transformed B27+ve B cell lines, with natural expression of MHCI, do not express

HD6-reactive molecules, despite relatively high HC10 staining. Therefore, I first sought to determine whether AS patient DCs which express relatively high levels of MHCI upon activation, could induce cell surface NC-B27 molecules.

The main obstacle in studying B27 expression in blood-derived DCs from AS patients is the low number of circulating DCs and the small volume of patient blood sample approved by clinical research ethics. Consequently, my first approach was to establish a working protocol to generate a high number of DCs from peripheral blood-derived monocytes (moDCs). CD14 MicroBeads (MACS Miltenyi) were used for positive selection of monocytes from PBMCs and cultured in R10 supplemented with GM-CSF and IL-4 for 5 days to obtain immature moDCs (see Materials and methods).

Immature DCs are characterized by low levels of MHCI expression, hence ultrapure lipopolysaccharide (LPS) was used to induce DC maturation and thus increase levels of MHCI. LPS, a main component of the outer cell membrane of Gram-negative bacteria, can activate immune responses both via Toll-like receptor 4 (TLR4), or in a TLR4-independent manner. Notably, Gram-negative bacteria, *Esherichia coli* (*E. coli*) and *Salmonella typhimurium* (*S. typhimurium*), have been suggested to be environmental factors involved in AS pathogenesis. I therefore tested ultrapure LPS from both *E.coli* and *S.typhimurium* to stimulate moDCs on day 5 of culture.

Few, if any, HD6-reactive molecules were detected in immature B27+ve moDCs or in LPS (*E.coli* or *S. typhimurium*) stimulated (24h) moDCs (Figure 4.1, A - HD6 MFIs (blue) vs isotype control MFIs (grey)). Moreover longer incubation times (48h and 72h) with LPS also failed to induce HD6 staining (data not shown).

In contrast, LPS stimulation from both *E. coli* or *S. typhimurium* increased HC10 staining (Figure 4.1, A –HC10 MFIs (green) vs isotype control MFIs (grey)). HC10 staining was also observed in healthy control moDCs (Figure 4.1, B –green histograms). Importantly, the B27+ve AS patient moDCs consistently expressed higher levels of HC10-reactive molecules upon *E. coli* or *S. thyphimurium* LPS stimulation compared with healthy controls (Figure 4.2, A).

Figure 4.1 HD6-reactive molecules are not detectable in AS moDCs even after stimulation with LPS *E. coli* or *S. thyphimurium*, despite the presence of HC10-reactive molecules. HD6 (blue histograms) and HC10 (green histograms) staining in A) B27+ve AS patient moDCs and B) B27-ve healthy control moDCs. Numbers in histogram legends – GeoMean MFIs. Representative flow cytometry data from n=3 independent experiments.

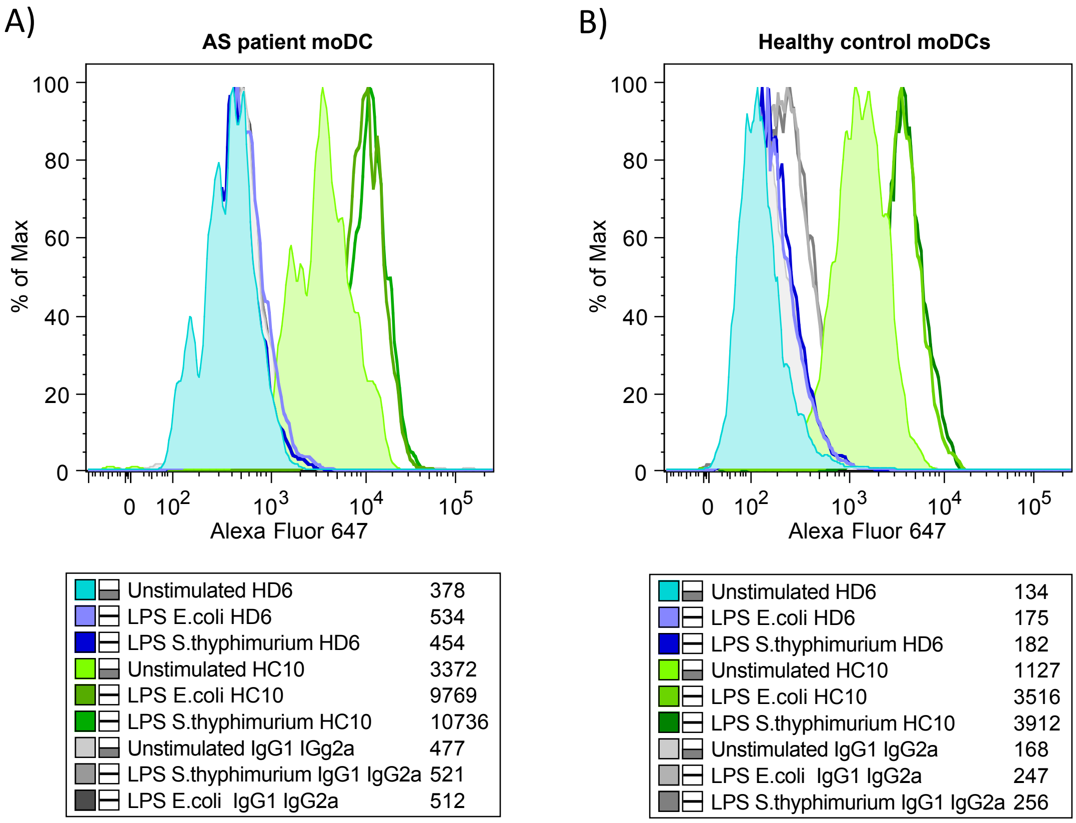

Figure 4.2 AS patient moDCs express elevated levels of HC10-rective molecules upon LPS stimulation compared with healthy controls. A) HC10 expression at the surface of AS patient (Grey bars) and healthy control (Black and white bars) in unstimulated moDCs or after 24h treatment with LPS *E. coli* or *S. thyphimurium*. Data obtained in two independent experiments from n=3 AS patient and n=2 healthy control samples. Error bars - Mean with SEM.

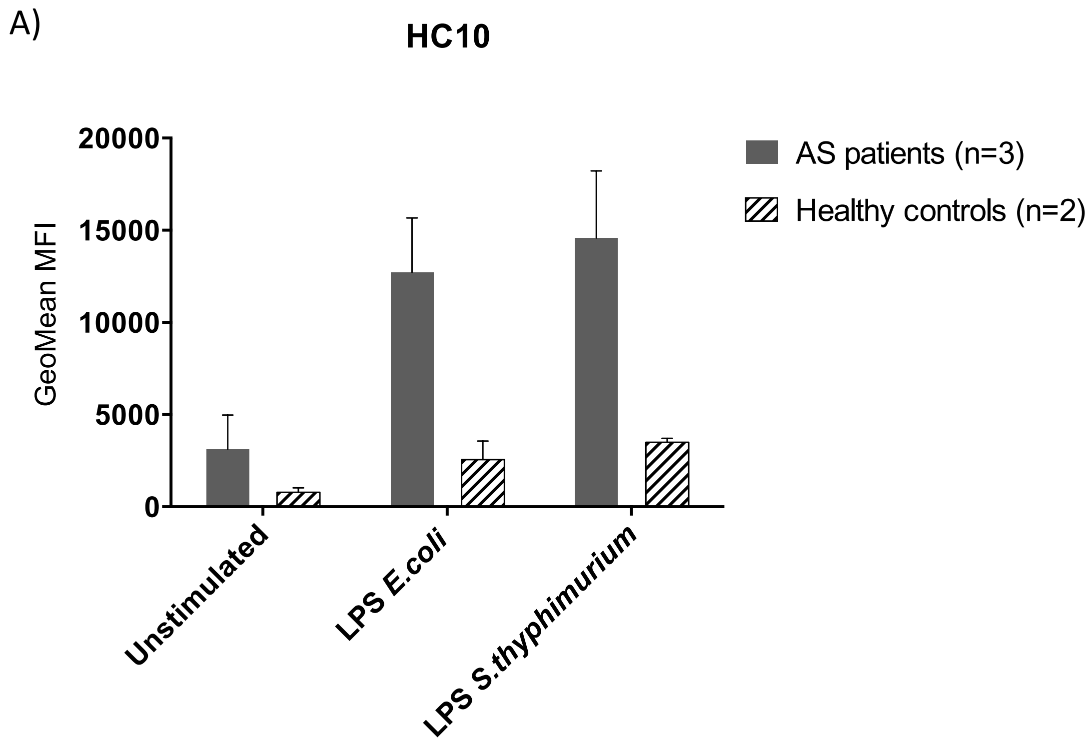

In order to test whether NC-B27 can be induced on moDCs via other TLR stimuli I next cultured immature moDC with CpG oligodeoxynucleotide (CpG ODN) or polyinosinic:polycytidylic acid (Poly I:C). CpGs are short single-stranded DNA molecules that contain repeated motifs of cytosine triphosphate deoxynucleotide (C) followed by guanine triphosphate deoxynucleotide (G), abundantly present in microbial genomes, that are recognized by Toll-like receptor 9 (TLR9). Poly I:C is a synthetic analogue of double-stranded RNA (dsRNA), which can stimulate anti-viral responses via Toll-like receptor 3 (TLR3).

Neither CpG nor Poly I:C were able to induce expression of HD6-reactive molecules at the surface of AS patient-derived moDCs (Figure 4.3, A). Notably, CpG and Poly I:C treated moDCs expressed relatively low levels of HC10-reactive molecules compared to LPS stimulation (Figure 4.3, B). However, neither CpG nor Poly I:C induced increased levels of properly folded B27 (ME1), although an increase in W6/32 staining was seen with Poly I:C stimulation (Figure 4.3, C and D).

Figure 4.3 HD6-reactive molecules are not detectable in moDCs after stimualtion with CpG or Poly I:C. A) HD6, B) HC10, C) ME1 and D) W6/32 staining in unstimulated moDCs or 24h after LPS S.*thyphimurium*, CpG or Poly I:C stimulation. Representative flow cytometry data from AS patients - grey bars (n=2) and healthy control - black and white bars (n=1). Each flow cytometry staining condition for individual sample was performed in duplicates. Error bars for data obtained from AS patients - Mean with SEM.

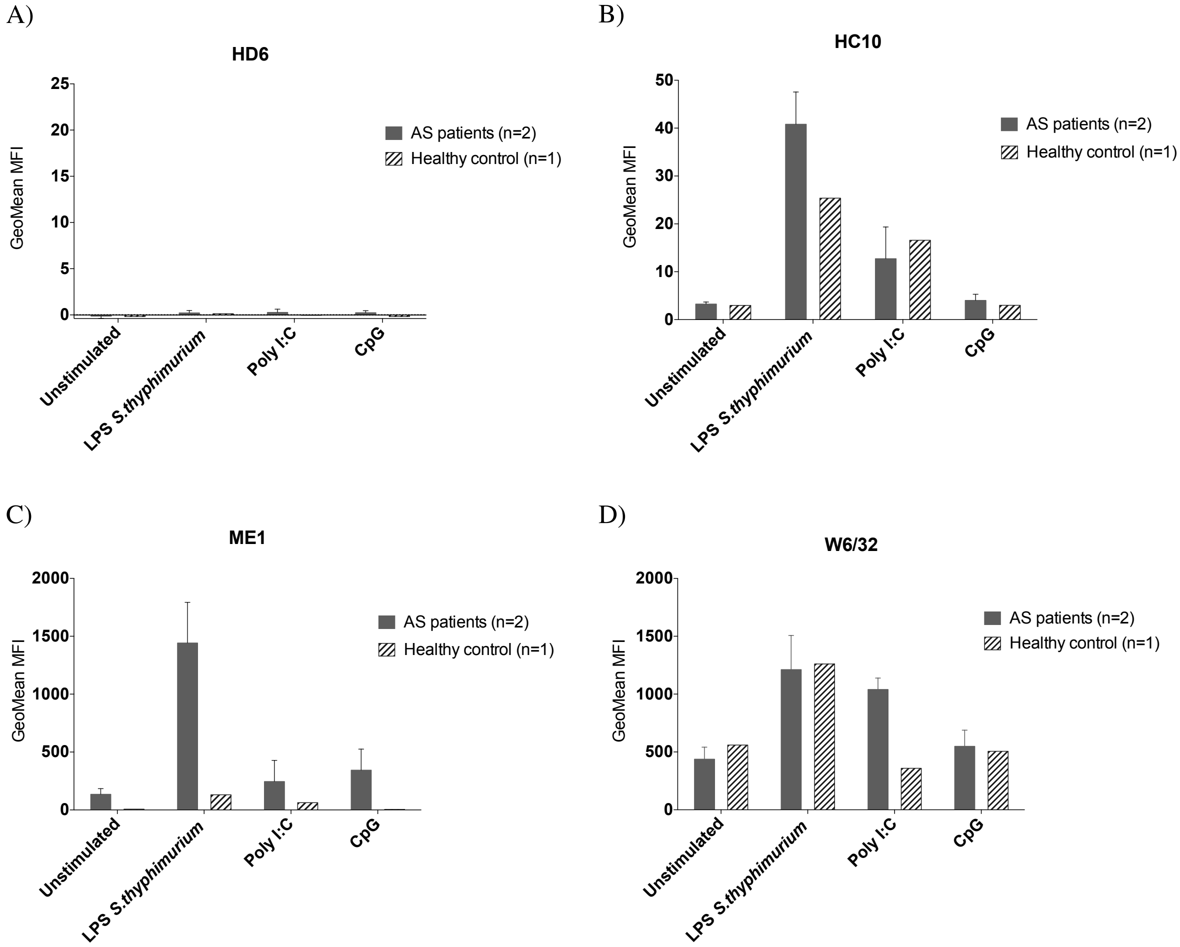

TNFα and interferons (IFNα, IFNβ, and IFNγ) may play a role in pro-inflammatory responses in SpA. Therefore, I next sought to investigate the influence of TNFα, IFNα, IFNβ or IFNγ treatment on the expression of cell surface non-classical forms of MHC class I molecules in AS patient and healthy control moDCs using flow cytometry.

After 24h of stimulaton with TNFα, IFNα, IFNβ or IFNγ, no detectable levels of HD6-reactive molecules were observed in AS or healthy control moDCs (Figure 4.4, A). HC10 (Figure 4.4, B) and ME1 (Figure 4.4, C) staining indicated no difference between AS patients and healthy control after cytokine stimulation. Cell surface expression of W6/32-reactive molecules was measured as a postitive control to confirm that the cytokine stimulation upregulated MHC class I expression. Increased W6/32 staining was observed in both AS and healthy control moDCs after treatment with IFNα, IFNγ or TNFα, but not IFNβ, to levels comparable with those observed after LPS stimulation (Figure 4.4, D).

Figure 4.4 HD6-reactive molecules are undetectable after interferons (IFNα, IFNβ, IFNγ) or TNFα stimulation in moDCs. A) HD6, B) HC10, C) ME1 and D) W6/32 expression in unstimulated or after 24h of stimulation with IFNα, IFNβ, IFNγ or TNFα in AS patient (grey bars) and healthy control (black and white bars) moDCs. Representative flow cytometry data from AS patients (n=2) and healthy control (n=1). Each flow cytometry staining condition for individual sample was performed in duplicates. Error bars for data obtained from AS patients Mean with SEM.

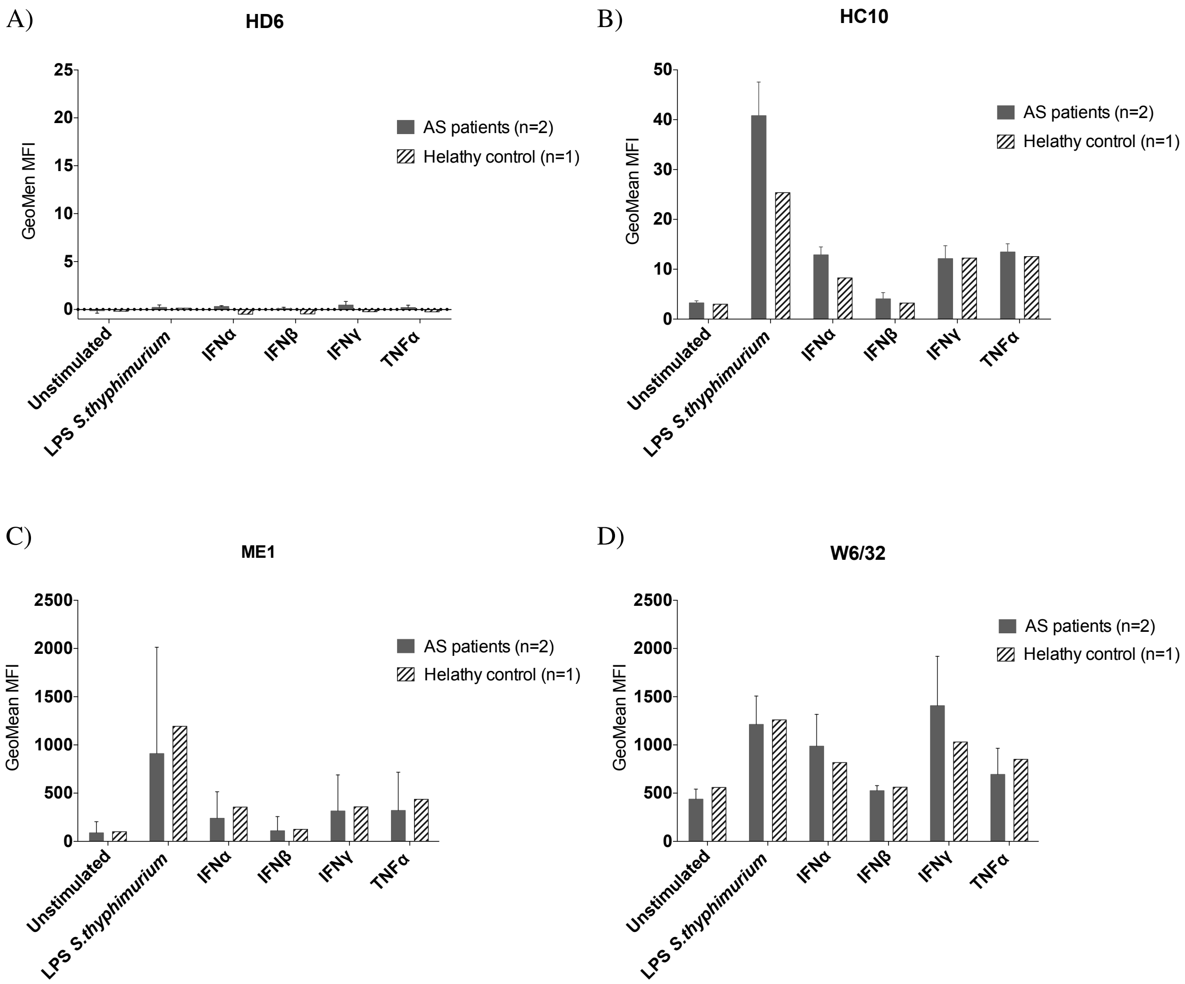

Although no HD6-reactive molecules were detected following stimulation with LPS alone, an increase in both properly folded and free heavy chains was observed. On the other hand, cytokine stimulation alone increased W6/32-reactive molecules, but failed to have a significant effect on the B27 molecules themselves. Therefore, I next combined LPS and cytokine treatment (TNFα or IFNγ) to determine if NC-B27 molecules could be upregulated in response to a mixture of TLR and cytokine stimulation, a situation more reminiscent of the inflamed joint environment.

Stimulation of AS moDCs with either the combination of LPS with IFNγ or with TNFα also failed to induce the expression of cell surface HD6-reactive molecules (Figure 4.5, A and B). Combining cytokine stimulation with LPS treatment also had no additive effect on the levels of HC10 staining, with levels comparable to those seen with LPS treatment alone. Notably, when LPS derived from *S. typhimurium* was used in combination with TNFα, HC10 staining seemed to decrease to the levels seen with TNFα treatment alone (Figure 4.6, A and B).

Interestingly, the ratio of HC10:W6/32 cell surface staining seemed to be consistently elevated in the moDCs derived from AS patients compared with healthy controls (Figure 4.7, A and B). Therefore, despite similar amounts of properly folded MHC class I molecules, AS patient-derived moDCs consistently expressed more unfolded HC10-reactive species compared to controls.

Figure 4.5 Combined LPS and cytokine moDC stimulation does not induce HD6-reactive molecules. HD6 staining in unstimulated or LPS *E. coli* or *S. thyphimurium* and cytokine stimulation in A) B27+ve AS patient and B) B27-ve helathy control moDCs. Numbers in histogram legends – GeoMean MFIs. Representative flow cytometry data from n=3 AS patients and n=3 healthy controls.

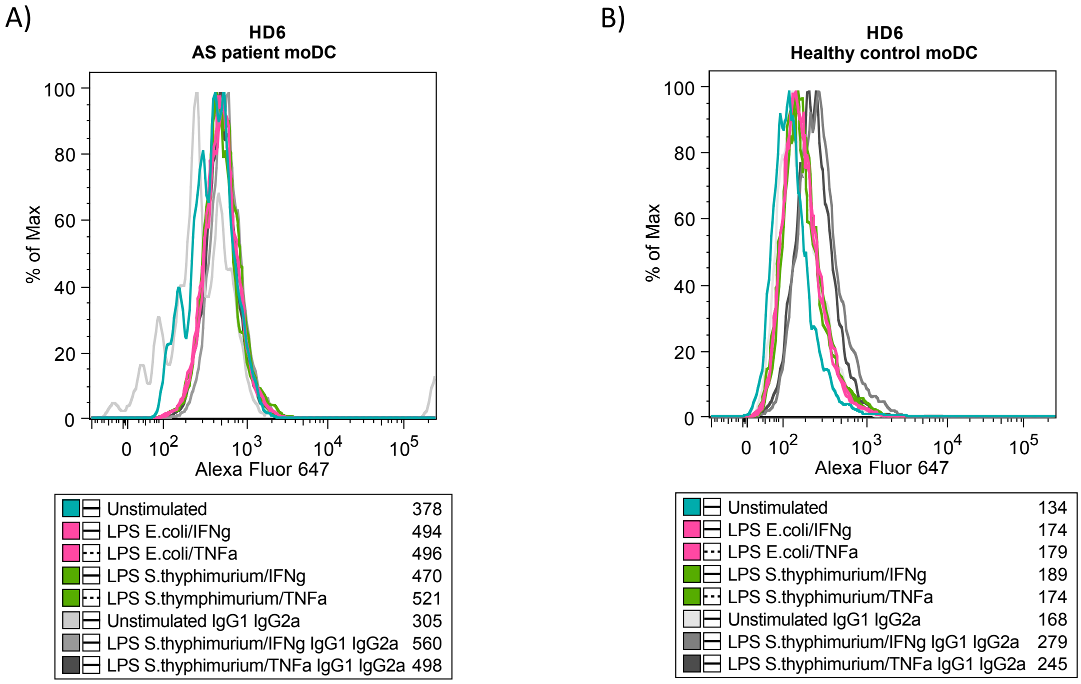

Figure 4.6 Cell surface expression levels of HC10-reactive molecules are increased in B27+ve AS patient moDCs compared with healthy controls. HC10 expression in AS patient (grey bars) and healthy control (black and white bars) unstimulated moDCs, after A) LPS *E. coli* or B) LPS *S. thyphimurium* and/or cytokine stimulation. Representative data from n=3 experiments. Number of samples included in analysis: AS patients n=3; healthy controls n=2. Error bars on graphs – Mean with SEM.

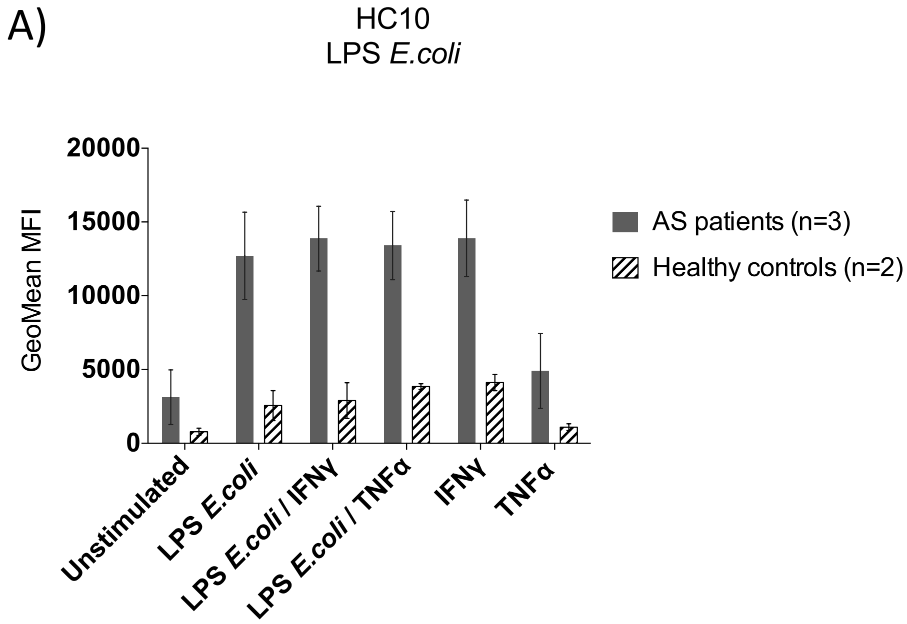

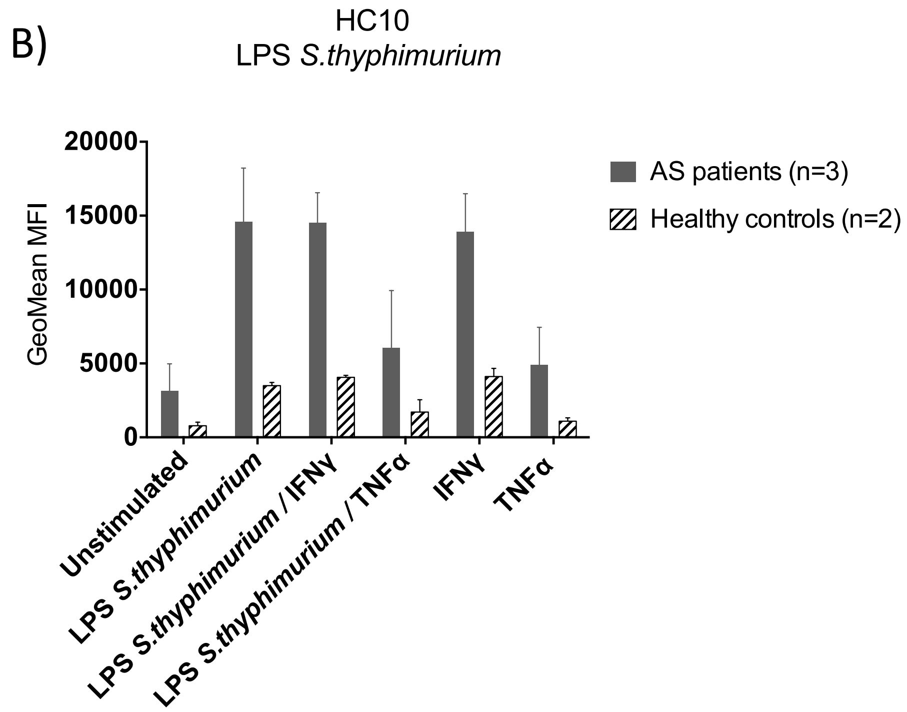

Figure 4.7 AS patient moDCs express higher ratios of cell surface HC10:W6/32 molecules compared to healthy controls. Ratios of cell surface HC10:W6/32 molecules in AS patient (Grey bars) and healthy control (Black and white bars) unstimulated moDCs or after A) LPS *E. coli* and B) LPS *S. thyphimurium* and/or cytokine stimulation. Representative data from n=3 experiments, number of samples included in analysis presented in graph legends. Error bars on graphs – Mean with SEM.

A)

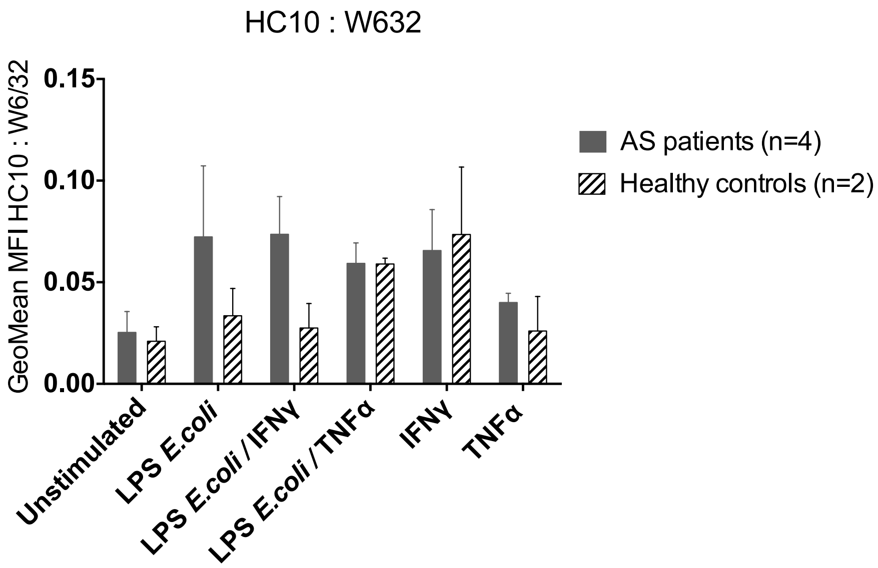

B)

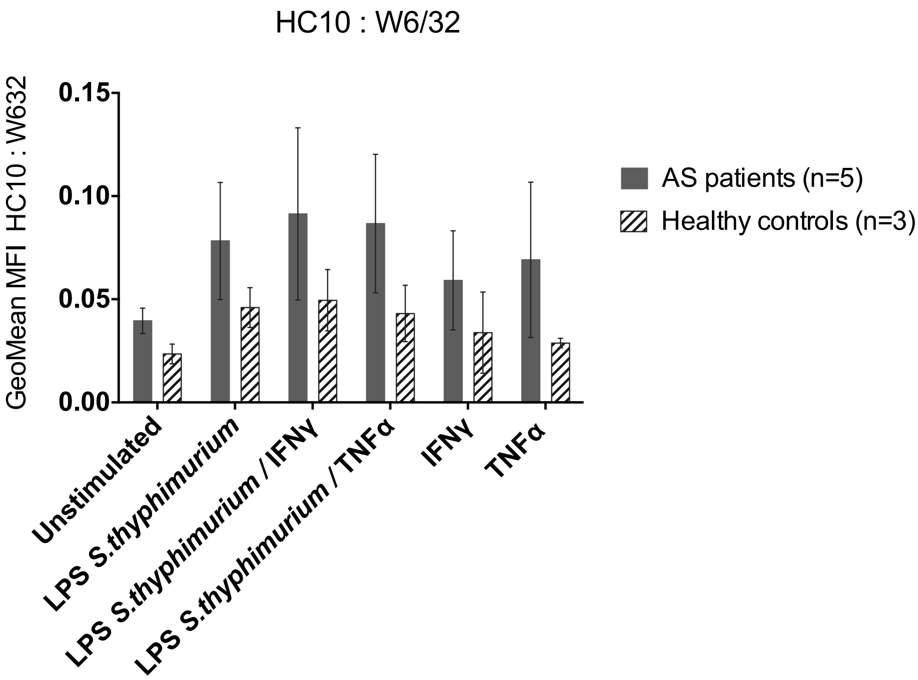

4.2.2 HD6-reactive molecules can be detected in B27+ve AS patient-derived moDCs following acid treatment

HD6-reactive molecules can be induced upon acid treatment in 220-B27 and 221-B27 cells, B27+ve BCLs (with natural expression of MHC class I molecules) and in B27+ve AS patient PBMCs (Chapter 3 and McHugh et al., 2014). As shown above, HD6 expression in B27+ve AS moDCs is undetectable even after DC maturation and upregulation of MHC class I molecules. Hence, I next sought to determine whether HD6-reactive molecules could be detected in AS patient moDCs following acid treatment. Unstimulated and mature (LPS-treated) moDCs from AS patients and healthy controls were treated with low pH iso-osmotic buffer as described previously, and then stained according to the standard flow cytometry protocol (see Materials and methods).

HD6-reactive molecules were detected in B27+ve AS patient moDCs but not B27-ve control moDCs following acid treatment (Figure 4.8, A vs B). In contrast, acid treatment increased levels of HC10-reactive molecules for both AS and healthy control moDCs (Figure 4.8, C and D). As expected, the levels of folded MHC class I molecules were decreased following acid treatment of all moDCs (Figure 4.9, A-D).

Figure 4.8 Induction of HD6-reactive molecules at the surface of B27+ve AS moDCs after acid treatment. HD6 staining before and after acid treatment in unstimulated (green) and LPS-treated (orange) A) B27+ve AS patient moDCs and B) B27-ve healthy control. HC10 staining before and after acid treatment in unstimulated (blue) and LPS-treated (pink) C) B27+ve AS patient moDCs and D) B27-ve healthy control moDCs. Dashed line histograms – before acid treatment. Solid line histograms – after acid treatment. Numbers in legends – GeoMean MFI.

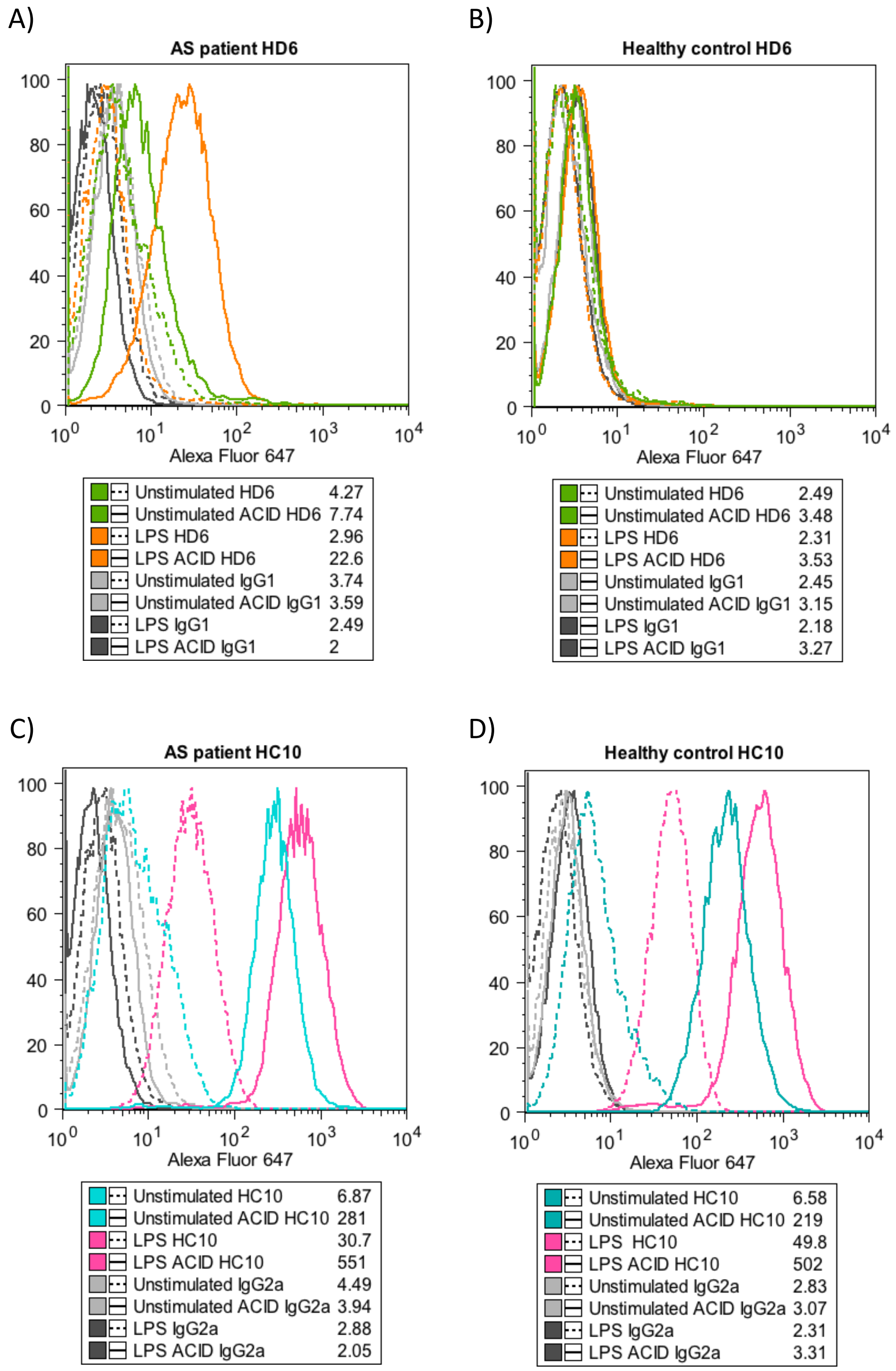

Figure 4.9 Changes in ME1- and W6/32-reactive molecules following acid treatment. ME1 staining before and after acid treatment in unstimulated (green) and LPS-treated (orange). A) B27+ve AS patient moDCs and B) B27-ve healthy control moDCs. HC10 staining before and after acid treatment in unstimulated (blue) and LPS-treated (pink) C) B27+ve AS patient moDCs and D) B27-ve healthy control moDCs. Representative flow cytometry data from n=5 independent experiments. Dashed line histograms – before acid treatment. Solid line histograms – after acid treatment. Numbers in legends – GeoMean MFI.

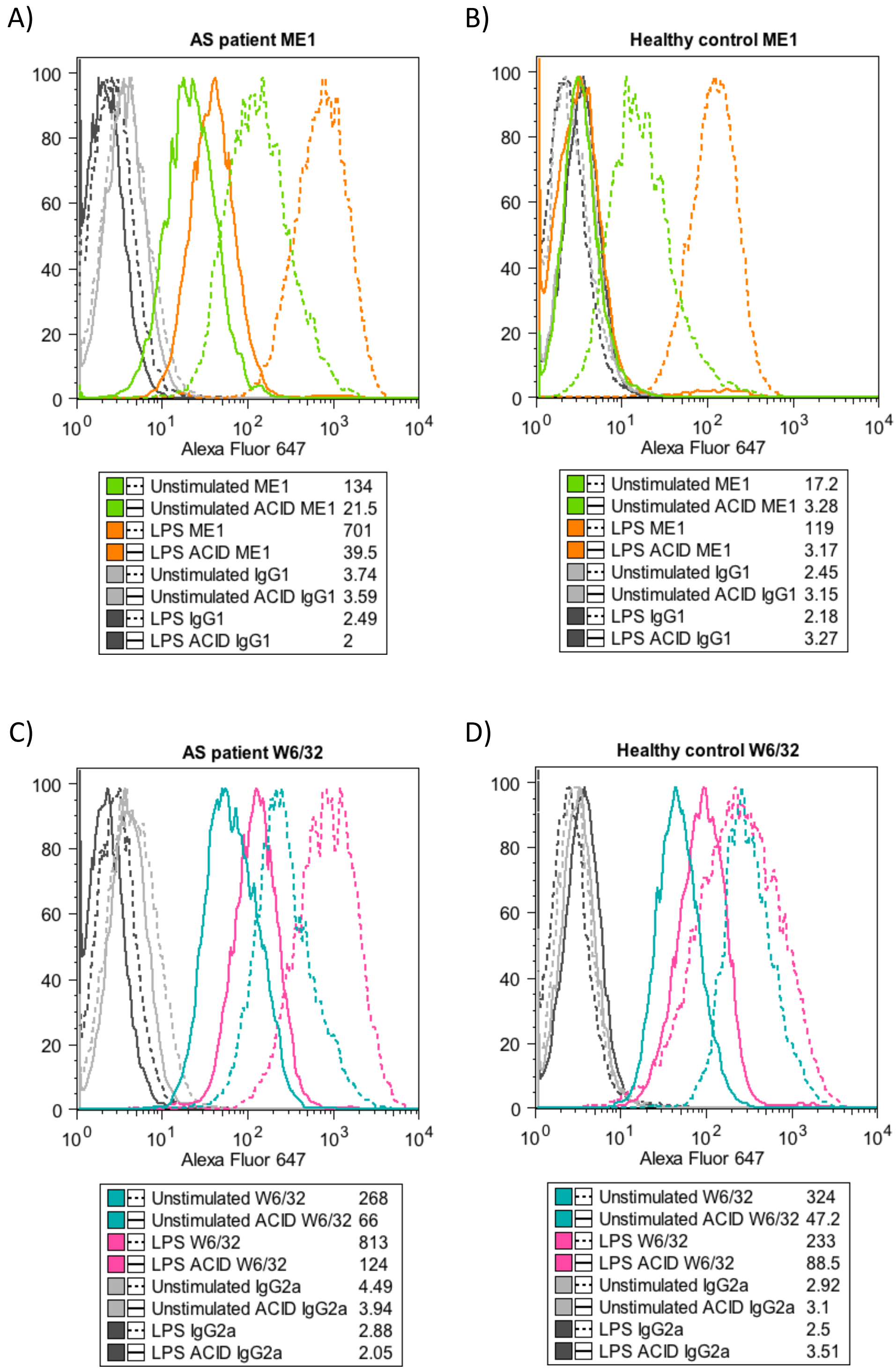

4.2.4 Confocal microscopy analysis of acid-induced HD6- and HC10-reactive molecules

Despite extensive studies on the nature of HLA-B27 molecules in cell lines, there are no published scientific reports investigating distribution of MHCI molecules at the cell surface of AS patient blood-derived cells. In B27 TG rats, B27 expression at the DC appears responsible for an impaired synapse formation with $CD4^{+}$ T cells (Hacquard-Bouder et al., 2007). Additionally, B27 TG rat APCs have been shown to have a defective costimulatory function, and can also stimulate $CD4^{+}$ T cells in an antigen-independent manner (Hacquard-Bouder et al., 2004). In the previous chapter I demonstrated that HD6- and HC10-reactive molecules could form clusters at the cell surface of B27-expressing cell lines. However, the detection of clustering was dependent on the levels of antibody staining, and therefore became more difficult upon acid treatment of cells, which upregulated both HD6 and HC10 staining. Altered seggregation patterns of MHC class I molecules in AS patient moDCs may be a cause of impaired synapse formation and functional interaction with $CD8^{+}$ and/or $CD4^{+}$ T cells.

Hence, I next sought to investigate whether HD6- and HC10-reactive molecules are distributed within the cell membrane in a distinct manner compared with ME1- and W6/32-reactive molecules using confocal microscopy. moDCs were cultured as before and unstimulated or LPS treated moDCs were than stained according to the standard flow cytometry protocol and visualized on 24-well fluorocarbon bottom microscopy plates using a Zeiss LSM710 confocal microscope and analyzed with ZEN software (see Materials and methods).

Cell surface HD6 staining was present in some of the LPS stimulated B27+ve AS moDCs (Figure 4.10, A), but not in immature moDCs (data not shown), seemingly inconsistent with my previous flow cytometry findings. However, these observed HD6+ve cells were relatively rare (≤5 cells per well). In agreement with my flow cytometry data, the majority of LPS stimulated moDCs expressed HC10-reactive molecules (Figure 4.10, B). ME1 and W6/32 staining were abundant at the cell surface of B27+ve AS moDCs (Figure 4.11, A and C).

Although only a fraction of moDCs expressed HD6-reactive molecules, these molecules did appear to form clusters (Figure 4.10, A). Clustering was also observed with the HC10 antibody (Figure 4.10, B), however this was not B27-specific as clusters could be seen in both B27+ve AS and B27-ve healthy control moDCs (Figure 4.10, D). Moreover, clustering was not specific for FHC, as ME1- and W6/32-reactive molecules seemed to also form clusters (Figure 4.11, A-D).

I next investigated the effect of acid treatment on cluster formation at the cell surface. Fluorescence intensity increased for both HD6 and HC10 following acid treatment of B27+ve moDCs (Figure 4.12, A vs B, C vs D), while ME-1 surface staining was decreased (Figure 4.12, E vs F). Importantly, and consistent with my previous flow cytometry findings, I did not observe any specific HD6 staining in samples from healthy controls carrying different than B27 HLA alleles (Figure 4.10, B).

Figure 4.10 Free heavy chains aggregate in small clusters at the surface of moDCs. HD6 (top row) and HC10 (bottom row) staining in LPS stimulated A) AS patient and B) healthy control moDCs. C) HC10 aggregates at the surface of AS patient moDCs, higher resolution (3X) of A) HC10 picture. Red – HD6 and HC10 secondary antibody, Alexa Fluor 647, Green – nuclear stain, Syto Green 24. Representative confocal microscopy data from n=5 independent experiments. Pictures taken with 40X objective using ZEISS LSM710 confocal microscope and analysed using ZEN software.

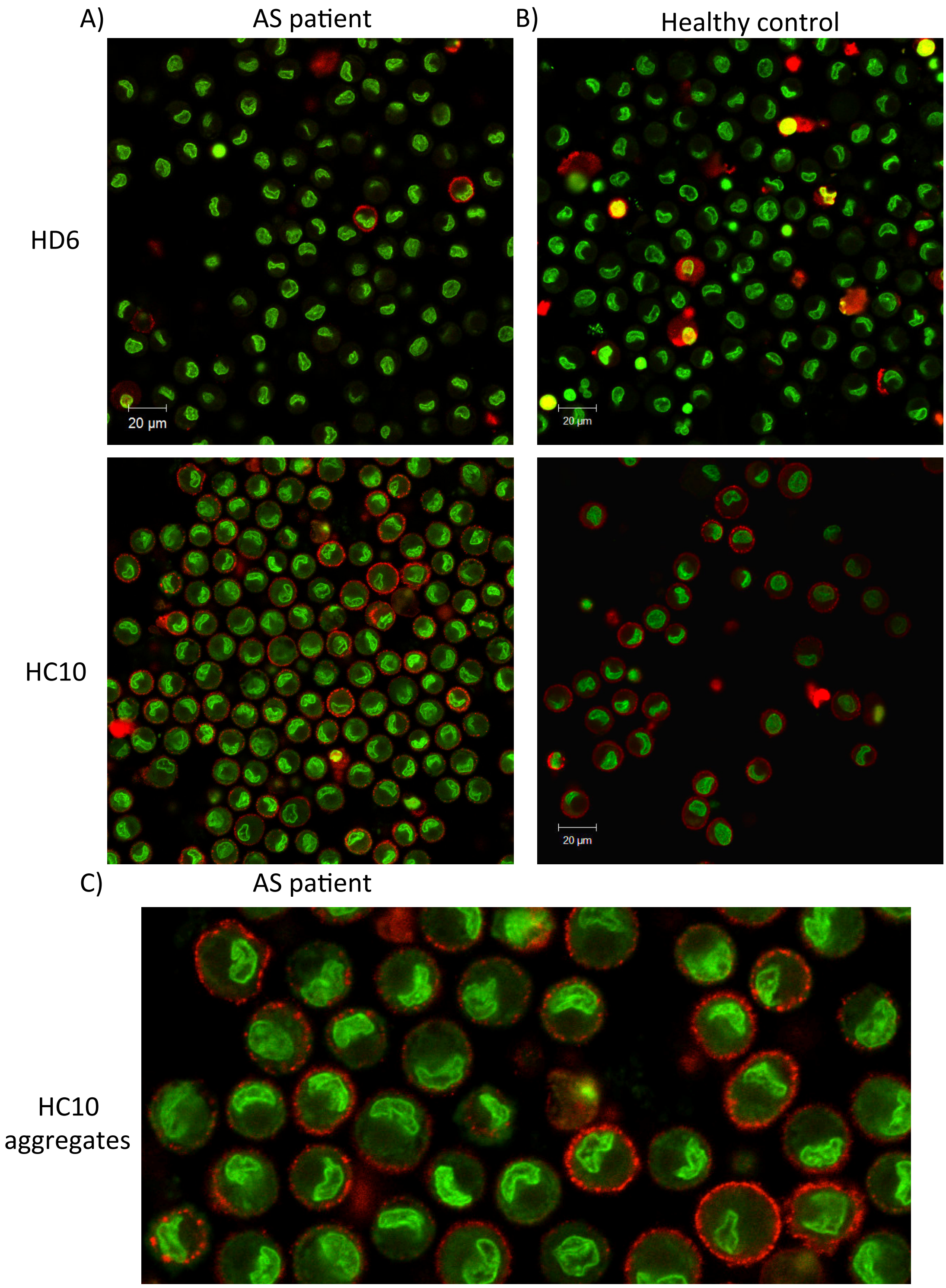

Figure 4.11 Aggregates of properly folded MHC class I molecules can be detected at the cell surface of moDCs. ME1 (top row) and W6/32 (bottom row) staining in LPS stimulated A) AS patient and B) healthy control moDCs. Red – ME1 and W6/32 secondary antibody, Alexa Fluor 647, Green – nuclear stain, Syto Green 24. Representative confocal microscopy data from n=5 independent experiments. Pictures taken with 40X objective using ZEISS LSM710 confocal microscope and analysed using ZEN software.

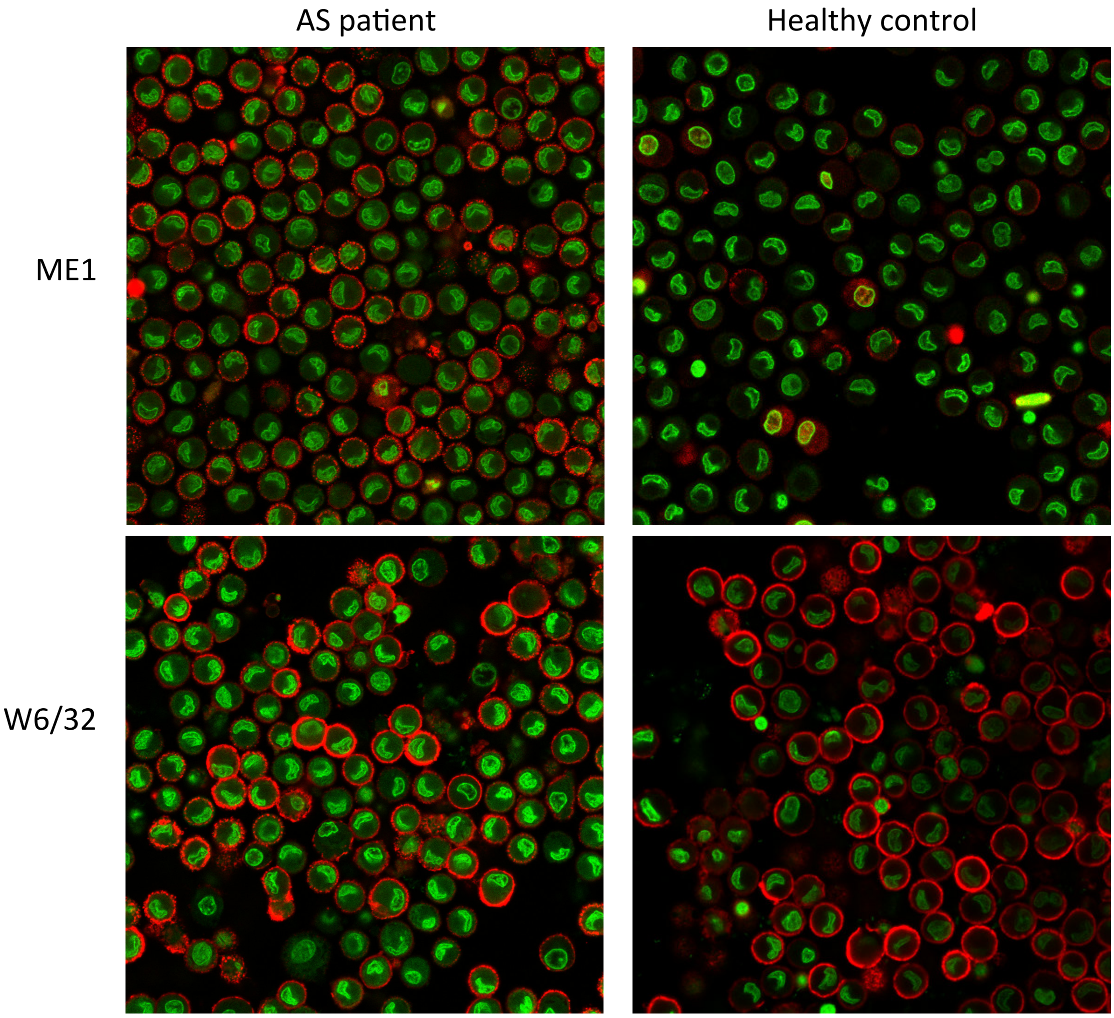

Figure 4.12 HD6-reactive molecules are induced at the surface of LPS stimulated AS patient moDCs upon acid treatment. A) HD6; B) Acid HD6; C) HC10; D) Acid HC10; E) ME1; F) Acid ME1. Confocal microscopy staining. Red (Alexa Fluor 633, secondary antibody); Green (nuclear stain SytoGreen 24). Pictures taken with 40X objective using Zeiss LSM710 confocal microscope and analysed using ZEN software. Representative data of n=3 experiments.

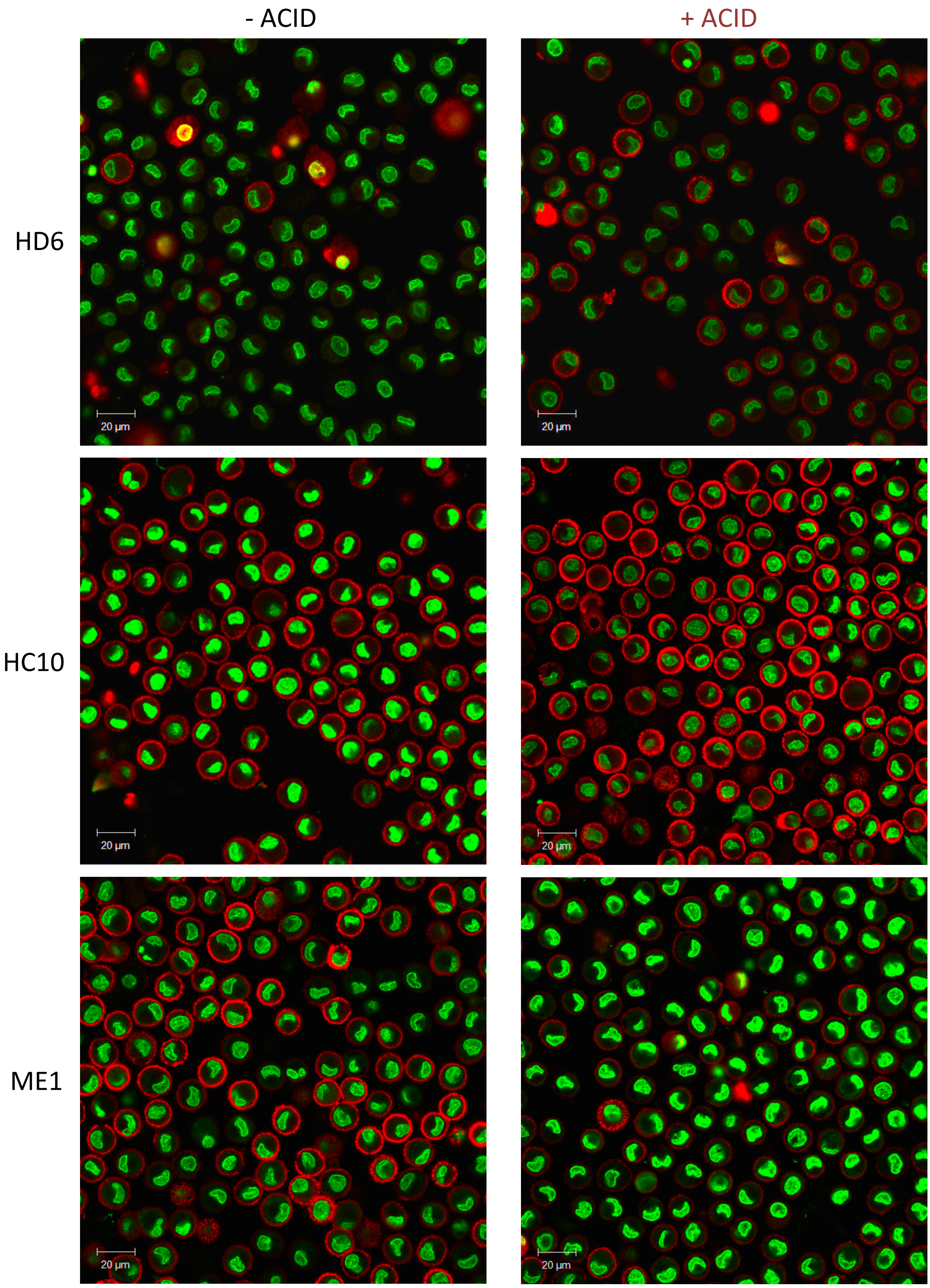

Summary Chapter 4.2

My results suggest that cell surface expression of HD6-reactive molecules was not induced through stimulation of moDCs via TLR4 (LPS), TLR9 (CpG) or TLR3 (Poly I:C), or at least it may require additional environmental factors. Notably, expression of HC10 in AS patient moDCs was higher after LPS stimulation compared with healthy controls. In AS moDCs LPS stimulation seemed to induce higher levels of HC10 and ME1 compared with CpG and Poly I:C.

Furthermore, cytokine stimulation (TNFα, IFNα, IFNβ, or IFNγ) or with either the combination of LPS with IFNγ or with TNFα also failed to induce the expression of cell surface HD6-reactive molecules in AS patient moDCs. Combining cytokine stimulation with LPS treatment also had no additive effect on the levels of HC10 staining, with intensities comparable to those seen with LPS treatment alone. Notably, when LPS derived from *S. typhimurium* was used in combination with TNFα, HC10 staining seemed to decrease to the levels seen with TNFα treatment alone.

However, at the same time the ratio of cell surface FHCs (HC10) to properly folded MHCI molecules (W6/32) seemed to be consistently elevated in the moDCs derived from AS patients compared with healthy controls. Hence, despite similar cell surface expression levels of properly folded MHCI molecules, AS patient-derived moDCs consistently presented more unfolded HC10-reactive species compared with healthy controls.

HD6-reactive molecules were induced following acid treatment specifically in B27+ve AS patient moDCs, but were absent in B27-ve healthy control moDCs. Confocal microscopy analysis of LPS stimulated moDCs suggested that HD6 staining can be detected at the surface of AS patient moDCs even before acid treatment, however HD6+ve cells were relatively rare (≤ 5 per well of 24-well microscopy plate). Furthermore, acid treatment had no influence on the cell surface seggregation patterns of NC-B27 and clasical MHCI molecules in moDCs. Clusters formation was visible both before and after acid treatment, with all used anti-MHC class I antibodies (HD6, HC10, ME1 and W6/32) and was not specific to B27+ve AS patient moDCs as was also observed in B27-ve control moDCs (HC10 and W6/32).

4.3 AS patient monocyte-derived Mφ do not express HD6-reactive molecules in *in vitro* culture

Macrophages have been found in AS patient synovial tissues and joints. Moreover, AS patient monocyte-derived macrophages have been shown to induce IL-23 production upon stimulation (Prevosto, Goodall, & Gaston, 2012). Hence, they may be implicated in the disease pathogenesis and might express NC-B27.

Therefore, next I sought to investigate whether HD6-reactive molecules can be expressed by monocyte-derived Mφ. $CD14^+$ monocytes were isolatated as previously described. Monocytes were cultured according to the standard Mφ generation protocol in R10 media supplemented with rh M-CSF for 5 days (see Materials and methods). 100ng/ml of *S.thyphimurium* LPS or 20ng/ml of IFNγ or combination of both stimuli, was used in overnight culture in order to induce higher levels of MHC class I expression. Typical macrophage morphology was observed on day 5 and 6. HD6, HC10, ME1 and W6/32 antibodies were used to stain Mφ by flow cytometry and confocal microscopy. Given that, monocyte-derived Mφ grow as adherent cells, a gentle detachment method with lidocaine was used to prepare cells immediately prior staining for flow cytometry. An alternative and commonly used detachment method employs trypsin/EDTA, however I have found that this can affect cell surface MHC class I molecules, in particular antibody epitopes, including those for HD6 and HC10. For microscopy analysis, the adherent Mφ were stained directly on fluorocarbon-bottom microscopy plates (see Materials and methods).

Both unstimulated and LPS and/or cytokine-treated AS patient Mφ expressed few, if any HD6- and low levels of HC10-reactive molecules (Figure 4.13, A and C). Combined stimulation with LPS/IFNγ induced the highest levels of ME1 and W6/32 staining compared with unstimulated Mφ and LPS or IFNγ (Figure 4.14, A and C). Confocal microsocpy data were consistent with my flow cytometry findings (Figure 4.15, A-D).

Consistent with my flow cytometry data, confocal microscopy analysis of both unstimulated and treated AS Mφ also revealed little if any HD6 and HC10 staining (Figure 4.13, B and D). Similar HC/10 and W6/32 staining was observed in healthy control Mφ (Figure 4.14, B and D).

Thus, my results suggest that *in vitro* cultured monocyte-derived Mφ do not express HD6-reactive molecules, even after stimulation with LPS and/or IFNγ. Furthermore, these Mφ are characterized by low levels of cell surface HC10 staining, despite the presence of properly folded MHC class I molecules (ME1 and W6/32).

Summary Chapter 4.3

AS patient and healthy control monocyte-derived Mφ expressed few if any HD6- and HC10-reactive molecules, despite the presence of significant levels of cell surface properly folded MHCI (ME1 and W6/32).

Figure 4.13 AS patient monocyte-derived Mφ express few if any HD6- and HC10-reactive molecules. HD6 staining in A) AS patient and B) healthy control monocyte-drived Mφ. HC10 staining in C) AS patient and D) helathy control monocyte-derived Mφ. Light blue histograms – unstimulated cells; Pink histograms – LPS; Dark blue histograms – IFNγ; Green histograms – LPS and IFNγ stimulated cells. Representative flow cytometry data from n=3 AS patient and n=2 healthy control samples. Numbers in legends – geometric mean MFI.

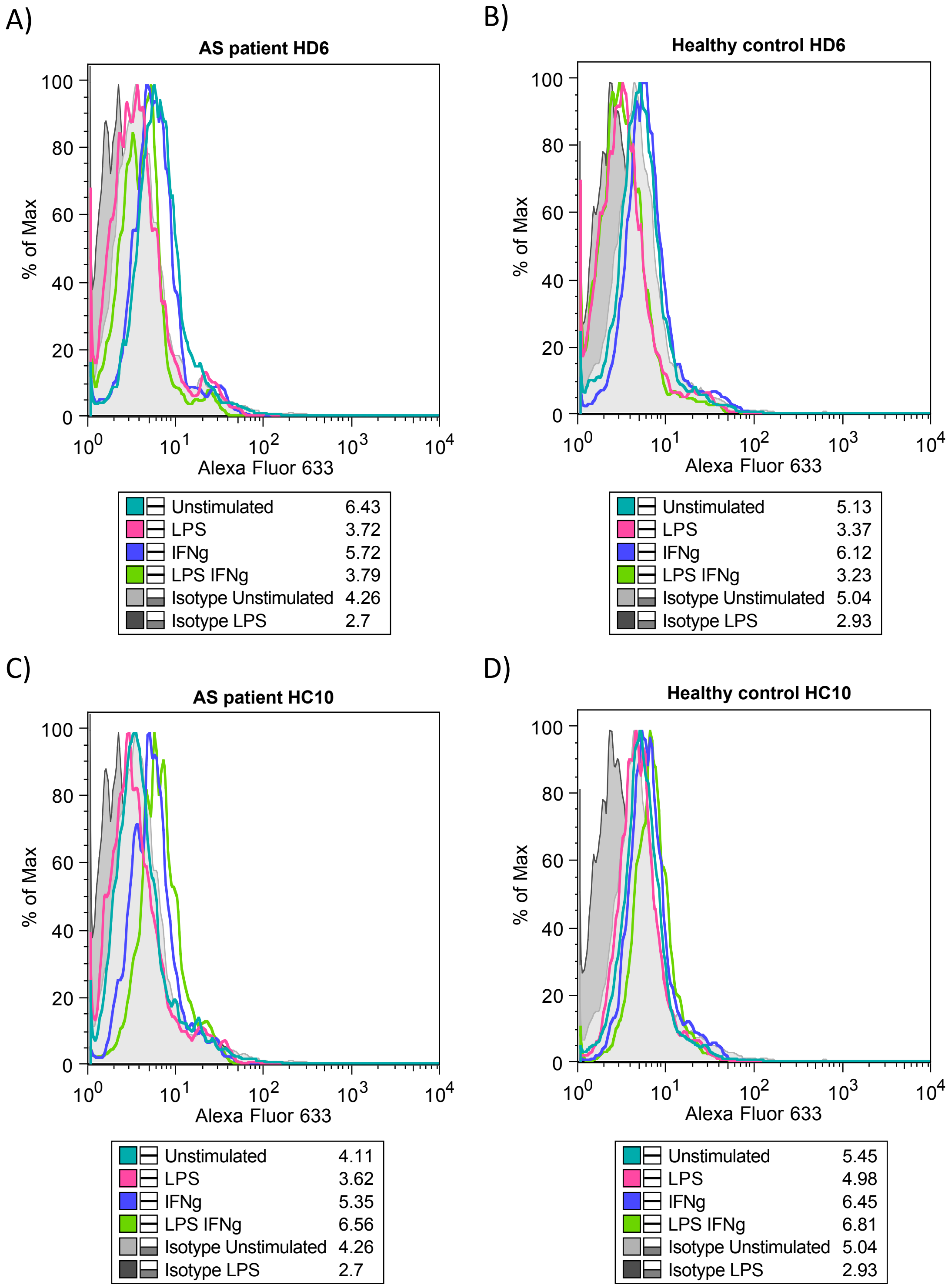

Figure 4.14 Expression of properly folded MHCI molecules in monocyte-derived Mφ. ME1 staining in A) AS patient and B) healthy control monocyte-drived Mφ. W6/32 staining in C) AS patient and D) helathy control monocyte-derived Mφ. Light blue histograms – unstimulated cells; Pink histograms – LPS; Dark blue histograms – IFNγ; Green histograms – LPS and IFNγ stimulated cells. Representative flow cytometry data from n=3 AS patient and n=2 healthy control samples. Numbers in legends – geometric mean MFI.

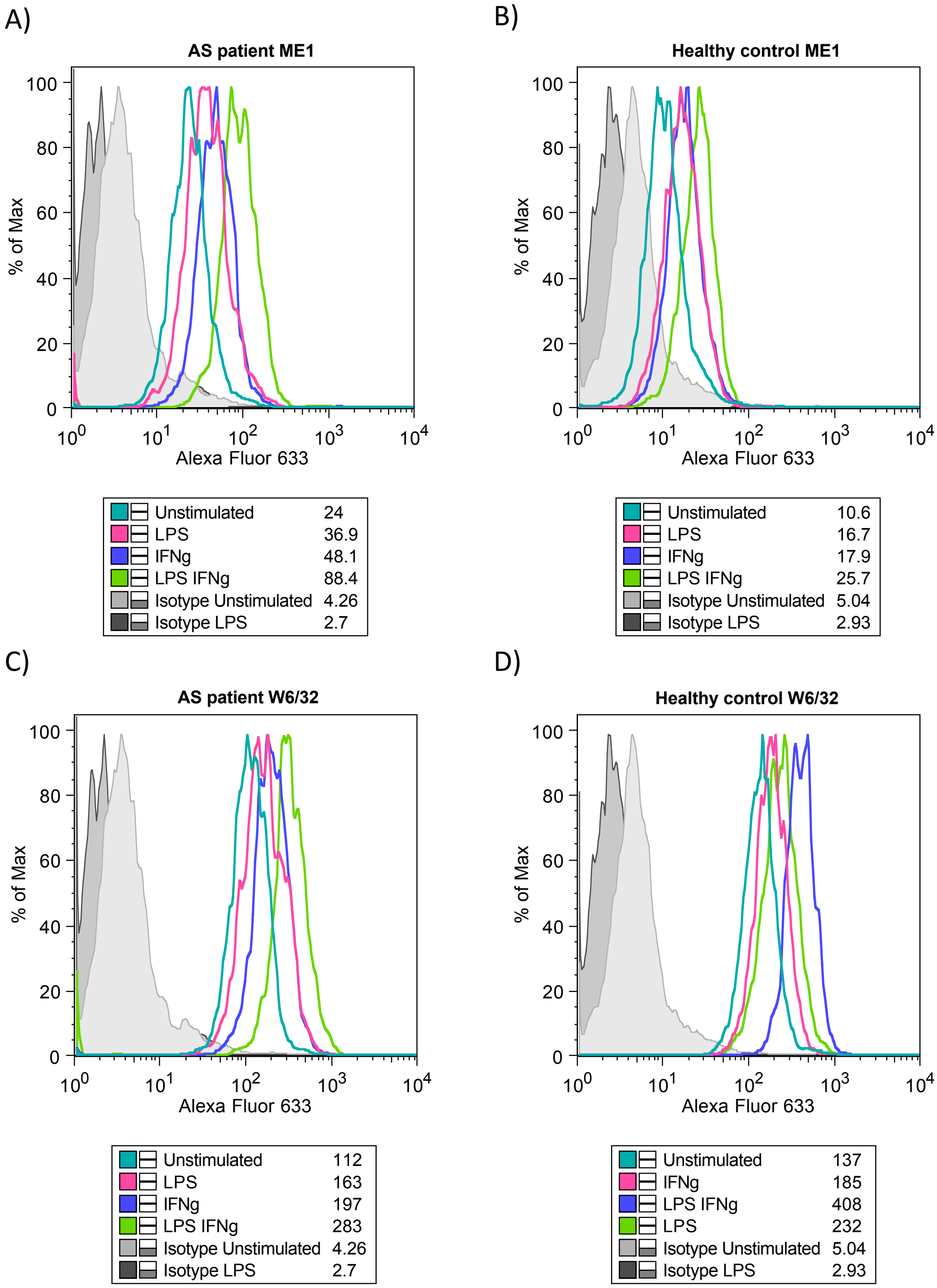

Figure 4.15 No significant HD6 and HC10 staining was detected at the cell surface of AS patient monocyte-derived Mφ. Confocal microscopy analysis of A) HD6, B) HC10, C) ME1 and D) W6/32 in AS patient monocyte-derived Mφ after 24h stiulation with LPS**.** Magenta - secondary antibody, Alexa Fluor 633; Green - nuclear stain, SytoGreen 24. Pictures were taken with 40X objective using Zeiss LSM510 confocal microscope and analyzed using ZEN software.

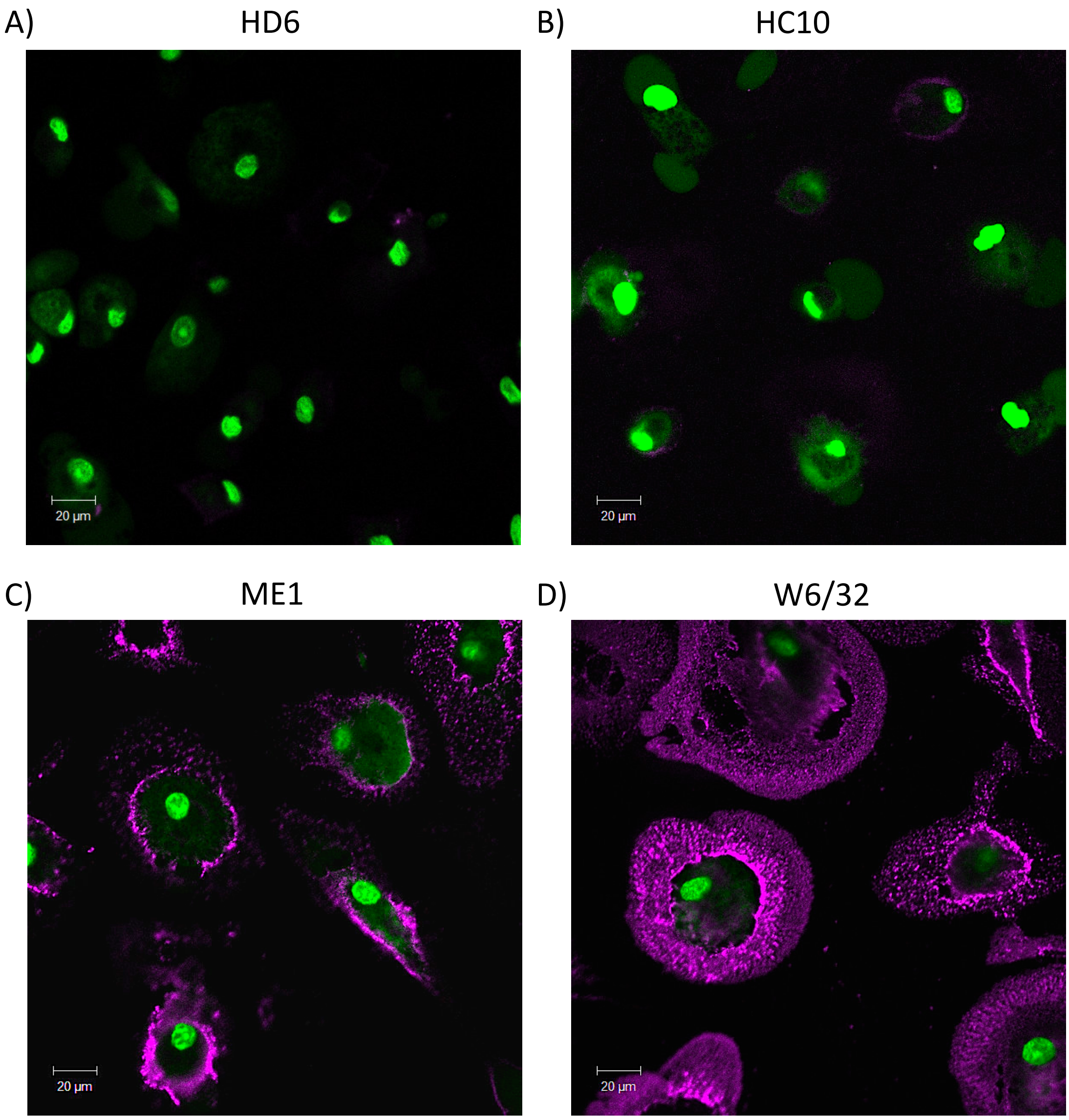

4.4 HD6-reactive molecules are detectable in B27+ve AS patient-derived osteoclasts

Osteoclasts are important bone remodeling cells, which can function as APCs, can secrete immunomodulatory factors, and have been shown to be involved in pathophysiology of SpA joints. Therefore, I next sought to investigate whether AS patient monocyte-derived osteoclasts could express potentially pathogenic NC-B27 molecules.

Osteoclasts were generated using two different methods. In the first method, osteoclasts were generated in a monoculture from pure monocytes. $CD14^{+}$ monocytes from 4 AS patients (3 B27+ve, 1 B27-ve) and 2 healthy controls (unknown HLA type) were cultured on 24-well microscopy plates for 13 days, in R10 media supplemented with 100ng/ml of rhRANKL and 25ng/ml of rhM-CSF. Every 3 days culture media was replaced with fresh media and rhRANKL/rhM-CSF. This allows the investigation of the osteoclastogenic properties of monocytic cells and the expression of HD6-reactive molecules in osteoclasts that have not been exposed to contact with other cell types present in PBMCs (e.g. T cells, NK cells). In the second method, osteoclasts were generated from whole PBMCs. PBMCs from AS patients and healthy controls were cultured on microscopy plates in R10 supplemented with 100ng/ml of rhRANKL and 25ng/ml of rhM-CSF. After 2-3 days of culture, when adherent, monocytic cells reached confluency, suspension cells were removed from wells and adherent cells were resuspended in a fresh R10 with 100ng/ml of rhRANKL and 25ng/ml of rhM-CSF (see Material and Methods). In this method, the activation state and potentially cell surface MHCI expression of osteoclasts may be affected by cell-cell interactions and cytokines present in the initial 2 day co-culture. Osteoclasts derived by both methods were subsequently stained directly on plates using HD6, HC10, ME1, W6/32 (see Materials and Methods).

Osteoclasts generated from AS patient B27+ve monocytes showed higher number of large multinucleated cells compared with the B27-ve AS patient and healthy control cells. Furthermore, the numbers of cells presenting characteristic "activated osteoclast"-like morphology (a large cell surface, "foamy" cytoplasm and ruffled edges) were higher in samples obtained from AS patient B27+ve monocytes compared with the B27-ve AS patient and control cells (Table 1). Of potential interest, a 2.5-3 fold decrease in the number of large cells was observed in two of the B27+ve AS patients recieving anti-TNFα treatment compared with the untreated AS patient (Table 1, AS 1417 - no treatment vs AS 1419 - Etanercept or AS 1422 - Adalimumab). Moreover, osteoclasts generated from the B27-ve AS 1423 patient and healthy control 2 showed very low number of large cells with osteoclast-like morphology (Table 1).

A relatively high intensity of HD6 staining was detected after osteoclasts generation from the B27+ve AS patients (Figure 4.16, A). The majority of these HD6-reactive molecules were present on the mononuclear monocytic-like cells present in the culture, possibly representing the activated monocytes or pre-osteoclasts, whereas a low intensity staining was observed in the multinucleated cells (Figure 4.16, A). Importantly, HD6 staining was absent in the B27-ve AS patient (AS 1423) and in one of the healthy controls (Healthy control 2), both of which presented a low number of activated osteoclast-like cells (data not shown). However, HD6 staining was detected in healthy control 1 (Figure 4.16, B), despite the fact that I did not observe ME1 staining (suggesting that healthy individual was B27-ve) (Figure 4.17, B).

Intensities of HC10 (Figure 4.16, C vs D) and W6/32 (Figure 4.17, C vs D) staining were similar in both AS patient and healthy control samples.

Therefore, HD6 staining observed in osteoclast culture from B27-ve healthy control could be due to the unspecific antibody binding. Despite the use of a standard FcR blocking buffer, 2%FCS/10% normal goat serum (NGS) and 10% normal rabbit serum (NRS), in the osteoclast staining protocol, I can not exclude the possibility of insufficent FcR blockage or non-specific binding of HD6 antibody to osteoclast surface under specific conditions. Hence, I next sought to test whether FcR blocking with a commercial Fc gamma receptor (FcγR) blocking reagent (MACS Miltenyi, UK) (containing anti-CD32, anti-CD16 antibodies) could affect HD6 staining in osteoclast cultures.

Importantly, HD6 staining on all mononuclear cells was completely abolished after the use of a commercial FcγR block. However, low levels of fluorescence signals were still present on multinucleated, osteoclast-like cells in AS patient samples (Figure 4.18, A-D). Moreover, the intenstities of HC10 (Figure 4.16, C vs 4.19, B), ME1 (Figure 4.17, A vs 4.19, C) and W6/32 (Figure 4.17, C vs 4.19, D) staining were significantly lower after the use of a commercial FcγR block compared with 2%FCS/10%NGS/10%NRS.

Thus, these findings suggested that MHCI staining on mononuclear cells was dependent on FcR blocking reagent and high intensity HD6 staining observed previously even in healthy control sample could be due to the insufficient FcR block. At the same time, HD6 staining on multinucleated cell was not affected by the FcR blocking method and likely represents specific binding.

No HD6 staining was observed in healthy control OCs when the commercial FcγR blocking reagent was used.

Next I generated osteoclasts from whole PBMCs to test whether direct cell-cell intractions or the presence of cytokines and other immune modulators induced in co-culture conditions could affect osteoclast expression of cell surface NC-B27 molecules. A commericial FcγR blocking reagent was used in the staining protocol (see Materials and methods).

HD6-reactive molecules were detected mainly at the surface of large, multinucleated cells derived from B27+ve AS patient PBMCs, similar to the previous findings with osteoclasts generated from a pure monocyte population and in the presence of the Fc blocking reagent (Figure 4.20, A-C). HC10 (Figure 4.21, A), ME1 (Figure 4.21, B) and W6/32 (Figure 4.21, C) staining were also expressed at similar levels compared with osteclasts derived from $CD14^{+}$ cells.

Thus, my data suggests that expression levels of classical and non-classical MHCI molecules on osteoclasts is not affected by the presence of other cell types and/or cytokines and immune mediators produced in the osteoclasts culture from the whole PBMCs.

Table 4.1 HLA-B27+ AS patient monocytes forms higher numebr of multinucleated, large osteoclast-like cells when cultured in media supplemented with rhRANKL and rhM-CSF. Number of cells evaluated on semi-quantitavie analysis of at least 18 confocal microscopy pictures taken from different areas of n=6 independent culture wells.

SAMPLE	HLA-B27 status*	Treatment	Number of multinucleated cells/picture	Number of large osteoclasts/ picture area
AS 1417	+	No treatment	2.39	0.83
AS 1419	+	Etanercept	2.46	0.27
AS 1422	+	Adalimumab	4.59	0.35
AS 1423	-	No treatment	2.41	0.03
Healthy control 1	-	NA	3.45	0.2
Healthy control 2	-	NA	1.9	0.03

* AS patients HLA-B27 status determined on a PCR-based routine diagnostic test; Healthy controls – ME1-negative staining

Figure 4.16 High levels of HD6-reactive molecules are dtected at the cell surface of both B27+ve AS patient and B27-ve healthy control monocyte-derived osteoclasts after blocking with 2%FCS/10%NGS/10%NRS. HD6 staining in A) AS patient and B) healthy control monocyte derived osteoclasts. HC10 staining in C) AS patient and D) healthy control monocyte derived osteoclasts. Red – HD6 or HC10, secondary antibody, Alexa Fluor 647. Green – nuclear stain, SytoGreen 24. Pictures taken using 40X objective, Zeiss LSM710 confocal microscope and analyzed using ZEN software.

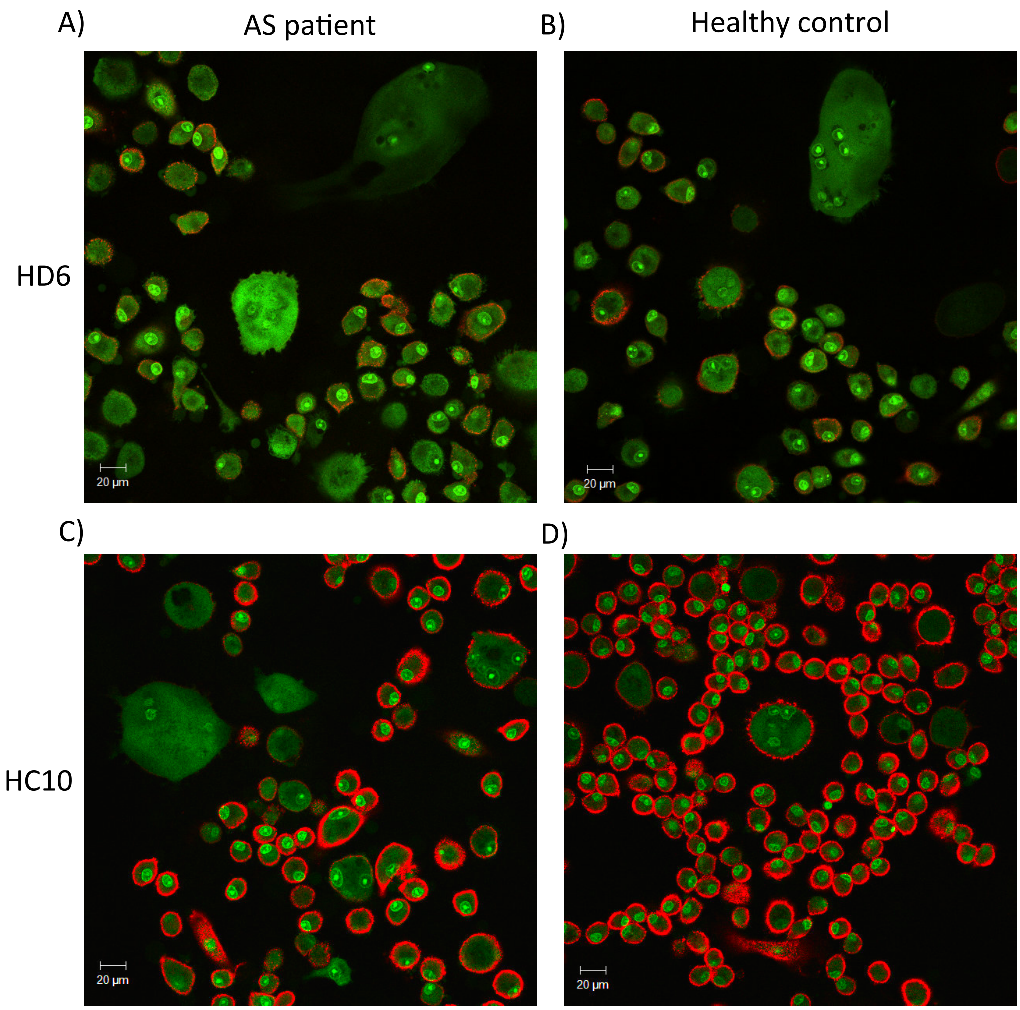

Figure 4.17 Expression of ME1- and W6/32-reactive molecules in B27+ve AS patient and B27-ve healthy control monocyte-derived osteoclasts. ME1 staining in A) AS patient and B) healthy control monocyte derived osteoclasts. W6/32 staining in C) AS patient and D) healthy control monocyte derived osteoclasts. Red – ME1 or W6/32, secondary antibody, Alexa Fluor 647. Green – nuclear stain, SytoGreen 24. Pictures taken using 40X objective, Zeiss LSM710 confocal microscope and analyzed using ZEN software.

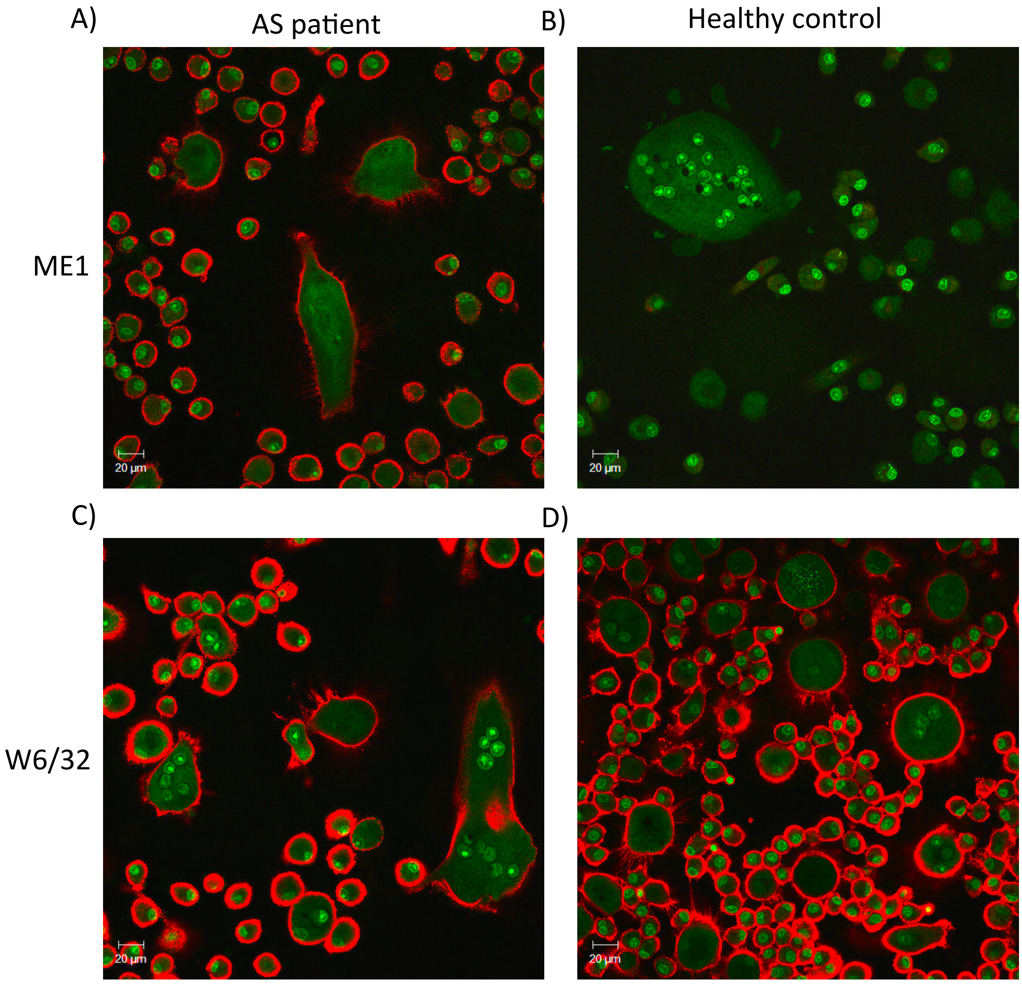

Figure 4.18 HD6-reactive molecules are present at the cell surface of B27+ve AS patient monocyte-derived osteoclasts even after using a commercial FcγR blocking reagent. HD6 staining in AS patient monocyte derived osteoclasts pictures A) and B) 2D view; C) and D) 3D view of areas in picture A) and B). Red – HD6, secondary antibody, Alexa Fluor 647. Green – nuclear stain, SytoGreen 24. Pictures taken using 40X objective, Zeiss LSM710 confocal microscope and analyzed using ZEN software.

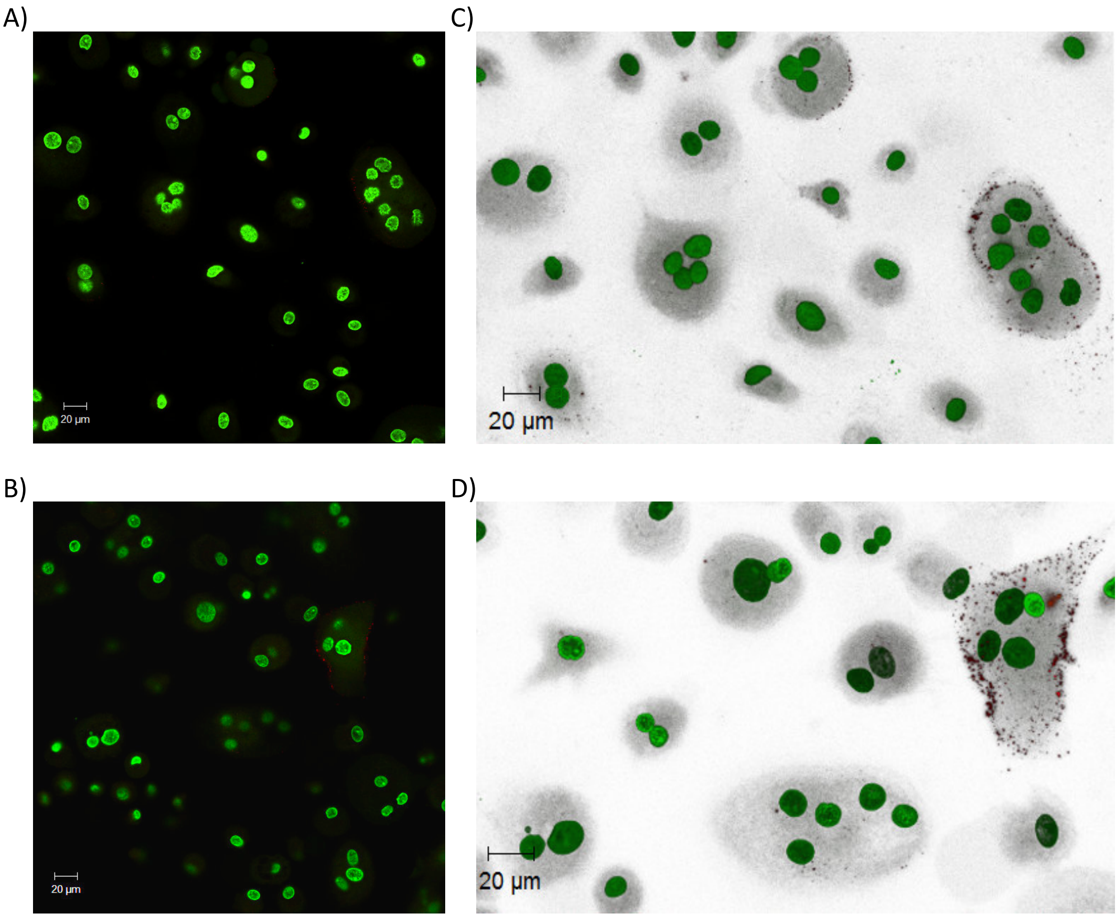

Figure 4.19 Cell surface expression of MHCI molecules in B27+ve AS patient monocyte-derived osteoclasts after using a commercial FcγR blocking reagent. A) HD6, B) HC10, C) ME1 and D) W6/32 staining in AS patient monocyte derived osteoclasts pictures. Red – HD6, secondary antibody, Alexa Fluor 647. Green – nuclear stain, SytoGreen 24. Pictures taken using 40X objective, Zeiss LSM710 confocal microscope and analyzed using ZEN software.

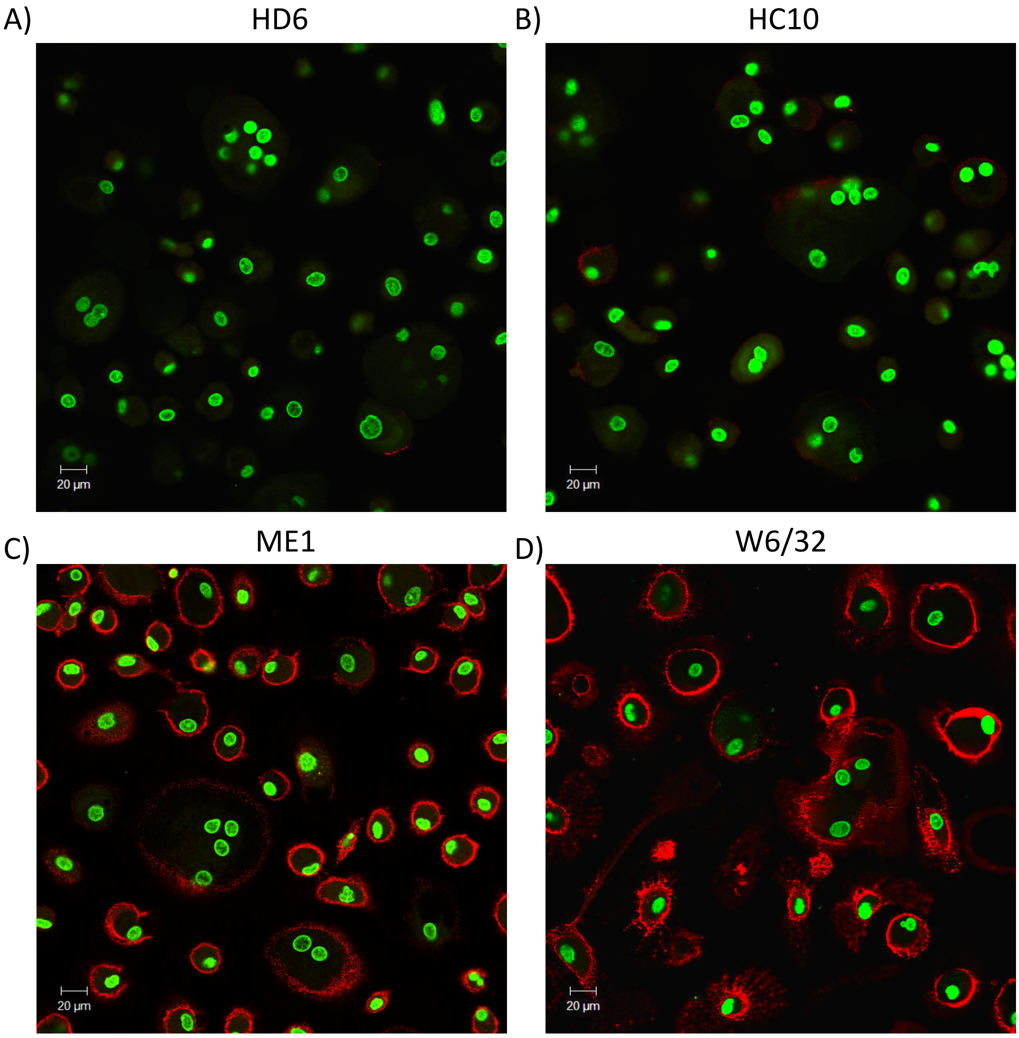

Figure 4.20 HD6-reactive molecules are present at the cell surface of B27+ve AS patient PBMC-derived osteoclasts after using a commercial FcγR blocking reagent. HD6 staining in AS patient PBMC-derived osteoclasts pictures A) and C) 2D view; B) 3D view of the area from picture A. D) IgG1 – isotype control. Red arrows indicating HD6 staining. Red – HD6, secondary antibody, Alexa Fluor 647. Green – nuclear stain, SytoGreen 24. Pictures taken using 40X objective, Zeiss LSM710 confocal microscope and analyzed using ZEN software.

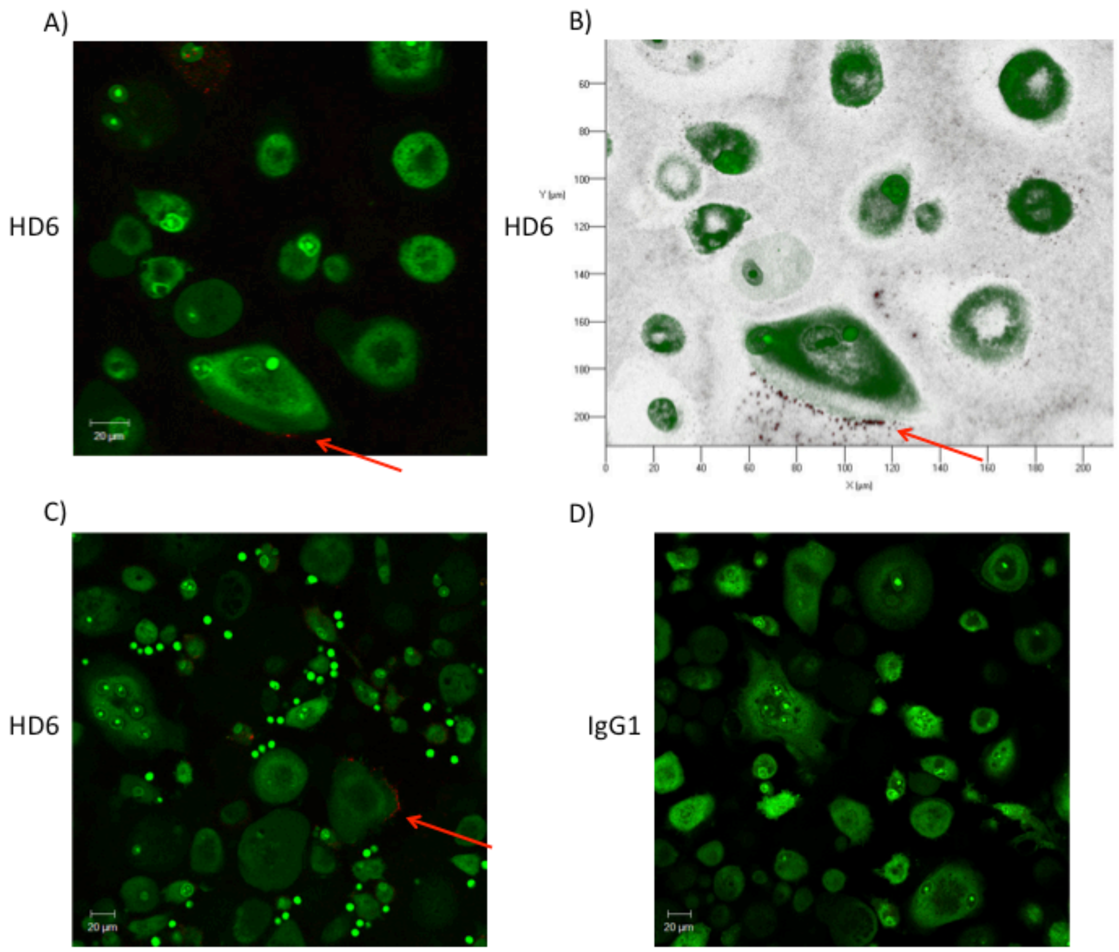

Figure 4.21 Cell surface staining of MHC class I molecules in B27+ve AS patient PBMC-derived osteoclasts after using a commercial FcγR blocking reagent. Free heavy chains - A) HC10, and properly folded MHCI molecules - B) ME1 and C) W6/32 in osteocasts derived from AS patient PBMCs. D) IgG2a - isotype control. Red - MHCI, secondary antibody, Alexa Fluor 647. Green – nuclear stain, SytoGreen 24. Pictures taken using 40X objective, Zeiss LSM710 confocal microscope and analyzed using ZEN software.

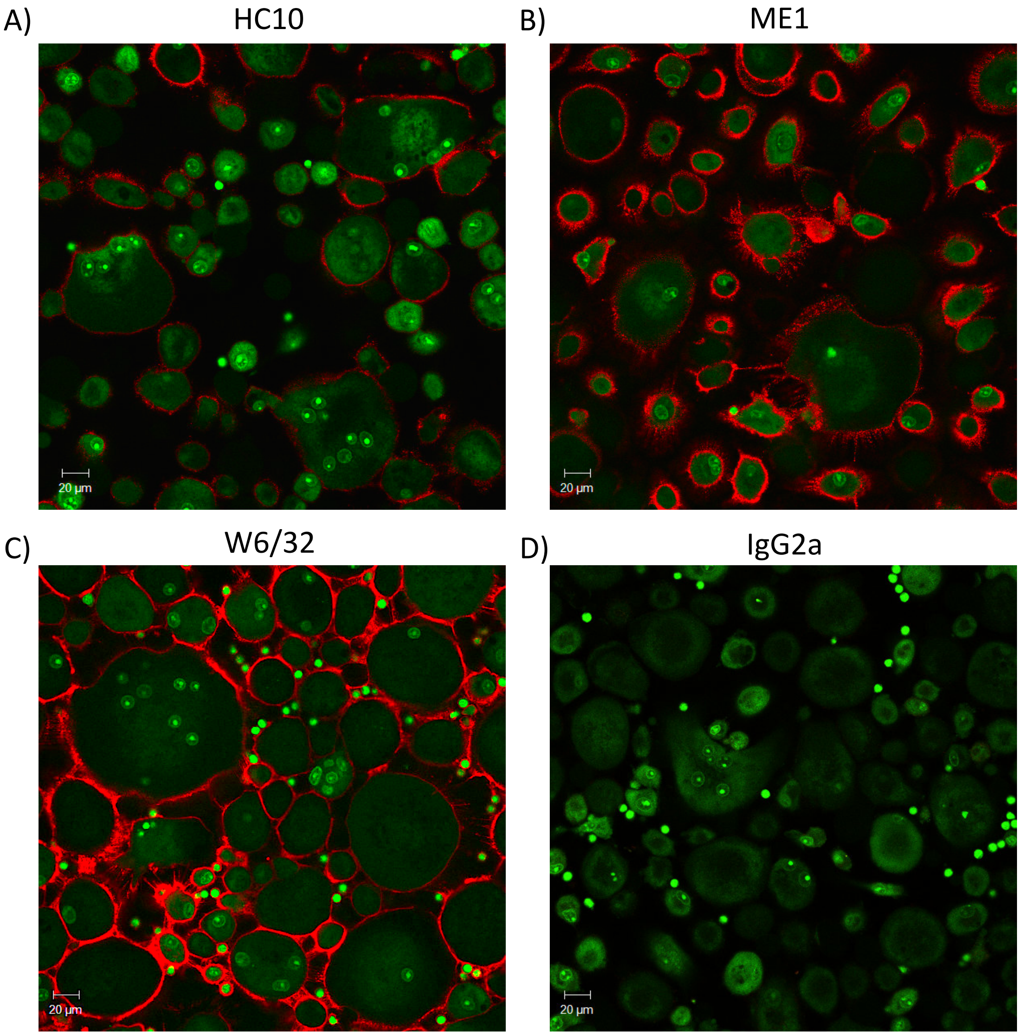

Notably, I observed a higher number of large, multinucleated cells (5 or more nuclei/osteoclast cell) with a characteristic osteoclast-like morphology (ruffled cell membrane are, “foamy” cytoplasm) when osteoclasts were generated from whole PBMCs compared with OCs derived from $CD14^+$ cells (Figure 4.16 and 4.17 vs 4.20 and 4.21). This suggests that the presence of other cell types, which can express osteoclastogenesis mediators or enable direct cell-cell interactions, can positively influence osteoclast formation process.

Summary Chapter 4.4

Confocal microsocpy analysis of AS patient-derived osteoclasts suggested that low levels of HD6 staining can be detected on multinucleated cells derived from both pure monocyte and whole PBMCs.

Monocytes derived from untreated B27+ve AS patients generated more large osteoclasts, with an activated-like morphology compared to B27+ve AS patients on anti-TNFα tretament, B27-ve AS patient and healthy controls.

4.5 HD6-reactive molecules are present at the surface of synovial tissue cells, but are not detectable in synovial fluid cell isolates

HD6-reactive molecules are not abundantly expressed at the cell surface of blood-derived cell populations in *in vitro* culture. However, NC-B27 molecules may be present at the cell surface of resident and/or infiltrating cells in the inflammed SpA joints. Therefore, I next sought to investigate HD6 staining in cells isolated from AS patient-derived knee synovial tissue and fluid using flow cytometry. Importantly, axial skeleton tissue and fluid samples are extremely rare due to the invasive and dangerous nature of the procedure. On the other hand, inflammatory manifestations in peripheral joints (e.g. knee, wrist, ankle) are relatively rare in AS patients. Hence, despite an access to a large number of blood samples the access to the synovial fluid and tissue samples was limited.

4.5.1 HD6-reactive molecules are detected by flow cytometry in cells isolated from AS patient synovial tissue

Synovial tissue cells were isolated in a collagenase-free method using a mesh cell strainer and syringe plunger. An enzyme-free tissue cell isolation allows to preserve untouched cell surface non-classical and classical forms of MHC class I molecules and thus avoid destroying any potential MHCI antibody epitopes. Synovial fluid cells were isolated according to the standard gradient centrifugation cell isolation protocol. Subsequently synovial tissue and fluid cells were stained according to the standard flow cytometry protocol and analyzed using flow cytometry and confocal microsocpy (see Materials and Methods).

Three cell populations (Figure 4.22 and 4.23 A, Population 1-3) were distinguished in synovial tissue and fluid samples using flow cytometry based on dot plots representing cell granularity (SS, side-scatter) vs cell size (FS, forward scatter). Based on these physical features population 1 most likely represent lymphocytes, population 2 - monocytic cells and population 3 -granulocytes.

Notably, HD6 staining was detected in cells with a monocyte-like morphology (population 2) isolated from B27+ve AS patient knee synovial tissue sample (Figure 4.22, B, HD6-dark blue histogram), but were absent in synovial fluid sample (Figure 4.23, B, HD6-dark blue histogram). Cells in both population 1 (lymphocyte morphology) (Figure 4.22 and 4.23, C) and population 3 (granulocyte morphology) (Figure 4.22 and 4.23, D) did not express HD6-reactive molecules (dark blue histograms).

HC10-reactive molecules were expressed on cells with a lymphocyte-like and monocyte-like morphology (populations 1 and 2), but were absent on granulocyte-like cells in both synovial tissue and fluid cell isolates (Figure 4.22 and 4.23, B-D, HC10-pink histograms).

Moreover, granulocyte-like cells expressed relatively low levels of properly folded MHCI molecules, compared with lymphocyte-like and monocyte-like cells (Figure 4.21 and 4.22, B-D, ME1-green and W6/32-light blue histograms).

Figure 4.22 Low levels of HD6 staining are detected in AS patient synovial tissue isolates in cells gated as population 2. A) FSC/SSC dot plot showing the population gating strategy. Expression of non classical (Dark blue histograms - HD6; Pink histograms - HC10) and properly folded (Green histograms - ME1; Light blue histograms – W6/32) MHCI molecules in B) Population 1; C) Population 2; D) Population 3. Grey histograms - isotype mix - IgG1 and IgG2a control. Number of AS patient samples analyzed n=1, n=3 replicates were performed for each staining condition. Numbers in legends – GeoMean MFI,

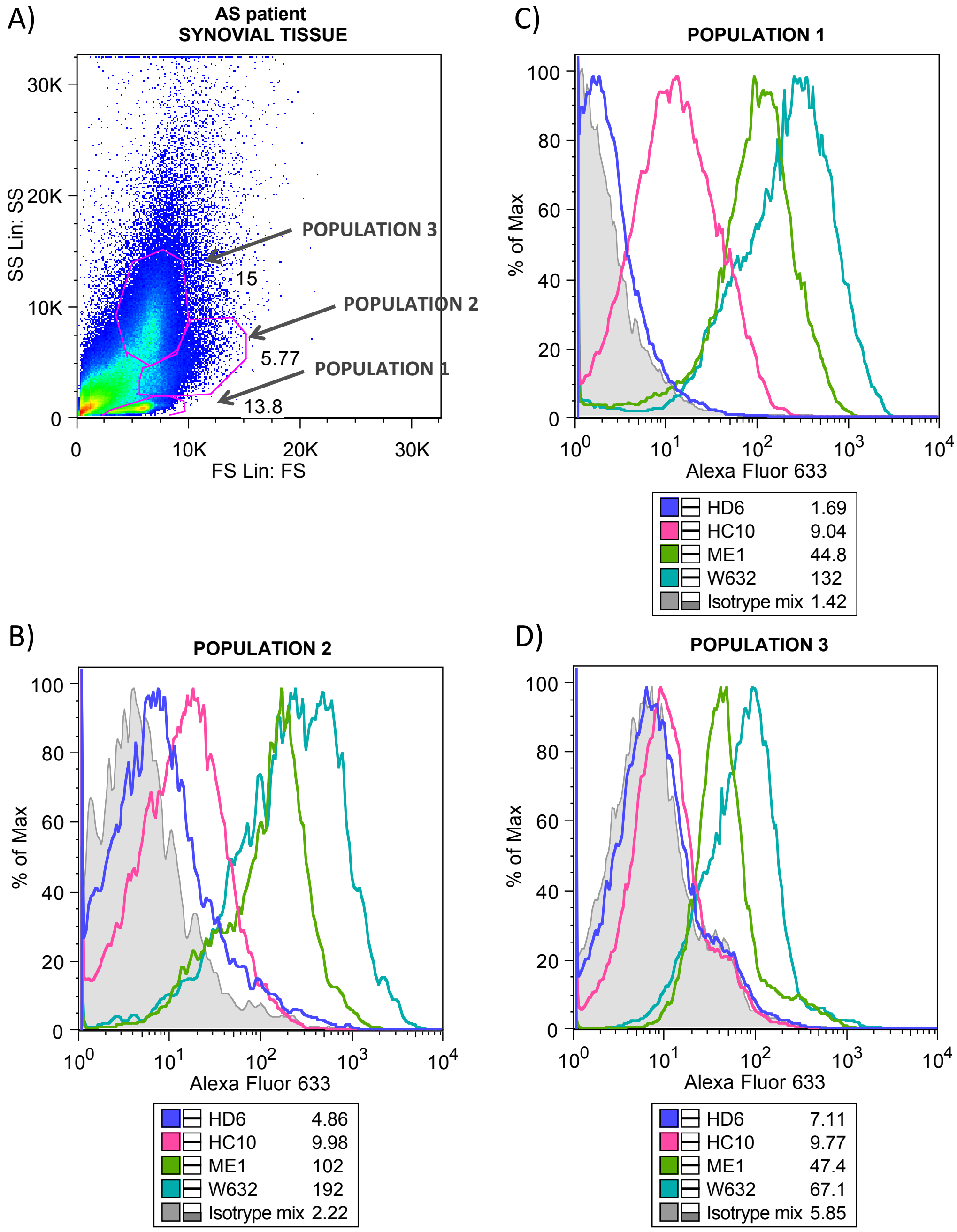

Figure 4.23 HD6-reactive molecules are undetectable in AS patient synovial fluid sample. A) FSC/SSC dot plot showing the population gating strategy. Expression of non classical (Dark blue histograms - HD6; Pink histograms - HC10) and properly folded (Green histograms - ME1; Light blue histograms – W6/32) MHCI molecules in B) Population 1; C) Population 2; D) Population 3. Number of AS patient samples analyzed n=1, n=3 replicates were performed for each staining condition. Numbers in legends – GeoMean MFI, secondary antibody Alexa Fluor 633.

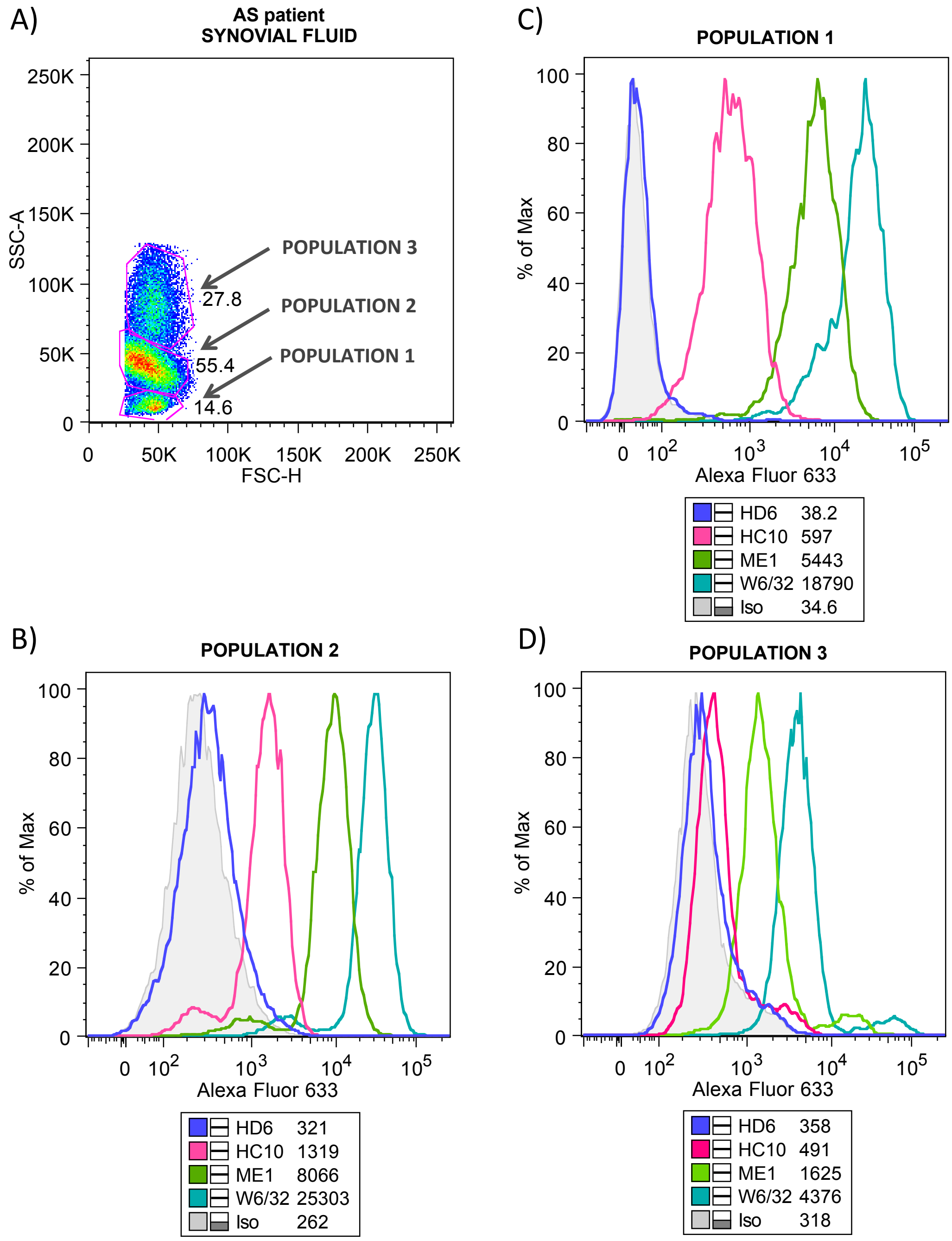

Simultaneously, confocal microscopy staining of SFMCs and PBMCs isolated from the same B27+ve AS patient was performed in order to investigate segregation patterns of non-classical and classical MHCI molecules.

Consistent with my flow cytometry findings, few, if any HD6-reactive molecules were detected in synovial fluid cell isolates and PBMCs (Figure 4.24, A and B). Notably, relatively high levels of FHCs (HC10) and properly folded B27 molecules (ME1) were detected at the surface of mononuclear cells (Figure 4.24, C and D and 4.25, A and B). Multinucleated cells with a granulocyte-like morphology expresed lower amounts of HC10- and ME-reactive molecules compared with mononuclear cells. Furthermore, cell surface FHCs and properly folded ME1-reactive molecules had a tendency to form clusters.

Figure 4.24 HD6-reactive molecules are not detected by confocal microscopy in SFMCs and PBMCs isolated from B27+ve AS patient. Mononuclear cells in SFMCs express relatively high levels of HC10. HD6 staining in A) SFMCs and B) PBMCs from B27+ve AS patient. HC10 staining in C) SFMCs and D) PBMCs. Red - MHCI, secondary antibody, Alexa Fluor 647. Green – nuclear stain, Syto Green 24. Number of AS patient samples analyzed n=1, n=3 replicates were performed for each staining condition. Pictures taken using 40X objective, Zeiss LSM710 confocal microscope and analyzed using ZEN software.

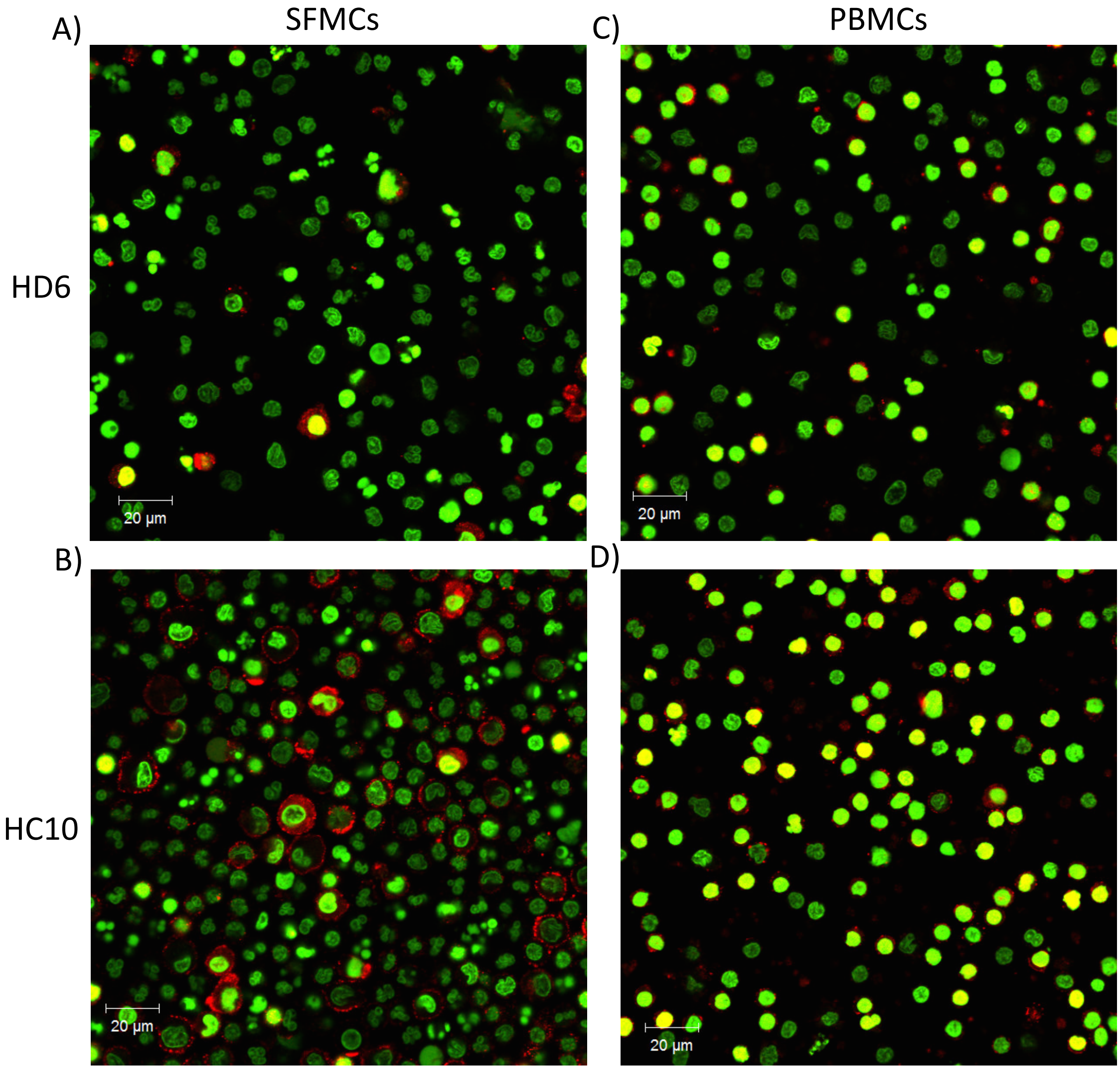

Figure 4.25 Cluster formation and abundant amounts of ME1-reactive molecules can be detected at the surface of mononuclear cells in SFMCs and PBMCs. ME1 staining in A) SFMCs and B) PBMCs from B27+ve AS patient. IgG1 - isotype control in C) SFMCs and D) PBMCs. Red - MHCI, secondary antibody, Alexa Fluor 647. Green – nuclear stain, Syto Green 24. Number of AS patient samples analyzed n=1, n=3 replicates were performed for each staining condition. Pictures taken using 40X objective, Zeiss LSM710 confocal microscope and analyzed using ZEN software.

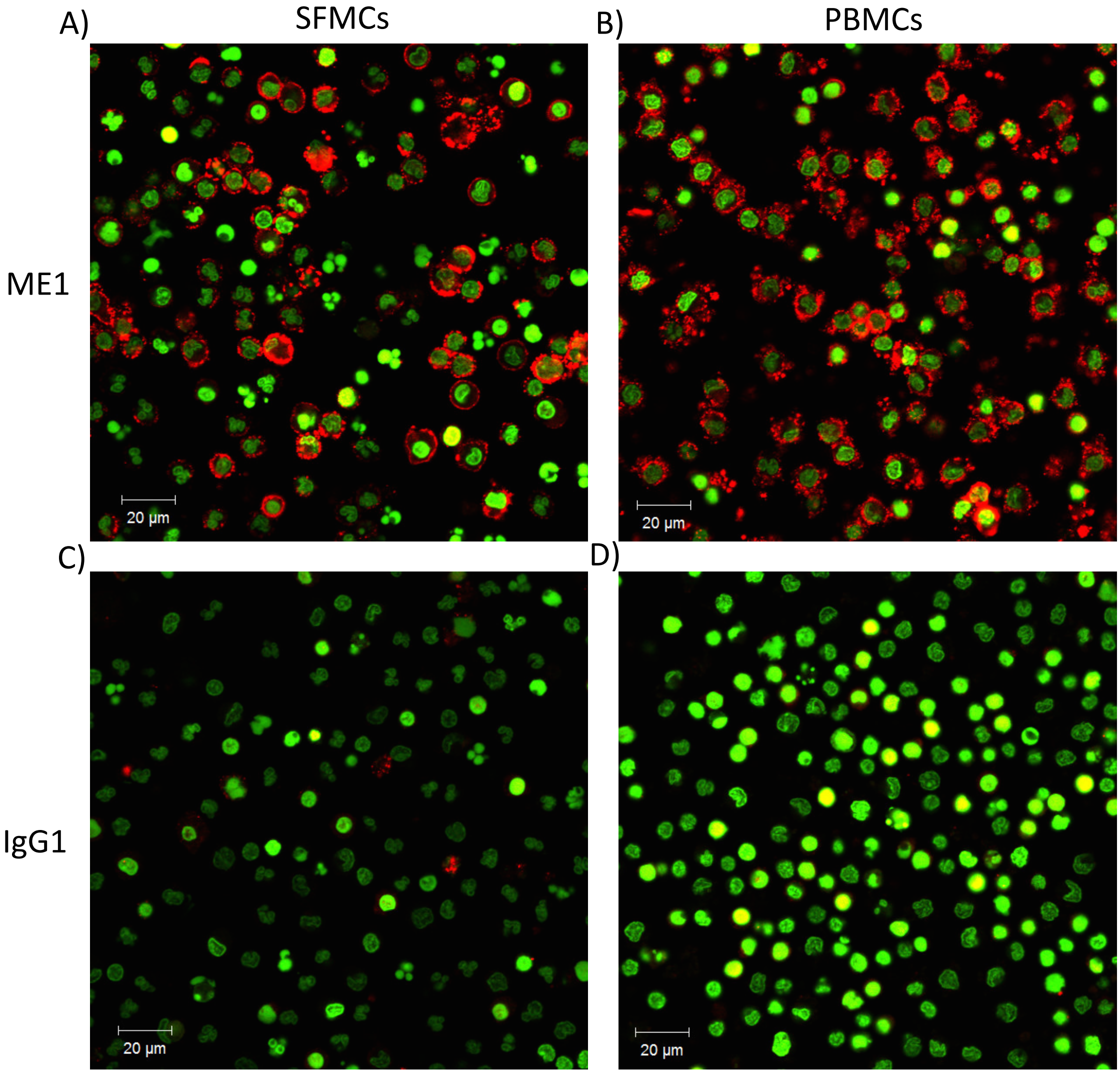

4.5.2 HD6-reactive molecules are present in knee synovial tissue sections derived from B27+ve SpA patients

Next I sought to investigate whether HD6-reactive molecules are expressed in the knee synovial tissue sections using immunohistochemistry (IHC). Formalin fixed, paraffin-embedded B27+ve and control B27-ve SpA (including PsA patients) knee synovial tissue sections were obtained from Prof. Baeten's lab, Academic Medical Centre, University of Amsterdam. Subsequently, I stained B27+ve and control B27-ve SpA tissue sections with primary HD6 and HC10 antibodies, followed by secondary-HRP conjugated antibody and scanned stained tissue sections using Aperio Scanner (see Materials and methods).

HD6 staining was detected specifically in tissues derived from B27+ve SpA patients (Figure 4.26, A), and was absent in B27-ve specimens (Figure 4.26, B). Furthermore, HD6-reactive molecules were present mainly in the intimal lining, the outer layer of synovial tissue (Figure 4.26 and 4.27, A; higher resolution images, 4.28, A and B, blue arrows). Lower number and intensity of HD6 staining was present in cells found in the sublining layer (Figure 4.28, A and B, red arrows). Additionally, HD6 staining was observed in multinucleated cells with osteoclast-like morphology found in a B27+ve SpA patient synovial tissue (Figure 4.29, A).

In contrast, high intensity of HC10 staining was observed in both intimal and sublining layers (Figure 4.26, C blue arrow) in tissue sections derived from B27+ve SpA patients. Moreover, high intensity of HC10 staining was found on mononuclear cell infiltrates (Figure 4.26, C, black arrows) present in moderate numbers in B27+ve and B27-ve PsA synovial tissue. However, B27+ve and –ve non-PsA SpA tissue samples were characterized by few if any mononuclear cell infiltrates.

Notably, I observed high intensity background staining in samples obtained from RA patients using HD6 antibody (data not shown). However, due to the poor quality of available RA samples and their limited number I was unable to optimize and repeat the HD6 staining. Although, it is most likely nonspecific binding of HD6 antibody to tissue, I cannot be certain that there are no HD6-reactive molecules present in the inflamed RA joints.

Summary Chapter 4.5

Analysis of cells isolated from AS patient synovial tissue and fluid using flow cytometry demonstrated that low levels of HD6-reactive molecules were detected on cells with a monocyte-like morphology isolated from the synovial tissue, but not synovial fluid.

Similarly to my flow cytometry findings, confocal microsocpy analysis of SFMC and PBMC samples obtained simulatneously from the same AS patient, failed to detect HD6 staining, despite relatively high intensities of HC10 staining.

Importantly, IHC analysis of B27+ve AS patient knee synovial tissue samples suggested that HD6-reactive molecules are present in the inflamed joints. Furthermore, HD6 staining was co-localized with mononuclear cells presenting monocyte/macrophage-like morphology found in the intimal lining and sublining of the synovial tissue. Additionally, few HD6+ve large, multinucleated, osteoclast-like cells were observed in

B27+ve AS tissues.

HC10-reactive molecules were abundantly expressed on mononuclear cells in both intimal lining and sublining of the synovial tissue. Notably, high intensity staining was also observed on the monoculear cells infiltrating inflamed synovial tissue.

Figure 4.26 HD6-reactive molecules are detected in B27+ve SpA knee synovial tissue, but are absent in B27-ve SpA samples. HD6 staining in A) B27+ve and B) B27-ve SpA knee synovial tissue. HC10 staining in C) B27+ve and D) B27-ve SpA knee synovial tissue. Immunohistochemistry staining using Ready-to-Use AEC+ High Sensitivity Substrate Chromogen Kit. Red – HD6 or HC10 staining. Blue – Mayer's Hematoxilin staining. Stained tissue sections were visualized using Aperio CS2 Scanner, Leica Biosystems. Pictures were analyzed using Aperio ImageScope software (Leica Biosystems).

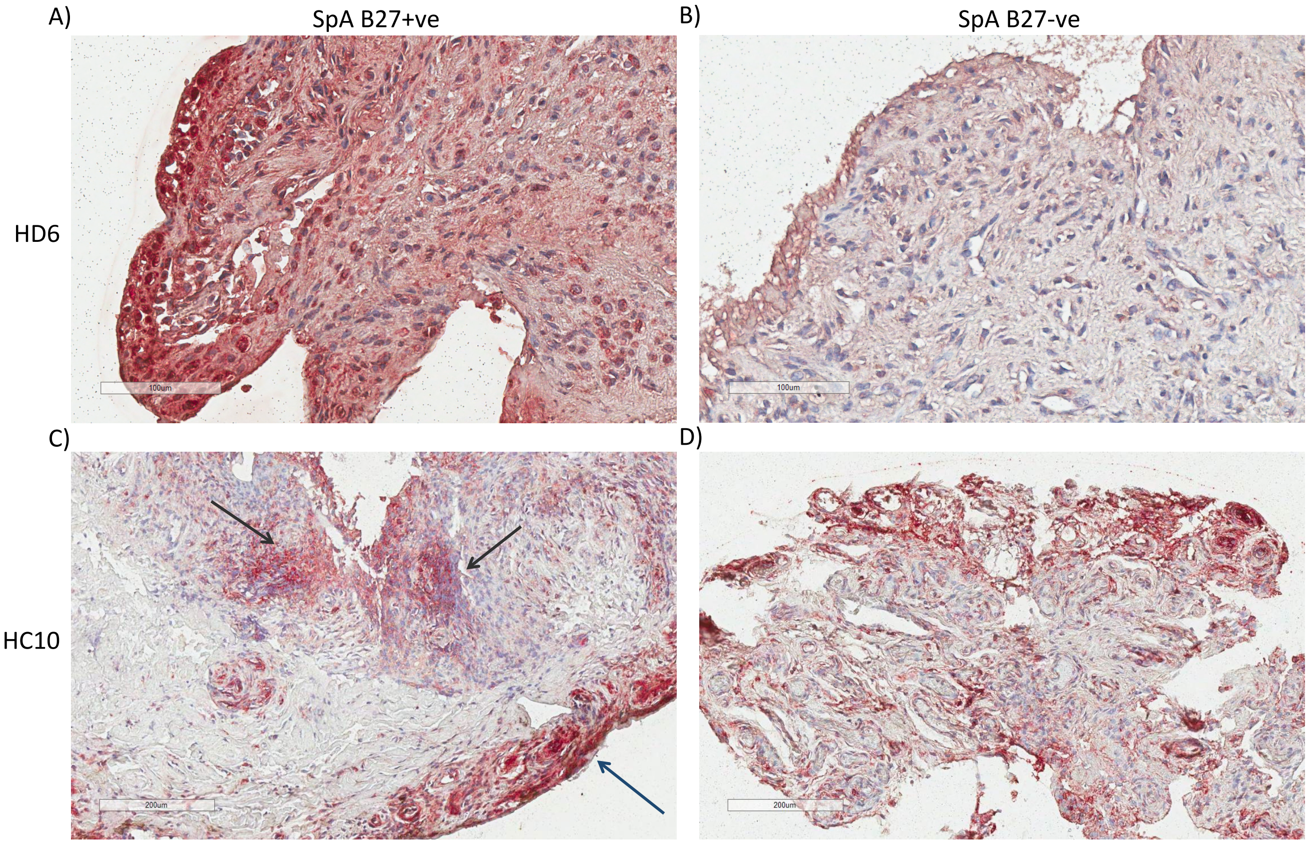

Figure 4.27 HD6-reactive molecules are mainly detected on cells in the intimal lining and sublining layer of B27+ve SpA knee synovial tissue. A) HD6 staining in B27+ve SpA knee synovial tissue, for higher resolution of the area A and B see Figure 4.27. B) IgG1, isotype control staining in B27+ve SpA knee synovial tissue. Immunohistochemistry staining using Ready-to-Use AEC+ High Sensitivity Substrate Chromogen Kit. Red - HD6 or HC10 staining. Blue - Mayer's Hematoxilin staining. Stained tissue sections were visualized using Aperio CS2 Scanner, Leica Biosystems. Pictures were analyzed using Aperio ImageScope software (Leica Biosystems).

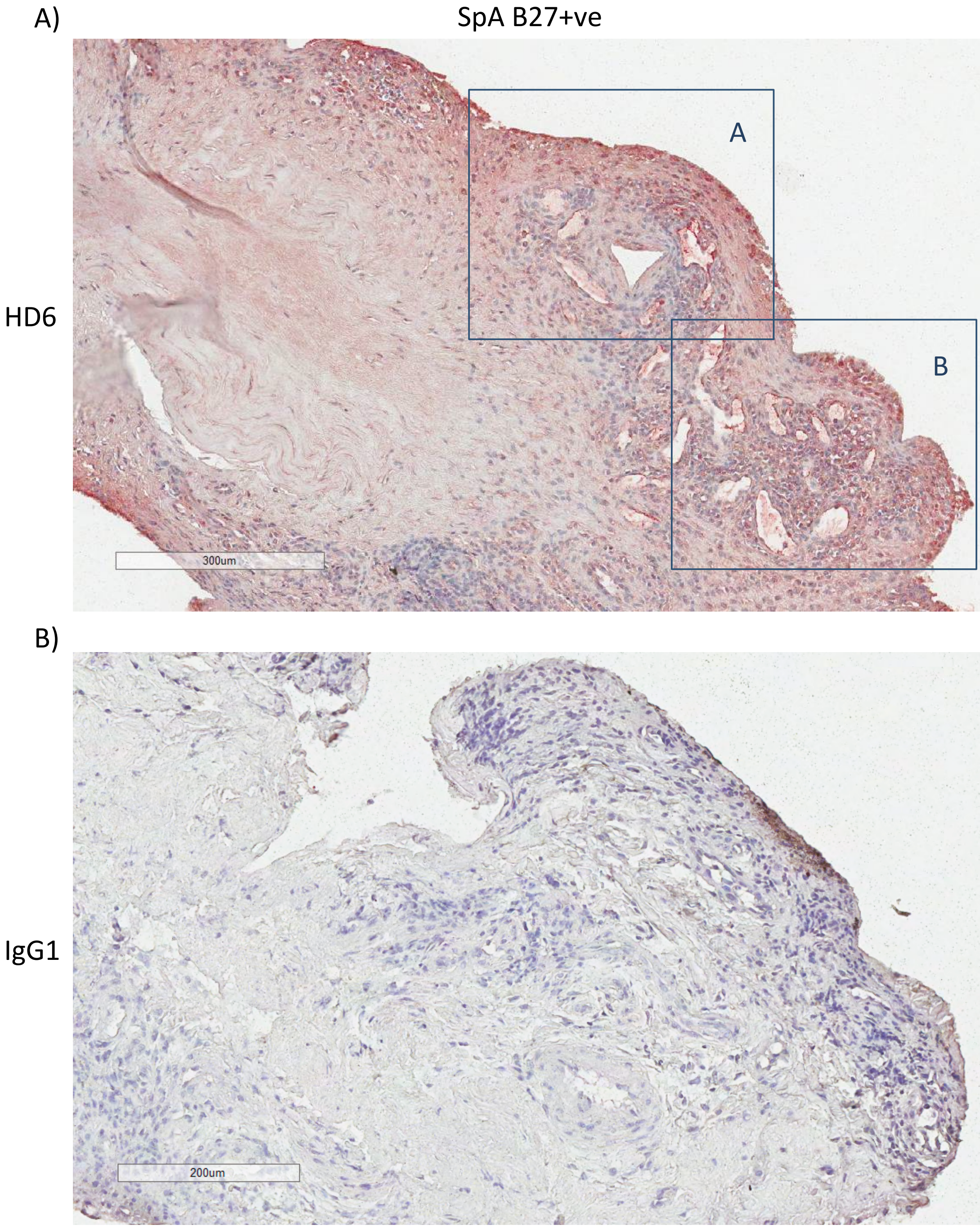

Figure 4.28 HD6 staining in cells found in the intimal lining and sublining of the B27+ve SpA knee synovial tissue. A) and B) higher resolution of areas A and B from Figure 4.26 showing HD6-reactive molecules present in cells located in the intimal lining layer (blue arrows) and sublining layer (red arrows) of the B27+ve SpA knee synovial tissue. Immunohistochemistry staining using Ready-to-Use AEC+ High Sensitivity Substrate Chromogen Kit. Red - HD6 or HC10 staining. Blue - Mayer's Hematoxilin staining. Stained tissue sections were visualized using Aperio CS2 Scanner, Leica Biosystems. Pictures were analyzed using Aperio ImageScope software (Leica Biosystems).

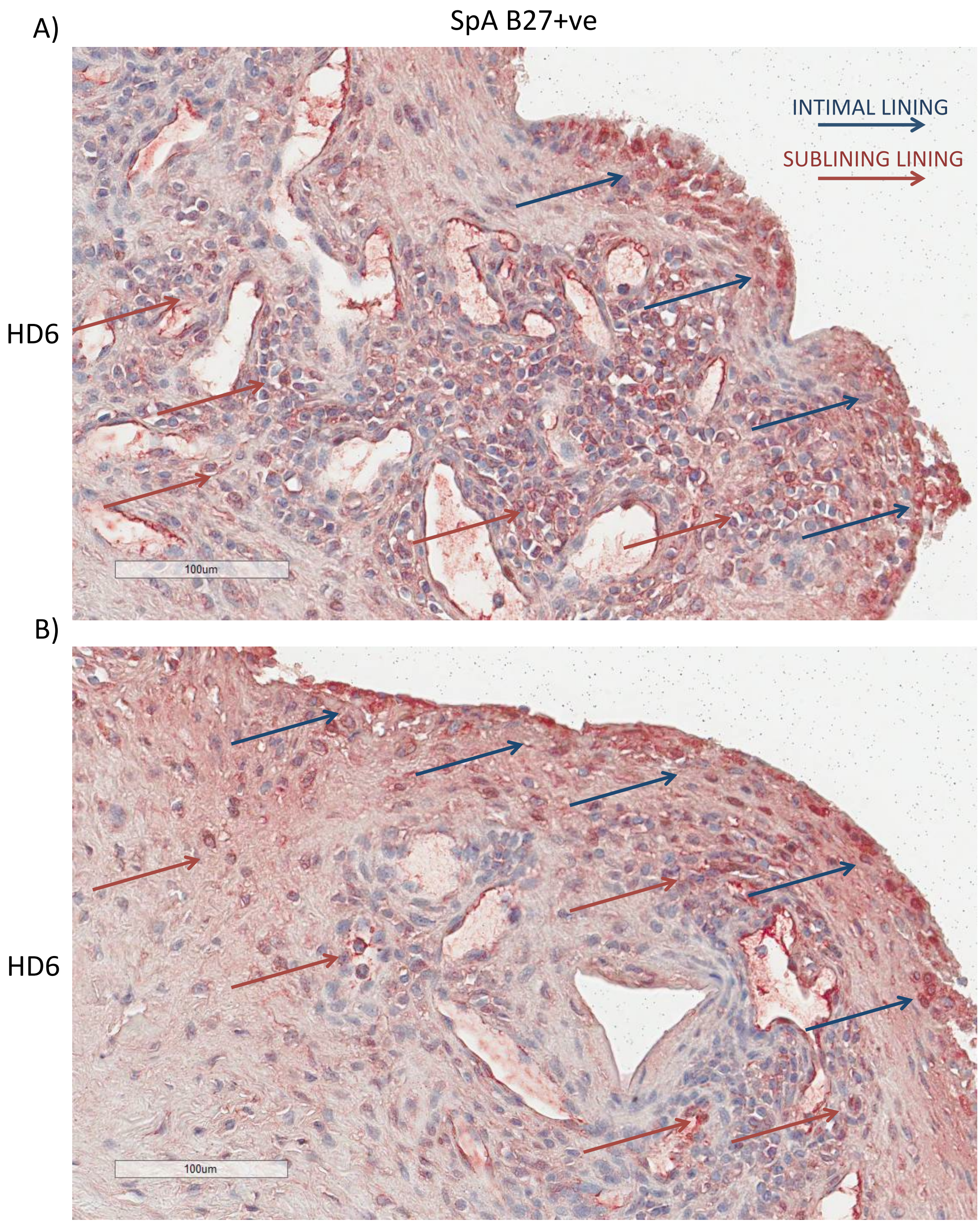

Figure 4.29 HD6 staining can be detected on multinucleated, osteoclast-like cells in B27+ve SpA knee synovial tissue. A) HD6 staining in the B27+ve SpA knee synovial tissue on multinucleated osteoclast-like cell (black arrow). Immunohistochemistry staining using Ready-to-Use AEC+ High Sensitivity Substrate Chromogen Kit. Red – HD6 or HC10 staining. Blue – Mayer's Hematoxilin staining. Stained tissue sections were visualized using Aperio CS2 Scanner, Leica Biosystems. Pictures were analyzed using Aperio ImageScope software (Leica Biosystems).

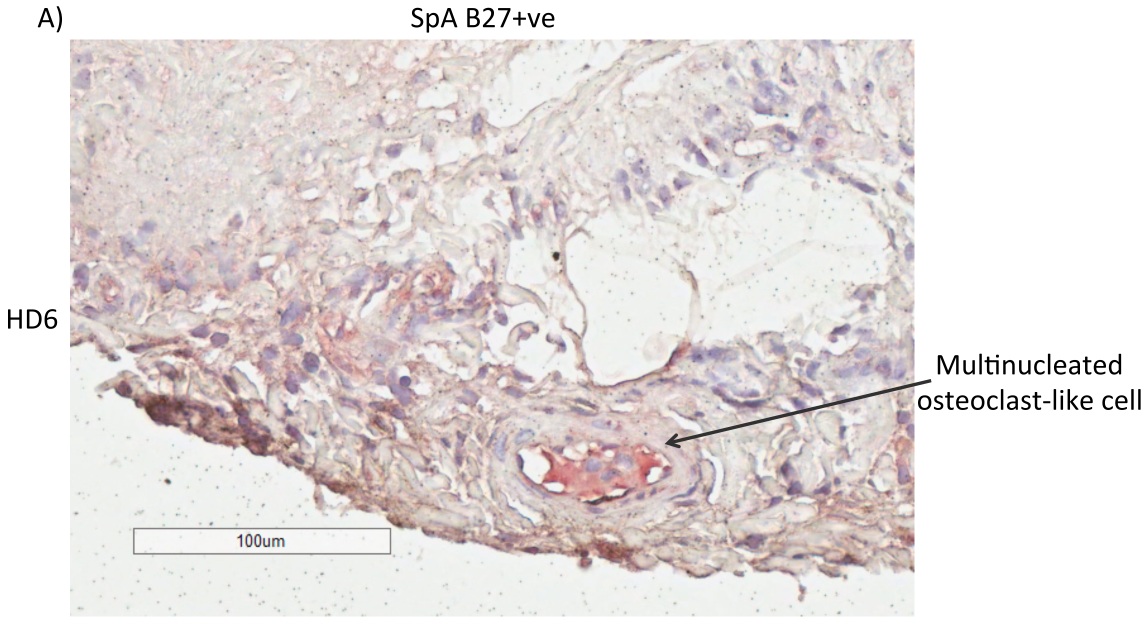

4.6 Discussion Chapter Four

In this chapter I have studied the expression of NC-B27 molecules in AS patient monocyte-derived DCs, Mφ and OCs, in PBMC-derived OCs, and in SpA patient-derived synovial fluid and tissue. Importantly, as yet nobody has investigated the expression of HD6-reactive molecules in these cells and tissues. Furthermore, although the HC10 antibody is commonly used to study the expression of MHCI FHC both intracellularly and at the cell surface, the number of studies using this antibody in SpA human primary blood-derived cells and tissues is limited.

I did not observe HD6 staining in AS patient monocyte-derived DCs by flow cytometry, even after stimulation with different types of TLR ligands and/or pro-inflammatory cytokines. Interestingly, my confocal microscopy analysis suggested that very few (≤ 5 of the $0.5x10^6$ stained cells) of the LPS activated AS moDCs presented relatively high levels of HD6-reactive molecules. However, HD6-reactive molecules were induced specifically in B27+ve AS patient moDCs after acid treatment. Notably, HC10-reactive FHCs were at the same time abundantly expressed in these cells and were further increased following acid treatment. There is a possibility that surface expression of HD6-reactive molecules may require specific environmental factors, such as a tissue-specific environment, a pro-inflammatory cytokine cocktail or direct contact with other cell types. Given that interaction of these NC-B27 molecules with KIR3DL2 can induce proliferation and enhance survival of pro-inflammatory Th17 cells and production of IL-17 (Bowness and Ridley et al., 2011; Chan, Kollnberger, Wedderburn, & Bowness, 2005; Wong-Baeza et al., 2013), there is a possibility that the expression of NC-B27 molecules is strictly regulated with yet unknown factors involved. Yet, these potentially pathogenic NC-B27 forms could be induced specifically in peripheral or axial joints of B27+ve SpA patients. Noteworthy, the phenotype, cell surface expression of MHCI molecules, cytokine production and function of moDCs derived in the *in vitro* culture may differ significantly from primary blood- and tissue-derived DCs. Hence, we cannot exclude the possibility that other types of dendritic cells, generated *in vivo* in the circulation or tissues of SpA patients, could express HD6-reactive molecules. As discussed in the previous chapter, another possibility is that the HD6 antibody epitope is absent and/or masked in the AS patient-derived cells, yet it can be accessed following brief acid treatment.

Interestingly the ratios of HC10-reactive FHCs to W6/32-reactive MHCI molecules were consistently increased in AS patient moDCs compared with healthy controls. These findings emphasize the role of MHCI FHCs in the disease pathogenesis, however based on my results we cannot conclude whether the higher expression levels of HC10 may trigger the inflammation in AS patients or they are simply a cause of an active disease state. Notably, Raine *et al.* have shown elevated levels of HC10-reactive FHCs in PBMCs obtained from B27+ve AS and RA patients compared with healthy controls (Raine et al., 2006). On the other hand, two studies demonstrated increased HC10 expression by $CD14^+$ blood monocytes in AS patients compared with RA patients and healthy controls (Ding et al., 2015; Tsai et al., 2002). Moreover, Ding *et al.* showed higher expression of HC10 in synovial fluid $CD14^+$ cells compared with peripheral blood in SpA patients. Interestingly, higher levels of HC10 staining were observed in B27+ve healthy control PBMCs compared with B27+ve AS patient cells (Cauli et al., 2002). Thus, given that the IL-23/Th17 pathway plays a key role in AS disease pathogenesis, there is a possibility that elevated levels of FHCs could be expressed at the surface of PBMCs simply as a consequence of Th17-driven inflammation. Increased expression of HC10-reactive molecules specifically in B27+ve AS monocytes, but not in RA monocytes, suggests that FHCs may play an additional role in driving the immune responses in B27+ve individuals. Thus, future investigation of the HC10 and HC10:W6/32 ratios in B27+ve SpA vs RA and/or OA moDCs could help us to answer the question whether increased levels of the NC-B27 molecules are characteristic for B27+ve SpA or could also be present in RA and/or OA moDCs.

Similar to my findings using moDCs, I did not observe HD6 staining in AS patient monocyte-derived Mφ, even after stimulation with LPS and/or IFNγ, by both flow cytometry and confocal microscopy. Additionally, unlike moDCs, Mφ expressed very low levels of HC10. The possible explanation of these observations could be that Mφ are not predisposed to express NC-B27 molecules abundantly in the same way as moDCs. Furthermore, there is a possibility that only *in vivo* generated macrophages and/or resident tissue Mφ in SpA, but not *in vitro*-derived Mφ, could express HD6-reactive molecules.

My data using monocyte-derived OCs showed evidence of relatively high intensity HD6 staining of a mononuclear cell population, possibly monocytic OC precursor, in B27+ve AS patients, and surprisingly in one of the B27-ve healthy controls. Additionally low intensity HD6 staining was observed at the surface of multinucleated, osteoclast-like cells and this was specific to B27+ve AS patients. Notably, circulating CD14+ve pre-osteoclasts present in blood from PsA and psoriatic patients can express high levels of FcRγIII (CD16) (Chiu et al., 2010). Moreover, it has been recently shown that FcRγIV expression on monocytic osteoclast precursors can enhance osteoclastogenesis and consequently lead to bone destruction (Seeling et al., 2013). Hence, there is a possibility that despite the use of a standard FcR blocking buffer (2% FCS/10% normal goat serum (NGS) and 10% normal rabbit serum (NRS)) made in-house in my confocal microscopy staining protocol, the blocking was not sufficient to eliminate unspecific binding of HD6. Notably, in the subsequent experiments I demonstrated that the commercial FcγR blocking reagent, containing anti-CD32 and anti-CD16 antibodies, eliminated HD6 staining on the mononuclear, pre-osteoclast-like cells, yet the low intensity staining on the multinucleated B27+ve osteoclast-like cells remained unaffected. Furthermore, similar low intensity HD6 staining was observed specifically in the B27+ve PBMC-derived multinucleated, osteoclast-like cells. Notably, simultaneous, abundant HC10 staining was detected at the surface of both monocyte- and PBMC-derived OCs. In summary my data do suggest low-level, but specific HD6 staining of B27+ve multinucleated, osteoclast-like cells, indicative of specific forms of NC-B27 expression.

Interestingly, my preliminary results suggested that monocytes isolated from B27+ve individuals are predisposed to generate higher number of large, multinucleated cells presenting the activated-like phenotype. However, more experiments with the monocyte-derived OCs need to be performed in the future to confirm my preliminary findings and further investigate their potential pathogenic role in SpA.

Regarding this, I demonstrated that B27+ve AS patient monocyte- and PBMC-derived OCs can express cell surface HD6-reactive molecules after *in vitro* culture. These findings suggest that OCs present *in vivo* in SpA joints could, similarly to the *in vitro* generated cells, express HD6-reactive forms of B27 molecules and possibly be involved in driving the immune responses *in situ*. Additionally, the B27-specific pro-osteoclastogenic properties suggest that expression of these NC-B27 forms at the surface of monocytic osteoclast precursors could be directly involved in the enhanced development of the activated osteoclasts. Further investigation of the HLA-B27 expression and function in the SpA-derived OCs is of the potential future interest and could give us better understanding of the B27 involvement in the joint pathogenesis.

Importantly, in this part of my project I have investigated for the first time the expression of HD6- and HC10-reactive molecules in SpA- and RA-derived paraffin embedded synovial tissue sections. Notably, HD6+ve cells, likely Mφ, DCs or activated monocytes were found in the intimal and sublining layers of the B27+ve SpA tissues. Yet, the specificity of HD6 staining to the B27+ve SpA tissues was unclear due to the high background staining observed in the RA samples and the limited number of specimens. On the other hand, HC10 staining was present not only in the intimal and sublining areas of the SpA tissues, but additionally abundant expression of HC10-reactive molecules was found in the mononuclear cell infiltrates. Furthermore, these high intensity HC10+ve cell infiltrates were also observed in the RA synovial tissue. Hence, there is a possibility that HD6- and HC10-reactive molecules expressed at the surface of resident tissue cells may be involved in driving the immune responses. Whereas, the abundant expression of the HC10-reactive MHCI FHCs in the mononuclear cell infiltrates could be simply a consequence of the ongoing inflammation and the increased cell turnover rate. Previous studies suggested that different mechanisms and cell types of both resident and infiltrating synovial tissue cells are involved in the SpA, RA and OA joint pathology. Notably, increased number of

CD68$^+$ macrophages was found in the inflamed hip synovial tissues derived from AS patients compared with OA patients (Chen et al., 2009). Moreover, it has been shown that in inflammatory conditions such as SpA, RA or gout, synovial tissue is infiltrated by the heterogeneous population of mixed-phenotype M1/M2 Mφ (Ambarus et al., 2012). This unique, highly plastic Mφ population originates from blood monocytes and can express both M1 and M2 phenotypic markers depending on the local cytokine milieu. Furthermore, Ambarus *et al*. suggested that the synovial intimal lining layer in SpA, unlike in RA, consists mainly of resident tissue-differentiated M2-like Mφ. Thus, there is a possibility that the HD6 staining observed in my experiments in the B27+ve SpA synovial tissue could be specific to the resident tissue Mφ population and/or infiltrating heterogenic M1/M2 cells.

Thus, subsequent future experiments with additional phenotypic markers would allow us to identify the phenotype of cells expressing these differing patterns of NC-B27 molecules in the inflamed SpA synovial tissue. Furthermore, additional optimization of the background staining and use of the additional control RA and OA tissue sections could address the question whether HD6 and HC10 expression by intimal and sublining cells is specific to SpA or could be also present in RA and/or OA synovial tissue. Noteworthy, due to limitations of IHC, tissue fixation and paraffin embedding procedure, I cannot be certain that observed staining of the NC-B27 molecules was present at the cell surface. Thus, there is a possibility that the observed HD6 and HC10 staining could be a cause of the use of fixatives in the tissue preparation procedure, as ME1- and W6/32-reactive epitopes are removed following PFA fixation. Future investigation of the HD6 and HC10 staining in frozen synovial tissue sections could help us to address this problem.

In conclusion, my findings suggest that HD6-reactive molecules are not abundantly expressed in the circulation, but are rather specifically found in the site of inflammation, in the peripheral joints obtained from SpA patients with an active disease. The mechanism behind the induction of HD6-reactive molecules in tissue requires further investigation. However, importantly HC10-reactive FHCs and the ratios of HC10:W6/32 are consistently increased in B27+ve AS patient moDCs compared with B27-ve healthy controls, suggesting that MHCI FHCs may play an important role in the inflammation.

Importantly, it is not yet clear which forms of NC-B27 may be pathogenic in SpA. The part of HC10-reactive molecules probably includes the smaller HD6-reactive subset. Although both HD6- and HC10-reactive forms of NC-B27 were demonstrated to bind to KIR3DL2 (Bowness and Ridley et al., 2011; McHugh et al., 2014; Payeli et al., 2012; Kollneberger et al. unpublished data) and have a potential pathogenic role in SpA, we cannot confirm that they have the same structure. Notably, cell surface HC10-reactive forms of MHCI FHCs are also expressed in healthy controls, these could suggest that not all of the HC10-reactive B27 species can be pathogenic.

Potential mechanisms by which NC-B27 can drive the SpA pathogenesis are discussed in Chapter six.

Chapter Five: Cell surface expression of non-classical forms of HLA-B27 in B27 TG^2 rat model

5.1 Introduction

As demonstrated in my previous chapter HD6-reactive molecules are expressed only at low levels in different types of AS patient blood-derived cells both in a steady state and after activation with pro-inflammatory factors. Low expression levels of HD6 were observed only in PBMC-derived osteoclasts and in synovial tissues from inflamed SpA patient joints. On the other hand, brief acid treatment induced relatively high levels of HD6 staining in AS patient blood-derived cells. Taken together our findings suggest that these non-classical forms of B27 molecules may be expressed particularly in joints or under specific environmental conditions. Studying SpA patient joints and axial skeleton tissue biopsies is limited due to the extremely rare availability of samples, therefore SpA animal models could give us a better opportunity for insight into the role of the HLA-B27 molecules in disease pathogenesis. Of the HLA-B27 transgenic rat models that have been developed the B27 TG^2 rat model most strongly resembles human SpA (Tran et al., 2006). We have previously demonstrated HD6 staining in the original B27 TG^1 rat model (McHugh et al., 2014). However, in this model gastrointestinal inflammation is a dominant inflammatory feature, and there is relatively little arthritis in axial skeleton. As proposed by Taurog *et al.*, HLA-B27 misfolding and subsequent abundance of cell surface free heavy chains might predispose these animals to gastritis and colitis, which than trigger musculoskeletal manifestations. Thus joint inflammation may be less dependent on the expression of HLA-B27.

In the B27 TG^2 SpA model the introduction of additional copies of huβ2m to reduce B27 misfolding eliminated gut inflammation, but exacerbated joint manifestations. This suggests that HLA-B27 is required to drive joint inflammation. Additionally, for the first time in the B27 TG^2 rat model all male rats developed clinical manifestations in the axial skeleton characteristic for human SpA (van Duivenvoorde et al., 2012). The inflammatory processes observed in histological sections from rat vertebral joints consisted of new bone formation, spondylitis, fibrosis and enthesitis. Importantly, B27 TG^2 male rats had no symptoms of gut inflammation (Tran et al., 2006).

Thus this model seems to resemble human HLA-B27-related forms of SpA to a greater degree compared with previous animal models. Therefore, studying expression of classical and non-classical HLA-B27 molecules at different stages of the disease in this rat model could indicate whether cell surface HLA-B27 FHC homodimers could be a key factor leading to the disease onset and/or manifestations perpetuation.

5.2 HD6-reactive molecules are expressed in splenic and lymph node cells in B27 TG^2 rats

Our group has previously studied expression of HLA-B27 molecules in spleens in the original B27 TG^1 model (McHugh et al., 2014). They demonstrated that cell surface expression levels of both properly folded and non-classical forms of HLA-B27 molecules in splenic cells were dependent on animal age. HD6-reactive molecules were expressed at low levels in the first 3 months of age and increased with age. Moreover, non-classical forms of HLA-B27 were abundantly expressed on mononuclear cells and to a lower extent on granulocytes.

Hence, next I sought to investigate, in collaboration with Prof Dominique Baeten's group in the Academic Medical Centre, University of Amsterdam, expression patterns of classical and non-classical HLA-B27 molecules in B27 TG^2 male rats. In particular I investigated whether HD6-reactive molecules are expressed before the disease onset in that rat model. Consequently, spleens (SPLC) and lymph nodes (LNs) from asymptomatic B27 TG^2 animals (3 months old) and healthy control animals (HLA-B7 TG and wild type Lewis) were shipped from Amsterdam, on ice, in R10 media straight after isolation. I isolated splenic and lymph node cells using mesh cell strainers and stained according to the standard flow cytometry protocol (Material and methods). Five cell surface markers were selected to distinguish cell populations. Four main populations were determined on the basis of CD4, CD8α, CD11b, CD45R/MHC class II cell surface expression. CD4 is expressed on thymocytes and mature T lymphocytes (MHC class II restricted T helper cells), as well as at lower levels on monocytes, macrophages and some dendritic cells. CD8α is characteristic for mature class I restricted T lymphocytes and on the majority of NK cells. CD11b can be found mainly on macrophages, dendritic cells and granulocytes. CD45 receptor (CD45R) is expressed on most B lymphocytes and its expression levels varies in different B cell subsets and maturation states. MHC class II is found on peripheral B lymphocytes, epidermal Langerhans cells, dendritic cells and some tissue macrophages.

Figure 5.1 HD6-reactive molecules are expressed on $CD4^+$ and $CD8^+$ splenic and lymph node cells from B27 TG^2. Representative FSC versus SSC flow cytometry dot plots of A) lymph node and B) splenic cells. Population gating strategy - CD4 versus CD8α dot plots C) in LNs and D) in SPLC. HD6 staining on $CD4^+$ and $CD8^+$ cells in LNs (E) and spleens (F). Spleens and lymph nodes were obtained from n=6 animals (n=2 B27 TG^2, n=2 B7 TG, n=2 WT Lewis). Each flow cytometry staining condition for individual sample was performed in duplicates.

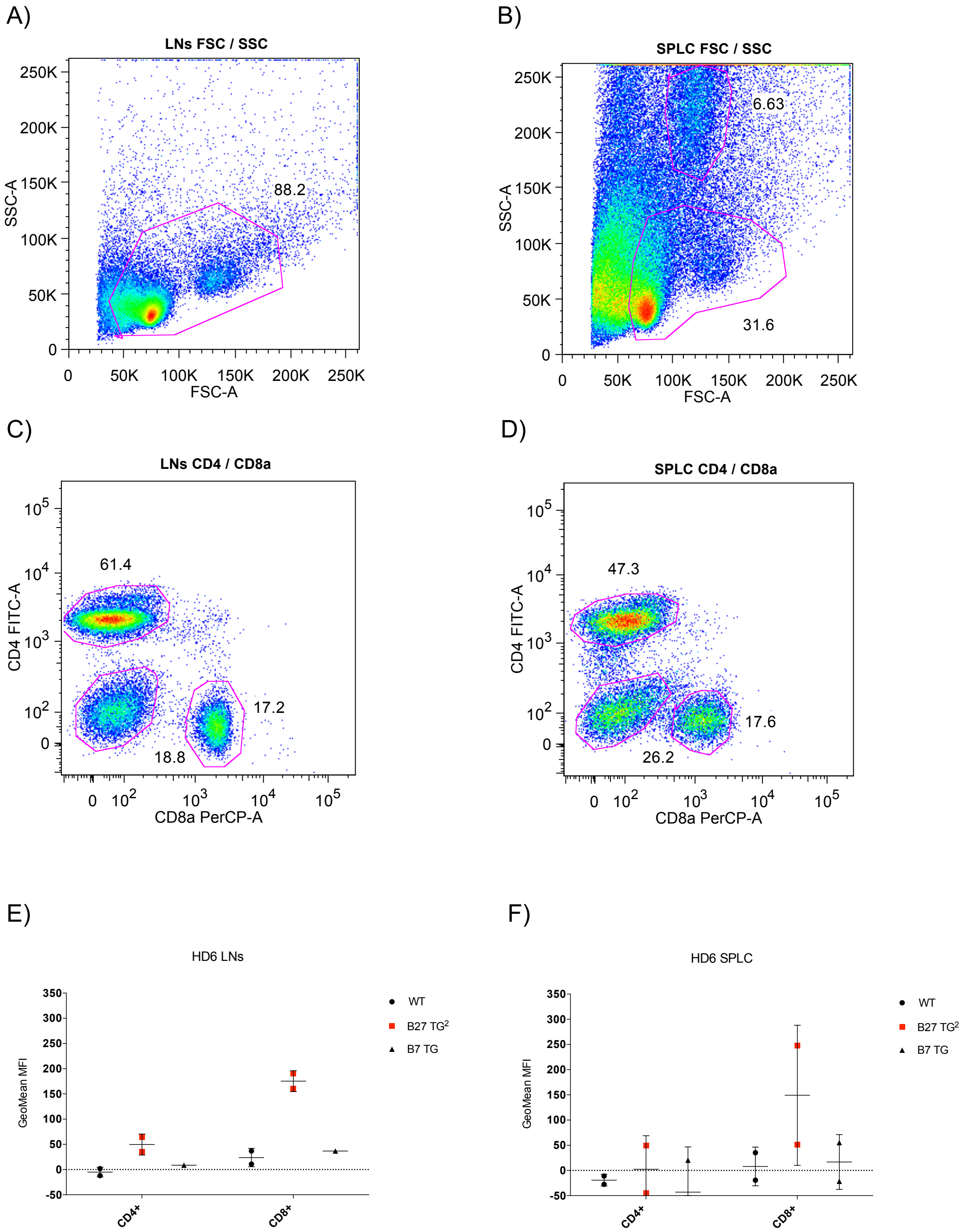

I observed an elevated expression of HD6-reactive molecules in the $CD4^+$ and $CD8^+$ LNs cells isolated from B27 TG^2 animals compared with controls (Figure 5.1, E). However, in splenic cells, a higher expression level of HD6 was observed only in one of the two B27 TG^2 rats (Figure 5.1, F). Notably, HD6 was expressed at greater amounts in $CD8^+$ cells (Figure 5.1, E vs F).

For $CD4^+$ and $CD8^+$ cell populations isolated from B27 TG^2 rat LNs had higher HC10 expression FHCs compared with control B7 TG and WT rats (Figure 5.2, A). Moreover, at the same time in B27 TG^2 animals HC10 staining levels were higher than levels of properly folded B27 molecules (Figure 5.2, C). Hence, HC10 to ME1 ratios were increased in $CD4^+$ and $CD8^+$ B27 TG^2 LNs compared with the ones obtained from control animals (Figure 5.2, E). Interestingly, both B27 TG and B7 TG $CD8^+$ cells in LNs consistently expressed more human MHC class I molecules (folded and FHC) compared with $CD4^+$ cells. Additionally, on both $CD4^+$ and $CD8^+$ cells in B27 TG^2 and B7 TG animals HC10 expression levels increased with ME1 expression.

Splenic $CD4^+$ and $CD8^+$ populations expressed lower levels of HC10 (Figure 5.2, B) and similar or decreased levels of properly folded HLA-B27 molecules (ME1 staining) (Figure 5.2, D) compared with HLA-B7 transgenic animals. Interestingly, my data consistently showed that the ratio between cell surface FHC and properly folded B27 molecules was significantly higher in B27 TG^2 animals compared with B7 TG rats (Figure 5.2, F).

Figure 5.2 High levels of FHCs are expressed on both $CD4^+$ and $CD8^+$ cells in LNs from B27 TG^2 rats. HC10 to ME1 ratios are significantly higher in B27 TG^2 rats compared with HLA-B7 TG animals. Expression of HC10 on $CD4^+$ and $CD8^+$ cells in LNs (A) and spleens (B). Expression of ME1 on $CD4^+$ and $CD8^+$ cells in LNs (C) and spleens (D). HC10 : ME1 ratio on $CD4^+$ and $CD8^+$ in LNs (E) and in spleen (F). Spleens and lymph nodes were obtained from n=6 animals (n=2 WT Lewis; n=2 B27 TG^2; n=2 B7 TG). Each flow cytometry staining condition for individual sample was performed in duplicates.

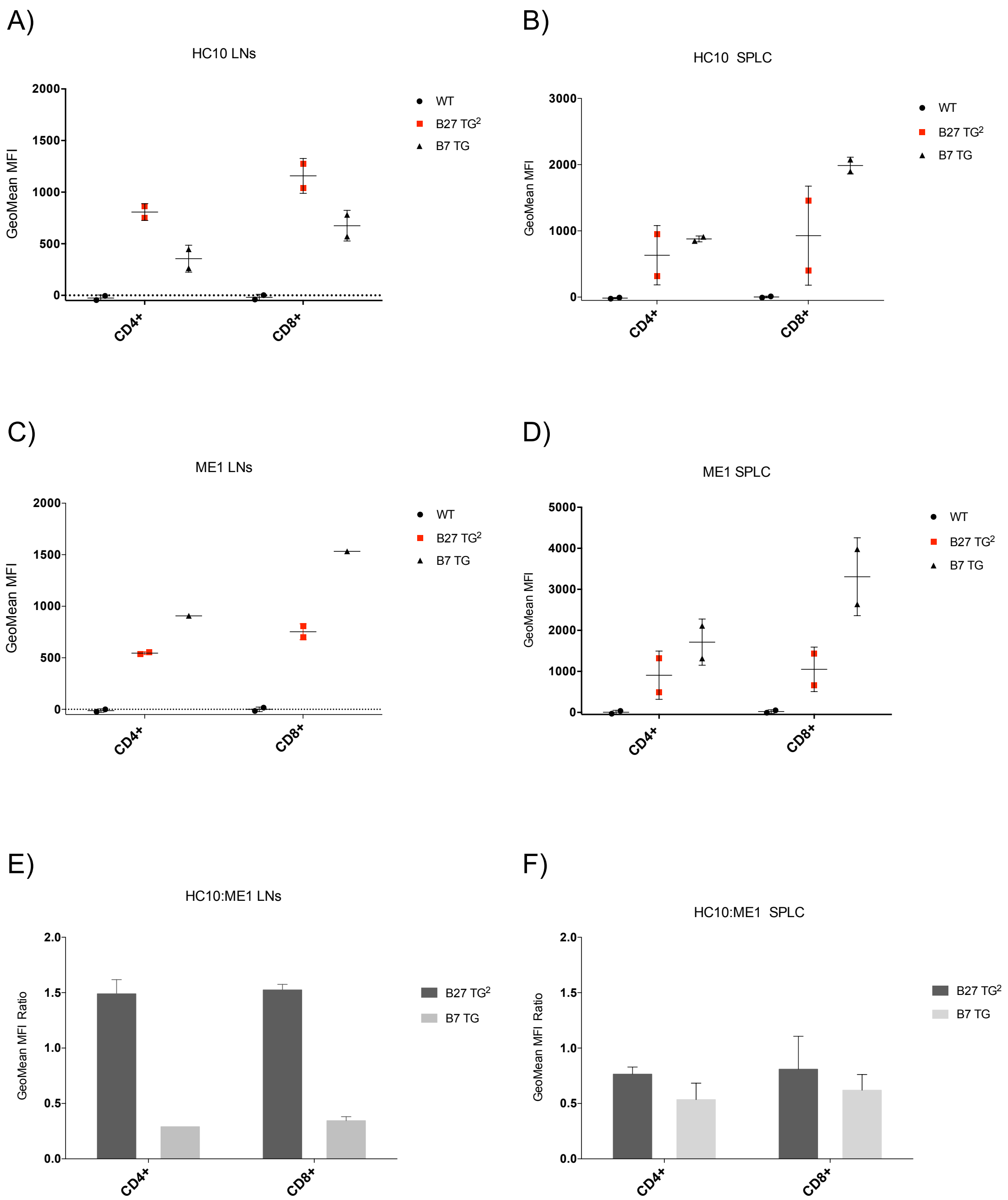

Three main cell populations expressing CD45R and MHC class II were detected in LNs: CD45R ^{low}, CD45R^{+}/MHC II^{+} and MHC II ^{low} (Figure 5.3, A). However, HD6-reactive molecules were expressed mainly on CD45R^{low} cell population. In spleens, unlike in LNs, only one cell population was present CD45R^{low}/MHC II^{+} (Figure 5.4, A). These cells did not show HD6 staining (Figure 5.4, B).

Two main cell populations expressing CD11b were observed in LNs: CD11b^{low}/FSC^{low} and CD11b^{low}/FSC^{high} (Figure 5.5, A). However, none of them expressed HD6-reactive molecules (Figure 5.5, B and C). I did not detect a clear CD11b cell population (CD11b^{low}) in splenic isolates in any of the animals (Data not shown). The percentages of CD11b^{low} cells were decreased in B27 TG^{2} rats compared with control animals. Again, similar to LNs, HD6 staining was not present on splenic CD11b^{low} cells.

Summary Chapter 5.2

Taken together, HD6-reactive molecules can be detected exclusively in B27 TG^{2} rats and seem to be more abundant in LNs than in a spleen. CD8^{+} cells expressed higher levels of HD6 compared with CD4^{+} cells. Moreover, HD6-reactive molecules were also found on CD45R^{low} cells. Additionally, B27 TG^{2} rats expressed higher levels of HC10-reactive molecules in LNs and ME1 to HC10 ratios in both LNs and spleens compared with B7 TG rats. These findings suggest that non-classical B27 molecules are abundantly expressed in diseased-prone B27 TG^{2} rat, but not B7 TG animals, and may be consistent with their possible role in driving the immune responses.

Figure 5.3 CD45R^{low} cells express higher levels of HD6 in B27 TG^2 lymph nodes. A) Population gating strategy CD45R versus MHC II in LNs. B) Representative histograms of HD6 expression in CD45R$^+$/MHC II$^+$ LNs population (left), CD45R^{low} (middle) and MHC II^{low} (right). C) Representative histograms of HC10 expression in the CD45R$^+$/MHC II$^+$ LNs population (left), CD45R^{low} (middle) and MHC II^{low} (right). LNs were obtained from n=6 animals (n=2 WT Lewis; n=2 B27 TG^2; n=2 B7 TG). Each flow cytometry staining condition for individual sample was performed in duplicates. Numbers in histogram legends - GeoMean MFIs.

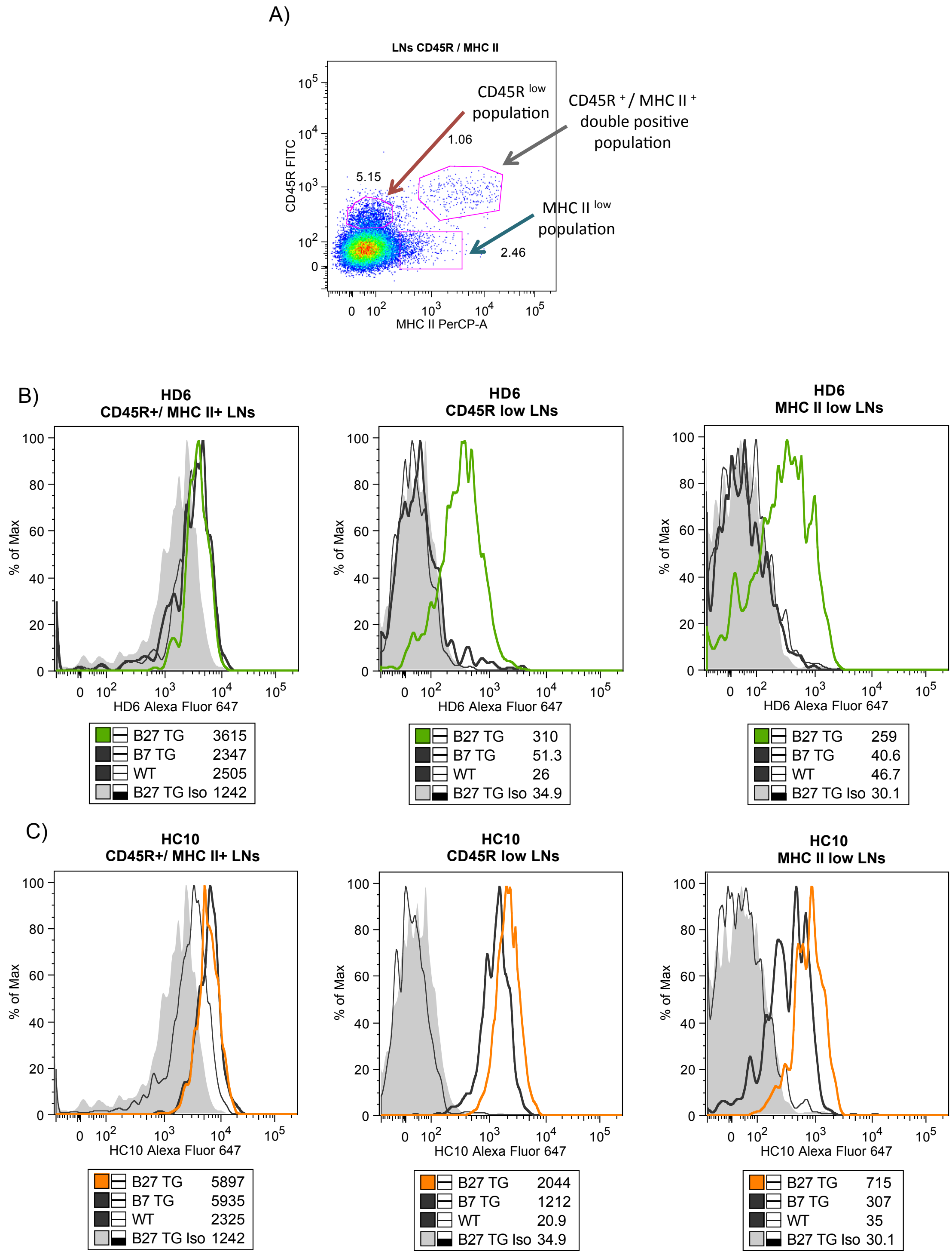

Figure 5.4 Splenic CD45R^{low}/MHC II^{+} cells express low levels of HD6- and HC10-reactive molecules. A) CD45R versus MHC II population gating strategy in spleens. B) HD6 and C) HC10 expression on double positive CD45R^{low}/MHC II $^{+}$ population in spleen. Spleens were obtained from n=6 animals (n=2 WT Lewis; n=2 B27 TG^{2}; n=2 B7 TG). Each flow cytometry staining condition for individual sample was performed in duplicates. Numbers in histogram legends - GeoMean MFIs.

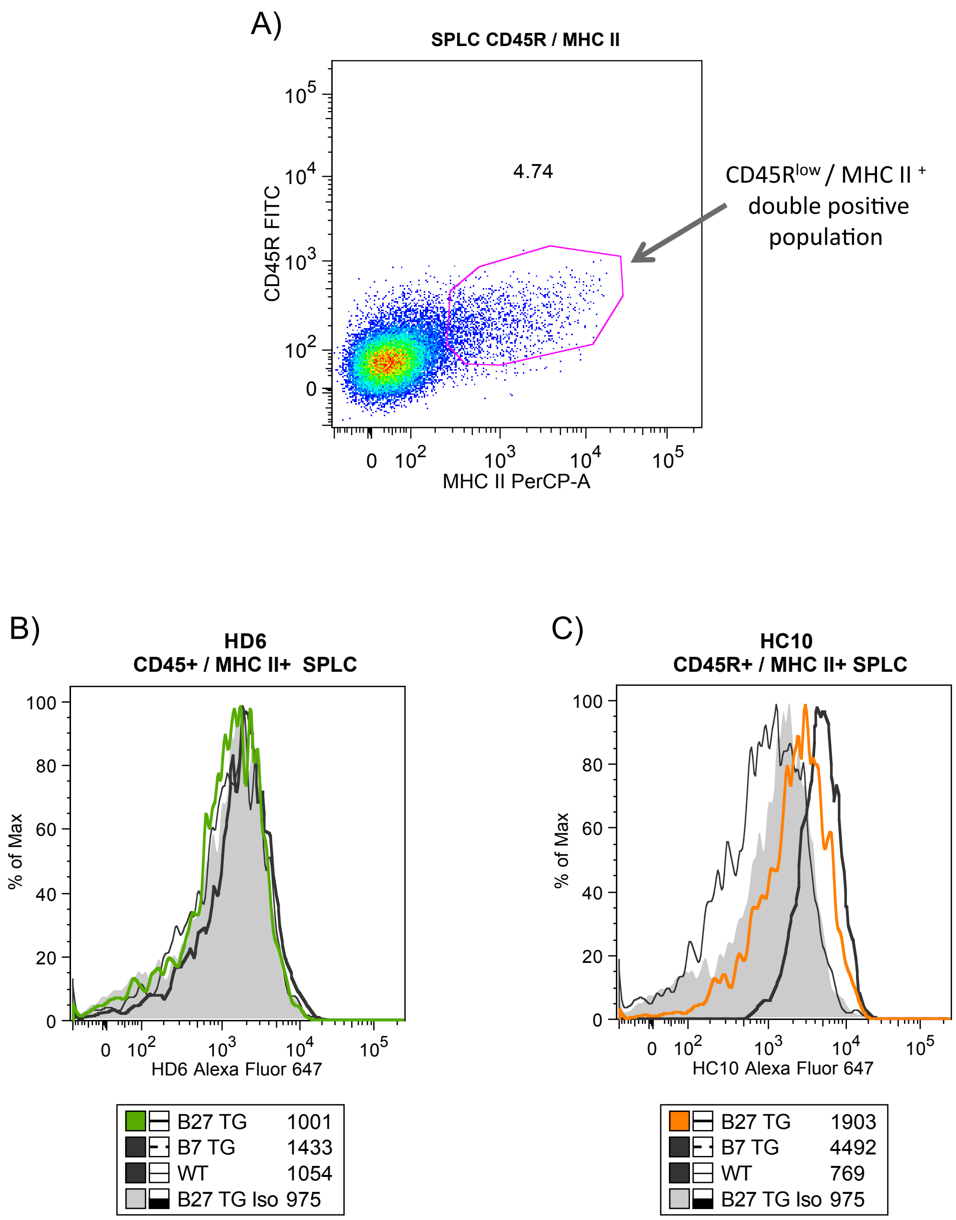

Figure 5.5 CD11b^{low} cell populations in LNs express low levels of non-classical HD6- and HC10-reactive molecules. A) Representative flow cytometry dot plot showing CD11b versus FSC gating strategy in LNs. Expression of HD6 in LNs B) CD11b^{low}/FSC^{low} and C) CD11b^{low}/FSC^{high} populations. Expression of HC10 in LNs D) CD11b^{low}/FSC^{low} and E) CD11b^{low}/FSC^{high} populations. LNs were obtained from n=6 animals (n=2 WT Lewis; n=2 B27 TG[2]; n=2 B7 TG). Each flow cytometry staining condition for individual sample was performed in duplicates. Numbers in histogram legends - GeoMean MFIs.

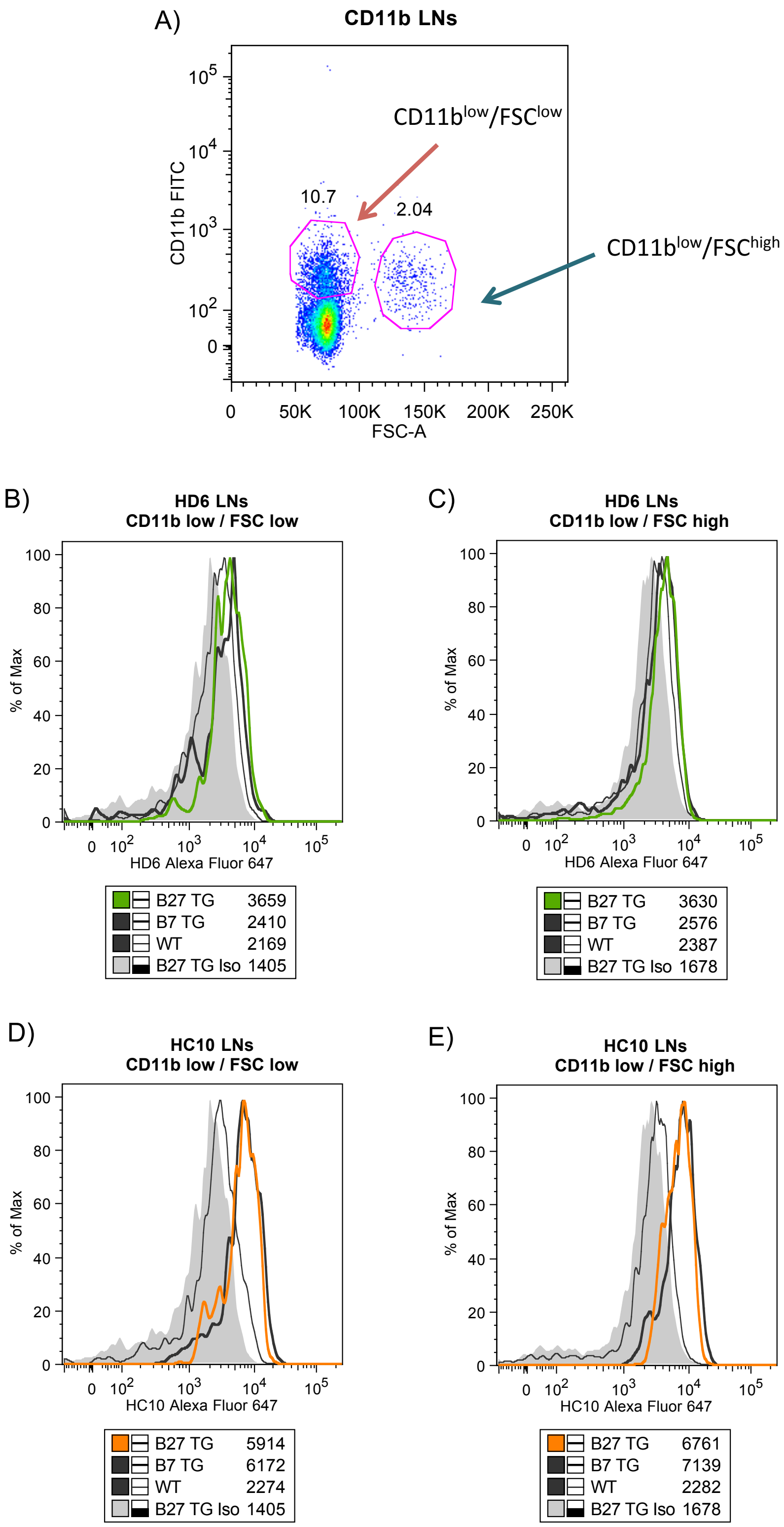

5.3 Expression of HD6-reactive molecules in the innate immune triggered (B27 TG^3) rat model

Van Duivenvoorde *et. al.* (2011, ACR published abstract) recently developed a further model of SpA. They injected B27 TG^2 rats (6 weeks old males) with 30-90mg of *M.tb* in incomplete Freund's adjuvant (IFA). Notably, *M.tb* has previously been used to trigger adjuvant-induced arthritis (AIA) in a rat model of RA, but at significantly higher doses. In the B27 TG^2 model *M.tb* injection accelerated the appearance of disease symptoms with arthritis and spondylitis appearing 2-3 weeks after immunization. This is at least a month earlier than when the symptoms develop in this model spontaneously. Taken together these findings put forward this new model of innate immune-driven SpA as an excellent animal model to study B27-driven disease.

Therefore, my next approach was to investigate whether there are any significant differences in expression patterns of HLA-B27 in B27 TG^2 rats 2 and 3 weeks after immunization with 30mg of *M.tb* and in control non-immunized study group of the same strain.

B27 TG^2 male rats (6 weeks old) were injected subcutaneously with 30mg of *M.tb* in IFA. Peripheral blood mononuclear cells (PBMCs), LNs and spleens were isolated at 2 and 3 weeks post injection (p.i.) (4 animals per group) and non-immunized B27 TG^2 animals (2 per time point) were used to stain classical and non-classical forms of HLA-B27 molecules. Similar to previous experiments four main populations were determined on a basis of CD4, CD8α, CD11bc, CD45R/MHC class II cell surface expression. Notably, in these experiments I used anti-CD11bc antibody, which detect macrophages, activated monocytes and dendritic cells to a better extent than previously used CD11b antibody (Chapter 5.1). As shown previously in the original B27 TG[1] rat model (May et al., 2003) CD161$^+$ cells could be involved in the disease pathogenesis. Hence, I used additionally this surface marker to identify rat NK cells. Notably, CD161 can be expressed as well on dendritic cells, activated monocytes and some subsets of T cells (Th17 cells).

HD6 staining of PBMCs CD4$^+$ cells was similar in immunized and non-immunized animals at both time points investigated (Figure 5.6, A). This was also the case for CD8$^+$ cells, although higher mean fluorescence intensities (MFIs) were observed compared with CD4$^+$ cells (Figure 5.6, B).

In LNs, there were no statistically relevant differences in HD6 staining between *M.tb* treated and untreated B27 TG[2] animals in both CD4$^+$ and CD8$^+$ cell populations (Figure 5.6, A and B). However, immunized animals at 2 weeks p.i. presented decreased levels of HD6-reactive molecules.

Similarly, for both splenic CD4$^+$ and CD8$^+$ cell populations, *M.tb* treatment also appeared to decrease HD6 staining at 2 and 3 weeks p.i. (Figure 5.6, A and B). However, importantly 3 weeks post immunization the decrease in HD6 staining was statistically relevant.

These observed differences in HD6 staining in both LNs and spleens were not linked to changes in ME1 staining, which remained similar at both time points and in both study groups (Figure 5.6, E and F).

HC10 staining of $CD4^+$ and $CD8^+$ cells from PBMCs, LNs and spleens was similar in immunized and non-immunized animals at both time points investigated (Figure 5.6, B and C). Interestingly, when comparing HC10 staining at 2 and 3 weeks p.i. in LNs there was significant decrease in the latter time point. Again this difference did not coincide in changes with ME1 expression levels.

Interestingly, although *M.tb* injection did not affect the levels of HD6 and HC10 staining in PBMCs, their levels were increased with age (Figure 5.6, A, B, C and D). In contrast, ME1 staining on $CD4^+$ and $CD8^+$ cells was decreased in *M.tb* treated rats 3 weeks p.i. (Figure 5.6, E and F).

Figure 5.6 HD6 staining is decreased in spleens 3 weeks post *M.tb* injection. HD6 staining in CD4⁺ (A) and CD8⁺ (B) cells, HC10 staining in CD4⁺ (C) and CD8⁺ (D) cells and ME1 in CD4⁺ (E) and CD8⁺ (F) in PBMCs, LNs and SPLC 2 and 3 weeks +/- 30mg *M.tb* injection in B27 TG^2 rats. Number of B27 TG^2 rats per time point: 2 untreated and 4 treated with 30mg *M.tb*.

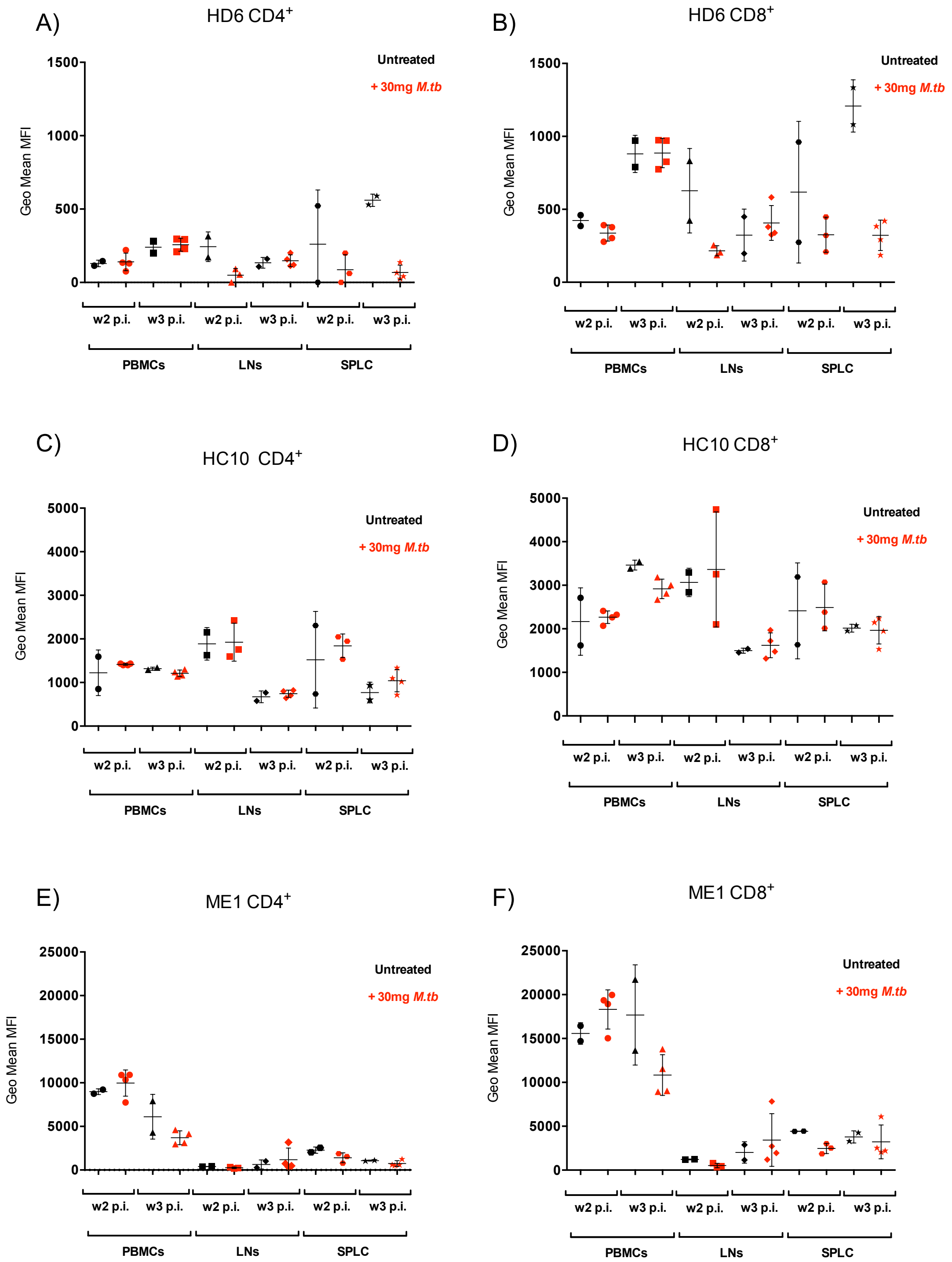

CD45R$^+$/MHC II$^+$ cells (Figure 5.7, A) were present in PBMCs, LNs and spleens both at 2 and 3 weeks p.i. *M. tb* injection did not alter HD6 and HC10 staining on this cell population in blood and periphery lymphoid organs (Figure 5.7, B and C). Notably, the raised ME1 levels observed in PBMCs (Figure 5.7, D), irrespective of *M.tb* treatment, did not correlate with changes in expression levels of non-classical B27 molecules.

CD11bc$^+$ cells (Figure 5.8, A) were detected in PBMCs at both experimental time points and in spleens 3 weeks after *M.tb* injection. There was no significant difference in surface expression of non-classical B27 on CD11bc$^+$ cells between immunized and non-immunized animals (Figure 5.8, B and C). However, HD6 and HC10 staining were higher on CD11bc$^+$ cells from PBMCs compared with splenic cells. Interestingly, expression of both classical (ME1) (Figure 5.8, D) and non-classical (HC10 and HD6) B27 molecules was decreased in the older animals, irrespective of *M.tb* treatment.

Figure 5.7 Increased levels of non-classical B27 molecules are observed on CD45R⁺/MHC II⁺ cells in LNs from B27 TG² rats 2 weeks p.i. +/- *M.tb*. A) CD45R/MHCII population gating strategy. Expression of B) HD6-, C) HC10-) and D) ME1-reactive molecules in PBMCs, LNs and SPLC from B27 TG² animals 2 and 3 weeks +/- *M.tb*. B) Representative flow cytometry dot plot CD45R versus MHC II showing population gating strategy. Number of B27 TG² rats per time point: 2 untreated and 4 treated with 30mg *M.tb*.

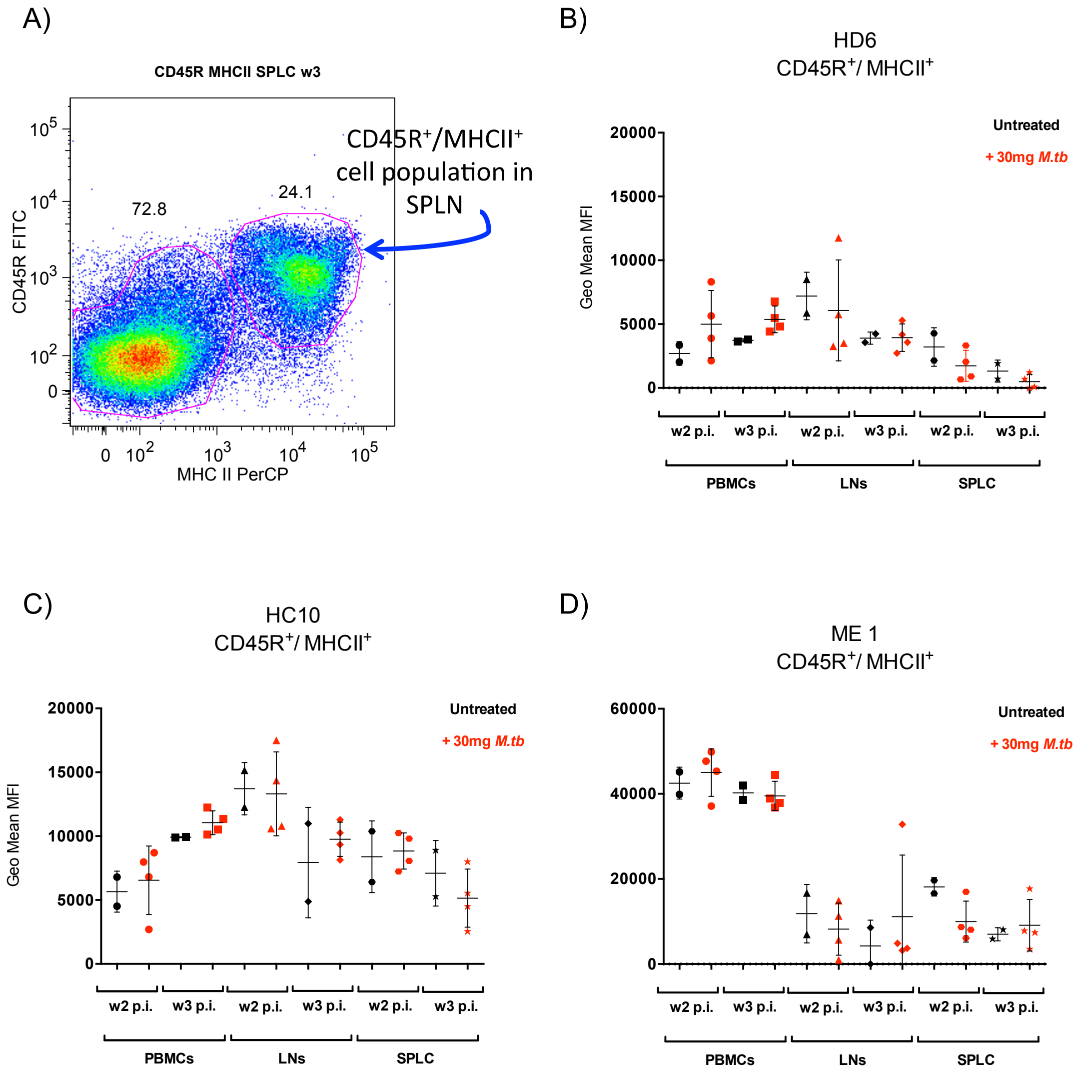

Figure 5.8 Increased levels of non-classical B27 molecules are detected on CD11bc$^+$ cells in PBMCs from B27 TG^2 rats 2 weeks p.i. +/- *M.tb*. A) CD11bc Population gating strategy. Expression of B) HD6-, C) HC10- and D) ME1-reactive molecules in PBMCs, SPLC from B27 TG^2 animals 2 and 3 weeks +/- *M.tb*. B) Representative flow cytometry dot plot CD11bc versus FSC showing population gating strategy. Number of B27 TG^2 rats per time point: 2 untreated and 4 treated with 30mg *M.tb*.

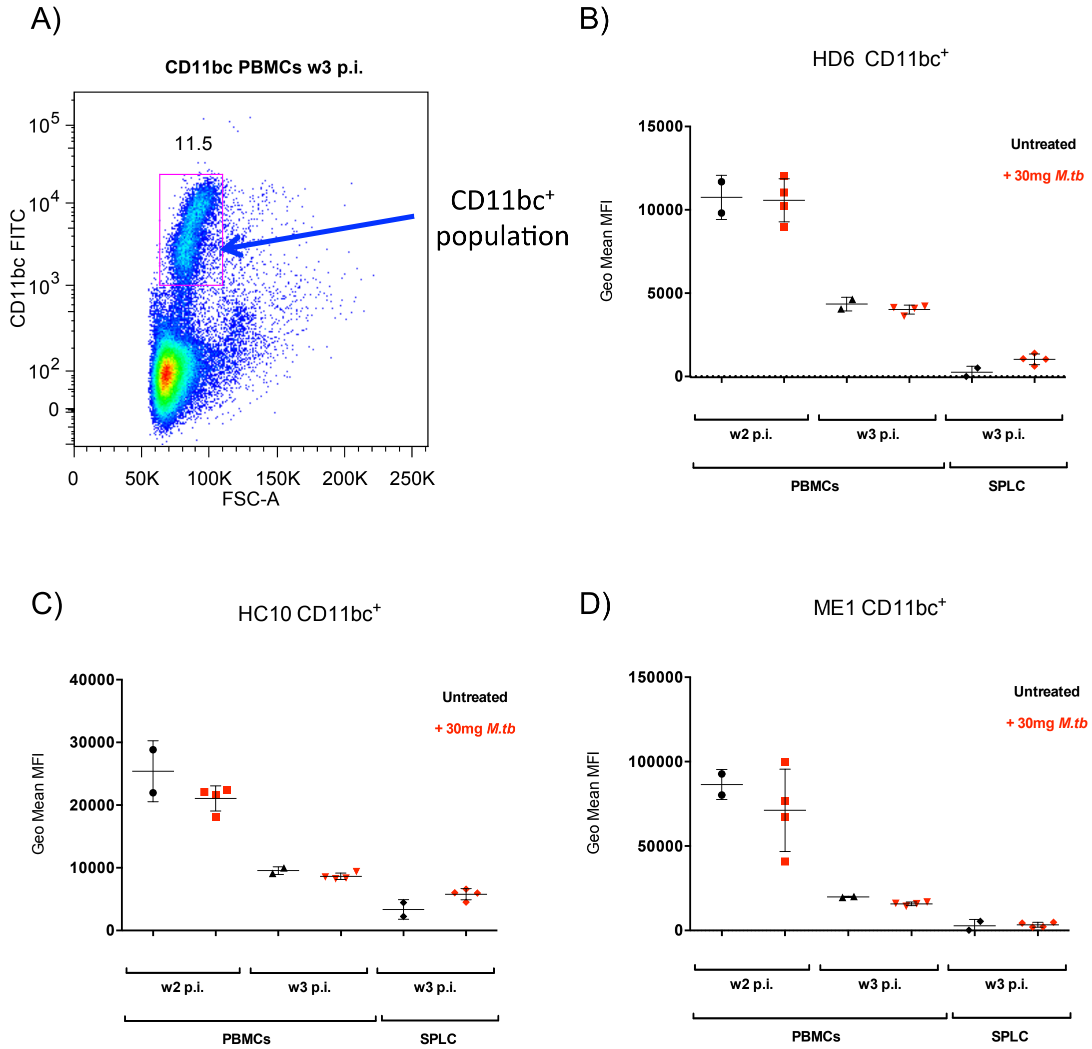

Figure 5.9 Characterization of CD161-positive cell populations in B27 TG^{2} rat spleen 3 weeks post *M.tb* injection. A) Representative CD161 versus FSC flow cytometry dot plot showing gating strategy. Red arrow – CD161^{high} cell population; Blue arrow – CD161^{med} cell population.

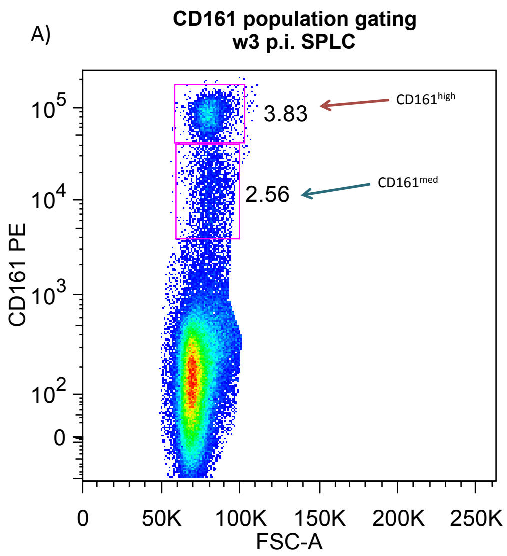

Two main populations expressing CD161 were detected in cells isolated from the B27 TG^{2} rats: CD161^{high} (expressing high levels of CD161 molecules) and CD161^{med} (characterized by the medium expression levels of CD161) (Figure 5.9, A).

In both PBMC CD161^{high} and CD161^{med} cell populations HD6-reactive molecules were expressed at similar levels at both studied time points (Figure 5.10, A and B). Similar observations were found for HC10 staining (Figure 5.10, C and D). However, raised levels of ME1 were present on PBMC CD161^{high} population on week 2 p.i. compared to week 3, irrespective of *M.tb* injection.

Interestingly, in LNs both HD6 and HC10 staining on CD161^{high} cells were increased in *M.tb* treated rats at 2 weeks post injection (Figure 5.10, A and C, middle data set). This difference did not correspond to changes in ME1 expression levels, which remained similar in all study groups, regardless of animal age (Figure 5.10, E).

Splenic CD161^{high} cells expressed elevated levels of HD6 and HC10 at 2 weeks p.i, irrespective of *M.tb* immunization (Figure 5.10, A and C). In splenic CD161^{med} population *M.tb* injection seemed to decrease HD6 levels at both 2 and 3 weeks p.i (Figure 5.10, B). However, at the same time a slight increase in HC10 staining was detected in *M.tb* treated animals (Figure 5.10, D). ME1 expression levels in both CD161 cell populations were similar in all study groups (Figure 5.10, F).

Figure 5.10 HD6- and HC10-reactive molecules are increased on CD161^{high} LNs cells 2 weeks post *M.tb* injection. Expression of HD6 (A and B), HC10 (C and D) and ME1 (E and F) in CD161^{high} and CD161^{med} cells from PBMCs, LNs and SPLC 2 and/or 3 weeks p.i. +/- *M.tb* injection. Number of B27 TG^{2} rats per time point: 2 untreated and 4 treated with 30mg *M.tb*.

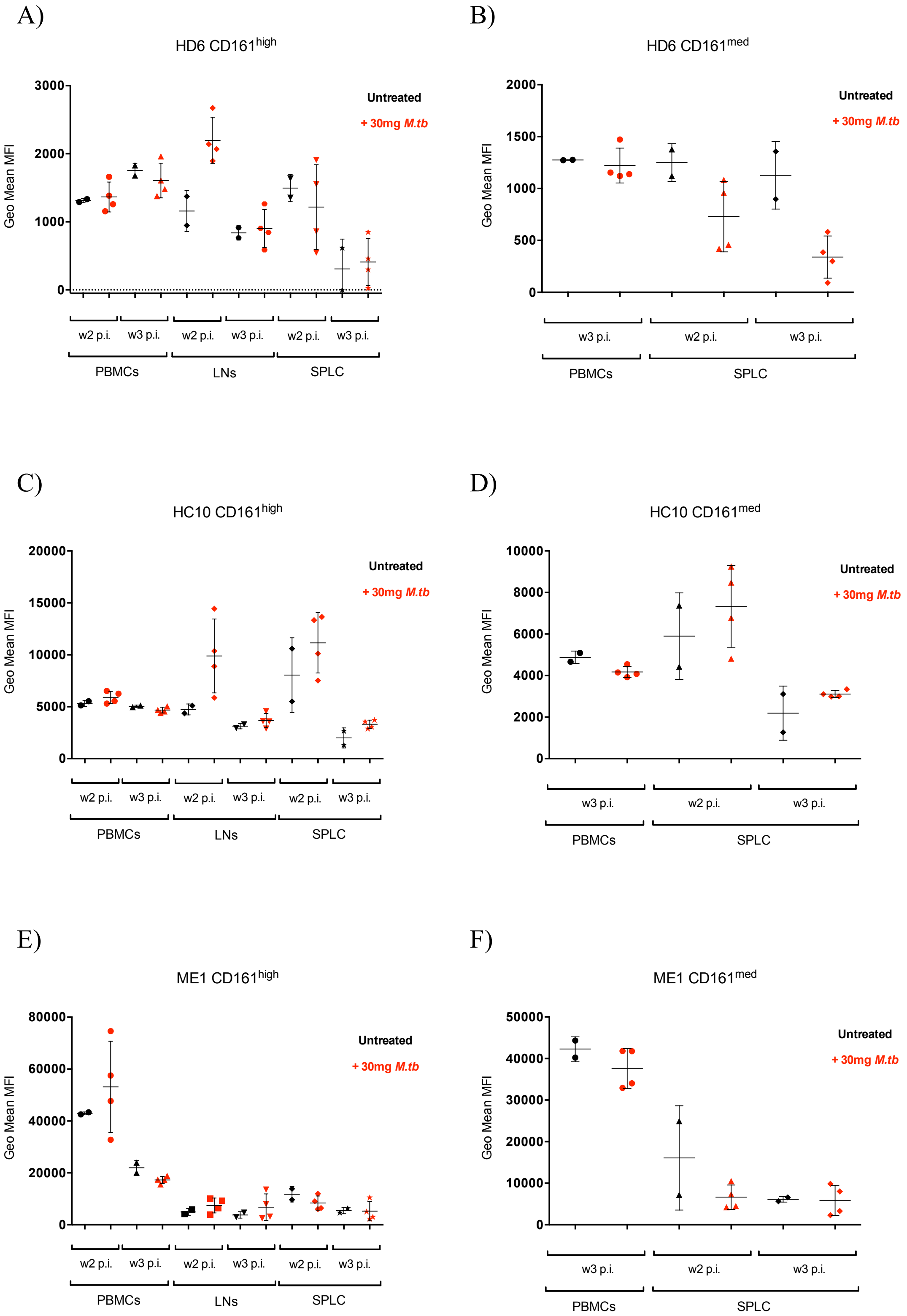

We have shown previously that granulocyte numbers were consistently increased in the original B27 TG^{1} rat model (7-9 months old) (McHugh et al., 2014). However, only splenic cells were investigated. These could be simply a consequence of severe gut and joint inflammation or it might implicate the role of granulocytes in disease pathogenesis.

Consequently I sought to investigate whether *M.tb* injection, which accelerates the disease onset in the B27 TG^{2} rat model, influences granulocyte population.

Granulocyte population was characterized on a basis of cell granularity (side scatter, SSC) and cell size (forward scatter, FSC) (Figure 5.11). I did not observe a clear granulocyte population in blood and lymph nodes in 8 weeks old animals (Appendix). Similarly, untreated 9 weeks old animals did not present a clear granulocyte population in PBMCs and LNs (Figure 5.11, A and C). However, at this time point granulocytes were observed in spleens independently of *M.tb* injection (Figure 5.11, E and F). Granulocytes could only be detected in PBMCs and LNs in B27 TG^{2} rats 3 weeks p.i. (Figure 5.11, B and D).

Figure 5.11 Granulocytes are more abundant in blood and lymph nodes 3 weeks post *M.tb* injection. Representative SSC versus FSC flow cytometry dot plots showing PBMCs, LNs and SPLC from untreated and *M.tb* treated animals 3 weeks post injection. Pink gates – granulocyte population, numbers in dot plots – percentages of gated cells.

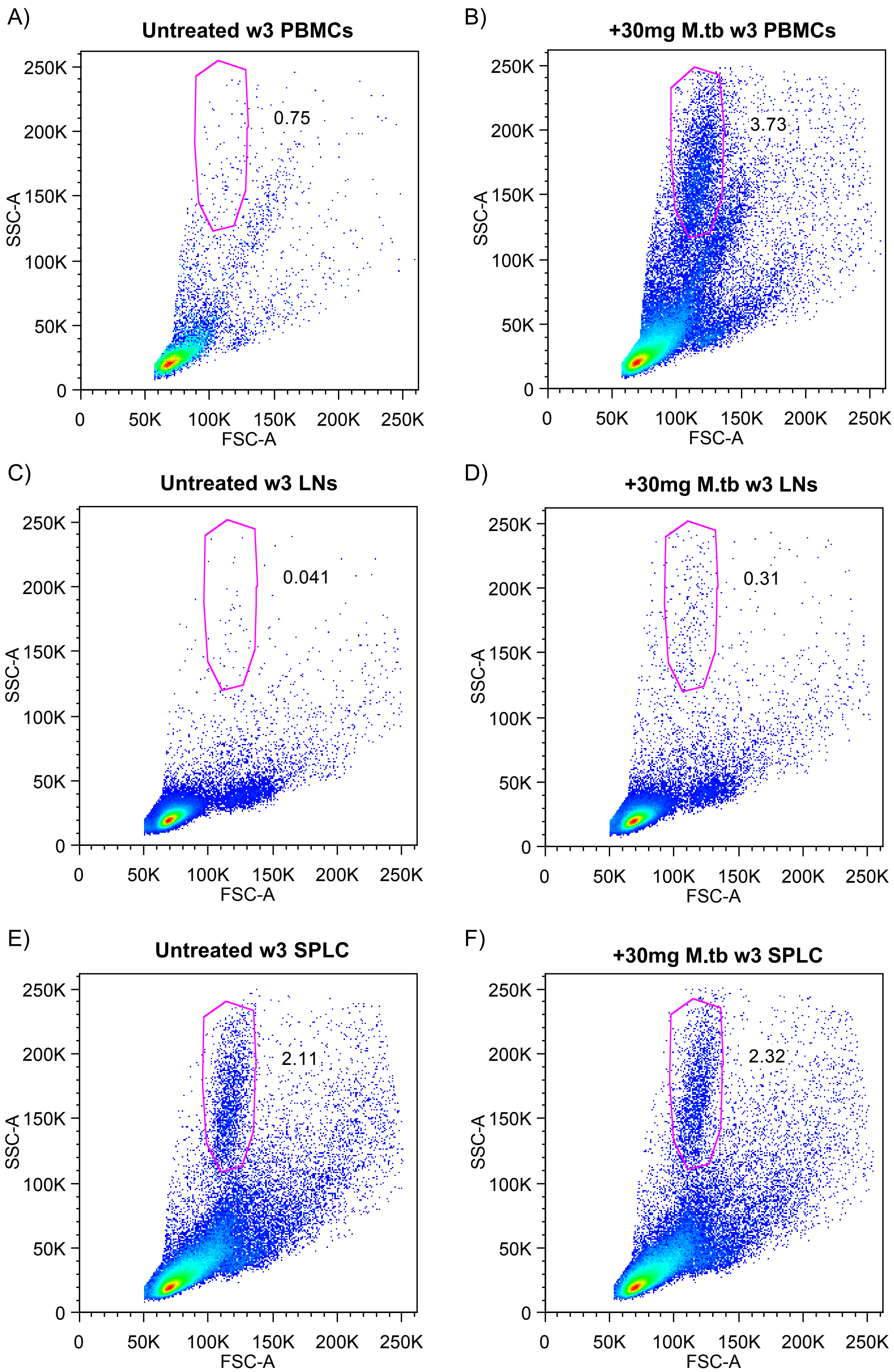

Table 5.1 Summary comparisons of changes in the expression of HD6-, HC10- and ME-reactive molecules between 2 and 3 weeks p.i. in untreated B27 TG[2] rats. The arrows show changes on week 3 relative to week 2 p.i.

	PBMCs			LNs			SPLC		
	HD6	HC10	ME1	HD6	HC10	ME1	HD6	HC10	ME1
$CD4^+$	↑	↔	↓	↓	↓	↔	↑	↓	↓
$CD8^+$	↑	↑	↔	↓	↓	↔	↑	↓	↔
$CD45R^+$/ MHC II^+	↑	↑	↔	↓	↓	↓	↓	↓	↓
$CD11bc^+$	↓	↓	↓	No $CD11bc^+$ cell population			$CD11bc^+$ cell population was present only on w3 p.i. and expression levels lower compared with PBMCs		
$CD161^{high}$	↑	↔	↓	↓	↓	↔	↓	↓	↓
$CD161^{med}$	$CD161^{med}$ cell population was present only on w3 p.i. and expression levels lower compared with SPLC w3 p.i.			No $CD161^{med}$ cell population			↓	↓	↓

↑ INCREASE

↑ INCREASE TREND

↔ NO CHANGES

↓ DECREASE TREND

↓ DECREASE

Table 5.2 Summary comparisons of changes in the expression of HD6-, HC10- and ME-reactive molecules between 2 and 3 weeks p.i. in *M.tb* treated B27 TG^2 rats. The arrows show changes on week 3 relative to week 2 p.i.

	PBMCs			LNs			SPLC		
	HD6	HC10	ME1	HD6	HC10	ME1	HD6	HC10	ME1
CD4$^+$	↑ INCREASE TREND	↔ NO CHANGES	↓ DECREASE	↑ INCREASE TREND	↓ DECREASE	↑ INCREASE TREND	↔ NO CHANGES	↓ DECREASE	↔ NO CHANGES
CD8$^+$	↑ INCREASE	↑ INCREASE	↓ DECREASE	↑ INCREASE	↓ DECREASE	↔ NO CHANGES	↔ NO CHANGES	↓ DECREASE TREND	↔ NO CHANGES
CD45R$^+$/ MHC II$^+$	↔ NO CHANGES	↑ INCREASE	↓ DECREASE TREND	↓ DECREASE TREND	↓ DECREASE	↔ NO CHANGES	↓ DECREASE TREND	↓ DECREASE	↔ NO CHANGES
CD11bc$^+$	↓ DECREASE	↓ DECREASE	↓ DECREASE	No CD11bc$^+$ cell population			CD11bc$^+$ cell population present only on w3 p.i. and expression levels lower compared with PBMCs		
CD161^{high}	↑ INCREASE TREND	↓ DECREASE TREND	↓ DECREASE	↓ DECREASE	↓ DECREASE	↔ NO CHANGES	↓ DECREASE	↓ DECREASE	↓ DECREASE TREND
CD161^{med}	CD161^{med} cell population was present only on w3 p.i. and expression levels lower compared with SPLC w3 p.i.			No CD161^{med} cell population			↓ DECREASE	↓ DECREASE	↔ NO CHANGES

↑ INCREASE
↑ INCREASE TREND
↔ NO CHANGES
↓ DECREASE TREND
↓ DECREASE

Table 5.3 Summary comparison of changes in HD6, HC10 and ME1 expression between *M.tb* treated and untreated B27 TG^2 rats. The arrows show changes between *M.tb* treated realtive to untreated rats.

		PBMCs			LNs			SPLC		
		HD6	HC1	ME1	HD6	HC10	ME1	HD6	HC10	ME1
CD4+	Week 2 p.i	↔	↔	↔	↓	↔	↔	↓	↑	↔
	Week 3 p.i	↔	↔	↓	↔	↔	↔	↓	↑	↔
CD8+	Week 2 p.i	↔	↔	↑	↓	↔	↔	↓	↔	↓
	Week 3 p.i	↔	↓	↓	↑	↔	↔	↓	↔	↔
CD45R+/ MHC II+	Week 2 p.i	↑	↑	↑	↓	↔	↔	↓	↔	↓
	Week 3 p.i	↑	↑	↔	↔	↑	↔	↓	↓	↔
CD11bc+	Week 2 p.i	↔	↓	↓	No CD11bc+ cell population			CD11bc+ cell population was present only on w3 p.i. and expression levels lower compared with PBMCs		
	Week 3 p.i	↔	↔	↔						
CD161high	Week 2 p.i	↔	↔	↑	↑	↑	↔	↓	↑	↔
	Week 3 p.i	↔	↔	↓	↑	↔	↔	↔	↑	↔
CD161med	Week 2 p.i	CD161med cell population was present only on w3 p.i. and expression levels lower compared with SPLC w3 p.i.			No CD161med cell population			↓	↑	↔
	Week 3 p.i							↓	↑	↔

↑ INCREASE
↑ INCREASE TREND
↔ NO CHANGES
↓ DECREASE TREND
↓ DECREASE

Summary Chapter 5.3

In PBMCs from both untreated and treated animals HD6- and HC10-reactive molecules were increased on $CD8^+$ and slightly elevated on $CD4^+$ cells at 3 weeks p.i. Similarly, in $CD45^+$/MHC II^+ cells HC10 staining was increased at 3 weeks p.i.

Interestingly, decreased amounts of both HD6- and HC10-reactive molecules were detected in $CD11bc^+$ cells from PBMCs, $CD45R^+$/MHC II^+ cells from LNs and spleens and $CD161^{med}$ cells from spleens at 3 weeks p.i, irrespective of *M.tb* treatment.

Moreover, in both study groups an increase trend in HD6 staining was observed in $CD161^{high}$ population at 3 weeks p.i present in blood.

M.tb injection increased cell surface expression of HD6- and HC10-reactive molecules in $CD161^{high}$ population obtained from LNs at 2 weeks p.i. At the same time a slightly elevated levels of HD6 and HC10 staining were found in $CD45R^+$/MHC II^+ cells isolated from blood.

On the other hand, in $CD4^+$ and $CD8^+$ cells isolated 2 weeks p.i from LNs and 3 weeks p.i. from spleens, treatment with *M.tb* led to the decrease in HD6 staining. Interestingly, the decrease in expression levels of HD6-reactive molecules in splenic $CD4^+$ cells and $CD161^{med}$ cells was correlated with elevated levels of HC10-reactive molecules.

5.4 HD6-reactive molecules are expressed in peripheral joints and spine of B27 TG^2 rats

One of the principal advantages of the SpA rat model is the opportunity to study the progression of the disease in peripheral joints and spine. As mentioned before, studying affected joints in humans, especially spine tissue, is limited due to the extremely rare availability of samples.

Peripheral joint inflammation in AS may be driven by pathogenic B27 molecules present on joint resident cells or it could be a consequence of HLA-B27 expression on infiltrating cells from periphery. Therefore, I was interested in whether potentially pathogenic forms of B27, including HD6- and HC10-reactive molecules, can be detected in joints.

Ankle joints were obtained from both spontaneous and accelerated B27 TG^2 rat model. As controls ankles from B7 TG rats with *M.tb* induced arthritis and from collagen induced arthritis (CIA) Lewis rats were used. As described previously (van Duivenvoorde et al., 2012) inflammation in ankle joints was scored by two independent observers on a scale from 0 to 3 (Grade 0 = no inflammation, no pathological arthritic tissue manifestations; Grade 2 = moderate inflammation, with mononuclear cell infiltrates in the connective and synovial tissue, visible osteoclasts and bone erosions; Grade 3 = severe inflammation, with cell infiltration into the bone, many multinucleated, osteoclast-like cells and extensive bone erosions).

Immunohistochemical (IHC) analysis of paraffin embedded tissue sections from non-inflamed (grade 0) ankles of B27 TG^2 male rats showed significant HD6 staining in mature chondrocytes in the outer layer of the joint cartilage (Figure 5.12 A and B, area 4). Furthermore, fibroblast-like cells in a connective tissue and fibrocartilage expressed significant amounts of HD6-reactive molecules (Figure 5.12 A and B, C left bottom corner). In addition, chondrocyte-like cells from fibrocartilage were characterized by significant HD6 (Figure 5.12 C and D, area 6). Importantly no HD6 staining was detected in control ankles from WT Lewis rats with CIA (Figure 5.12, C and D) and no non-specific staining was observed with isotype controls (Figure 5.12, E and F).

In B27 TG^2 rat ankles with a moderate inflammation (grade 2) HD6 staining was also observed in chondrocyte-like cells as well as osteoblast-like cells (Figure 5.14). Again, similar findings were observed in fibrocartilage and connective tissue (Figure 5.14, C, area 6 and 3). Additionally, HD6 also stained a population of smaller, multinuclear cells in bone marrow zones, which may represent “inactive” osteoclasts (Figure 5.14, D, area 1).

Moreover, the HD6-positive osteoblast-like cells and chondrocyte-like cells in grade 2 tissue sections were found inside circular zones, which resembled new cartilage formation sites with multinucleated osteoclasts and osteoblasts in a surrounding perichondrium (Figure 5.14, A and B, area 10).

Furthermore, HD6 stained the majority of multinucleated osteoclast-like cells, which were present in bone erosion and remodeling sites and in bone marrow (Figure 5.14 A, B and D, area 1 and 9). Interestingly, the synovial tissue mononuclear cell infiltrates did not show significant HD6 staining (Figure 5.14, A and C, area 8).

Sites containing “active” osteoclasts that were eroding the bone matrix and associated with increased numbers of bone erosion and remodeling sites were characteristic for the severe inflammation (score 3) (Figure 5.15, A, B, C and D area 9). Notably, HD6 staining was restricted to these “activated” osteoclasts. Large mononuclear cell infiltrates were observed in ankle joints with grade 3 inflammation (Figure 5.16, C, area 8). Moreover high intensity of HD6 staining was observed in bone marrow sites on osteoclast-like cells (Figure 5.16 A and B). Interestingly, the fibroblast-like, osteoblast-like and chondrocyte-like cell populations stained with HD6 to a lesser extent in grade 3 tissue compared with grade 0 and grade 2 (Figure 5.16, C and D, area 3 and 4).

Figure 5.12 HD6-reactive molecules are abundantly expressed on chondrocyte-like cells in articular cartilage in B27 TG^2 ankle joints at early stages (score 0) of the disease without a visible mononuclear cell infiltrates. Chondrocytes staining in an outer layer of cartilage – A, 4 (10X) and B, 4 (20X) higher resolution of the black square area from picture A. C) and D) HD6 staining in ankle joints from CIA WT Lewis rat with score 3 inflammation (5X). E) and F) IgG1 isotype staining in ankle from B27 TG^2 rat. Numbers in pictures: 1 – bone marrow; 2 – bone matrix with osteocytes; 4 – articular cartilage with chondrocytes; 5 – synovial tissue. Immunohistochemistry staining using Ready-to-Use AEC+ High Sensitivity Substrate Chromogen Kit. Red – HD6 antibody staining. Blue – Mayer's Hematoxilin staining. Tissue sections were scanned on AperioScanner and analyzed in ImageScope.

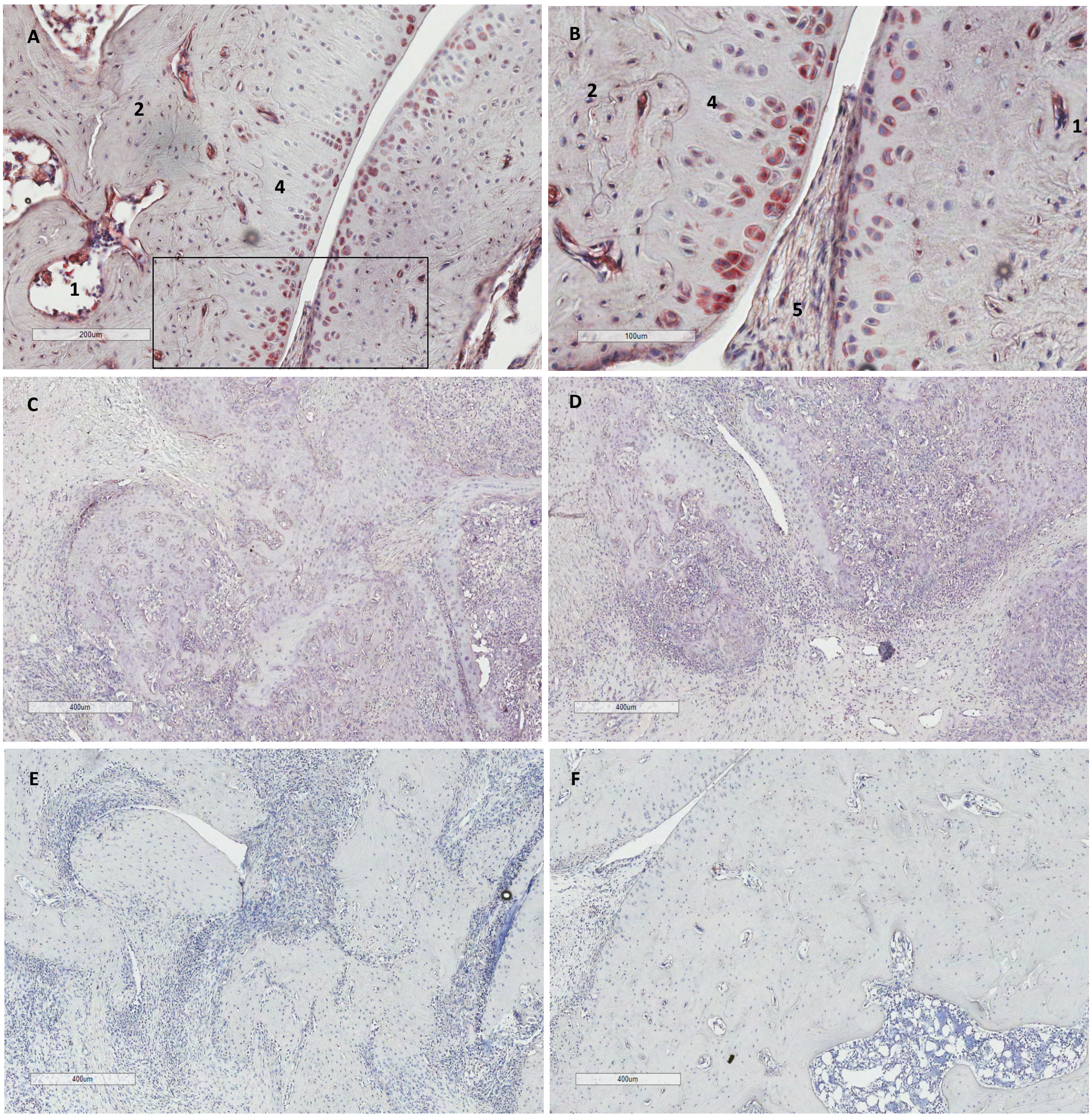

Figure 5.13 HD6-reactive molecules are expressed in fibroblast-like cells in connective tissue and chondrocyte-like cells in fibrocartilage in ankles from B27 TG[2] rats with no inflammation (score 0). Fibroblast-like cells staining in a connective tissue – A), 3 (10X). B) (20X) higher resolution of a black square area from picture A. C and D, HD6 staining of chondrocyte-like and fibroblast-like cells in a fibrocartilage. Paraffin embedded B27 TG[1] ankle tissue sections were obtained from rats without clinical symptoms (score 0). Numbers in pictures: 2 – bone matrix with osteocytes; 3 – connective tissue with fibroblasts; 6 – fibrocartilage with chondrocytes and fibroblasts; 7 – blood vessels. Immunohistochemistry staining using Ready-to-Use AEC+ High Sensitivity Substrate Chromogen Kit. Red – HD6 antibody staining. Blue – Mayer's Hematoxilin staining. Tissue sections were analysed on AperioScanner.

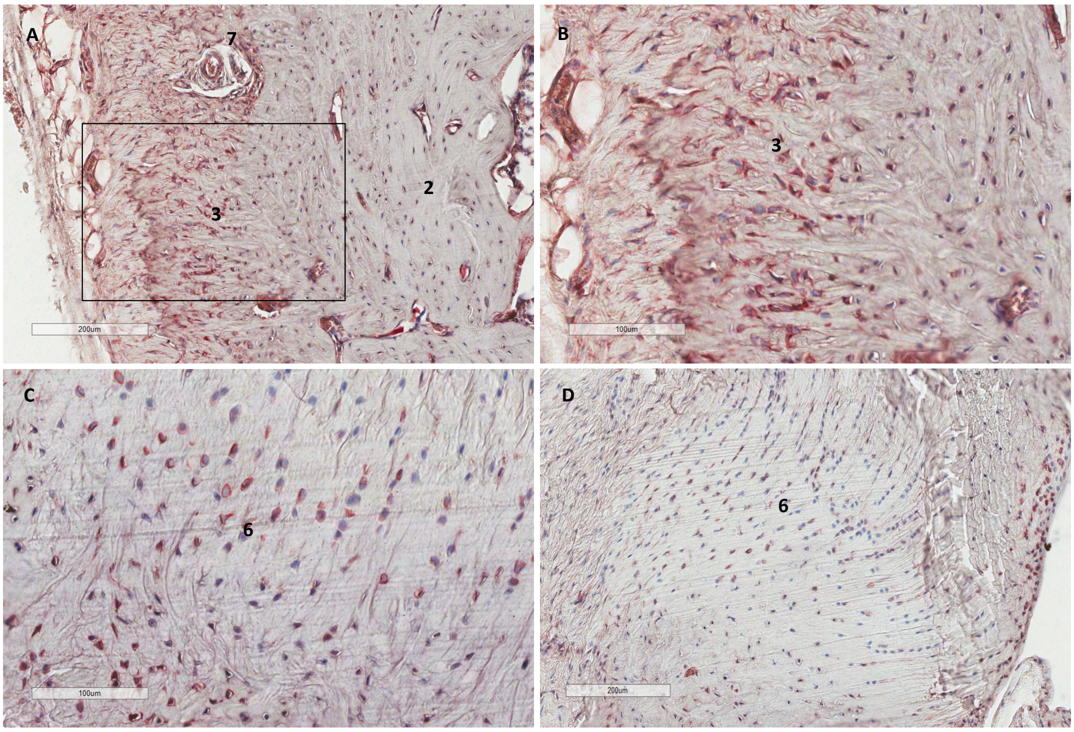

Figure 5.14 Expression of HD6-reactive molecules in grade 2 ankle joints from B27 TG[1] rats. A) 10X and B) 20X higher resolution of the black square area from picture A. Chondrocytes staining in an outer layer of articular cartilage - A and B, 4. Osteoclasts staining in bone remodeling, erosion zones (A and B, 9) and in bone marrow (D, 1). Chondrocyte staining in fibrocartilage (C, 6) and fibroblasts staining in connective tissue (C, 3). Single cells staining in a mononuclear cell infiltrates zone in synovial tissue (A and B, 8). Numbers in pictures: 1 – bone marrow with multinucleated osteoclasts; 2 – bone matrix with osteocytes; 3 – connective tissue with fibroblasts; 4 – articular cartilage with chondrocytes; 6 – fibrocartilage with chondrocytes and fibroblasts; 8 – mononuclear cell infiltrates zones in synovial tissue; 9 – bone remodeling, erosion sites with multinucleated osteoclasts; 10 – circular zones with osteoblast-like and chondrocyte-like cells, resembling new cartilage formation sites. Immunohistochemistry staining using Ready-to-Use AEC+ High Sensitivity Substrate Chromogen Kit. Red – HD6 antibody staining. Blue – Mayer's Hematoxilin staining.

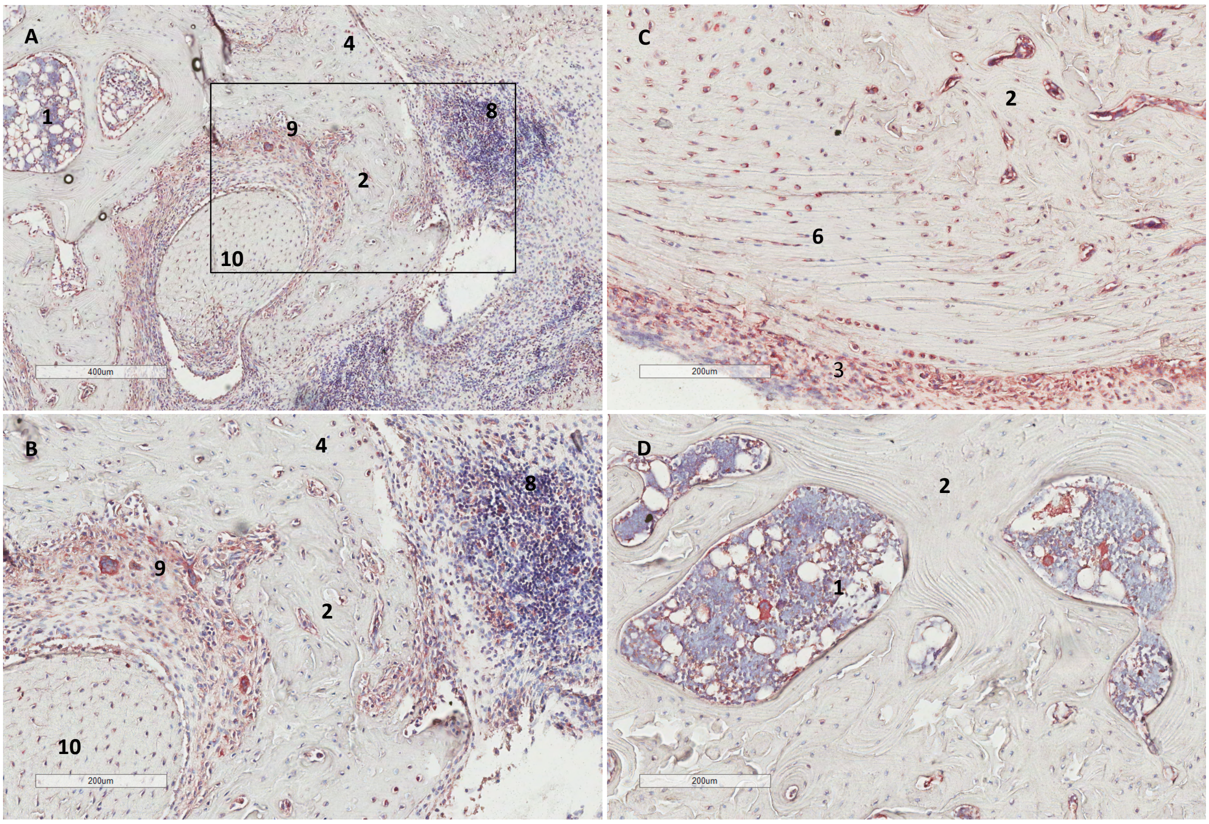

Figure 5.15 HD6 is expressed on osteoclast-like cells in bone remodeling zones present in abundant numbers in ankle joints from B27 TG[2] rats with severe inflammation (score 3). Multinucleated, activated osteoclasts and mononuclear cell infiltrates in bone erosion, remodeling zones – A) 9 (10X) and B) 9 (20X, higher resolution of the black square area from picture A), C) 9 (10X) and D) 9 (20X, higher resolution of the black square area from picture C). Low intensity HD6 staining in cells present in mononuclear cell infiltrates zones and surrounding synovial tissue (C, 8). Numbers in pictures: 2 – bone matrix with osteocytes; 8 – mononuclear cell infiltrates in a synovial tissue; 9 – bone erosion, remodeling sites with mononuclear cell infiltrates. Immunohistochemistry staining using Ready-to-Use AEC+ High Sensitivity Substrate Chromogen Kit. Red – HD6 antibody staining. Blue – Mayer's Hematoxilin staining.

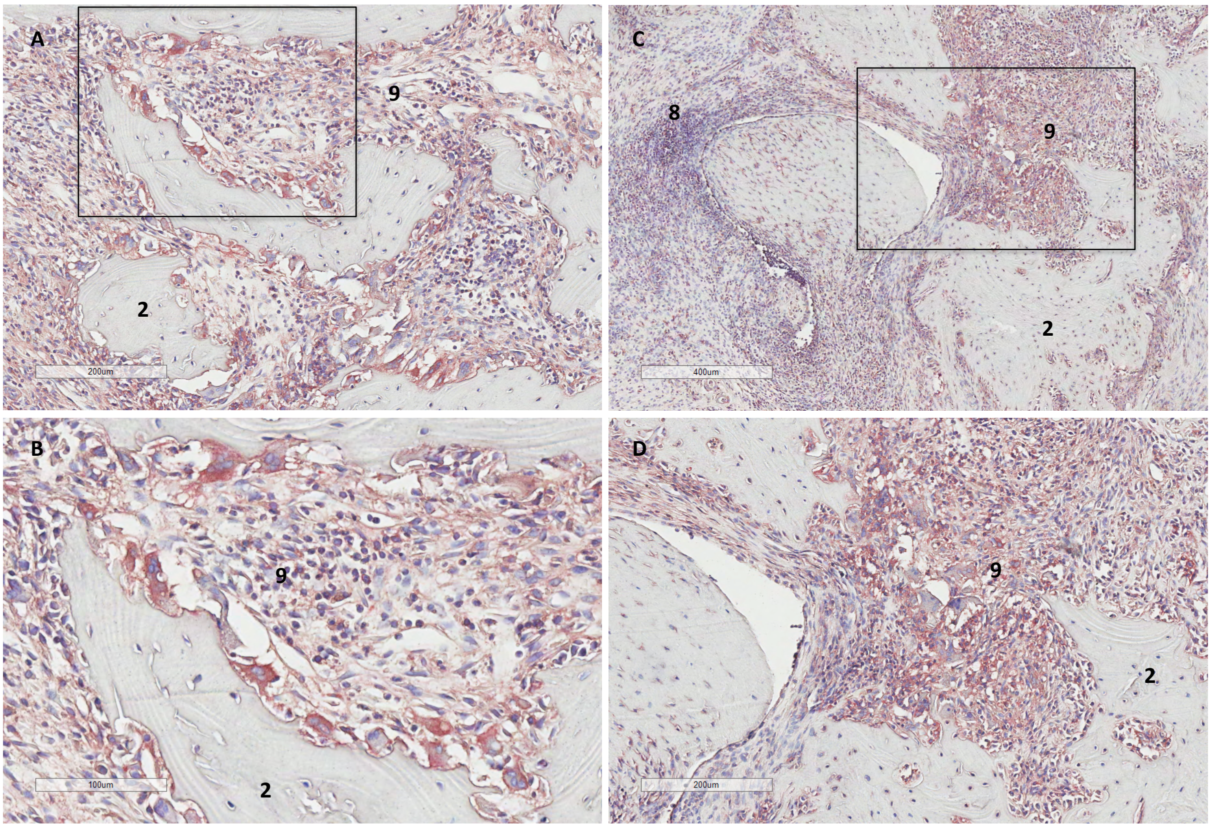

Figure 5.16 HD6 staining is abundant on osteoclast-like cells in bone marrow in severely inflamed ankle joints from B27 TG[2] rats. HD6 staining on multinucleated, osteoclast-like cells in bone marrow (A and C, 1). Low intensity HD6 staining in connective tissue (B, 3) and synovial tissue mononuclear cell infiltrates (B, 8). Low intensity chondrocyte staining in articular cartilage (D, 4) and synovial tissue (D, 5). Numbers in pictures: 1 – bone marrow; 2 – bone matrix with osteocytes; 3 – connective tissue with fibroblasts; 4 – articular cartilage with chondrocytes; 5 – synovial tissue; 8 – mononuclear cell infiltrates in connective tissue. Immunohistochemistry staining using Ready-to-Use AEC+ High Sensitivity Substrate Chromogen Kit. Red – HD6 antibody staining. Blue – Mayer's Hematoxilin staining.

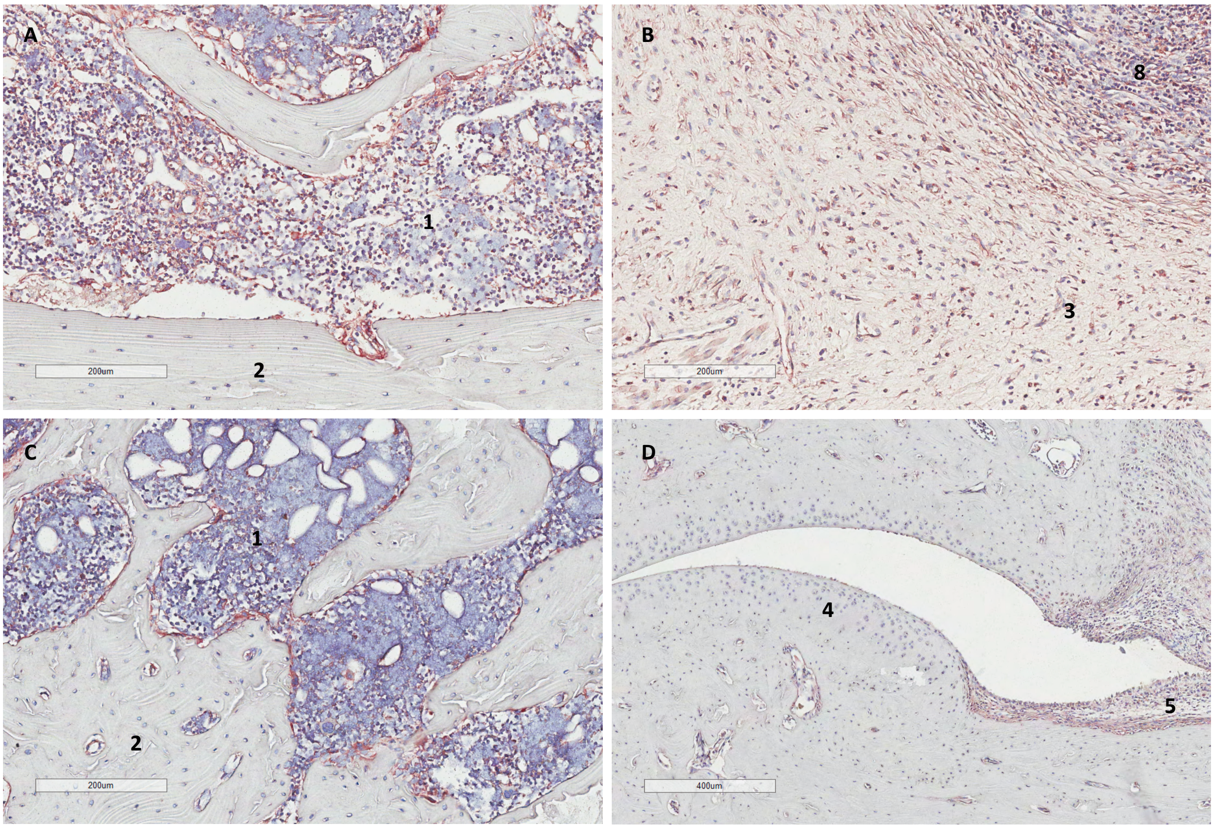

Moreover, no detectable difference of HD6 staining was observed in the severely inflamed joints compared with moderate inflammation, despite the increased number of infiltrating cells and progression of histopathological features (Figure 5.14 versus Figure 5.15).

In non-inflamed and moderately inflamed ankle joints low levels of HC10 staining were detected on chondrocyte-like cells in articular cartilage and fibrocartilage, as well as in a fibroblast-like cells in connective tissue (Figure 5.17 and 5.18, area 4 and 6). Hence, these data are consistent with the staining patterns observed with HD6. However, unlike HD6, HC10 significantly stained the infiltrating mononuclear cells (Figure 5.18 and 5.19, area 8). Moreover, the expression levels of HC10 staining were increased on infiltrating cells present in bone remodeling sites in severely inflamed (grade 3) tissues (Figure 5.19, A, E and F, are 9). These observations suggest that at early stages of the disease HC10-reactive inflammatory cells infiltrate the synovial and connective tissue and subsequently migrate further into the tissue, where they can be found in bone erosion and remodeling sites. Notably, only low levels of HD6-reactive molecules can be detected on these infiltrating cells.

Figure 5.17 HC10 staining is present on chondrocytes in articular cartilage and fibrocartilage in ankle joints from B27 TG[2] rats with no inflammation (score 0). Chondrocyte staining in the outer layer of articular cartilage (A and C, 4) and in fibrocartilage (B and C, 6). Numbers in pictures: 1 –bone marrow; 2 – bone matrix with osteocytes; 4 – articular cartilage with chondrocytes; 5 – synovial tissue; 6 – fibrocartilage with chondrocytes and fibroblasts; 7- blood vessels. Immunohistochemistry staining using Ready-to-Use AEC+ High Sensitivity Substrate Chromogen Kit. Red – HC10 antibody staining. Blue – Mayer's Hematoxilin staining.

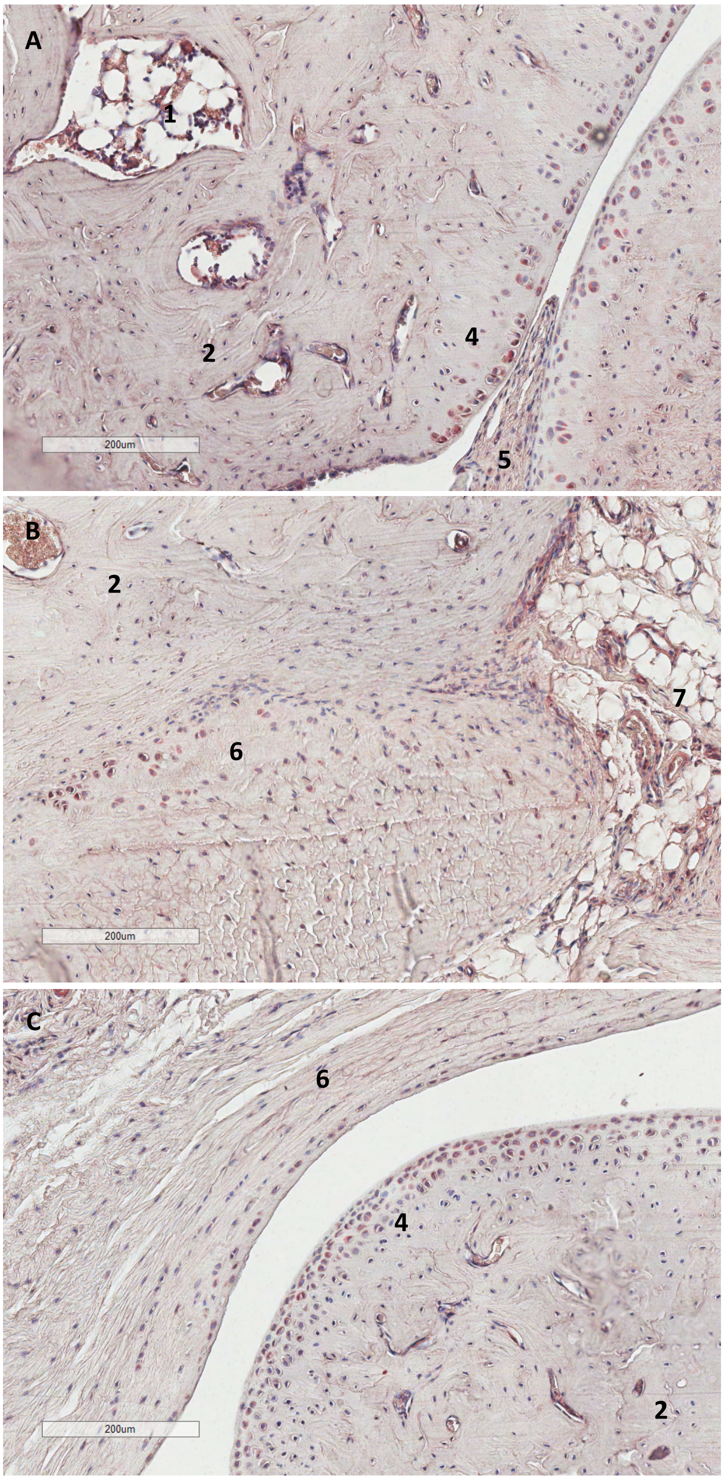

Figure 5.18 Significant HC10 staining is observed in mononuclear cell infiltration zones in the synovial tissue and bone remodeling zones in ankle joints from B27 TG² rats with moderate inflammation (score 2). High intensity FHC staining in mononuclear cell infiltrate zones in synovial tissue (A and B, 8) and on multinucleated and mononuclear cells present in bone remodeling zones (A and B, 9). A (10X) and B (20X) higher resolution of the black square area from picture A. HC10 staining visible in a bone marrow (A and C, 1). Low intensity HC10 staining on chondrocytes in articular cartilage (B and C, 4). Numbers in pictures: 1 – bone marrow; 2 – bone matrix with osteocytes; 4 – articular cartilage with chondrocytes; 5 – synovial tissue; 8 – mononuclear cell infiltrates in synovial and connective tissue; 9 – bone remodeling, erosion zones with mononuclear cell infiltrates and multinucleated osteoclasts. Immunohistochemistry staining using Ready-to-Use AEC+ High Sensitivity Substrate Chromogen Kit. Red – HC10 antibody staining. Blue – Mayer's Hematoxilin staining.

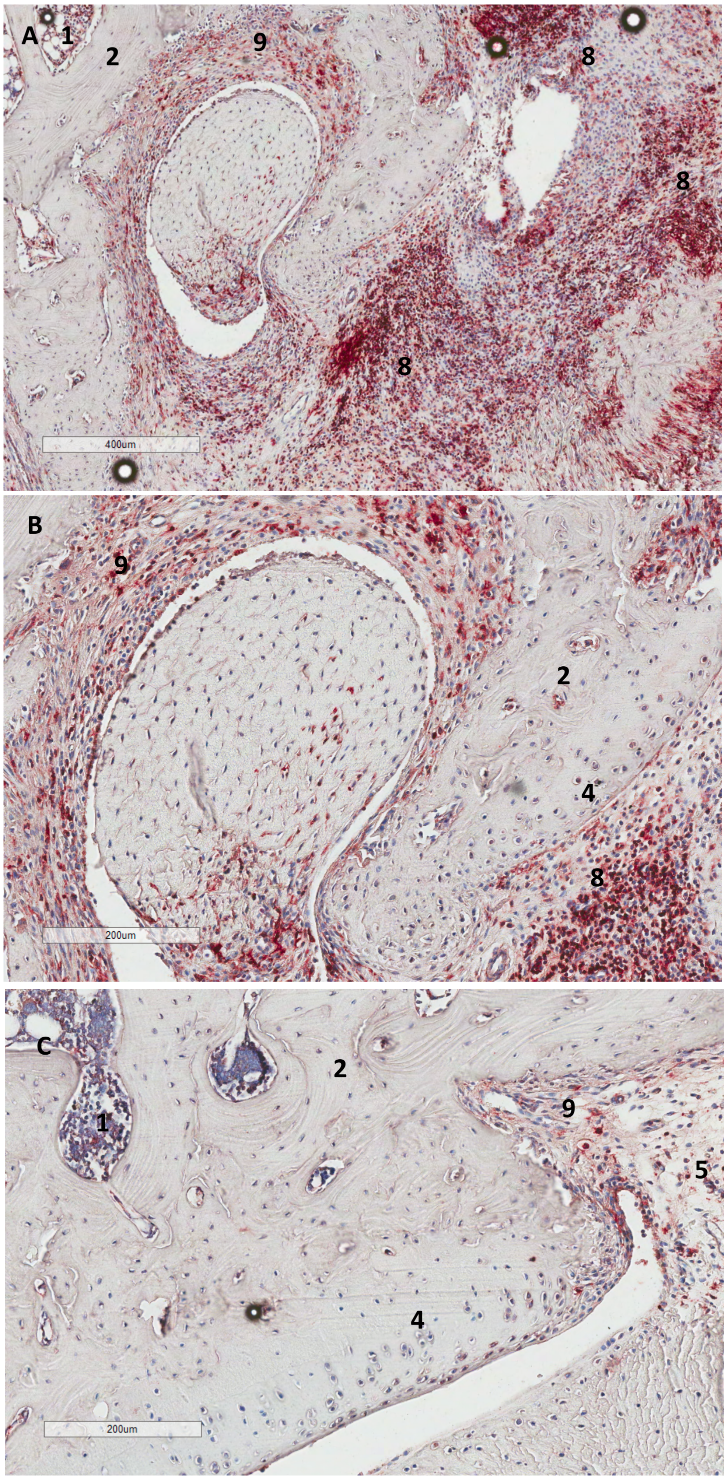

Figure 5.19 High intensity HC10 staining is located in mononuclear cell infiltrates in connective and synovial tissue and in bone erosion and remodeling sites in ankle joints from B27 TG^2 rats with severe inflammation (score 3). HC10 staining on mononuclear cell infiltrates (A, B and E, 8). HC10 staining on mononuclear cells in synovial tissue (C and D, 5). HC10-positive mononuclear cells and multinucleated osteoclasts in bone erosion and remodeling zones (A, E and F, 9). E (10X) and F (20X, higher resolution of a black square area from picture E). Numbers in pictures: 1 – bone marrow; 2 – bone matrix with osteocytes; 4 – articular cartilage with chondrocytes; 5 – synovial tissue; 8 – mononuclear cell infiltrates zones in a connective and synovial tissue; 9 – bone erosion and remodeling sites with mononuclear cell infiltrates and multinucleated osteoclasts. Immunohistochemistry staining using Ready-to-Use AEC+ High Sensitivity Substrate Chromogen Kit. Red – HC10 antibody staining. Blue – Mayer's Hematoxilin staining.

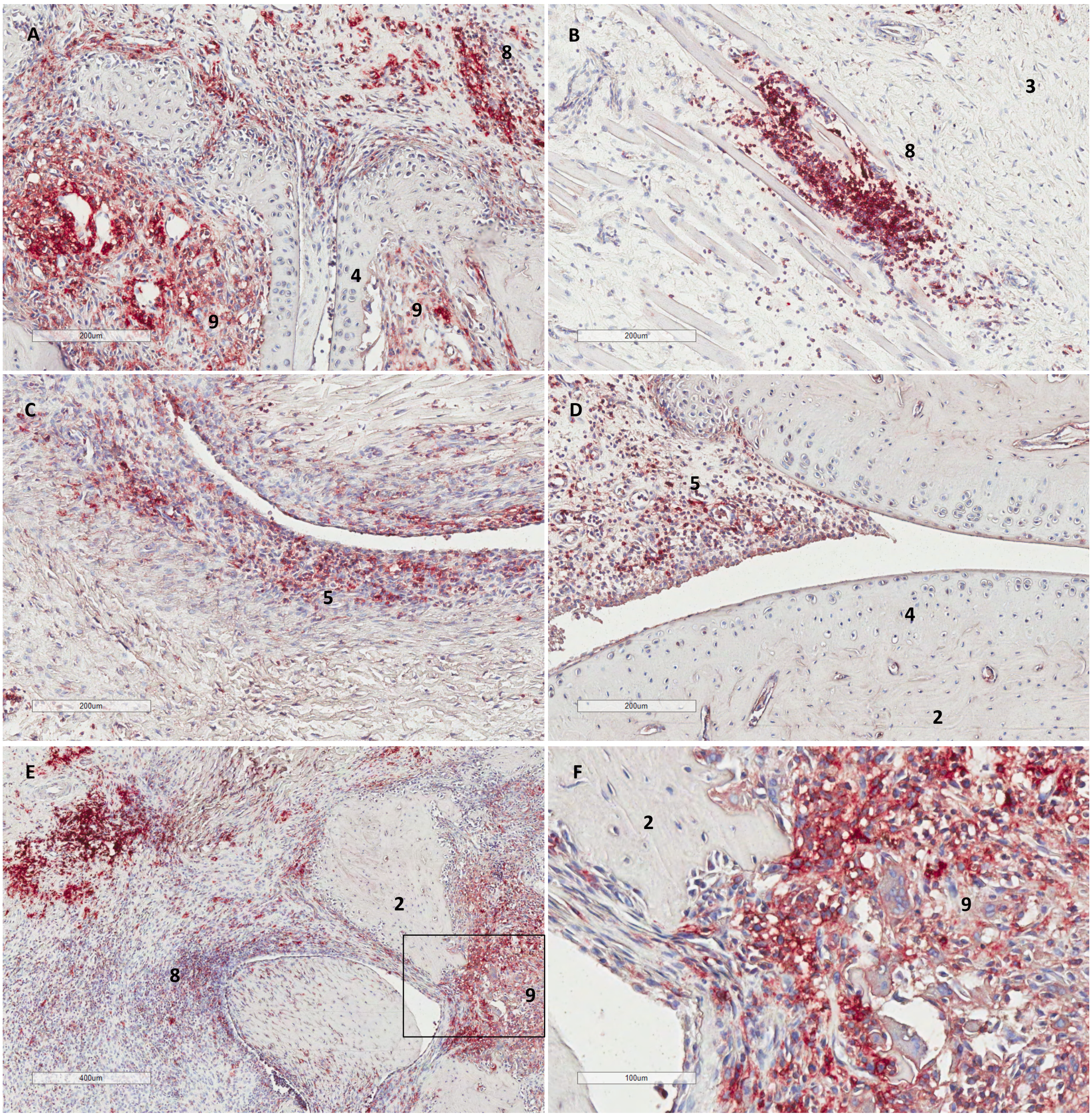

Importantly, B7 TG animals injected with *M.tb* develop similar joint manifestations to B27 TG^2 rats (van Duivenvoorde, ACR published abstract). I observed that the mononuclear cell infiltrates in peripheral joints can be detected earlier (grade 0) than in B27 TG^2 rats (grade 2). Unfortunately, no B7 TG rat tissue sections without *M.tb* injection were available. HD6 staining was mainly found on chondrocyte-like, fibroblast-like and osteoblast-like cells in B7 TG animals. Similar to my findings from B27 TG^2 rats some of these HD6 staining was specific to cells present inside circular zones resembling new cartilage formation sites with chondrocyte-like and osteoblast-like cells in a surrounding perichondrium.

Furthermore, HC10 staining patterns in B7 TG rats were also analogous to the ones observed in B27 TG^2 animals.

Summary Chapter 5.4

Ankle joints with no inflammation (score 0) or moderate inflammation (score 2) isolated from B27 TG^2 rats presented significant HD6 staining on chondrocyte-like cells in articular cartilage and fibrocartilage, as well as on fibroblast-like cells in fibrocartilage and connective tissue. Additionally, HD6-positive “inactive” and “active”, multinucleated osteoclast-like cells were present in bone marrow and bone erosion and remodeling sites in grade 2 and 3 ankle joints. At the same time, relatively low number of cells expressing HD6-reactive molecules was found in mononuclear cell infiltrates. On the other hand, high intensity of HC10 staining was detected in mononuclear cell infiltrates in tissues with moderate and severe inflammation. Furthermore, HC10 stained mononuclear and multinuclear cells in bone erosion and remodeling sites, synovial and connective tissue to the lesser extent compared with mononuclear cell infiltrates.

5.5 HD6-reactive molecules are expressed on resident cells in axial skeleton joints from B27 TG^2 rats

Sacroiliac joint inflammation and ankylosis in lower axial skeleton are characteristic clinical features in human SpA. However, due to the limited availability of spinal and sacroiliac joint biopsis from patients there is little known about the pathology of these joint manifestations in human. In the B27 TG^2 spontaneous and *M.tb* induced vertebral joint inflammation in tails is seen in 100% of male animals making it a suitable model to study axial skeleton SpA-like manifestations.

Consequently, I sought to investigate expression of HLA-B27 in axial skeleton joints. To identify whether potentially pathogenic NC-B27 molecules are present tail tissues were obtained from 4 B27 TG^2 male rats at 1, 2 and 3 weeks after injection of the lowest *M.tb* dose (30mg) and from 2 animals without innate immune stimulation at the same time points.

The axial joint tissue sections consisted of 2 vertebrae. Axial joints are formed from vertebral bones (VB), which are separated by intervertebral discs (ID) (Figure 5.20, A and B). Intervertebral disc consists of annulus fibrosus (AF), which forms concentric layers of fibrocartilage that surround the central matter of nucleus pulposus (NP). The space between intervertebral disc and end bone plate (EBP) of the vertebrae consists of articular cartilage (AC) and some adipose tissue (AT).

Figure 5.20 Rat tail vertebral joint structure. A) A full view of the tail tissue section showing 2 vertebral bones separated by vertebral discs. B) Higher resolution of small black square area from picture A showing enthesal site. C) Higher resolution large black square are from picture A showing the structure of vertebrates and intervertebral discs junction. D) Higher resolution of black square area from picture C demonstrating the structure of end bone plate and intervertebral disc junction. ID – intervertebral disc; LL – longitudinal ligament; SM – skeletal muscle; VB – vertebral bone; AF – annulus fibrosus; AT – adipose tissue; CT – connective tissue; L – ligament; ACS – articular cartilage sites; BM – bone marrow; EBP – end bone plate; ES – enthesal site; NP – nucleus pulposus; HC – hyaline cartilage. Immunohistochemistry staining using Ready-to-Use AEC+ High Sensitivity Substrate Chromogen Kit. Red – HD6 antibody staining. Blue – Mayer's Hematoxilin staining.

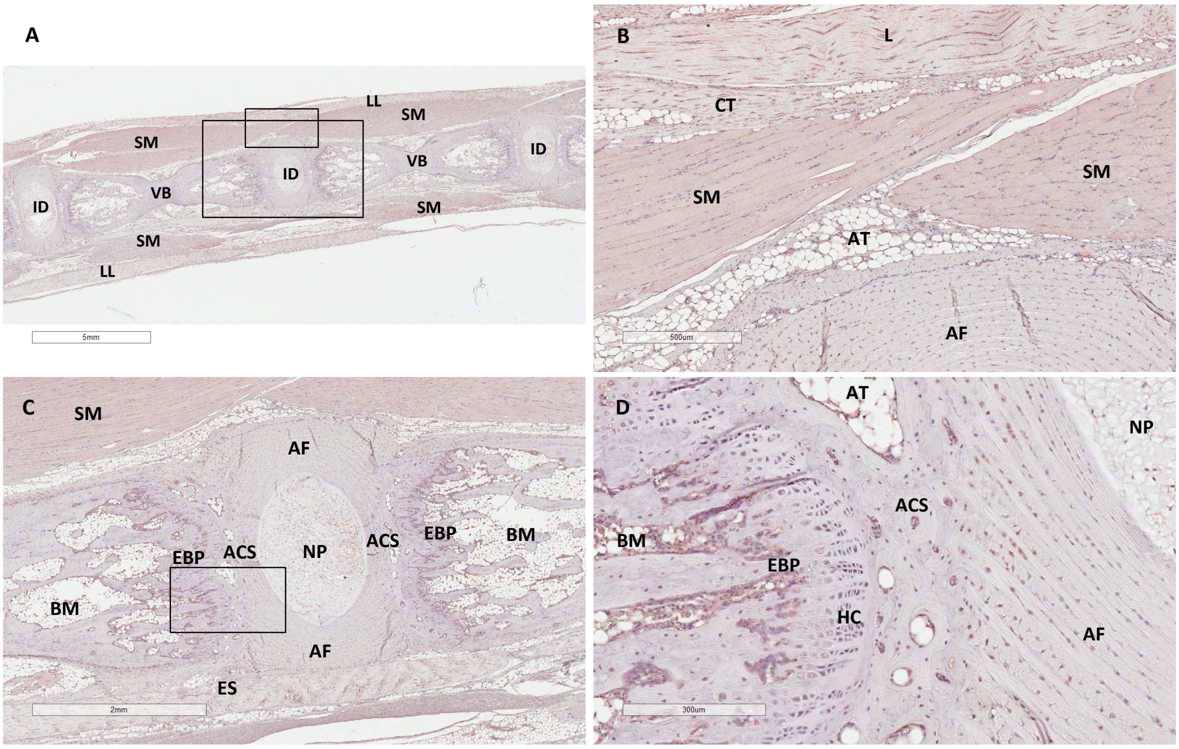

Skeletal muscles (SM) present in the axial joints can be attached directly to the vertebral bone or alternatively muscle can be inserted into tendons or ligaments, which are attached to bone (enthesis). In the first case, the area of muscle and bone attachment is extensive (Figure 5.20, B and C), while in the second case the attachment area is more localized. In both cases attachment occurs in periosteum, which consists of irregular, dense connective tissue with some areas of adipose tissue (Figure 5.20 B, AT). Although, enthesitis is a common clinical feature of ankylosing spondylitis, it is unclear whether inflammation is restricted to the enthesis and/or occurs in sites of direct muscle attachment. In enthesitis inflammatory cells infiltrate tissue via blood vessels (BV) in the connective tissue (CT). Therefore it is possible that inflammation may occur in the periosteum without the involvement of ligaments and tendons.

Immunohistochemical analysis of the axial joints obtained from B27 TG^2 male rats 1 week after *M.tb* injection demonstrated significant HD6 staining on cells present in annulus fibrosus, fibroblast-like cells in neighboring connective tissue and chondrocyte-like cells in the vertebral end bone plate (Figure 5.21 B, C, D). Importantly, my data suggested that intensity of HD6 staining was significantly higher in junctions of annulus fibrosus, connective tissue adjacent to enthesis or direct muscle-bone attachment sites and vertebral end bone plate (Figure 5.21, B, C, D).

Notably, similar HD6 staining was also observed in the age-matched non-immunized B27 TG^2 animals (data not shown).

Furthermore, the numbers of HD6-reactive molecules were increased in joints from the older rats (8 and 9 weeks) irrespective of *M.tb* injection. Firstly, HD6 staining was detected on chondrocyte-like cells in the vertebral end bone plate (EBP) and articular cartilage sites (ACS), fibroblast-like cells in a connective tissue (CT) and on cells present in annulus fibrosus (AF) (8 weeks no *M.tb* – Figure 5.22; 8 weeks *M.tb* – Figure 5.23; 9 weeks no *M.tb* – Figure 5.24; 9 weeks *M.tb* – Figure 5.25). Secondly, a higher number of bone remodeling sites (BRS) with HD6-positive cells can be seen in articular cartilage separating vertebral end bone plate from intervertebral disc (Figure 5.24, B and C, BRS). In the bone marrow (BM) both mononuclear and multinucleated cells also expressed HD6-reactive molecules (Figure 5.23 and 5.25, BM, EBP). Thirdly, I observed cells migrating between concentric collagen fibers in annulus fibrosus in the older rats (8 and 9 weeks) (Figure 5.20 and 5.21). Moreover, in 9 weeks old animals increased number of migratory cells was found specifically in areas of annulus fibrosus neighboring highly vascularized connective tissue (Figure 5.25, C and D). Interestingly, the vascularized connective tissue, which appears to develop with disease progression, generally contained more HD6-reactive molecules with a higher intensity of staining.

Finally I also observed HD6-positive proliferating fibroblast-like and/or macrophage-like cells in the periosteum, but only in tissue section from B27 TG^2 rats 2 weeks post *M.tb* injection (Figure 5.23 A and B). These potentially inflammatory cells seem to invade and migrate into a vertebral bone matrix at a distant location from the intervertebral disc zone. Importantly, I did not observe similar infiltrates in untreated animals.

Figure 5.21 HD6-reactive molecules are abundantly expressed on resident cells in non-inflamed (score 0) axial joints obtained from B27 TG^2 male rats +/- 1 week after *M.tb* injection. A) Intervertebral disc and vertebral bone end plate zone with observed HD6 staining. B) HD6 staining on chondrocyte-like cells in vertebral end bone plate and on fibroblast like cells in connective tissue. C and D) cells staining in annulus fibrosus, enthesis and vertebral end bone plate. ACS – articular cartilage sites; AF – annulus fibrosus; AT – adipose tissue; BM – bone marrow; CT – connective tissue; EBP – end bone plate; ES – enthesal site; NP – nucleus pulposus; SM – skeletal muscle. Immunohistochemistry staining using Ready-to-Use AEC+ High Sensitivity Substrate Chromogen Kit. Red – HD6 antibody staining. Blue – Mayer's Hematoxilin staining.

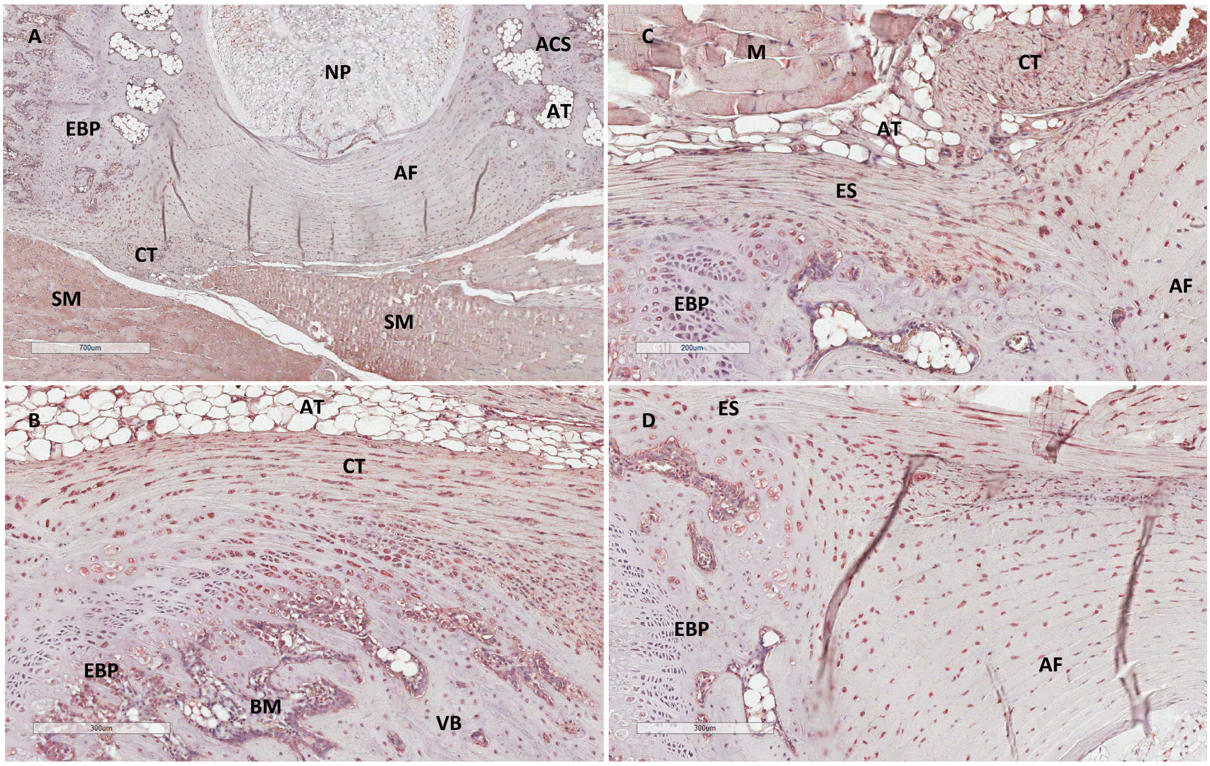

Figure 5.22 The intensity of HD6 staining and number of HD6-positive cells increase with animal age and the progression of the disease. Tail tissue sections obtained from 8 weeks old B27 TG[2] male rats A) HD6 positive cells present in the junction between intervertebral disc and vertebral end bone plate. B) Higher resolution (10X) of the large black square area from picture A representing HD6 staining on chondrocyte-like cells in vertebral end bone plate, bone marrow cells and fibroblast like cells in connective tissue. C) Higher resolution (10X) of a small black square aarea in picture A, showing high intensity HD6-staining on cells in annulus fibrosus. D) Staining on cells in bone remodeling sites and on fibroblast-like cells in connective tissue. AF – annulus fibrosus; AT – adipose tissue; BM – bone marrow; BRS – bone remodeling sites; BV – blood vessels; CT – connective tissue; EBP – end bone plate; Immunohistochemistry staining using Ready-to-Use AEC+ High Sensitivity Substrate Chromogen Kit. Red – HD6 antibody staining. Blue – Mayer's Hematoxilin staining.

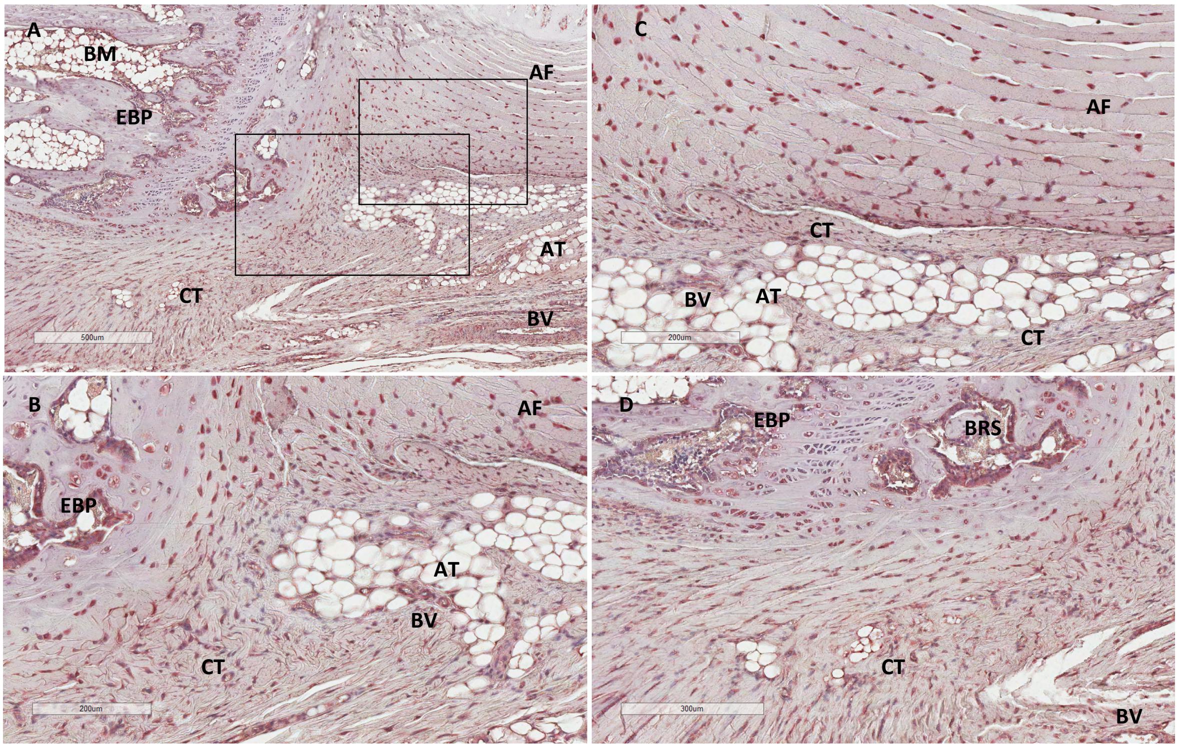

Figure 5.23 HD6 staining on cells in B27 TG[2] rats 2 weeks after *M.tb* injection. High intensity staining on fibroblast-like and macrophage-like cells in the site where connective tissue invade vertebral bone. A) Connective tissue with fibroblast-like and macrophage-like cells infiltrating vertebral bone matrix (10X). B) Higher resolution (20X) of picture A. C) HD6 staining in the enthesal site. D) High intensity HD6 staining on chondrocytes in articual cartilage site and on cells in bone marrow. ACS – articular cartilage sites; AF – annulus fibrosus; AT – adipose tissue; B – bone matrix; BM – bone marrow; CT – connective tissue; EBP – end bone plate; ES – enthesal site; NP – nucleus pulposus; SM – skeletal muscle. Immunohistochemistry staining using Ready-to-Use AEC+ High Sensitivity Substrate Chromogen Kit. Red – HD6 antibody staining. Blue – Mayer's Hematoxilin staining.

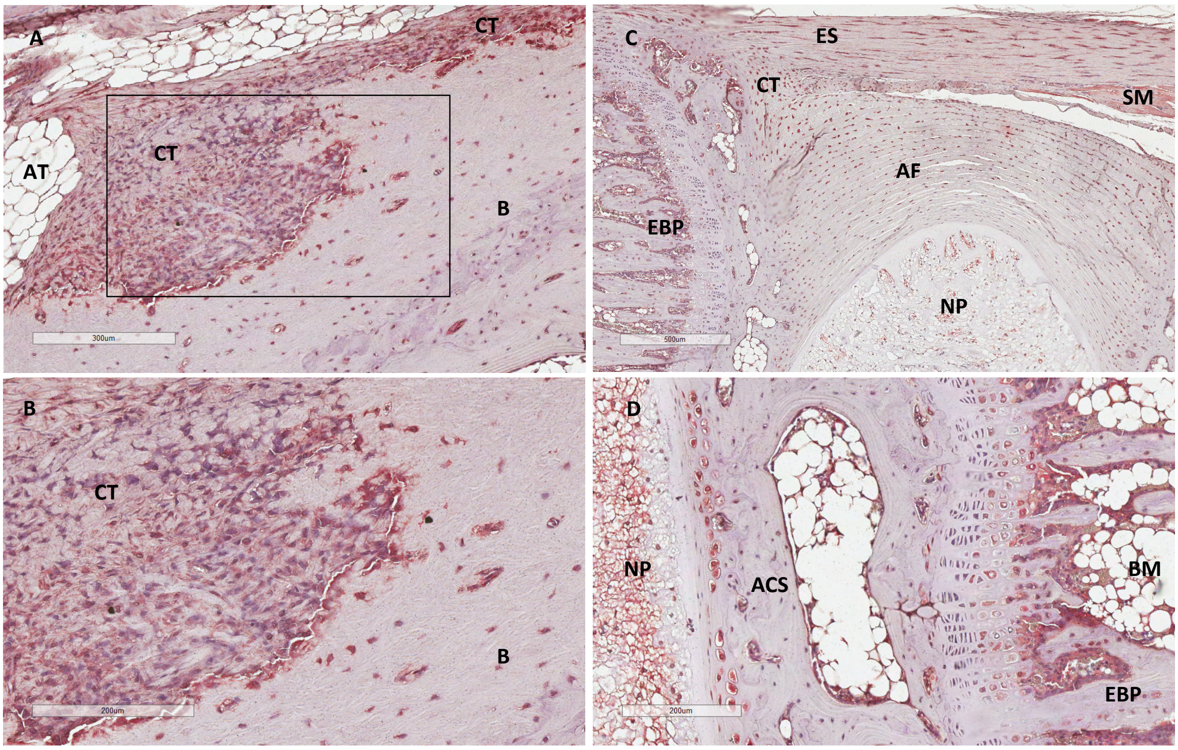

Figure 5.24 Abundant HD6 expression at the junction of vertebral end bone plate, connective tissue and intervertebral discs in axial joints from untreated B27 TG[2] rats 3 weeks p.i. Pictures A) and C) (8X) Pictures B) and D) 20X resolution. A) HD6 staining on fibroblast-like cells in a connective tissue and chondrocyte-like cells in a vertebral end bone plate. B) Higher resolution of black square area in picture A. C) and D) Staining in bone remodeling sites present in articular cartilage sites neighboring annulus fibrosus and connective tissue. ACS – articular cartilage sites; AF – annulus fibrosus; B – bone matrix; BM – bone marrow; CT – connective tissue; EBP – end bone plate. Immunohistochemistry staining using Ready-to-Use AEC+ High Sensitivity Substrate Chromogen Kit. Red – HD6 antibody staining. Blue – Mayer's Hematoxilin staining.

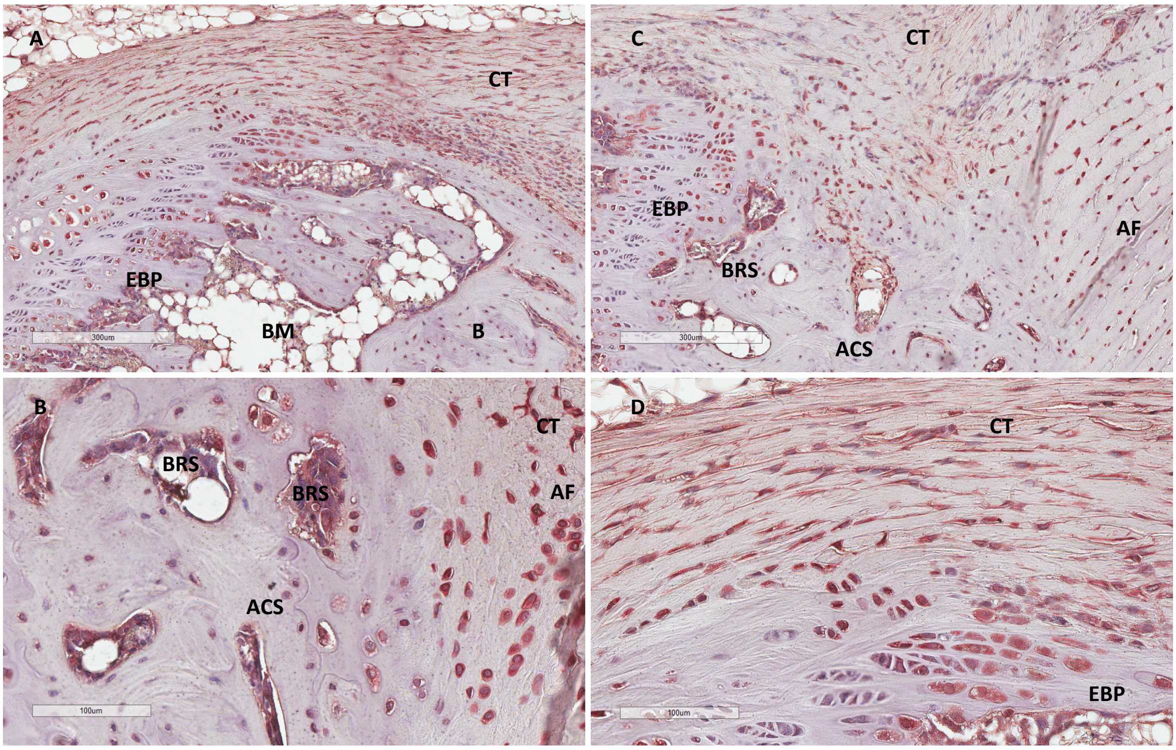

Figure 5.25 High intensity of HD6 staining and number of HD6+ve cells in annulus fibrosus, connective tissue and vertebral end bone plate in ankle joints from 9 weeks old animals 3 weeks after *M.tb* injection. A) HD6 staining in enthesal site neighboring intervertebral disc space. B) Higher resolution of large black square area from picture A. C) Higher resolution of small black square area from picture A demonstrating high intensity and number of cells staining with HD6 in annulus fibrosus. D) 40X resolution of the black square area from picture C representing HD6 positive cells migrating between colagenous fibres in annulus fibrosus. ACS – articular cartilage sites; AF – annulus fibrosus; AT – adipose tissue; BV – blood vessels; BRS – bone remodeling sites; CT – connective tissue; EBP – end bone plate; ES – enthesal site; NP – nucleus pulposus. Immunohistochemistry staining using Ready-to-Use AEC+ High Sensitivity Substrate Chromogen Kit. Red – HD6 antibody staining. Blue – Mayer's Hematoxilin staining.

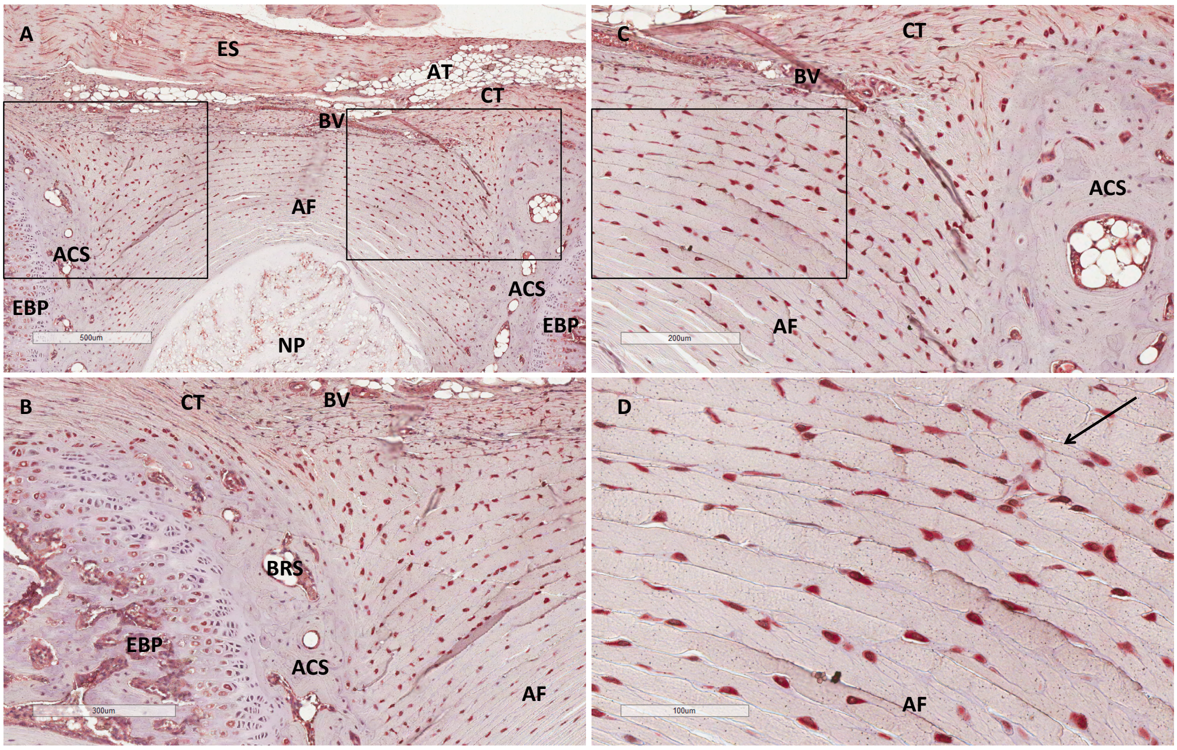

Summary Chapter 5.5

My immunohistochemistry analysis of HD6 staining in spinal joints obtained from young B27 TG[2] male rats before and after *M.tb* treatment demonstrated that, HD6-reactive molecules are expressed by resident cells in the very early stages of the disease (clinical inflammation score 0). HD6 staining was observed in three main cell types: chondrocyte-like cells in vertebral end bone plates and articular cartilage sites separating vertebrae from intervertebral disc; fibroblast-like cells in connective tissue; and cells found in between collagen fibers in the annulus fibrosus. The intensity of staining and number of HD6-positive cells increased with animal age. Furthermore, more abundant vascularization in connective tissue surrounding intervertebral disc space in the older animals was associated with increased number of HD6-positive cells within annulus fibrosus. Interestingly, my data suggested that HD6 staining also increased with age in bone marrow cells in the axial vertebral bones. Importantly, similar HD6 staining patterns were observed in both immunized animals and age-matched control untreated animals, what may indicate that expression of these potentially pathogenic forms of HLA-B27 on resident cells in rat joints is independent from innate immune stimulation at the early stages of the disease.

5.6 Discussion Chapter Five

The susceptibility to disease in the B27 TG[1] animals strictly depends on the B27 copy number, and consequently mRNA and protein levels of HLA-B27 (J D Taurog, Maika, Simmons, Breban, & Hammer, 1993). Bird *et. al.* demonstrated the presence of surface homodimers in LN cells, splenocytes and DCs isolated from 33-3 TG rats using cell surface iodination and immunoprecipitation with HC10 mAb. Nevertheless, so far only one study has used the novel HD6 antibody to investigate cell surface expression of NC-B27 molecules in B27 TG[1] rats. McHugh *et al.* showed that the levels of both HD6 and HC10 staining in B27 TG[1] rats strictly depends on the animal age, with only low levels detected under 3 months of age (McHugh et al., 2014). Notably, HD6 and HC10 staining was abundant on splenic mononuclear cells, but granulocytes expressed few if any NC-B27 molecules. As yet, nobody has studied the expression of cell surface HD6- and HC10-reactive molecules in the B27 TG[2] model. The additional hβ2m in the B27 TG[2] rats was found to decrease intracellular B27 misfolding, UPR responses and inhibited colitis, however significantly increased the prevalence of arthritis and spondylitis. One interpretation of these findings is that cell surface expression of HLA-B27 molecules contribute to the development of joint inflammation. Yet, it is still unclear whether disease onset in B27 TG[2] rats is a consequence of the surface expression of properly folded HLA-B27 molecules, or rather could be driven by the cell surface NC-B27 molecules, perhaps arising from the ME1-reactive species. Hence, investigation of the expression patterns of HD6- and HC10-reactive molecules in PBMCs, secondary lymphoid organs (SLOs) and joints of the B27 TG[2] animals could give us a clue about the key players and potential mechanisms of the inflammatory responses in SpA.

Notably, in agreement with the previous study using B27 TG[1] rat splenocytes, I have demonstrated that HD6-reactive molecules are specifically expressed in B27 TG[2] rat SPLCs and LNs, as I did not detect HD6 staining in control B7 TG and WT cells. Importantly, HD6 staining was increased on LN cells compared with SPLCs and $CD8^+$ cells expressed higher levels of NC-B27 molecules compared with $CD4^+$ cells. However, the overall expression of MHCI molecules in the $CD8^+$ population was elevated. All susceptible to arthritis B27 TG animals carry a high copy number of HLA-B27, hence the presence of HD6-reactive molecules on $CD4^+$ and $CD8^+$ cells could be simply a consequence of its overexpression.

A previous study by May *et al*. suggested that gut inflammation in 21-4H and 33-3 rats is independent of the classical $CD8\alpha^+$ T cells (May et al., 2003). However, they identified several other CD8α-expressing cell types, such as $CD161^+$ NK cells, $CD11bc^+$ macrophages/dendritic cells and $CD8\alpha^+\beta^-$ T cells, which were not permanently depleted by the administration of anti-CD8α mAb. Furthermore, only PBMC-derived cells were analyzed in this study, hence there is a possibility that CD8α-expressing cells were still present in SLOs and tissues even after depletion. Additionally, a $CD4^+CD8\alpha^+CD161^+CD11bc^+CD172a^+$ monocyte population was expanded in diseased B27 TG animals. Moreover, the majority of animals developed gut inflammation, however the presence of arthritis varied significantly among different study groups (20-52%). Finally, the onset of arthritis was significantly delayed compared with gastrointestinal manifestations and animals were sacrificed as soon as the clinical symptoms in joints have appeared. Thus the severity of arthritis was not comprehensively evaluated. In conclusion, based on this study we can not exclude the possibility that some of the $CD8\alpha^+$ cell populations could play a role in the development of arthritis.

Importantly, in the B27 TG^2 rat model the majority of male rats spontaneously develop peripheral and axial joint manifestations without IBD-like symptoms. Therefore the mechanisms driving pro-inflammatory immune responses in the B27 TG^2 rats can be different to those in the 21-4H and 33-3 B27 TG animals. As previously mentioned, it has been shown that MHCI molecules can bind to the KIRs and LILRs immune receptors both in the *tans* and *cis* conformations. These interactions are important for the development of CD8$^+$ T cell-dependent self-tolerance and maintenance of the balance between the steady and active state of the immune system. Hence, cell surface NC-B27 species expressed by CD8α^+ cells may bind immune receptors with the strong affinity in *cis*. Consequently the *trans* binding could be inhibited, resulting in the impaired self-tolerance. Alternatively, these cells may represent CD8α^+ NK cells or activated monocytes/dendritic cells. NC-B27 molecules expressed by NK cells could similarly affect the balance between tolerance and activation, whereas their expression on APCs could be involved in the induction of Th17 immune responses. It has been demonstrated that CD4$^+$ KIR3DL2$^+$ T cells are expanded in AS patient PBMCs and that their interaction with B27-expressing B cell lines can lead to the induction of Th17 differentiation and IL-17 production. Hence, there is a possibility that HD6-reactive molecules present at the surface of APCs, could activate pro-inflammatory Th17 responses in B27 TG^2 rats via binding to PIRs, a rodent homologs of human KIRs.

Subsequent study using CD8$^{-/-}$ B27 TG rats, generated by the induction of heritable CD8α-null mutation, suggested that arthritis and spondylitis arise in the absence of any functional CD8$^+$ T cells (Joel D. Taurog et al., 2009). However, the severity and prevalence to axial and peripheral joint manifestations were not described consistently, as rats from different study groups were observed for dissimilar time periods. Additionally, due to the relatively small number of animals per group, the data were unable to confirm statistical relevance of their obervations. As they suggested, it is unlikely that classical $CD8^+$ T cells may initiate joint inflammation, nevertheless they may play a role in the amplification and/or acceleration of the disease. Furthermore, it is possible that other cell populations which will normally express CD8α, such as monocytes and suppressor cells, can differentiate and function even in its absence. Thus, although they presented strong evidence against the arthritogenic peptide theory and showed that joint inflammation can occur independently of classical $CD8^+$ T cell, they did not exclude the potential role of other cell populations in the induction of the disease.

I also demonstrated that HD6 staining was present in spleens and LNs on cells characterized by $CD45R^{low}$ expression, but not on $CD11b^+$ cells (found only in LNs and absent in spleens). The population expressing CD45R could represent B cells. CD11b is mainly found on macrophages, however could also be expressed by dendritic cells and granulocytes. Expression of HD6-reactive molecules on $CD45R^+$ cells, possibly an antigen presenting B cell population, could lead to the activation and expansion of Th17 cells. Notably, the splenic and LN cells that I studied hadn't been freshly isolated, thus there is a possibility that some cell populations (e.g. activated APCs) did not survive the transport procedure.

My results showed that the ratio of HC10:ME1 was elevated in LNs isolated from B27 TG^2 animals compared with splenic cells and control B7 TG rats. Notably, the absolute levels of HC10 staining were higher in cells isolated from B7 TG animals compared with B27 TG^2 rats. Nevertheless, B7 TG rats expressed significantly higher levels of ME1-reactive molecules, resulting in the lower ratio of HC10:ME1 compared with B27 TG^2. I cannot exclude the possibility that observed increased intensity of ME1 staining in the B7 TG animals was simply due to the higher affinity of ME1 antibody for HLA-B7 molecules compared with HLA-B27. Nevertheless, elevated levels of NC-B27 at the surface of B27 TG^2 LN cells suggest that these molecules may play a role in disease pathogenesis. Notably, LNs are an important organ of our immune system, where the circulating T cells can interact with APCs, be activated and consequently migrate to the site of inflammation. Therefore, there is a possibility that pathogenic Th17 cells driving joint inflammation may be primarily induced in LNs upon the interaction of NC-B27 with immune receptors.

In the subsequent experiments, I have investigated whether *M.tb* injection could affect the surface expression of potentially pathogenic, NC-B27 molecules in SPLCs, LNs, PBMCs and axial skeleton joints obtained from B27 TG^2 rats. The *M.tb* injection of B27 TG^2 rats, described for the first time by van Duivenvoorde *et al.*, aimed to accelerate and synchronize the disease onset (van Duivenvoorde et al., 2011, ACR published abstract). Notably, in this novel, accelerated model of the disease (B27 TG^3), male rats developed arthritis and spondylitis 2-3 weeks post *M.tb* (30μg)/IFA injection, over 40 days before the disease onset in the spontaneous B27 TG^2 model. However, importantly higher doses of *M.tb* (60μg and 90 μg)/IFA can also induce SpA-like symptoms in B27 TG females and male B7 TG animals. In the original AIA rat model injection of high doses of *M.tb* (1mg)/IFA (or CFA) trigger the development of arthritis in disease-prone rat lines, such as Lewis and DA. Rats susceptible to arthritis can develop delayed type hypersensitivity (DTH) driven by $CD4^+$ T cells recognizing a peptide epitope derived from bacterial heat-shock protein 65 (HSP65) (Hogervorst et al., 1991; van Eden et al., 1989). HSP65 is highly homologous to the rat HSP60, which has ~96% homology to the human HSP60. Thus it has been proposed that $CD4^+$ T cells activated with the HSP 180-188 epitope can cross-react with self-antigens present in the cartilage. Notably, immunization with low doses of HSP65 or HSP65 peptides before the injection of adjuvant can prevent the development of AIA in disease-prone rats (Haque et al., 1996). Further studies demonstrated reduced number of $CD4^+CD25^+FoxP3^+$ regulatory T cells post *M.tb* injection in susceptible to arthritis rat strains (Bai et al., 2014). Moreover, abundant number of "arthritogenic" leukocytes (monocytes, macrophages and T cells), and to a lesser extent neutrophils, migrated into synovium before the appearance of clinical symptoms (Bush, Walker, Lee, & Kirkham, 2001; Pearson & Wood, 1963). Bush *et al*. demonstrated transient increase in the IL-17, TNFα, IL-2 and IFNγ production in inguinal LNs 6-9 days post *M.tb* injection. In synovial tissue IL-17, IL-2 and IFNγ were transiently induced on day 13 p.i., whereas TNFα and TGFβ were increased between day 13-18 for prolonged times. Moreover, the removal of LNs before the fifth day post *M.tb*. injection in Lewis rats resulted in the complete inhibition of the disease development (Newbould, 1964). It has been suggested that in the AIA-resistant rat strains splenic suppressor T cells can reduce the susceptibility to arthritis (Piatier-Tonneau, Mach, Kahan, & Delbarre, 1982). Furthermore, the production of high levels of pro-inflammatory Th1 cytokines, IFNγ and TNFα, directly post *M.tb* injection in the resistant WKY rats reduced the severity of arthritis (E. E. Y. Kim, Chi, Bouziane, Gaur, & Moudgil, 2008; E. Y. Kim, Chi, Rajaiah, & Moudgil, 2008). Thus, it has been proposed that the amount and timing of the production of Th1 pro-inflammatory cytokines post *M.tb* treatment have a significant influence on the outcome of the bacterial challenge. Additionally, differences in the frequencies and activity of $CD8^+$ suppressor T cells and Th2 cytokine producing cells in the susceptible vs resistant rat strains are key decision factors in the induction of arthritis (Bersani-Amado, Barbuto, & Jancar, 1990; Fournié et al., 2001; Piatier-Tonneau et al., 1982). In summary, these findings suggest that disease-prone rats cannot properly resolve immune responses after *M.tb* injection due to the imbalance between tolerance and activation of immune responses and aberrant timing and amounts of produced Th1 and Th2 cytokines. Notably, the B27 TG^2 rats are particularly susceptible to arthritis, as they can develop peripheral and axial joint manifestations spontaneously even in the absence of adjuvant challenge. Hence, there is a possibility that HLA-B27 expression may play a role in the impaired immune tolerance and activation.

While, I here propose that cell surface expression of HLA-B27 is a key factor predisposing B27 TG^2 rats to arthritis and spondylitis, whether the acceleration of the disease in B27 TG^2 rats post *M.tb* treatment requires the expression of NC-B27 molecules remains unclear. My data do not convincingly support this hypothesis and suggest that although B27 TG^2 rats require cell surface NC-B27 for the development of the disease, *M.tb* injection do not significantly affect the expression of HD6- and HC10-reactive molecules. Thus, I propose that *M.tb* can accelerate the progression of the SpA-like symptoms via activation of cell populations infiltrating axial and peripheral joints. Subsequently, direct interaction of activated, infiltrating mononuclear cells with HD6- and/or HC10-reactive molecules present in joints may drive immune responses. However, whether mononuclear cell populations infiltrating joints in the spontaneous model are activated independently of B27 or require its expression need further investigation.

Interestingly, my results from experiments using *M.tb* (30µg) treated B27 TG^2 rats suggested that bacterial challenge could increase cell surface expression levels of both HD6- and HC10-reactive molecules in $CD161^{high}$ cells found in LNs at 2 weeks post treatment. CD161 molecules are mainly expressed by NK cells, but importantly can also be found in subsets of T cells, dendritic cells and activated monocytes. The presence of HD6-reactive molecules at the surface of NK cells could possibly impair the balance between tolerance and activation of the immune responses. The interaction of KIRs (rats PIRs) expressed at the surface of NK cells with self-antigens presented in the MHCI context by APCs is crucial for the development and maintenance of self-tolerance. Notably, KIRs can be also expressed by activated or memory $CD8^+$ T cells present in circulation, however the role of these molecules in the induction of self-tolerance is unclear (Mingari et al., 1996; Speiser et al., 1999). Interestingly, KIRs can be downregulated on $CD8^+$ T upon binding to their ligands expressed at the surface of APCs in the absence of the TCR stimulation (Huard & Karlsson, 2000). Hence, it has been proposed that KIR expression in $CD8^+$ T cells depends on the quantity and quality of antigens present in the circulation, as well as the strength of the TCR signal. Thus, surface NC-B27 on both NK cells and $CD8^+$ T cells may interact with KIRs in *cis* and affect their interactions in *trans*, resulting in the impaired self-tolerance and hypersensitiveness.

Alternatively, the $CD161^{high}$ population may represent APCs, such as activated monocytes or dendritic cells. As mentioned before, May *at al.* observed expansion of the $CD4^+CD8\alpha^+CD161^+CD11bc^+CD172a^+$ monocyte population in diseased rats in the original B27 TG^1 model suggesting the importance of these cells in SpA pathogenesis. HD6-reactive NC-B27 molecules expressed on APCs could be ligands for PIRs (KIRs).

Furthermore, a small increase in the HD6 and HC10 staining was detected in PBMC-derived $CD45R^+/MHCII^+$ cell population at 2 weeks p.i. The $CD45R^+/MHCII^+$ population could represent B cells and, as mentioned previously, I propose that NC-B27 present at the surface of these circulating APCs may bind to PIRs and activate Th17 responses. NC-B27 were up regulated at the surface of B cells specifically in circulation, hence it is possible that these cells migrated to/from the affected joints.

Notably, I observed an age dependent changes in both NC-B27 and ME1 staining irrespective of *M.tb* treatment. HD6 staining on $CD8^+$ T cells and $CD45^+/MHCII^+$ cells was increased in PBMCs and spleen, and at the same time decreased in LNs at 9 weeks of age compared with 8 weeks. Additionally, HD6-reactive molecules were expressed at elevated levels on PBMC-derived $CD161^{high}$ cells from older rats. Interestingly, HC10 levels were increased in the circulation only on $CD8^+$ and $CD45R^+/MHCII^+$ cells, but not on $CD161^{high}$ cells. Furthermore, I did not observe any changes in HC10 staining on splenic and LN cells. Notably, ME1 staining in these cell populations remained unchanged or decreased, thus there was an increase in the cell surface ratios of NC-B27:ME1 in older rats. Increased HC10:ME1 ratios at the cell surface in older animals could influence the balance of *cis* and *trans* interactions between NC-B27 and its receptors. As a consequence the equilibrium between immune tolerance and activation could be affected leading to the induction of immune responses.

In conclusion, the increase in HD6 and/or HC10 staining in $CD161^{high}$, $CD45R^+/MHCII^+$ cell populations indicate their potential role in driving the immune responses possibly by earlier proposed mechanisms. Moreover, expression of HD6 at the surface of $CD8^+$ cells could also contribute to the severity of disease. As mentioned before decreased number and/or activity of $CD8^+$ suppressor/regulatory T cells in susceptible to arthritis rat strains result in the development of inflammatory responses in joints. Hence, there is a possibility that the expression of NC-B27 by $CD8^+$ T cells may inhibit development/activity of suppressor/regulatory T cells.

Additionally, in this chapter I have used IHC to investigate the expression of HD6- and HC10-reactive molecules in the B27 TG rats. Importantly, my IHC data show that HD6-reactive molecules are abundantly expressed on resident cells in B27 TG^2 rat axial joints before the onset of the clinical symptoms and irrespective of *M.tb* injection. However, their expression seemed to increase with animal age, perhaps explaining why very young animals do not develop arthritis. HD6 staining was found on chondrocyte-like, fibroblast-like and osteoclast-like cells at the junction of: annulus fibrosus, connective tissue and the vertebral end plate. Van Duivenvoorde *et al.* have previously demonstrated that axial joint inflammation in B27 TG^2 rats starts at this areas with the infiltration of mononuclear pro-inflammatory leukocytes. Hence, I hypothesize that resident joint cells expressing NC-B27 could interact with infiltrating cells and induce the differentiation of pro-inflammatory Th17 cells. Notably, *M.tb* injection could accelerate the onset of joint inflammation by the activation of cells in the circulation and/or SLOs and by accelerating/enhancing their migration to the peripheral and axial joints. These infiltrating cells could be activated irrespective of HLA-B27 expression, or via previously proposed mechanisms dependent on the cell surface NC-B27 molecules. Notably, HC10 staining, unlike HD6, was additionally abundant on infiltrating pro-inflammatory mononuclear leukocytes. Thus there is a possibility that surface HC10-reactive FHCs could be increased due to the cell activation and turnover (apoptosis), or by a hypoxic environment caused by a high number of cells present locally in the site of infiltration. However, HC10-reactive forms can also be found in healthy cells, thus the classical MHCI FHCs present in cell infiltrates may not necessarily be pathogenic. Moreover, the HC10 mAb can also bind HD6-reactive molecules hence there is a possibility that these forms of NC-B27 are particularly involved in the joint pathogenesis. Importantly, due to the tissue preparation, fixation and IHC staining procedure I cannot conclude for certain whether observed NC-B27 staining is located to the cell surface or in intracellular compartments. Furthermore, the fixation of paraffin embedded tissue sections with PFA removes ME1 and W6/32 antibodies epitopes, so I did not observe any staining with these mAbs. Therefore, there is a possibility that it could also alter HD6 and HC10 staining.

Interestingly, I observed HD6 and HC10 staining in tissue sections derived from diseased B7 TG rats. As mentioned before, higher doses of *M.tb* (60µg and 90 µg) can also trigger peripheral and axial manifestations in B7 TG rats (van Duivenvoorde et al., 2011, ACR published abstract). Hence, there is a possibility that similar mechanisms drive joint inflammation in both B27 TG and B7 TG animals. Notably, overexpression of HLA-B7 in rats could lead to the unnatural behavior of this human MHCI molecule. I cannot exclude the possibility that human HLA-B7 molecules in B7 TG rats can also misfold and form NC-B7 species (e.g. recognized by HD6 antibody) after *M.tb* stimulation. Indeed my data suggest that this could be the case. Importantly HLA-B27 and HLA-B7 MHCI molecules have a high homology, therefore overexpression of HLA-B7 in TG rats may lead to SpA onset similar to the one observed in HLA-B27 animals. Moreover, there are some publications reporting that individuals expressing both HLA-B27 and HLA-B7 have a higher prevalence of Juvenile Spondyloarthropathies (Harjaček, Margetić, Martinez, & Grubić, 2008). Interestingly, recent studies reported that HLA-B*07 is strongly associated with HLA-B27-negative SpA in a Western Indian population (Parasannanavar, Rajadhyaksha, & Ghosh, 2014).

In conclusion, I hypothesize that the expression of potentially pathogenic HD6- and HC10-reactive molecules on resident cells in joints is necessary for driving joint pathogenesis. Furthermore, I propose that the expression of NC-B27 in the circulation and SLOs may lead to activation of inflammatory cells, infiltrating axial and peripheral joints, via both APC-immune receptor interactions and impaired balance between immune tolerance and activation. Thus, HLA-B27 expression in B27 TG^2 rats may contribute to the disease pathogenesis by several independent mechanisms.

Chapter Six: DPhil project concluding remarks and future perspectives

The main aim of my DPhil project was to investigate cell surface expression of NC-B27 forms, primarily in AS patients and in the B27 TG[2] rat model of SpA. I used both existing reagents and the novel HD6 monoclonal antibody. The B27 FHC homodimer theory suggests that NC-B27 can not only be present intracellularly, but also at the cell surface, and that their interaction with immune receptors such as KIRs may induce Th17-driven immune responses in SpA patients. Although, this theory has been studied for the past two decades using the HC10 mAb, only recently a novel HD6 mAb was generated against $B27_2$ using a phage display library (Payeli et al., 2012). Notably, Payeli *et al.* demonstrated HD6 staining in B27-expressing cell lines and on a $CD14^+$ population from AS patient PBMCs and SFMCs. In a second study HD6-reactive molecules were detected at significant levels in B27+ve cell lines and B27 TG[1] rat splenocytes, however were absent in AS patient PBMCs in a standard conditions, but could be induced by brief acid treatment (McHugh et al., 2014). The contradicting results from experiments using AS patient PBMC observed in these studies could be due to the use of different blocking reagents in the flow cytometry staining procedure and/or different batches of the HD6 antibody. Alternatively, there is a possibility that the expression of HD6-reactive molecules in the circulation may vary amongst B27+ve AS patients and may be dependent of disease activity and treatment regimen. Therefore, further investigation of the expression patterns of HD6-reactive molecules in SpA patient- and B27 TG rat-derived cells and tissues could help us to answer the question whether these NC-B27 forms are commonly and abundantly expressed or are rather restricted to specific cell types and/or sites, such as joints, in the disease setting. Nevertheless, B27-expressing cell lines are important tools in studying the unusual nature of HLA-B27 molecules using HD6 mAb.

Investigation of cell surface NC-B27 molecules by confocal microscopy could give us a clue about their segregation at the cell surface that could be related with their role as immune receptor ligands. However, as yet nobody has investigated cell surface segregation patterns of HD6- and HC10-reactive molecules in B27-expressing cell lines by confocal microscopy. My confocal microscopy experiments using HeLa-B27 and 221-B27 cell lines suggested that HD6- and HC10-reactive molecules have a tendency to cluster at the cell surface. My results suggested that NC-B27 molecules, unlike properly folded MHCI, are not evenly distributed at the cell surface, but rather accumulate in organized cell membrane domains, possibly in lipid rafts. However, whether observed clustering is a consequence of their potential role as immune receptor ligands (e.g. KIR3DL2) or simply occurs due to the FHC endocytosis and recycling events requires further investigation. Importantly, cluster formation of HD6-reactive molecules and HC10-reactive molecules in AS patient-derived moDCs was not specific to B27+ve individuals and furthermore ME1- and W6/32-reactive molecules could also form clusters. Notably, HD6 staining could be detected in AS moDCs only after acid treatment. The presence of aggregates was more striking with antibodies recognizing non-classical MHCI species, perhaps due to the lower intensity of staining.

Secondly, I have confirmed the presence of cell surface HD6-reactive B27 molecules in B27+ve 220 and 221 LCLs by IP and subsequent western blot using HC10 mAb. The majority of which was immunoprecipitated in a HMW form, suggesting the presence of $B27_2$ or other B27 complexes. Notably, in agreement with previous findings, my IP results demonstrated that HLA-B27 molecules could reach cell surface even in the absence of TPN. Furthermore, surface levels of NC-B27 HMW species were increased in 220-B27 cells (lacking functional TPN) suggesting higher levels of misfolded MHCI molecules at cell surface. Interestingly, 220-B27 TPN and 221-B27 cells with functional TPN and an increased amount of properly folded B27 molecules at the surface were more sensitive to acid treatment. Consequently more NC-B27 molecules were immunoprecipitated from these cells following acid treatment compared with 220-B27 cells. Thus, although HLA-B27 molecules are relatively independent of TPN, my results suggest that MHCI complexes reaching cell surface in the absence of TPN are less stable. On the other hand, my findings also suggest that in B27+ve cell lines with functional TPN, acid-induced NC-B27 species originate from properly folded B27 molecules present at the cell surface.

My findings using B27+ve BCLs and AS patient monocyte- and PBMC-derived cells suggested that only few if any surface HD6-reactive molecules could be detected in B27+ve cells with the natural expression of HLA class I alleles. This was in agreement with previous observations by McHugh *et al.*, although distinct from Payeli *et. al*. Moreover, I did not observe HD6-reactive molecules on B27+ve AS patient moDCs and macrophages even after stimulation with LPS and/or pro-inflammatory cytokines. But importantly, HD6 staining was induced specifically on B27+ve AS moDCs following acid treatment. Furthermore, my preliminary data suggested that low levels of HD6 staining could be detected on B27+ve AS patient monocyte- and PBMC-derived multinucleated OCs. Since activated OCs present *in vivo* in bone can dissolve bone by the local secretion of acid, there is a possibility that

HD6 staining observed in blood-derived OCs in cell culture was due to the exposure to the local acidic environment. Furthermore, although pH measurement in joints is problematic, it has been shown that, unlike in healthy tissues, pH in inflamed joints is acidic. Hence, HD6-reactive molecules may be induced specifically and locally in AS patient joints, but may be absent in the circulation under normal circumstances. My preliminary data using SpA knee synovial tissue sections demonstrated the presence of HD6+ve cells in the intimal lining and sublining layer specifically in B27+ve, and not in B27-ve patients. Thus, these results further support the hypothesis that potentially pathogenic NC-B27 could be induced on specific cell types and/or by specific environmental factors, rather than abundantly expressed in the circulation. These could also explain that although the majority of nucleated cells can express HLA-B27 molecules in B27+ve individuals, HD6-reactive molecules could be found specifically in the site of inflammation. However, due to the restricted availability of human tissue samples at different stages of the disease, we cannot conclude whether HD6 staining observed in synovial tissue is the cause of joint inflammation or rather a side effect of local pro-inflammatory responses (local hypoxic or acidic environment, cell exhaustion, apoptosis). Future investigation of both paraffin-embedded and frozen tissue sections derived from SpA and control RA and/or OA synovial tissues could help to confirm the specificity of HD6 staining, and identify potentially pathogenic, HD6+ve resident and infiltrating cell populations.

Importantly, HC10:W6/32 ratios were consistently increased on B27+ve AS patient-derived moDCs compared with B27-ve healthy controls. This finding further emphasize the potential role of NC-B27 molecules in the disease pathogenesis. However, since I did not detect any HD6 staining on AS moDCs, even in the presence of relatively high HC10 staining, my results may suggest that NC-B27 forms recognized by HC10 mAb, rather than HD6, may play a key role in the disease pathogenesis. Abundantly expressed HC10-reactive molecules probably represent a heterogeneous population, where some aberrant B27 FHC forms, similar to HD6-reactive molecules, may be pathogenic, whereas others may be neutral and simply be a result of ongoing inflammation. Further investigation of the HC10-expression in cells and tissues derived not only from SpA, but also control diseased RA and/or OA patients could provide an answer as to whether the observed increased levels of cell surface HC10 reactive molecules are characteristic for B27+ve individuals or can be also observed in other inflammatory conditions.

Due to the delayed disease diagnosis in SpA patients combined with the highly restricted availability of tissue samples, studying disease mechanisms *in situ* is extremely challenging. Therefore, the use of the B27 TG^2 rat model, which resembles human SpA, could give us a better insight into the disease pathology and help us to understand why individuals carrying HLA-B27 gene are predisposed to SpA. In my flow cytometry experiments using young B27 TG^2 rats I have identified several cell populations in the circulation and SLOs with increased levels of HD6-reactive molecules. These cell types could be potentially key players in the disease pathogenesis. My results demonstrated that HD6 staining could be detected not only in APCs, but also in $CD161^+$ and $CD8^+$ cells, potentially NK and T cells. Thus, these findings could suggest that cell surface expression of HD6-reactive molecules may contribute to the disease pathogenesis not only via the induction of immune responses, but may also impair immune tolerance. As mentioned previously it has been demonstrated that $CD4^+$ $KIR3DL2^+$ cells derived from AS patient blood can be expanded and induce the production of IL-17 after incubation with B27-expressing cell lines (Bowness and Ridley et al., 2011). Moreover, it has been proposed that observed activation of Th17 responses is driven by direct interaction of KIRs and NC-B27 molecules, as co-culture in the presence of KIR3DL2 specific DX-31 mAb inhibited cell proliferation and activation. Notably, the B27 TG^2 animals that I studied did not present yet clinical manifestations in their peripheral and axial joints. Hence cell populations with increased cell surface levels of HD6-reactive molecules could be key players in the early stages of the disease, before the onset of inflammatory responses in joints. This could also explain the lack of HD6-reactive molecules on AS patient blood-derived cells, both whole PBMCs and monocyte-derived cell populations. There is a possibility that potentially pathogenic NC-B27 in AS patients could be expressed on circulating cells only at certain stages of the disease and in the presence of a specific mixture of environmental and genetic factors. Notably, B27 TG^2 rats carry high gene copy numbers of both HLA-B27 and hβ2m and express relatively high levels of cell surface B27 molecules. Hence, I cannot exclude possibility that observed HD6 staining in B27 TG^2 rats in the circulation and SLOs, and the lack of staining in samples obtained from AS patients is due to the overexpression of HLA-B27 in rats. Interestingly, B27 TG^2 rats have increased hβ2m gene copy number compared with B27 TG^1 animals, and they develop axial and peripheral manifestations without any symptoms of gastrointestinal inflammation. In the presence of additional hβ2m UPR, ER stress responses and intracellular misfolding is significantly decreased in B27 TG^2 animals compared with B27 TG^1, whereas cell surface levels of properly folded HLA-B27 molecules are increased. These findings suggest that cell surface expression of HLA-B27, but not UPR and ER stress responses, are crucial for the development of peripheral and axial joint inflammation. As proposed here and by Bird *et al*. (Bird et al., 2003) cell surface NC-B27 species arise from properly folded HLA-B27 molecules, hence B27 TG^2 rats the higher susceptibility to arthritis may be caused by increased expression of NC-B27 molecules.

Importantly, I have demonstrated the expression of HD6-reactive molecules on resident cells (chondrocytes, fibroblasts, osteoclasts) in axial and peripheral joints obtained from B27 TG^2 rats before the disease onset. Notably, their expression increased with animal age, suggesting that these cells may be essential for driving bone and synovial tissue pathology in B27 TG^2 rat model, and possibly in human SpA. Notably, similar to my observations using human SpA-derived synovial tissues, in B27 TG^2 ankles and tails HC10 staining was also abundant on infiltrating mononuclear cells, with few if any HD6+ve cells. Therefore, the interaction of HD6-reactive molecules expressed by joint resident cells with activated in the periphery PIR^+ lymphocytes (or $KIR3DL2^+$ in human) could drive the sequence of pro-inflammatory events *in situ* and be responsible for joint pathology. Future experiments using B27 TG^2 rats could help us to identify the phenotype of joint resident cells expressing HD6-reactive molecules, as well as cell populations infiltrating joint tissues, which could possibly directly interact with NC-B27 species *in situ*. Notably, further investigation of the expression patterns of NC-B27 molecules in the circulation and SLOs in younger animals and at later time points, with more severe inflammation, could give us additional insight in the sequence of inflammatory events in circulation, SLOs and peripheral and axial joints.

Taken together, the work described in this thesis contributes to our knowledge about cell and tissue types expressing potentially pathogenic HD6- and HC10-reactive NC-B27 molecules. Notably, I have demonstrated that in AS patients HD6 staining is rather restricted to specific cell types *in vitro* (osteoclasts) and possibly determined by environmental factors and tissue types *in vivo* (synovial and joint tissue). Furthermore, based on my data using B27 TG^2 rats, APC populations with increased levels of HD6-reactive molecules found at different time points in the circulation and SLOs, such as B cells ($CD45R^+/MHCII^+$), activated monocytes, macrophages or dendritic cells ($CD11bc^+$) cells, may also play an important role in the disease pathogenesis. However, such cells may be absent in AS patient PBMCs obtained at late stages of the disease and with active inflammation. Interestingly, my data also suggest that $CD161^+$ and $CD8^+$ cells found in PBMCs and SLOs in B27 TG^2 animals expressed elevated levels of surface NC-B27 molecules. Hence, these cell populations may additionally contribute to the development of SpA by impaired control of immune tolerance. Thus, the work presented Importantly, given that NC-B27 seemed to be expressed only under certain conditions, in restricted cell types and joint tissues, HD6 mAb could possibly be used in the future as a therapeutic agent in SpA patients. Blocking NC-B27 molecules with HD6 mAb directly in B27+ve SpA joints, ideally at early stages of the disease, could potentially inhibit the progression of pro-inflammatory immune responses and bone and synovial tissue pathology. Lastly, future investigation of the NC-B27 interactions with immune receptors and their role in immune tolerance could open new possibilities for treatment targets.

Figure 6.1 HLA-B27 in health and disease - proposed mechanisms of action and the role of NC-B27 in SpA pathogenesis

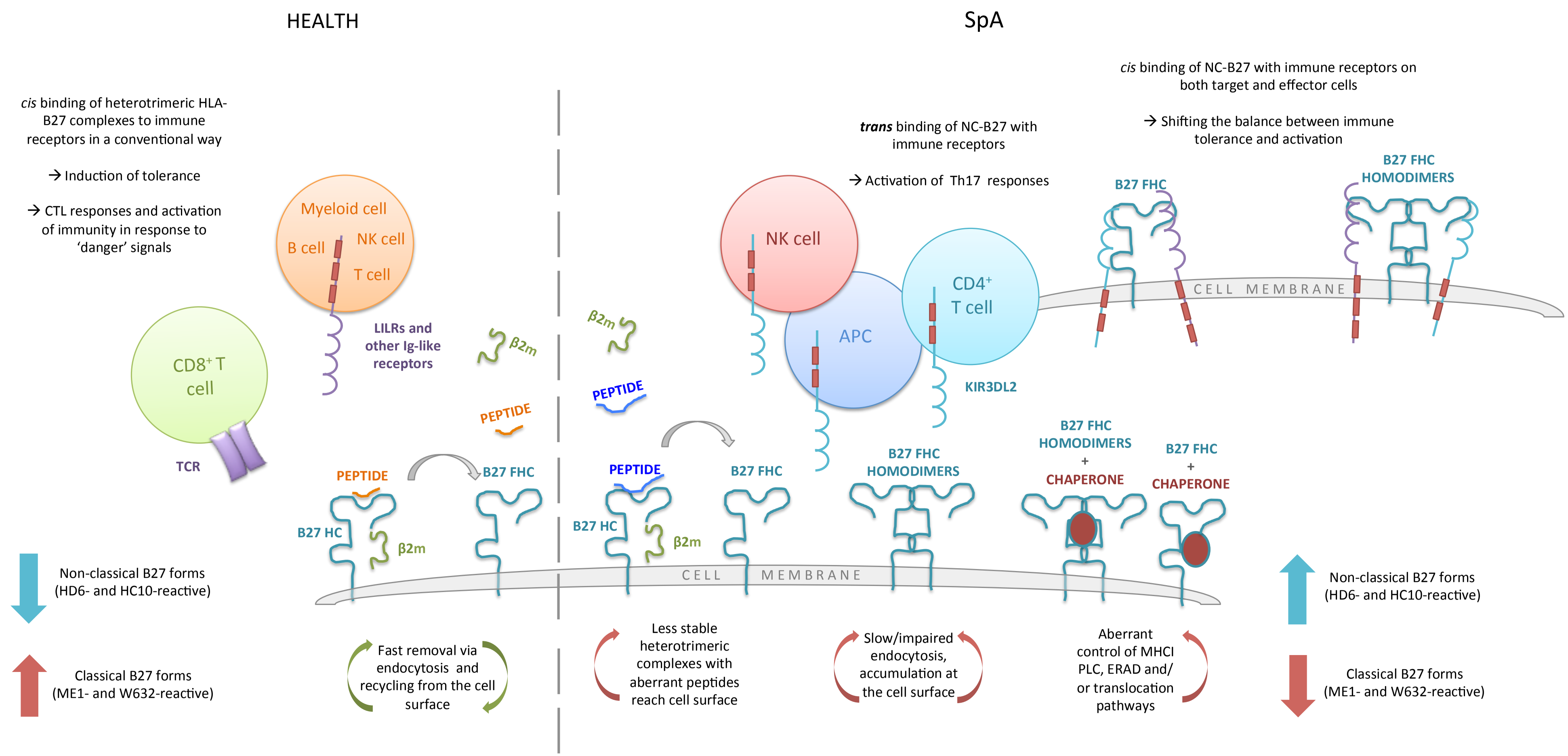

References

Agrawal, N., and Brown, M., 2014. 'Genetic Associations and Functional Characterization of M1 Aminopeptidases and Immune-Mediated Diseases.' *Genes and immunity*:1–7.

Aguirre, J. Ignacio et al. 2007. 'Effects of Basic Fibroblast Growth Factor and a Prostaglandin E2 Receptor Subtype 4 Agonist on Osteoblastogenesis and Adipogenesis in Aged Ovariectomized Rats.' *Journal of bone and mineral research : the official journal of the American Society for Bone and Mineral Research* 22:877–88.

Allen, R. L., C. A. O'Callaghan, A. J. McMichael, and P. Bowness. 1999. 'Cutting Edge: HLA-B27 Can Form a Novel Beta 2-Microglobulin-Free Heavy Chain Homodimer Structure.' *Journal of immunology (Baltimore, Md.: 1950)* 162:5045–48.

Altfeld, Marcus et al. 2006. 'HLA Alleles Associated with Delayed Progression to AIDS Contribute Strongly to the Initial CD8+ T Cell Response against HIV-1.' *PLoS Medicine* 3(10):1851–64.

Alvarez-Navarro, Carlos et al. 2013. 'Novel HLA-B27-Restricted Epitopes from Chlamydia Trachomatis Generated upon Endogenous Processing of Bacterial Proteins Suggest a Role of Molecular Mimicry in Reactive Arthritis.' *Journal of Biological Chemistry* 288:25810–25.

Ambarus, Carmen a, Troy Noordenbos, Maria J. H. de Hair, Paul P. Tak, and Dominique L. P. Baeten. 2012. 'Intimal Lining Layer Macrophages but Not Synovial Sublining Macrophages Display an IL-10 Polarized-like Phenotype in Chronic Synovitis.' *Arthritis research & therapy* 14(2):R74.

Ammaranond, Palanee et al. 2011. 'HIV Immune Escape at an Immunodominant Epitope in HLA-B*27-Positive Individuals Predicts Viral Load Outcome.' *Journal of immunology (Baltimore, Md.: 1950)* 186(1):479–88.

Amor, B. et al. 1995. 'Are Classification Criteria for Spondylarthropathy Useful as Diagnostic Criteria?' *Revue du rhumatisme (English ed.)* 62:10–15.

Amor, B., M. Dougados, and M. Mijiyawa. 1990. *Criteria of the Classification of Spondylarthropathies*.

Andersen, M. H., D. Schrama, P. Thor Straten, and J. C. Becker. 2006. 'Cytotoxic T Cells.' *J Invest Dermatol* 126(April 2005):32–41.

Appel, Heiner et al. 2006. 'Immunohistochemical Analysis of Hip Arthritis in Ankylosing Spondylitis: Evaluation of the Bone-Cartilage Interface and Subchondral Bone Marrow.' *Arthritis and rheumatism* 54(6):1805–13.

Appel, Heiner et al. 2009. 'Altered Skeletal Expression of Sclerostin and Its Link to Radiographic Progression in Ankylosing Spondylitis.' *Arthritis and Rheumatism* 60:3257–62.

Appel, Heiner et al. 2011. 'Analysis of IL-17+ Cells in Facet Joints of Patients with Spondyloarthritis Suggests That the Innate Immune Pathway Might Be of Greater Relevance than the Th17-Mediated Adaptive Immune Response.' *Arthritis Research & Therapy* 13(3):R95.

Appenzeller-Herzog, Christian, and Hans-Peter Hauri. 2006. 'The ER-Golgi Intermediate Compartment (ERGIC): In Search of Its Identity and Function.' *Journal of cell science* 119:2173–83.

Armaka, Maria et al. 2008. 'Mesenchymal Cell Targeting by TNF as a Common Pathogenic Principle in Chronic Inflammatory Joint and Intestinal Diseases.' *The Journal of experimental medicine* 205:331–37.

Atagunduz, Pamir et al. 2005. 'HLA-B27-Restricted CD8+ T Cell Response to Cartilage-Derived Self Peptides in Ankylosing Spondylitis.' *Arthritis and Rheumatism* 52:892–901.

Baas, E. J. et al. 1992. 'Peptide-Induced Stabilization and Intracellular Localization of Empty HLA Class I Complexes.' *The Journal of experimental medicine* 176(1):147–56.

Baeten, Dominique et al. 2013. 'Anti-Interleukin-17A Monoclonal Antibody Secukinumab in Treatment of Ankylosing Spondylitis: A Randomised, Double-Blind, Placebo-Controlled Trial.' *The Lancet* 382:1705–13.

Baeten, Dominique, and Filip Keyser. 2004. 'The Histopathology of Spondyloarthropathy.' *Current Molecular Medicine* 4(1):1–12.

Bai, Shu-tong et al. 2014. 'Ethyl Acetate Extract from Celastrus Aculeatus Merr . Suppresses Synovial Inflammation in Adjuvant Arthritis Rats through Apoptosis Induction of CD4 + CD25 + FOXP3 + T Cells.' 2014.

Bang, So Young et al. 2011. 'Genetic Studies of Ankylosing Spondylitis in Koreans Confirm Associations with ERAP1 and 2p15 Reported in White Patients.' *Journal of Rheumatology* 38:322–24.

Baraliakos, Xenofon et al. 2005. 'Clinical Response to Discontinuation of Anti-TNF Therapy in Patients with Ankylosing Spondylitis after 3 Years of Continuous Treatment with Infliximab.' *Arthritis research & therapy* 7:R439–44.

Bárdos, T. et al. 2005. 'A Longitudinal Study on an Autoimmune Murine Model of Ankylosing Spondylitis.' *Annals of the rheumatic diseases* 64:981–87.

Barkham, Nick et al. 2009. 'Clinical and Imaging Efficacy of Infliximab in HLA-B27-Positive Patients with Magnetic Resonance Imaging-Determined Early Sacroiliitis.' *Arthritis and Rheumatism* 60:946–54.

Barrow, Alexander David, and John Trowsdale. 2006. 'You Say ITAM and I Say ITIM, Let's Call the Whole Thing off: The Ambiguity of Immunoreceptor Signalling.' *European Journal of Immunology* 36(7):1646–53.

Bartelds, G. M. et al. 2010. 'Anti-Infliximab and Anti-Adalimumab Antibodies in Relation to Response to Adalimumab in Infliximab Switchers and Anti-Tumour Necrosis Factor Naive Patients: A Cohort Study.' *Annals of the rheumatic diseases* 69:817–21.

Bautista-caro, María Beĺn et al. 2013. 'Decreased Th17 and Th1 Cells in the Peripheral Blood of Patients with Early Non-Radiographic Axial Spondyloarthritis: A Marker of Disease Activity in HLA-B27+ Patients.' *Rheumatology (United Kingdom)* 52(2):352–62.

Benjamin, R., and P. Parham. 1990. 'Guilt by Association: HLA-B27 and Ankylosing Spondylitis.' *Immunology today* 11:137–42.

Bernasconi, Riccardo, and Maurizio Molinari. 2011. 'ERAD and ERAD Tuning: Disposal of Cargo and of ERAD Regulators from the Mammalian ER.' *Current Opinion in Cell Biology* 23:176–83.

Bersani-Amado, C. A., J. A. Barbuto, and S. Jancar. 1990. 'Comparative Study of Adjuvant Induced Arthritis in Susceptible and Resistant Strains of Rats. II. Effect of Oral Administration of BCG and PPD.' *J Rheumatol* 17(6):738–42.

Bird, Lucy A. et al. 2003. 'Lymphoblastoid Cells Express HLA-B27 Homodimers Both Intracellularly and at the Cell Surface Following Endosomal Recycling.' *European Journal of Immunology* 33:748–59.

Blackwell, Katherine A., Lawrence G. Raisz, and Carol C. Pilbeam. 2010. 'Prostaglandins in Bone: Bad Cop, Good Cop?' *Trends in Endocrinology and Metabolism* 21:294–301.

Van den Bosch, F. et al. 2000. 'Effects of a Loading Dose Regimen of Three Infusions of Chimeric Monoclonal Antibody to Tumour Necrosis Factor Alpha (infliximab) in Spondyloarthropathy: An Open Pilot Study.' *Annals of the rheumatic diseases* 59:428–33.

Bowness and Ridley et al. 2011. 'Th17 Cells Expressing KIR3DL2 + and Responsive to HLA-B27 Homodimers Are Increased in Ankylosing Spondylitis: Commentary.' *The Journal of Immunology* 186:2672–80.

Bowness, Paul, Nathan Zaccai, Lucy Bird, and E. Yvonne Jones. 1999. 'HLA-B27 and Disease Pathogenesis : New Structural and Functional Insights.' (October):1–10.

Braem, Kirsten, and Rik J. Lories. 2012. 'Insights into the Pathophysiology of Ankylosing Spondylitis: Contributions from Animal Models.' *Joint, bone, spine : revue du rhumatisme* 79(3):243–48.

Brandt, J. et al. 2000. *Successful Treatment of Active Ankylosing Spondylitis with the Anti-Tumor Necrosis Factor Alpha Monoclonal Antibody Infliximab*.

Brandt, J. et al. 2003. 'Six-Month Results of a Double-Blind, Placebo-Controlled Trial of Etanercept Treatment in Patients with Active Ankylosing Spondylitis.' *Arthritis and Rheumatism* 48:1667–75.

Brandt, J. et al. 2005. 'Long-Term Efficacy and Safety of Etanercept after Readministration in Patients with Active Ankylosing Spondylitis.' *Rheumatology* 44:342–48.

Braun, J., R. Van Den Berg, et al. 2012. '2010 Update of the ASAS/EULAR Recommendations for the Management of Ankylosing Spondylitis.' *Revmatologiia (Bulgaria)* 20:5–16.

Braun, J., X. Baraliakos, et al. 2012. 'Golimumab Reduces Spinal Inflammation in Ankylosing Spondylitis: MRI Results of the Randomised, Placebo- Controlled GO-RAISE Study.' *Annals of the Rheumatic Diseases* 71:878–84.

Braun, Juergen, Uta Kiltz, Frank Heldmann, and Xenofon Baraliakos. 2015. 'Emerging Drugs for the Treatment of Axial and Peripheral Spondyloarthritis.' 1–14.

Braun, Jürgen et al. 1998. 'Prevalence of Spondylarthropathies in HLA-B27 Positive and Negative Blood Donors.' *Arthritis and Rheumatism* 41(January):58–67.

Braun, Jürgen et al. 2013. 'The Effect of Two Golimumab Doses on Radiographic Progression in Ankylosing Spondylitis: Results through 4 Years of the GO-RAISE Trial.' *Annals of the rheumatic diseases* 73:1–7.

Breban, M. et al. 1996. 'T Cells, but Not Thymic Exposure to HLA-B27, Are Required for the Inflammatory Disease of HLA-B27 Transgenic Rats.' *Journal of immunology (Baltimore, Md.: 1950)* 156:794–803.

Breban, M. et al. 2002. *Efficacy of Infliximab in Refractory Ankylosing Spondylitis: Results of a Six-Month Open-Label Study*.

Breban, M., Hammer, R. E., Richardson, J. A. & Taurog, J. D. 1993. 'Transfer of the Inflammatory Disease of HLA-B27.' *J Exp Med* 178(November):1607–16.

Brennan, F. M., D. Chantry, A. Jackson, R. Maini, and M. Feldmann. 1989. 'Inhibitory Effect of TNF Alpha Antibodies on Synovial Cell Interleukin-1 Production in Rheumatoid Arthritis.' *Lancet* 2:244–47.

Brochhausen, Christoph, Pia Neuland, C. James Kirkpatrick, Rolf M. Nüsing, and Günter Klaus. 2006. 'Cyclooxygenases and Prostaglandin E2 Receptors in Growth Plate Chondrocytes in Vitro and in Situ--Prostaglandin E2 Dependent Proliferation of Growth Plate Chondrocytes.' *Arthritis research & therapy* 8(3):R78.

Brode, Sven, and Paul A. MacAry. 2004. 'Cross-Presentation: Dendritic Cells and Macrophages Bite off More than They Can Chew!' *Immunology* 112(3):345–51.

Burness, Celeste B., and Emma D. Deeks. 2012. 'Adalimumab: In Non-Radiographic Axial Spondyloarthritis.' *Drugs* 72:2385–95.

Bush, K. a., J. S. Walker, C. S. Lee, and B. W. Kirkham. 2001. 'Cytokine Expression and Synovial Pathology in the Initiation and Spontaneous Resolution Phases of Adjuvant Arthritis: Interleukin-17 Expression Is Upregulated in Early Disease.' *Clinical and Experimental Immunology* 123(3):487–95.

Cain, Joel a., Nestor Solis, and Stuart J. Cordwell. 2014. 'Beyond Gene Expression: The Impact of Protein Post-Translational Modifications in Bacteria.' *Journal of Proteomics* 97:265–86.

Calin, A. et al. 1994. 'A New Approach to Defining Functional Ability in Ankylosing Spondylitis: The Development of the Bath Ankylosing Spondylitis Functional Index.' *Journal of Rheumatology* 21:2281–85.

Campbell, Elaine C., Franziska Fettke, Smita Bhat, Kenneth D. Morley, and Simon J. Powis. 2011. 'Expression of MHC Class I Dimers and ERAP1 in an Ankylosing Spondylitis Patient Cohort.' *Immunology* 133(3):379–85.

Campbell, Kerry S., and Amanda K. Purdy. 2011. 'Structure/function of Human Killer Cell Immunoglobulin-like Receptors: Lessons from Polymorphisms, Evolution, Crystal Structures and Mutations.' *Immunology* 132:315–25.

Campbell, S. M., S. M. Crowe, and J. Mak. 2001. 'Lipid Rafts and HIV-1: From Viral Entry to Assembly of Progeny Virions.' Pp. 217–27 in *Journal of Clinical Virology*, vol. 22.

Cao, Stewart Siyan, and Randal J. Kaufman. 2012. 'Unfolded Protein Response.' *Current biology : CB* 22(16):R622–26.

Carrington, Mary, and Stephen J. O'Brien. 2003. 'The Influence of HLA Genotype on AIDS.' *Annual review of medicine* 54:535–51.

Carter, Gemma C. et al. 2009. 'HIV Entry in Macrophages Is Dependent on Intact Lipid Rafts.' *Virology* 386(1):192–202.

Cauli, a. et al. 2002. 'Increased Level of HLA-B27 Expression in Ankylosing Spondylitis Patients Compared with Healthy HLA-B27-Positive Subjects: A Possible Further Susceptibility Factor for the Development of Disease.' *Rheumatology* 41(12):1375–79.

Cauli, Alberto et al. 2013. 'The Arthritis-Associated HLA-B*27:05 Allele Forms More Cell Surface B27 Dimer and Free Heavy Chain Ligands for KIR3DL2 than HLA-B*27:09.' *Rheumatology (Oxford, England)* 52(11):1952–62.

Chan, a. T., S. D. Kollnberger, L. R. Wedderburn, and P. Bowness. 2005. 'Expansion and Enhanced Survival of Natural Killer Cells Expressing the Killer Immunoglobulin-like Receptor KIR3DL2 in Spondylarthritis.' *Arthritis and Rheumatism* 52(11):3586–95.

Cheatum, D. E. 1975. 'Ankylosing Spondylitis and Related Diseases: Significance of HL-A W27 Histocompatibility Antigen.' *Comprehensive therapy* 1:20–25.

Chen, C., X. Zhang, J. Li, and Y. Wang. 2012. 'Associations of IL-23R Polymorphisms with Ankylosing Spondylitis in East Asian Population : A New Case – Control Study and a Meta-Analysis.' 126–30.

Chen, J., and C. Liu. 2005. 'Sulfasalazine for Ankylosing Spondylitis.' *Cochrane database of systematic reviews (Online)* (11):CD004800.

Chen, J., C. Liu, and J. Lin. 2006. 'Methotrexate for Ankylosing Spondylitis.' *Cochrane database of systematic reviews (Online)* (2):CD004524.

Chen, Liye et al. 2014. 'Critical Role of Endoplasmic Reticulum Aminopeptidase 1 in Determining the Length and Sequence of Peptides Bound and Presented by HLA-B27.' *Arthritis & rheumatology (Hoboken, N.J.)* 66(2):284–94.

Chen, W. S. et al. 2009. 'Immunohistological Features of Hip Synovitis in Ankylosing Spondylitis with Advanced Hip Involvement.' *Scandinavian journal of rheumatology* 38(2):154–55.

Chiu, Yahui Grace et al. 2010. 'CD16 (FcRgammaIII) as a Potential Marker of Osteoclast Precursors in Psoriatic Arthritis.' *Arthritis research & therapy* 12(1):R14.

Colbert, Robert a, Monica L. DeLay, Gerlinde Layh-Schmitt, and Dawn P. Sowders. 2009. 'HLA-B27 Misfolding and Spondyloarthropathies.' *Advances in experimental medicine and biology* 649(March):217–34.

Colonna, M., H. Nakajima, F. Navarro, and M. López-Botet. 1999. 'A Novel Family of Ig-like Receptors for HLA Class I Molecules That Modulate Function of Lymphoid and Myeloid Cells.' *Journal of leukocyte biology* 66(3):375–81.

Committee for Medicinal Products for Human Use. 2012. *Positive Recommendations of Committee for Medicinal Products for Human Use (CHMP) on Extensions of Therapeutic Indications for Humira (Adalimumab).*

Copeman, James, Naveen Bangia, James C. Cross, and Peter Cresswell. 1998. 'Elucidation of the Genetic Basis of the Antigen Presentation Defects in the Mutant Cell Line . 220 Reveals Polymorphism and Alternative Splicing of the Tapasin Gene.' 3783–91.

Cragnolini, Juan J., and José a López de Castro. 2008. 'Identification of Endogenously Presented Peptides from Chlamydia Trachomatis with High Homology to Human Proteins and to a Natural Self-Ligand of HLA-B27.' *Molecular & cellular proteomics : MCP* 7:170–80.

Cryan, Lorna M., and Michael S. Rogers. 2011. 'Targeting the Anthrax Receptors, TEM-8 and CMG-2, for Anti- Angiogenic Therapy.' *Front Biosci* 16:1574–88.

Dagfinrud, H., and K. Hagen. 2001. 'Physiotherapy Interventions for Ankylosing Spondylitis.' *Cochrane database of systematic reviews (Online)* CD002822.

Dahan, Arik, and Gordon L. Amidon. 2009. 'Small Intestinal Efflux Mediated by MRP2 and BCRP Shifts Sulfasalazine Intestinal Permeability from High to Low, Enabling Its Colonic Targeting.' *American journal of physiology. Gastrointestinal and liver physiology* 297(2):G371–77.

Davidson, Stuart I. et al. 2009. 'Association of ERAP1, but Not IL23R, with Ankylosing Spondylitis in a Han Chinese Population.' *Arthritis and Rheumatism* 60(11):3263–68.

Davidson, Stuart I. et al. 2013. 'High-Throughput Sequencing of IL23R Reveals a Low-Frequency, Nonsynonymous Single-Nucleotide Polymorphism That Is Associated with Ankylosing Spondylitis in a Han Chinese Population.' *Arthritis and Rheumatism* 65(7):1747–52.

DeLay, Monica L. et al. 2009. 'HLA-B27 Misfolding and the Unfolded Protein Response Augment Interleukin-23 Production and Are Associated with Th17 Activation in Transgenic Rats.' *Arthritis and Rheumatism* 60:2633–43.

Dennis, Megan K. et al. 2012. 'NIH Public Access.' 127(7):358–66.

Desreumaux, P., and S. Ghosh. 2006. 'Review Article: Mode of Action and Delivery of 5-Aminosalicylic Acid - New Evidence.' *Alimentary pharmacology & therapeutics* 24 Suppl 1:2–9.

Deuquet, Julie, Ekkehart Lausch, Andrea Superti-Furga, and F. Gisou van der Goot. 2011. 'The Dark Sides of Capillary Morphogenesis Gene 2.' *The EMBO Journal* 31:3–13.

Devlin, R. D. et al. 2003. 'Skeletal Overexpression of Noggin Results in Osteopenia and Reduced Bone Formation.' *Endocrinology* 144:1972–78.

Dhaenens, Maarten et al. 2009. 'Dendritic Cells from Spondylarthritis-Prone HLA-B27-Transgenic Rats Display Altered Cytoskeletal Dynamics, Class II Major Histocompatibility Complex Expression, and Viability.' *Arthritis and Rheumatism* 60(9):2622–32.

Diana, Julien et al. 2013. 'Crosstalk between Neutrophils, B-1a Cells and Plasmacytoid Dendritic Cells Initiates Autoimmune Diabetes.' *Nature medicine* 19:65–73.

Díaz-Peña, R., A. López-Vázquez, and C. López-Larrea. 2012. 'Old and New HLA Associations with Ankylosing Spondylitis.' *Tissue Antigens* 80(3):205–13.

Dietrich, J. W., J. M. Goodson, and L. G. Raisz. 1975. 'Stimulation of Bone Resorption by Various Prostaglandins in Organ Culture.' *Prostaglandins* 10(2):231–40.

Ding, Jin et al. 2015. 'Increased Expression of Human Leucocyte Antigen Class I Free Heavy Chains on Monocytes of Patients with Spondyloarthritis and Cells Transfected with HLA-B27.' *International Journal of Immunogenetics* 42(1):4–10.

Dong, Gang, Pamela a Wearsch, David R. Peaper, Peter Cresswell, and Karin M. Reinisch. 2009. 'Insights into MHC Class I Peptide Loading from the Structure of the Tapasin-ERp57 Thiol Oxidoreductase Heterodimer.' *Immunity* 30(1):21–32.

Dong, Hongtao, Qiuming Li, Ying Zhang, Wei Tan, and Z. Jiang. 2013. 'IL23R Gene Confers Susceptibility to Ankylosing Spondylitis Concomitant with Uveitis in a Han Chinese Population.' *PLoS ONE* 8(6):2–6.

Dong, W. et al. 2008. 'Upregulation of 78-kDa Glucose-Regulated Protein in Macrophages in Peripheral Joints of Active Ankylosing Spondylitis.' *Scandinavian journal of rheumatology* 37(6):427–34.

Dougados, M. et al. 1991. *The European Spondylarthropathy Study Group Preliminary Criteria for the Classification of Spondylarthropathy*.

Dresch, Christiane, Yann Leverrier, Jacqueline Marvel, and Ken Shortman. 2012. 'Development of Antigen Cross-Presentation Capacity in Dendritic Cells.' *Trends in Immunology* 33:381–88.

Duan, Fei, and Pramod K. Srivastava. 2012. 'An Invariant Road to Cross-Presentation.' *Nature Immunology* 13(3):207–8.

Duerr, R. H. et al. 2006. 'A Genome-Wide Association Study Identifies IL23R as an Inflammatory Bowel Disease Gene.' *Science* 314:1461–63.

Van Duivenvoorde, Leonie M. et al. 2012. 'Relationship between Inflammation, Bone Destruction, and Osteoproliferation in the HLA-B27/human β2 -Microglobulin-Transgenic Rat Model of Spondylarthritis.' *Arthritis and rheumatism* 64(10):3210–19.

Van Eden, W. et al. 1989. 'The Mycobacterial 65 kD Heat-Shock Protein and Autoimmune Arthritis.' *Rheumatology international* 9(3-5):187–91.

Eirís, Noemí et al. 2014. 'Genetic Variation at IL12B, IL23R and IL23A Is Associated with Psoriasis Severity, Psoriatic Arthritis and Type 2 Diabetes Mellitus.' *Journal of Dermatological Science* 75(3):167–72.

Ellis, S. A., C. Taylor, and A. McMichael. 1982. 'Recognition of HLA-B27 and Related Antigen by a Monoclonal Antibody.' *Human Immunology* 5(1):49–59.

Evnouchidou, Irini, Mirjana Weimershaus, Loredana Saveanu, and Peter van Endert. 2014. 'ERAP1-ERAP2 Dimerization Increases Peptide-Trimming Efficiency.' *Journal of immunology (Baltimore, Md.: 1950)*.

Feldmann, M., F. M. Brennan, and R. N. Maini. 1996. 'Role of Cytokines in Rheumatoid Arthritis.' *Annu Rev Immunol* 14:397–440.

Feldtkeller, Ernst, and Jon Erlendsson. 2008. 'Definition of Disease Duration in Ankylosing Spondylitis.' *Rheumatology International* 28(7):693–96.

Feltkamp, T. E. W., M. A. Khan, and J. A. Lopez de Castro. 1996. 'The Pathogenetic Role of HLA-B27.' *Immunology Today* 17:5–7.

Feng, Yuan, Jin Ding, Chun Mei Fan, and Ping Zhu. 2012. 'Interferon-γ Contributes to HLA-B27-Associated Unfolded Protein Response in Spondyloarthropathies.' *Journal of Rheumatology* 39(3):574–82.

Fert, Ingrid et al. 2014. 'Reverse Interferon Signature Is Characteristic of Antigen-Presenting Cells in Human and Rat Spondyloarthritis.' *Arthritis & rheumatology (Hoboken, N.J.)* 66(4):841–51.

Flanagan, A. M., and T. J. Chambers. 1992. 'Stimulation of Bone Nodule Formation in Vitro by Prostaglandins E1 and E2.' *Endocrinology* 130(1):443–48.

Fleischmann, Roy et al. 2012. 'Placebo-Controlled Trial of Tofacitinib Monotherapy in Rheumatoid Arthritis.' *New England Journal of Medicine* 367(6):495–507.

Fleur Sernee, M., Hidde L. Ploegh, and Danny J. Schust. 1998. 'Why Certain Antibodies Cross-React with HLA-A and HLA-G: Epitope Mapping of Two Common MHC Class I Reagents.' *Molecular Immunology* 35(3):177–88.

Fournié, G. J. et al. 2001. 'Cellular and Genetic Factors Involved in the Difference between Brown Norway and Lewis Rats to Develop Respectively Type-2 and Type-1 Immune-Mediated Diseases.' *Immunological reviews* 184:145–60.

François, R. J., L. Neure, J. Sieper, and J. Braun. 2006. 'Immunohistological Examination of Open Sacroiliac Biopsies of Patients with Ankylosing Spondylitis: Detection of Tumour Necrosis Factor Alpha in Two Patients with Early Disease and Transforming Growth Factor Beta in Three More Advanced Cases.' *Annals of the rheumatic diseases* 65(6):713–20.

Garg, Neha, Filip Van Den Bosch, and Atul Deodhar. 2014. 'Best Practice & Research Clinical Rheumatology The Concept of Spondyloarthritis : Where Are We Now ?' *Best Practice & Research Clinical Rheumatology* 28(5):663–72.

Garstka, Malgorzata et al. 2007a. 'Peptide-Receptive Major Histocompatibility Complex Class I Molecules Cycle between Endoplasmic Reticulum and Cis-Golgi in Wild-Type Lymphocytes.' *Journal of Biological Chemistry* 282:30680–90.

Garstka, Malgorzata et al. 2007b. 'Peptide-Receptive Major Histocompatibility Complex Class I Molecules Cycle between Endoplasmic Reticulum and Cis-Golgi in Wild-Type Lymphocytes.' *Journal of Biological Chemistry* 282(42):30680–90.

Gengenbacher, M., H. J. Sebald, P. M. Villiger, W. Hofstetter, and M. Seitz. 2008. 'Infliximab Inhibits Bone Resorption by Circulating Osteoclast Precursor Cells in Patients with Rheumatoid Arthritis and Ankylosing Spondylitis.' *Annals of the rheumatic diseases* 67(5):620–24.

Giles, Joanna et al. 2012. 'HLA-B27 Homodimers and Free H Chains Are Stronger Ligands for Leukocyte Ig-like Receptor B2 than Classical HLA Class I.' *Journal of immunology (Baltimore, Md. : 1950)* 188(12):6184–93.

Glant, Tibor T. et al. 2001. 'Variations in Susceptibility to Proteoglycan-Induced Arthritis and Spondylitis among C3H Substrains of Mice: Evidence of Genetically Acquired Resistance to Autoimmune Disease.' *Arthritis and Rheumatism* 44:682–92.

Goebel, Jens, Kathy Forrest, Dustie Flynn, Rakesh Rao, and Thomas L. Roszman. 2002. 'Lipid Rafts, Major Histocompatibility Complex Molecules, and Immune Regulation.' *Human Immunology* 63(10):813–20.

Gottlieb, A. B. et al. 2008. *An Open-Label, Single-Arm Pilot Study in Patients with Severe Plaque-Type Psoriasis Treated with an Oral Anti-Inflammatory Agent, Apremilast*.

Goulder, P. J. et al. 2001. 'Evolution and Transmission of Stable CTL Escape Mutations in HIV Infection.' *Nature* 412(6844):334–38.

Gowdie, Peter. 2011. 'Review of Disease - Modifying Anti Rheumatic Drugs in Paediatric Rheumatic Disease.' (March):1–50.

Guo, C. et al. 2012. 'Association of the ANTXR2 Gene Polymorphism and Ankylosing Spondylitis in Chinese Han.' *Scand J Rheumatol* 41:29–32.

Guo, Z. S. et al. 2010. 'Association of IL-1 Gene Complex Members with Ankylosing Spondylitis in Chinese Han Population.' *International Journal of Immunogenetics* 37:33–37.

Hacquard-Bouder, Cécile et al. 2004. 'Defective Costimulatory Function Is a Striking Feature of Antigen-Presenting Cells in an HLA-B27-Transgenic Rat Model of Spondylarthropathy.' *Arthritis and Rheumatism* 50:1624–35.

Hacquard-Bouder, Cécile et al. 2007. 'Alteration of Antigen-Independent Immunologic Synapse Formation between Dendritic Cells from HLA-B27-Transgenic Rats and CD4+ T Cells: Selective Impairment of Costimulatory Molecule Engagement by Mature HLA-B27.' *Arthritis and rheumatism* 56(5):1478–89.

Hammer, Robert E., Shanna D. Maika, James A. Richardson, J. P. Tang, and Joel D. Taurog. 1990. 'Spontaneous Inflammatory Disease in Transgenic Rats Expressing HLA-B27 and Human Beta 2m: An Animal Model of HLA-B27-Associated Human Disorders.' *Cell* 63:1099–1112.

Haque, M. Azizul et al. 1996. 'Suppression of Adjuvant Arthritis in Rats by Induction of Oral Tolerance to Mycobacterial 65-kDa Heat Shock Protein.' *European Journal of Immunology* 26(11):2650–56.

Harjaček, M., T. Margetić, N. Martinez, and Z. Grubić. 2008. 'Pediatric Rheumatology Allele Is Associated with Increased Susceptibility to Juvenile Spondyloarthropathies.' 498–504.

Hawkey, C. J., N. K. Boughton-Smith, and B. J. Whittle. 1985. 'Modulation of Human Colonic Arachidonic Acid Metabolism by Sulfasalazine.' *Digestive diseases and sciences* 30(12):1161–65.

Haworth, C. et al. 1991. 'Expression of Granulocyte-Macrophage Colony-Stimulating Factor in Rheumatoid Arthritis: Regulation by Tumor Necrosis Factor-Alpha.' *European journal of immunology* 21:2575–79.

Haynes, Katelin R. et al. 2012. 'Excessive Bone Formation in a Mouse Model of Ankylosing Spondylitis Is Associated with Decreases in Wnt Pathway Inhibitors.' *Arthritis research & therapy* 14:R253.

Heath, W. R., and F. R. Carbone. 2001. 'Cross-Presentation, Dendritic Cells, Tolerance and Immunity.' *Annual review of immunology* 19:47–64.

Van Der Heijde, D. et al. 2007. 'Infliximab Inhibits Progression of Radiographic Damage in Patients with Active Psoriatic Arthritis through One Year of Treatment: Results from the Induction and Maintenance Psoriatic Arthritis Clinical Trial 2.' *Arthritis and Rheumatism* 56:2698–2707.

Van Der Heijde, D. et al. 2008. 'Radiographic Progression of Ankylosing Spondylitis after up to Two Years of Treatment with Etanercept.' *Arthritis and Rheumatism* 58:1324–31.

Van der Heijde, D. et al. 2009. 'ASDAS, a Highly Discriminatory ASAS-Endorsed Disease Activity Score in Patients with Ankylosing Spondylitis.' *Ann Rheum Dis* 68:1811–18.

Van Der Heijde, Désirée et al. 2005. 'Evaluation of the Efficacy of Etoricoxib in Ankylosing Spondylitis: Results of a Fifty-Two-Week, Randomized, Controlled Study.' *Arthritis and Rheumatism* 52:1205–15.

Van der Heijde, Désirée et al. 2009. 'Assessment of Radiographic Progression in the Spines of Patients with Ankylosing Spondylitis Treated with Adalimumab for up to 2 Years.' *Arthritis research & therapy* 11:R127.

Van Der Heijde, Désirée et al. 2013. 'Tofacitinib (CP-690,550) in Patients with Rheumatoid Arthritis Receiving Methotrexate: Twelve-Month Data from a Twenty-Four-Month Phase III Randomized Radiographic Study.' *Arthritis and Rheumatism* 65(3):559–70.

Heijde, Van Der et al. 2008. 'Radiographic Findings Following Two Years of Infliximab Therapy in Patients with Ankylosing Spondylitis.' *Arthritis and rheumatism* 58:3063–70.

Heit, Antje et al. 2004. 'CpG-DNA Aided Cross-Priming by Cross-Presenting B Cells.' *Journal of immunology (Baltimore, Md.: 1950)* 172(3):1501–7.

Held, Werner, and Roy a Mariuzza. 2008. 'Cis Interactions of Immunoreceptors with MHC and Non-MHC Ligands.' *Nature reviews. Immunology* 8(4):269–78.

Heldmann, F. et al. 2011. 'The European Ankylosing Spondylitis Infliximab Cohort (EASIC): A European Multicentre Study of Long Term Outcomes in Patients with Ankylosing Spondylitis Treated with Infliximab.' *Clinical and experimental rheumatology* 29:672–80.

Hendel, H. et al. 1999. 'New Class I and II HLA Alleles Strongly Associated with Opposite Patterns of Progression to AIDS.' *Journal of immunology (Baltimore, Md.: 1950)* 162(11):6942–46.

Hermann, Clemens, Lisa M. Strittmatter, Janet E. Deane, and Louise H. Boyle. 2013. 'The Binding of TAPBPR and Tapasin to MHC Class I Is Mutually Exclusive.' *Journal of immunology (Baltimore, Md.: 1950)* 191(11):5743–50.

Hermann, E., D. T. Y. Yu, K. H. Meyer zum Buschenfelde, and B. Fleischer. 1993. 'HLA-B27-Restricted CD8 T Cells Derived from Synovial Fluids of Patients with Reactive Arthritis and Ankylosing Spondylitis.' *Lancet* 342:646–50.

Hinks, Anne et al. 2011. 'Subtype Specific Genetic Associations for Juvenile Idiopathic Arthritis: ERAP1 with the Enthesitis Related Arthritis Subtype and IL23R with Juvenile Psoriatic Arthritis.' *Arthritis research & therapy* 13:R12.

Hogervorst, E. J. et al. 1991. 'T Cell Reactivity to an Epitope of the Mycobacterial 65-kDa Heat-Shock Protein (hsp 65) Corresponds with Arthritis Susceptibility in Rats and Is Regulated by Hsp 65-Specific Cellular Responses.' *European journal of immunology* 21(5):1289–96.

Howe, Christopher et al. 2009. 'Calreticulin-Dependent Recycling in the Early Secretory Pathway Mediates Optimal Peptide Loading of MHC Class I Molecules.' *The EMBO journal* 28:3730–44.

Hsu, Leeyen, and April W. Armstrong. 2014. 'JAK Inhibitors: Treatment Efficacy and Safety Profile in Patients with Psoriasis.' *Journal of Immunology Research* 2014.

Huard, B., and L. Karlsson. 2000. 'KIR Expression on Self-Reactive CD8+ T Cells Is Controlled by T-Cell Receptor Engagement.' *Nature* 403(6767):325–28.

Hulpke, Sabine, Christoph Baldauf, and Robert Tampe. 2012. ‘Molecular Architecture of the MHC I Peptide-Loading Complex: One Tapasin Molecule Is Essential and Sufficient for Antigen Processing.’ *FASEB Journal* 26:5071–80.

Hulpke, Sabine, and Robert Tampé. 2013. ‘The MHC I Loading Complex:a Multitasking Machinery in Adaptiveimmunity.’ *Trends in biochemical sciences* 38(8):1–9.

Humphrey, Mary Beth, Lewis L. Lanier, and Mary C. Nakamura. 2005. ‘Role of ITAM-Containing Adapter Proteins and Their Receptors in the Immune System and Bone.’ *Immunological reviews* 208:50–65.

Im, C. H. et al. 2009. ‘Receptor Activator of Nuclear Factor Kappa B Ligand-Mediated Osteoclastogenesis Is Elevated in Ankylosing Spondylitis.’ *Clinical and experimental rheumatology* 27:620–25.

Iwakura, Yoichiro, and Harumichi Ishigame. 2006. ‘The IL-23 / IL-17 Axis in Inflammation.’ *The Journal of clinical investigation* 116(5):1218–22.

Jadon, Deepak et al. 2013. ‘Exploring Ankylosing Spondylitis-Associated ERAP1, IL23R and IL12B Gene Polymorphisms in Subphenotypes of Psoriatic Arthritis.’ *Rheumatology (United Kingdom)* 52(October 2012):261–66.

Jenkinson, T. R. et al. 1994. ‘Defining Spinal Mobility in Ankylosing Spondylitis (AS). The Bath AS Metrology Index.’ *Journal of Rheumatology* 21:1694–98.

Joffre, Olivier P., Elodie Segura, Ariel Savina, and Sebastian Amigorena. 2012. ‘Cross-Presentation by Dendritic Cells.’ *Nature Reviews Immunology* 12:557–69.

Jones, S. D., A. Steiner, S. L. Garrett, and A. Calin. 1996. ‘The Bath Ankylosing Spondylitis Patient Global Score (BAS-G).’ *British journal of rheumatology* 35:66–71.

Jongbloed, S. L. et al. 2009. ‘Plasmacytoid Dendritic Cells Regulate Breach of Self-Tolerance in Autoimmune Arthritis.’ *J Immunol* 182:963–68.

Karaderi, Tugce et al. 2009. ‘Association between the Interleukin 23 Receptor and Ankylosing Spondylitis Is Confirmed by a New UK Case-Control Study and Meta-Analysis of Published Series.’ *Rheumatology* 48(February):386–89.

Kaur, G., and N. Mehra. 2009. ‘Genetic Determinants of HIV-1 Infection and Progression to AIDS: Immune Response Genes.’ *Tissue Antigens* 74:373–85.

Keffer, J. et al. 1991. ‘Transgenic Mice Expressing Human Tumour Necrosis Factor: A Predictive Genetic Model of Arthritis.’ *EMBO J* 10(13):4025–31.

Kelleher, A. D. et al. 2001. ‘Clustered Mutations in HIV-1 Gag Are Consistently Required for Escape from HLA-B27-Restricted Cytotoxic T Lymphocyte Responses.’ *The Journal of experimental medicine* 193(3):375–86.

Khan, Muhammad Asim. 2013. ‘Polymorphism of HLA-B27 : 105 Subtypes Currently Known.’

Khare, S. D., H. S. Luthra, and C. S. David. 1995. ‘Spontaneous Inflammatory Arthritis in HLA-B27 Transgenic Mice Lacking Beta 2-Microglobulin: A Model of Human Spondyloarthropathies.’ *The Journal of experimental medicine* 182:1153–58.

Kiesel, Jennifer R., Zachary S. Buchwald, and Rajeev Aurora. 2009a. ‘Cross-Presentation by Osteoclasts Induces FoxP3 in CD8+ T Cells.’ *Journal of immunology (Baltimore, Md. : 1950)* 182:5477–87.

Kiesel, Jennifer R., Zachary S. Buchwald, and Rajeev Aurora. 2009b. ‘Cross-Presentation by Osteoclasts Induces FoxP3 in CD8+ T Cells.’ *Journal of immunology (Baltimore, Md. : 1950)* 182:5477–87.

Kim, E. Y., H. H. Chi, R. Rajaiah, and K. D. Moudgil. 2008. 'Exogenous Tumour Necrosis Factor Alpha Induces Suppression of Autoimmune Arthritis.' *Arthritis research & therapy* 10(1):R38.

Kim, EY Eugene Y., HH Howard H. Chi, Mohammed Bouziane, Amitabh Gaur, and Kamal D. Moudgil. 2008. 'Regulation of Autoimmune Arthritis by the pro-Inflammatory Cytokine Interferon-&#947'; *Clinical Immunology* 127(1):98–106.

Kim, Tae-Jong et al. 2008. 'Interleukin 1 Polymorphisms in Patients with Ankylosing Spondylitis in Korea.' *The Journal of rheumatology* 35(8):1603–8.

Kirino, Yohei et al. 2013. 'Genome-Wide Association Analysis Identifies New Susceptibility Loci for Behçet's Disease and Epistasis between HLA-B*51 and ERAP1.' *Nature genetics* 45:202–7.

Kollnberger, Simon et al. 2002. 'Cell-Surface Expression and Immune Receptor Recognition of HLA-B27 Homodimers.' *Arthritis and Rheumatism* 46:2972–82.

Kollnberger, Simon et al. 2004. 'HLA-B27 Heavy Chain Homodimers Are Expressed in HLA-B27 Transgenic Rodent Models of Spondyloarthritis and Are Ligands for Paired Ig-like Receptors.' *Journal of immunology (Baltimore, Md. : 1950)* 173:1699–1710.

Kollnberger, Simon et al. 2007. 'Interaction of HLA-B27 Homodimers with KIR3DL1 and KIR3DL2, Unlike HLA-B27 Heterotrimers, Is Independent of the Sequence of Bound Peptide.' *European journal of immunology* 37(5):1313–22.

Kontoyiannis, D., M. Pasparakis, T. T. Pizarro, F. Cominelli, and G. Kollias. 1999. 'Impaired On/off Regulation of TNF Biosynthesis in Mice Lacking TNF AU-Rich Elements: Implications for Joint and Gut-Associated Immunopathologies.' *Immunity* 10:387–98.

Krug, H. E., M. L. Mahowald, and C. Clark. 1989. 'Progressive Ankylosis (ank/ank) in Mice: An Animal Model of Spondyloarthropathy. III. Proliferative Spleen Cell Response to T Cell Mitogens.' *Clinical and experimental immunology* 78:97–101.

Van der Laken, C. J. et al. 2007. 'Imaging and Serum Analysis of Immune Complex Formation of Radiolabelled Infliximab and Anti-Infliximab in Responders and Non-Responders to Therapy for Rheumatoid Arthritis.' *Annals of the rheumatic diseases* 66:253–56.

Van der Laken, C. J. et al. 2008. 'The Formation of Infliximab and Anti-Infliximab Immune Complexes as an Explanation for Non-Responding to Infliximab Treatment of Rheumatoid Arthritis: Observational Study in 4 Patients.' *Nederlands tijdschrift voor geneeskunde* 152:1672–77.

Lande, Roberto et al. 2011. 'Neutrophils Activate Plasmacytoid Dendritic Cells by Releasing Self-DNA-Peptide Complexes in Systemic Lupus Erythematosus.' *Science translational medicine* 3:73ra19.

Langley, Richard G. et al. 2014. 'Secukinumab in Plaque Psoriasis - Results of Two Phase 3 Trials.' *The New England journal of medicine* 3–8.

Layh-Schmitt, Gerlinde, Eva Y. Yang, Grace Kwon, and Robert a Colbert. 2013. 'HLA-B27 Alters the Response to Tumor Necrosis Factor A and Promotes Osteoclastogenesis in Bone Marrow Monocytes from HLA-B27-Transgenic Rats.' *Arthritis and rheumatism* 65(8):2123–31.

Lee, Eun Bong et al. 2014. 'Tofacitinib versus Methotrexate in Rheumatoid Arthritis.' *The New England journal of medicine* 370(25):2377–86.

Lenart, Izabela et al. 2012. 'The MHC Class I Heavy Chain Structurally Conserved Cysteines 101 and 164 Participate in HLA-B27 Dimer Formation.' *Antioxidants & Redox Signaling* 16:33–43.

Li, H. et al. 2010. ‘Crosstalk between the Bone and Immune Systems: Osteoclasts Function as Antigen-Presenting Cells and Activate CD4+ and CD8+ T Cells.’ *Blood* 116(2):210–18.

Li, Nicholas L., Li Fu, Hannes Uchtenhagen, Adnane Achour, and Deborah N. Burshtyn. 2013. ‘Cis Association of Leukocyte Ig-like Receptor 1 with MHC Class I Modulates Accessibility to Antibodies and HCMV UL18.’ *European journal of immunology* 43(4):1042–52.

Li, Yili, and Roy a Mariuzza. 2014. ‘Structural Basis for Recognition of Cellular and Viral Ligands by NK Cell Receptors.’ *Frontiers in immunology* 5(March):123.

Lin, Zhiming et al. 2012. ‘A Genome-Wide Association Study in Han Chinese Identifies New Susceptibility Loci for Ankylosing Spondylitis.’ *Nature genetics* 44(1):73–77.

Liptay, Susanne et al. 2002. ‘Molecular Mechanisms of Sulfasalazine-Induced T-Cell Apoptosis.’ *British journal of pharmacology* 137(5):608–20.

López de Castro, José A. 2005. ‘HLA-B27: Portraying Immunodominant Viral Epitopes.’ *European Journal of Immunology* 35:336–40.

Lories, R. J., I. Derese, and F. P. Luyten. 2005. ‘Modulation of Bone Morphogenetic Protein Signaling Inhibits the Onset and Progression of Ankylosing Enthesitis.’ *J Clin Invest* 115:1571–79.

Lories, Rik J. U. et al. 2006. ‘Noggin Haploinsufficiency Differentially Affects Tissue Responses in Destructive and Remodeling Arthritis.’ *Arthritis and Rheumatism* 54:1736–46.

Lories, Rik J. U., I. Derese, and F. P. Luyten. 2008. ‘Inhibition of Osteoclasts Does Not Prevent Joint Ankylosis in a Mouse Model of Spondyloarthritis.’ *Rheumatology* 47:605–8.

Lories, Rik J. U., Inge Derese, and Frank P. Luyten. 2005. ‘Modulation of Bone Morphogenetic Protein Signaling Inhibits the Onset and Progression of Ankylosing Enthesitis.’ *The Journal of clinical investigation* 115:1571–79.

Lories, Rik J. U., Frank P. Luyten, and Kurt de Vlam. 2009. ‘Progress in Spondylarthritis. Mechanisms of New Bone Formation in Spondyloarthritis.’ *Arthritis research & therapy* 11:221.

Lories, Rik J. U., and Georg Schett. 2012. ‘Pathophysiology of New Bone Formation and Ankylosis in Spondyloarthritis.’ *Rheumatic Disease Clinics of North America* 38:555–67.

Lukas, C. et al. 2009. ‘Development of an ASAS-Endorsed Disease Activity Score (ASDAS) in Patients with Ankylosing Spondylitis.’ *Annals of the rheumatic diseases* 68:18–24.

Machado, Pedro et al. 2011. ‘Ankylosing Spondylitis Disease Activity Score (ASDAS): Defining Cut-off Values for Disease Activity States and Improvement Scores.’ *Annals of the rheumatic diseases* 70:47–53.

MacLean, L. et al. 1992. ‘Sulphydryl Reactivity of the HLA-B27 Epitope: Accessibility of the Free Cysteine Studied by Flow Cytometry.’ *Annals of the rheumatic diseases* 51:456–60.

Madden, D. R. 1995. ‘The Three-Dimensional Structure of Peptide-MHC Complexes.’ *Annual review of immunology* 13:587–622.

Malik, Pratap, Polina Klimovitsky, Lih-Wen Deng, Jonathan E. Boyson, and Jack L. Strominger. 2002. ‘Uniquely Conformed Peptide-Containing Beta 2-Microglobulin-Free Heavy Chains of HLA-B2705 on the Cell Surface.’ *Journal of immunology (Baltimore, Md.: 1950)* 169(8):4379–87.

Mamolo, C., J. Harness, H. Tan, and A. Menter. 2014. 'Tofacitinib (CP-690,550), an Oral Janus Kinase Inhibitor, Improves Patient-Reported Outcomes in a Phase 2b, Randomized, Double-Blind, Placebo-Controlled Study in Patients with Moderate-to-Severe Psoriasis.' *Journal of the European Academy of Dermatology and Venereology* 28(2):192–203.

Mariño, Eliana, Bernice Tan, Lauren Binge, Charles R. Mackay, and Shane T. Grey. 2012. 'B-Cell Cross-Presentation of Autologous Antigen Precipitates Diabetes.' *Diabetes* 61(11):2893–2905.

Martin, Annalise M., Jerzy K. Kulski, Campbell Witt, Pierre Pontarotti, and Frank T. Christiansen. 2002. 'Leukocyte Ig-like Receptor Complex (LRC) in Mice and Men.' *Trends in Immunology* 23(2):81–88.

Masuda, Ai, Akira Nakamura, Tsutomu Maeda, Yuzuru Sakamoto, and Toshiyuki Takai. 2007. 'Cis Binding between Inhibitory Receptors and MHC Class I Can Regulate Mast Cell Activation.' *The Journal of experimental medicine* 204(4):907–20.

Matko, Janos, Yuri Bushkin, Taiyin Wei, and Michael Edidinr. 1994. 'Clustering of Class.'

May, Ekkehard et al. 2003. 'CD8 Alpha Beta T Cells Are Not Essential to the Pathogenesis of Arthritis or Colitis in HLA-B27 Transgenic Rats.' *Journal of immunology (Baltimore, Md.: 1950)* 170:1099–1105.

McHugh, Kirsty et al. 2014. 'Expression of Aberrant HLA-B27 Molecules Is Dependent on B27 Dosage and Peptide Supply.' *Annals of the rheumatic diseases* 73(4):763–70.

McInnes, Iain B. et al. 2013. 'Efficacy and Safety of Ustekinumab in Patients with Active Psoriatic Arthritis: 1 Year Results of the Phase 3, Multicentre, Double-Blind, Placebo-Controlled PSUMMIT 1 Trial.' *Lancet* 382:780–89.

McInnes, Iain B. et al. 2014. 'Efficacy and Safety of Secukinumab, a Fully Human Anti-Interleukin-17A Monoclonal Antibody, in Patients with Moderate-to-Severe Psoriatic Arthritis: A 24-Week, Randomised, Double-Blind, Placebo-Controlled, Phase II Proof-of-Concept Trial.' *Annals of the rheumatic diseases* 73:349–56.

McKenzie, Brent S., Robert a. Kastelein, and Daniel J. Cua. 2006. 'Understanding the IL-23-IL-17 Immune Pathway.' *Trends in Immunology* 27(1):17–23.

McVicar, D. W., and D. N. Burshtyn. 2001. 'Intracellular Signaling by the Killer Immunoglobulin-like Receptors and Ly49.' *Science's STKE: signal transduction knowledge environment* 2001(75):re1.

Mear, J. P. et al. 1999. 'Misfolding of HLA-B27 as a Result of Its B Pocket Suggests a Novel Mechanism for Its Role in Susceptibility to Spondyloarthropathies.' *Journal of immunology (Baltimore, Md.: 1950)* 163:6665–70.

Mease, Philip J. et al. 2014. 'Brodalumab, an Anti-IL17RA Monoclonal Antibody, in Psoriatic Arthritis.' *The New England journal of medicine* 370:2295–2306.

Mei, Yang et al. 2011. 'Increased Serum IL-17 and IL-23 in the Patient with Ankylosing Spondylitis.' *Clinical Rheumatology* 30:269–73.

Merzougui, Nawel, Roland Kratzer, Loredana Saveanu, and Peter van Endert. 2011. 'A Proteasome-Dependent, TAP-Independent Pathway for Cross-Presentation of Phagocytosed Antigen.' *EMBO reports* 12(12):1257–64.

Metzner, Christoph, Brian Salmons, Walter H. Günzburg, and John A. Dangerfield. 2008. 'Rafts, Anchors and Viruses - A Role for Glycosylphosphatidylinositol Anchored Proteins in the Modification of Enveloped Viruses and Viral Vectors.' *Virology* 382(2):125–31.

Mielants, H. et al. 1995. 'The Evolution of Spondyloarthropathies in Relation to Gut Histology. I. Clinical Aspects.' *Journal of Rheumatology* 22:2266–72.

Mielants, H., E. M. Veys, C. Cuvelier, and M. de Vos. 1988. 'Ileocolonoscopic Findings in Seronegative Spondylarthropathies.' *British journal of rheumatology* 27 Suppl 2(suppl II):95–105.

Mielants, H., E. M. Veys, C. Cuvelier, M. De Vos, and L. Botelberghe. 1985. 'HLA-B27 Related Arthritis and Bowel Inflammation. Part 2. Ileocolonoscopy and Bowel Histology in Patients with HLA-B27 Related Arthritis.' *Journal of Rheumatology* 12:294–98.

Mielants, H., M. De Vos, C. Cuvelier, and E. M. Veys. 1996. 'The Role of Gut Inflammation in the Pathogenesis of Spondyloarthropathies.' *Acta Clinica Belgica* 51:340–49.

Mikecz, K., T. T. Glant, and A. R. Poole. 1987. 'Immunity to Cartilage Proteoglycans in BALB/c Mice with Progressive Polyarthritis and Ankylosing Spondylitis Induced by Injection of Human Cartilage Proteoglycan.' *Arthritis and rheumatism* 30:306–18.

Mingari, M. C. et al. 1996. 'Human CD8+ T Lymphocyte Subsets That Express HLA Class I-Specific Inhibitory Receptors Represent Oligoclonally or Monoclonally Expanded Cell Populations.' *Proceedings of the National Academy of Sciences of the United States of America* 93(22):12433–38.

Lo Monaco, Elisa et al. 2008. 'HLA-E: Strong Association with beta2-Microglobulin and Surface Expression in the Absence of HLA Class I Signal Sequence-Derived Peptides.' *Journal of immunology (Baltimore, Md. : 1950)* 181(8):5442–50.

Monnet, D. et al. 2012. 'Association between the IL-1 Family Gene Cluster and Spondyloarthritis.' *Annals of the Rheumatic Diseases* 71:885–90.

Morris, R. I., A. L. Metzger, R. Bluestone, and P. I. Terasaki. 1974. 'HL-A-W27--a Useful Discriminator in the Arthropathies of Inflammatory Bowel Disease.' *The New England journal of medicine* 290:1117–19.

Morris, R., A. L. Metzger, R. Bluestone, and P. I. Terasaki. 1974. 'HL-A W27--a Clue to the Diagnosis and Pathogenesis of Reiter's Syndrome.' *The New England journal of medicine* 290:554–56.

Neumann-Haefelin, C. 2011. 'Protective Role of HLA-B27 in HIV and Hepatitis C Virus Infection.' *Deutsche medizinische Wochenschrift (1946)* 136:320–24.

Neumann-Haefelin, Christoph et al. 2006. 'Dominant Influence of an HLA-B27 Restricted CD8+ T Cell Response in Mediating HCV Clearance and Evolution.' *Hepatology* 43(3):563–72.

Neumann-Haefelin, Christoph et al. 2011. 'Human Leukocyte Antigen B27 Selects for Rare Escape Mutations That Significantly Impair Hepatitis C Virus Replication and Require Compensatory Mutations.' *Hepatology* 54(4):1157–66.

Newbould, B. B. 1964. 'Role of Lymph Nodes in Adjuvant-Induced Arthritis in Rats.' *Annals of the rheumatic diseases* 23:392–96.

Nickerson, C. L., J. Hanson, and C. S. David. 1990. 'Expression of HLA-B27 in Transgenic Mice Is Dependent on the Mouse H-2D Genes.' *The Journal of experimental medicine* 172:1255–61.

Nocturne, G. et al. 2009. 'Lack of Efficacy of Rituximab in Spondylarthropathies: Data of 8 Patients Prospectively Followed in the French AIR ("auto-Immunity and Rituximab") Registry'. *Ann Rheum Dis* 68(Suppl3):626.

Noordenbos, Troy et al. 2012. 'Interleukin-17-Positive Mast Cells Contribute to Synovial Inflammation in Spondylarthritis.' *Arthritis and Rheumatism* 64(1):99–109.

Nordling, C., A. Karlsson-Parra, L. Jansson, R. Holmdahl, and L. Klareskog. 1992. 'Characterization of a Spontaneously Occurring Arthritis in Male DBA/1 Mice.' *Arthritis and Rheumatism* 35(6):717–22.

Papp, K. A. et al. 2013. 'Efficacy and Safety of Apremilast in Subjects with Moderate to Severe Plaque Psoriasis: Results from a Phase II, Multicenter, Randomized, Double-Blind, Placebo-Controlled, Parallel-Group, Dose-Comparison Study.' *Journal of the European Academy of Dermatology and Venereology* 27(3).

Papp, Kim et al. 2012. 'Efficacy of Apremilast in the Treatment of Moderate to Severe Psoriasis: A Randomised Controlled Trial.' *Lancet* 380(9843):738–46.

Papp, Kim A. et al. 2012. 'Brodalumab, an Anti–Interleukin-17–Receptor Antibody for Psoriasis.' *New England Journal of Medicine* 366:1181–89.

Paramarta, Jacqueline E., and Dominique Baeten. 2013. 'Spondyloarthritis: From Unifying Concepts to Improved Treatment.' *Rheumatology (Oxford, England)* (December 2013):1–13.

Paramarta, Jacqueline E., Tanja F. Heijda, and Dominique L. Baeten. 2013. 'Fast Relapse upon Discontinuation of Tumour Necrosis Factor Blocking Therapy in Patients with Peripheral Spondyloarthritis.' *Annals of the rheumatic diseases* 72(9):1581–82.

Parasannanavar, Devaraj J., Anjali Rajadhyaksha, and Kanjaksha Ghosh. 2014. 'Role of Hla-B Alleles and Clinical Presentation of b27 Negative Spondyloarthritis Patients from Mumbai, Western India.' *Autoimmune diseases* 2014:327315.

Parcej, David, and Robert Tampé. 2010. 'ABC Proteins in Antigen Translocation and Viral Inhibition.' *Nature chemical biology* 6(8):572–80.

Parham, Peter. 2005. 'MHC Class I Molecules and KIRs in Human History, Health and Survival.' *Nature reviews. Immunology* 5:201–14.

Passalent, Laura A. 2011. 'Physiotherapy for Ankylosing Spondylitis: Evidence and Application.' *Current opinion in rheumatology* 23:142–47.

Pathan, E. et al. 2012. 'Efficacy and Safety of Apremilast, an Oral Phosphodiesterase 4 Inhibitor, in Ankylosing Spondylitis.' *Annals of the Rheumatic Diseases*.

Payeli, Sravan K. et al. 2012. 'Inhibiting HLA – B27 Homodimer – Driven Immune Cell Inflammation in Spondylarthritis.' 64(10):3139–49.

Pearson, Carl M., and Fae D. Wood. 1963. 'Studies of Arthritis and Other Lesions Induced in Rats by The Injection of Mycobacterial Adjuvant.' *American Journal of Pathology* 42(1):73–95.

Peh, C. a et al. 1998. 'HLA-B27-Restricted Antigen Presentation in the Absence of Tapasin Reveals Polymorphism in Mechanisms of HLA Class I Peptide Loading.' *Immunity* 8(5):531–42.

Perosa, Federico et al. 2003. 'Beta 2-Microglobulin-Free HLA Class I Heavy Chain Epitope Mimicry by Monoclonal Antibody HC-10-Specific Peptide.' *Journal of immunology (Baltimore, Md.: 1950)* 171(4):1918–26.

Pfizer. 2013. 'Product Information Sulfasalazine.' (89730):89730.

Piatier-Tonneau, D., P. S. Mach, a Kahan, and F. Delbarre. 1982. 'T Suppressor Lymphocytes Regulation of Adjuvant Arthritis in Two Inbred Strains of Rats.' *Clinical and experimental immunology* 49(3):645–51.

Pimentel-Santos, F. M. et al. 2009. 'Association of IL23R and ERAP1 Genes with Ankylosing Spondylitis in a Portuguese Population.' *Clinical and experimental rheumatology* 27:800–806.

Poddubnyy, Denis et al. 2011. ‘Rates and Predictors of Radiographic Sacroiliitis Progression over 2 Years in Patients with Axial Spondyloarthritis.’ *Annals of the rheumatic diseases* 70:1369–74.

Poddubnyy, Denis, Kay-Geert a Hermann, Johanna Callhoff, Joachim Listing, and Joachim Sieper. 2014. ‘Ustekinumab for the Treatment of Patients with Active Ankylosing Spondylitis: Results of a 28-Week, Prospective, Open-Label, Proof-of-Concept Study (TOPAS).’ *Annals of the rheumatic diseases* 73:817–23.

Poddubnyy, Denis, and Joachim Sieper. 2012. ‘Radiographic Progression in Ankylosing Spondylitis/axial Spondyloarthritis.’ *Current Opinion in Rheumatology* 24:363–69.

Ports, W. C. et al. 2013. ‘A Randomized Phase 2a Efficacy and Safety Trial of the Topical Janus Kinase Inhibitor Tofacitinib in the Treatment of Chronic Plaque Psoriasis.’ *British Journal of Dermatology* 169(1):137–45.

Prevosto, Claudia, Jane C. Goodall, and J. S. Hill Gaston. 2012. ‘Cytokine Secretion by Pathogen Recognition Receptor-Stimulated Dendritic Cells in Rheumatoid Arthritis and Ankylosing Spondylitis.’ *Journal of Rheumatology* 39:1918–28.

Qian, Bi Feng, Susan L. Tonkonogy, and R. Balfour Sartor. 2006. ‘Luminal Bacterial Antigen-Specific CD4+ T-Cell Responses in HLA-B27 Transgenic Rats with Chronic Colitis Are Mediated by Both Major Histocompatibility Class II and HLA-B27 Molecules.’ *Immunology* 117:319–28.

Raine, T. et al. 2006. ‘Consistent Patterns of Expression of HLA Class I Free Heavy Chains in Healthy Individuals and Raised Expression in Spondyloarthropathy Patients Point to Physiological and Pathological Roles.’ *Rheumatology* 45(11):1338–44.

Ramos, Manuel et al. 2002. ‘Molecular Mimicry of an HLA-B27-Derived Ligand of Arthritis-Linked Subtypes with Chlamydial Proteins.’ *Journal of Biological Chemistry* 277(40):37573–81.

Rath, Heiko C. et al. 1996. ‘Normal Luminal Bacteria, Especially Bacteroides Species, Mediate Chronic Colitis, Gastritis, and Arthritis in HLA-B27/human β2 Microglobulin Transgenic Rats.’ *Journal of Clinical Investigation* 98:945–53.

Rath, Heiko C., Kenneth H. Wilson, and R. Balfour Sartor. 1999. ‘Differential Induction of Colitis and Gastritis in HLA-B27 Transgenic Rats Selectively Colonized with Bacteroides Vulgatus or Escherichia Coli.’ *Infection and Immunity* 67:2969–74.

Ravetch, J. V, and L. L. Lanier. 2000. ‘Immune Inhibitory Receptors.’ *Science (New York, N.Y.)* 290(5489):84–89.

Reveille, John D. 2011. ‘The Genetic Basis of Spondyloarthritis.’ *Annals of the rheumatic diseases* 70 Suppl 1:i44–50.

Rich, P. et al. 2012. ‘Secukinumab Induction and Maintenance Therapy in Moderate-to-Severe Plaque Psoriasis: A Randomised, Double-Blind, Placebo-Controlled, Phase II Regimen-Finding Study.’ *The British journal of dermatology* 2009:9–10.

Rizvi, Syed Monem et al. 2014. ‘Distinct Assembly Profiles of HLA-B Molecules.’ *Journal of immunology (Baltimore, Md. : 1950)* 192(11):4967–76.

Robinson, Philip C. et al. 2015. ‘Genetic Dissection of Acute Anterior Uveitis Reveals Similarities and Differences in Associations Observed With Ankylosing Spondylitis.’ 67(1):140–51.

Rudwaleit, M. et al. 2009. ‘The Development of Assessment of SpondyloArthritis International Society Classification Criteria for Axial Spondyloarthritis (part II): Validation and Final Selection.’ *Annals of the rheumatic diseases* 68(part II):777–83.

Rudwaleit, M. et al. 2011. 'The Assessment of SpondyloArthritis International Society Classification Criteria for Peripheral Spondyloarthritis and for Spondyloarthritis in General.' *Annals of the rheumatic diseases* 70:25–31.

Rudwaleit, M., J. Listing, J. Brandt, J. Braun, and J. Sieper. 2004a. 'Prediction of a Major Clinical (BASDAI 50) to Tumour Necrosis Factor A Blockers in Ankylosing Spondylitis.' *Annals of the Rheumatic Diseases* 63:665–70.

Rudwaleit, Martin et al. 2009. 'Effectiveness, Safety, and Predictors of Good Clinical Response in 1250 Patients Treated with Adalimumab for Active Ankylosing Spondylitis.' *Journal of Rheumatology* 36:801–8.

Saad, Carla GS et al. 2012. 'Low Sclerostin Levels: A Predictive Marker of Persistent Inflammation in Ankylosing Spondylitis during Anti-Tumor Necrosis Factor Therapy?' *Arthritis Research & Therapy* 14:R216.

Sandborn, William J. et al. 2008. 'A Randomized Trial of Ustekinumab, a Human Interleukin-12/23 Monoclonal Antibody, in Patients With Moderate-to-Severe Crohn's Disease.' *Gastroenterology* 135:1130–41.

Sandborn, William J. et al. 2012. 'Ustekinumab Induction and Maintenance Therapy in Refractory Crohn's Disease.' *New England Journal of Medicine* 367:1519–28.

Santos, Susana G., Simon J. Powis, and Fernando a Arosa. 2004. 'Misfolding of Major Histocompatibility Complex Class I Molecules in Activated T Cells Allows Cis-Interactions with Receptors and Signaling Molecules and Is Associated with Tyrosine Phosphorylation.' *The Journal of biological chemistry* 279(51):53062–70.

Schett, Georg et al. 2012. 'Oral Apremilast in the Treatment of Active Psoriatic Arthritis; Results of a Multicenter, Randomized, Double-Blind, Placebo-Controlled Study.' *Arthritis and Rheumatism* 64(10):3156–67.

Schlosstein, L., P. I. Terasaki, R. Bluestone, and C. M. Pearson. 1973. 'High Association of an HL-A Antigen, W27, with Ankylosing Spondylitis.' *The New England journal of medicine* 288:704–6.

Schneidewind, Arne et al. 2008. 'Structural and Functional Constraints Limit Options for Cytotoxic T-Lymphocyte Escape in the Immunodominant HLA-B27-Restricted Epitope in Human Immunodeficiency Virus Type 1 Capsid.' *Journal of virology* 82(11):5594–5605.

Van Schouwenburg, P. A. et al. 2012. 'Adalimumab Elicits a Restricted Anti-Idiotypic Antibody Response in Autoimmune Patients Resulting in Functional Neutralisation.' *Annals of the Rheumatic Diseases*.

Seeling, Michaela et al. 2013. 'Inflammatory Monocytes and Fcγ Receptor IV on Osteoclasts Are Critical for Bone Destruction during Inflammatory Arthritis in Mice.' *Proceedings of the National Academy of Sciences of the United States of America* 110(26):10729–34.

Shaw, Jacqueline, Hiroko Hatano, and Simon Kollnberger. 2014. 'The Biochemistry and Immunology of Non-Canonical Forms of HLA-B27.' *Molecular Immunology* 57(1):52–58.

Shen, Hui, Jane C. Goodall, and J. S. Hill Gaston. 2009. 'Frequency and Phenotype of Peripheral Blood Th17 Cells in Ankylosing Spondylitis and Rheumatoid Arthritis.' *Arthritis and Rheumatism* 60:1647–56.

Sherlock, Jonathan P. et al. 2012. 'IL-23 Induces Spondyloarthropathy by Acting on ROR-Γt+ CD3+CD4−CD8− Entheseal Resident T Cells.' *Nature Medicine* 18:1069–76.

Shimizu, Y., D. E. Geraghty, B. H. Koller, H. T. Orr, and R. DeMars. 1988. 'Transfer and Expression of Three Cloned Human Non-HLA-A,B,C Class I Major Histocompatibility

Complex Genes in Mutant Lymphoblastoid Cells.' *Proc Natl Acad Sci U S A* 85:227–31.

Sieper, J. et al. 2008. 'Comparison of Two Different Dosages of Celecoxib with Diclofenac for the Treatment of Active Ankylosing Spondylitis: Results of a 12-Week Randomised, Double-Blind, Controlled Study.' *Annals of the rheumatic diseases* 67:323–29.

Sieper, J. et al. 2012. 'Efficacy and Safety of Adalimumab in Patients with Non-Radiographic Axial Spondyloarthritis: Results of a Randomised Placebo-Controlled Trial (ABILITY-1).' *Annals of the Rheumatic Diseases*.

Sieper, J. et al. 2014. 'Efficacy and Safety of Infliximab plus Naproxen versus Naproxen Alone in Patients with Early, Active Axial Spondyloarthritis: Results from the Double-Blind, Placebo-Controlled INFAST Study, Part 1.' *Annals of the rheumatic diseases* 73:101–7.

Sieper, Joachim. 2007. 'Pathogenesis of Reactive Arthritis.' Pp. 181–87 in *Psoriatic and Reactive Arthritis: A Companion to Rheumatology*.

Sieper, Joachim, Martin Rudwaleit, Jürgen Braun, and Désirée Van Der Heijde. 2002. 'Diagnosing Reactive Arthritis: Role of Clinical Setting in the Value of Serologic and Microbiologic Assays.' *Arthritis and Rheumatism* 46(2):319–27.

Sims, a-M. et al. 2008. 'Prospective Meta-Analysis of Interleukin 1 Gene Complex Polymorphisms Confirms Associations with Ankylosing Spondylitis.' *Annals of the rheumatic diseases* 67:1305–9.

Šinkorová, Z., J. Čapková, J. Niederlová, R. Štěpánková, and J. Šinkora. 2008. 'Commensal Intestinal Bacterial Strains Trigger Ankylosing Enthesopathy of the Ankle in Inbred B10.BR (H-2k) Male Mice.' *Human Immunology* 69:845–50.

Smith, Judith a. et al. 2008. 'Endoplasmic Reticulum Stress and the Unfolded Protein Response Are Linked to Synergistic IFN-?? Induction via X-Box Binding Protein 1.' *European Journal of Immunology* 38(5):1194–1203.

Song, I. H. et al. 2011. *Treatment of Active Ankylosing Spondylitis with Abatacept: An Open-Label, 24-Week Pilot Study*.

Song, I. H. et al. 2012. 'Frequency and Duration of Drug-Free Remission after 1 Year of Treatment with Etanercept versus Sulfasalazine in Early Axial Spondyloarthritis: 2 Year Data of the ESTHER Trial.' *Annals of the Rheumatic Diseases* 71:1212–15.

Song, In-Ho et al. 2013. 'Similar Response Rates in Patients with Ankylosing Spondylitis and Non-Radiographic Axial Spondyloarthritis after 1 Year of Treatment with Etanercept: Results from the ESTHER Trial.' *Annals of the rheumatic diseases* 72:823–25.

Song, In-Ho, and Denis Poddubnyy. 2011. 'New Treatment Targets in Ankylosing Spondylitis and Other Spondyloarthritides.' *Current opinion in rheumatology* 23:346–51.

Sonkar, Gyanendra Kumar, Usha, and S. Singh. 2008. 'Is HLA-B27 a Useful Test in the Diagnosis of Juvenile Spondyloarthropathies?' *Singapore Medical Journal* 49:795–99.

Speiser, Daniel E. et al. 1999. 'CD28-Negative Cytolytic Effector T Cells Frequently Express NK Receptors and Are Present at Variable Proportions in Circulating Lymphocytes from Healthy Donors and Melanoma Patients.' *European Journal of Immunology* 29(6):1990–99.

Spel, Lotte, Jaap-Jan Boelens, Stefan Nierkens, and Marianne Boes. 2013. 'Antitumor Immune Responses Mediated by Dendritic Cells: How Signals Derived from Dying Cancer Cells Drive Antigen Cross-Presentation.' *Oncoimmunology* 2:e26403.

Spuls, Ph I., and L. Hooft. 2012. 'Brodalumab and Ixekizumab, Anti-Interleukin-17-Receptor Antibodies for Psoriasis: A Critical Appraisal.' *British Journal of Dermatology* 167:710–13.

Stam, N. J., H. Spits, and H. L. Ploegh. 1986. 'Monoclonal Antibodies Raised against Denatured HLA-B Locus Heavy Chains Permit Biochemical Characterization of Certain HLA-C Locus Products.' *Journal of immunology (Baltimore, Md.: 1950)* 137(7):2299–2306.

Stam, N. J., T. M. Vroom, P. J. Peters, E. B. Pastoors, and H. L. Ploegh. 1990. 'HLA-A- and HLA-B-Specific Monoclonal Antibodies Reactive with Free Heavy Chains in Western Blots, in Formalin-Fixed, Paraffin-Embedded Tissue Sections and in Cryo-Immuno-Electron Microscopy.' *International immunology* 2(2):113–25.

Strand, Vibeke, Georg Schett, Chiachi Hu, and Randall M. Stevens. 2013. 'Patient-Reported Health-Related Quality of Life with Apremilast for Psoriatic Arthritis: A Phase II, Randomized, Controlled Study.' *The Journal of rheumatology* 40(7):1158–65.

Suzuki, Takashi, and Yasuo Suzuki. 2006. 'Virus Infection and Lipid Rafts.' *Biological & pharmaceutical bulletin* 29(8):1538–41.

Tan, H. et al. 2013. 'Dose Response and Pharmacokinetics of Tofacitinib (CP-690,550) , an Oral Janus Kinase Inhibitor , in the Treatment of Chronic Plaque Psoriasis.' *Pharmacometrics & Systems Pharmacology* 2:e44.

Tanaka, Yoshiya, Makoto Suzuki, Hiroyuki Nakamura, Shigeyuki Toyoizumi, and Samuel H. Zwillich. 2011. 'Phase II Study of Tofacitinib (CP-690,550) Combined with Methotrexate in Patients with Rheumatoid Arthritis and an Inadequate Response to Methotrexate.' *Arthritis Care and Research* 63(8):1150–58.

Taugor, Joel D. et al. 1999. 'Inflammatory Disease in HLA-B27 Transgenic Rats.' *Immunological Reviews* 169(1):209–23.

Taurog, J. D. et al. 1994. 'The Germfree State Prevents Development of Gut and Joint Inflammatory Disease in HLA-B27 Transgenic Rats.' *The Journal of experimental medicine* 180:2359–64.

Taurog, J. D., L. Lowen, J. Forman, and R. E. Hammer. 1988. 'HLA-B27 in Inbred and Non-Inbred Transgenic Mice. Cell Surface Expression and Recognition as an Alloantigen in the Absence of Human Beta 2-Microglobulin.' *Journal of immunology (Baltimore, Md.: 1950)* 141(10):4020–23.

Taurog, J. D., S. D. Maika, W. A. Simmons, M. Breban, and R. E. Hammer. 1993. 'Susceptibility to Inflammatory Disease in HLA-B27 Transgenic Rat Lines Correlates with the Level of B27 Expression.' *Journal of immunology (Baltimore, Md.: 1950)* 150(9):4168–78.

Taurog, Joel D. et al. 2009. 'Spondylarthritis in HLA-B27/human ??2-Microglobulin-Transgenic Rats Is Not Prevented by Lack of CD8.' *Arthritis and Rheumatism* 60(7):1977–84.

Toussirot, Éric, Fabrice Michel, Matthieu Béreau, and Delphine Binda. 2013. 'Ustekinumab in Chronic Immune-Mediated Diseases: A Review of Long Term Safety and Patient Improvement.' *Patient Preference and Adherence* 7:369–77.

Townsend, A. et al. 1989. 'Association of Class I Major Histocompatibility Heavy and Light Chains Induced by Viral Peptides.' *Nature* 340:443–48.

Tran, Tri M., Martha L. Dorris, Nimman Satumtira, James A. Richardson, et al. 2006. 'Additional Human beta2-Microglobulin Curbs HLA-B27 Misfolding and Promotes

Arthritis and Spondylitis without Colitis in Male HLA-B27-Transgenic Rats.' *Arthritis and rheumatism* 54(4):1317–27.

Tran, Tri M., Martha L. Dorris, Nimman Satumtira, James a Richardson, et al. 2006. 'Additional Human beta2-Microglobulin Curbs HLA-B27 Misfolding and Promotes Arthritis and Spondylitis without Colitis in Male HLA-B27-Transgenic Rats.' *Arthritis and rheumatism* 54(4):1317–27.

Tsai, Wen Chan et al. 2002. 'Free HLA Class I Heavy Chain-Carrying Monocytes--a Potential Role in the Pathogenesis of Spondyloarthropathies.' *The Journal of rheumatology* 29(5):966–72.

Tsui, F. W., H. W. Tsui, F. Las Heras, K. P. Pritzker, and R. D. Inman. 2013. 'Serum Levels of Novel Noggin and Sclerostin-Immune Complexes Are Elevated in Ankylosing Spondylitis.' *Ann Rheum Dis*.

Tsui, Florence W. L. et al. 2010. 'Association of an ERAP1 ERAP2 Haplotype with Familial Ankylosing Spondylitis.' *Annals of the rheumatic diseases* 69:733–36.

Turner, Matthew J. et al. 2005. 'HLA-B27 Misfolding in Transgenic Rats Is Associated with Activation of the Unfolded Protein Response.' *Journal of immunology (Baltimore, Md.: 1950)* 175(4):2438–48.

Turner, Matthew J., Monica L. Delay, Shuzhen Bai, Erin Klenk, and Robert a Colbert. 2007. 'HLA-B27 up-Regulation Causes Accumulation of Misfolded Heavy Chains and Correlates with the Magnitude of the Unfolded Protein Response in Transgenic Rats: Implications for the Pathogenesis of Spondylarthritis-like Disease.' *Arthritis and rheumatism* 56(1):215–23.

Turner, Matthew J., Monica L. Delay, Shuzhen Bai, Erin Klenk, and Robert A. Colbert. 2007. 'HLA-B27 up-Regulation Causes Accumulation of Misfolded Heavy Chains and Correlates with the Magnitude of the Unfolded Protein Response in Transgenic Rats: Implications for the Pathogenesis of Spondylarthritis-like Disease.' *Arthritis and rheumatism* 56(1):215–23.

Uderhardt, S. et al. 2010. 'Blockade of Dickkopf (DKK)-1 Induces Fusion of Sacroiliac Joints.' *Annals of the rheumatic diseases* 69:592–97.

Ugrinovic, S., A. Mertz, P. Wu, J. Braun, and J. Sieper. 1997. 'A Single Nonamer from the Yersinia 60-kDa Heat Shock Protein Is the Target of HLA-B27-Restricted CTL Response in Yersinia-Induced Reactive Arthritis.' *Journal of immunology (Baltimore, Md.: 1950)* 159:5715–23.

Urban, R. G. et al. 1994. 'A Subset of HLA-B27 Molecules Contains Peptides Much Longer than Nonamers.' *Proceedings of the National Academy of Sciences of the United States of America* 91:1534–38.

Utriainen, Lotta et al. 2012. 'Expression of HLA-B27 Causes Loss of Migratory Dendritic Cells in a Rat Model of Spondylarthritis.' *Arthritis and rheumatism* 64(10):3199–3209.

Vastesaeger, Nathan et al. 2011. 'Predicting the Outcome of Ankylosing Spondylitis Therapy.' *Annals of the rheumatic diseases* 70:973–81.

Van Vollenhoven, Ronald F. et al. 2012. 'Tofacitinib or Adalimumab versus Placebo in Rheumatoid Arthritis.' *New England Journal of Medicine* 367(6):508–19.

De Vos, M., H. Mielants, C. Cuvelier, A. Elewaut, and E. Veys. 1996. 'Long-Term Evolution of Gut Inflammation in Patients with Spondyloarthropathy.' *Gastroenterology* 110:1696–1703.

De Vries, Mirjam K. et al. 2007. 'Decreased Clinical Response to Infliximab in Ankylosing Spondylitis Is Correlated with Anti-Infliximab Formation.' *Annals of the rheumatic diseases* 66:1252–54.

Wahl, C. et al. 1998. 'Sulfasalazine: A Potent and Specific Inhibitor of Nuclear Factor κB.' *Journal of Clinical Investigation* 101(5):1163–74.

Wan, Derrick C. et al. 2007. 'Noggin Suppression Enhances in Vitro Osteogenesis and Accelerates in Vivo Bone Formation.' *Journal of Biological Chemistry* 282:26450–59.

Wanders, Astrid et al. 2005. *Nonsteroidal Antiinflammatory Drugs Reduce Radiographic Progression in Patients with Ankylosing Spondylitis: A Randomized Clinical Trial*.

Wang, Xinwei, Zhiming Lin, Qiujing Wei, Yingjuan Jiang, and Jieruo Gu. 2009. 'Expression of IL-23 and IL-17 and Effect of IL-23 on IL-17 Production in Ankylosing Spondylitis.' *Rheumatology International* 29:1343–47.

Wang, Ying Nai et al. 2010. 'COPI-Mediated Retrograde Trafficking from the Golgi to the ER Regulates EGFR Nuclear Transport.' *Biochemical and Biophysical Research Communications* 399(4):498–504.

Weinreich, S., J. Capkova, B. Hoebe-Hewryk, C. Boog, and P. Ivanyi. 1996. 'Grouped Caging Predisposes Male Mice to Ankylosing Enthesopathy.' *Annals of the rheumatic diseases* 55:645–47.

Wendling, Daniel et al. 2012. 'Rituximab Treatment for Spondyloarthritis. A Nationwide Series: Data from the AIR Registry of the French Society of Rheumatology.' *Journal of Rheumatology* 39(12):2327–31.

Wessels, J. A. M., T. W. J. Huizinga, and H. Guchelaar. 2008. 'Recent Insights in the Pharmacological Actions of Methotrexate in the Treatment of Rheumatoid Arthritis.' (September 2007):249–55.

Van Wilgenburg, Bonnie, Michael D. Moore, William S. James, and Sally A. Cowley. 2014. 'The Productive Entry Pathway of HIV-1 in Macrophages Is Dependent on Endocytosis through Lipid Rafts Containing CD4.' *PLoS ONE* 9(1).

Wong-Baeza, Isabel et al. 2013. 'KIR3DL2 Binds to HLA-B27 Dimers and Free H Chains More Strongly than Other HLA Class I and Promotes the Expansion of T Cells in Ankylosing Spondylitis.' *Journal of immunology (Baltimore, Md.: 1950)* 190(7):3216–24.

Wu, Xue Bin et al. 2003. 'Impaired Osteoblastic Differentiation, Reduced Bone Formation, and Severe Osteoporosis in Noggin-Overexpressing Mice.' *Journal of Clinical Investigation* 112:924–34.

Zeh, H. J. et al. 1994. 'Flow-Cytometric Determination of Peptide-Class I Complex Formation: Identification of p53 Peptides That Bind to HLA-A2.' *Human Immunology* 39(2):79–86.

Zeng, Ling, Mary J. Lindstrom, and Judith A. Smith. 2011. 'Ankylosing Spondylitis Macrophage Production of Higher Levels of Interleukin-23 in Response to Lipopolysaccharide without Induction of a Significant Unfolded Protein Response.' *Arthritis and Rheumatism* 63:3807–17.

Zernich, Danielle et al. 2004. 'Natural HLA Class I Polymorphism Controls the Pathway of Antigen Presentation and Susceptibility to Viral Evasion.' *The Journal of experimental medicine* 200(1):13–24.